

DISSERTATION ZUR ERLANGUNG DES DOKTORGRADES
AN DER FAKULTÄT FÜR CHEMIE UND PHARMAZIE DER
LUDWIG-MAXIMILIANS-UNIVERSITÄT MÜNCHEN

**INVESTIGATION ON
OXYGEN-RICH
MATERIALS BASED ON
NITROCARBAMATES AND FOX-7**

Quirin Josef Axthammer

aus München, Deutschland

2016

ERKLÄRUNG

Diese Dissertation wurde im Sinne von §7 der Promotionsordnung vom 28. November 2011 von Herrn Prof. Dr. T. M. Klapötke betreut.

EIDESSTATTLICHE VERSICHERUNG

Diese Dissertation wurde eigenständig und ohne unerlaubte Hilfe erarbeitet.

München, den 03. Februar 2016

Quirin J. Axthammer

Dissertation eingereicht am:	05.02.2016
1. Gutachter:	Prof. Dr. T. M. Klapötke
2. Gutachter:	Prof. Dr. K. Karaghiosoff
Mündliche Prüfung:	29.02.2016

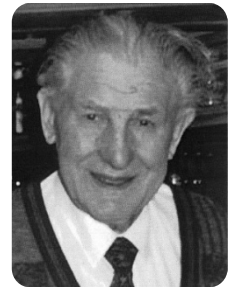
MEINER GELIEBTEN FAMILIE

UND IM BESONDEREN MEINEN GROßVATER

JOSEF MICHAEL AXTHAMMER

* 03.11.1921

† 13.03.2010



Danksagung

Mein Dank gilt an vorderster Stelle meinem Doktorvater Prof. Dr. Thomas M. Klapötke für die Aufnahme in den Arbeitskreis, die interessante Themenstellung, die stetige finanzielle und fachliche Unterstützung meiner Forschungsvorhaben sowie seine Begeisterung für die Wissenschaft.

Herrn Prof. Dr. Konstantin Karaghiosoff danke ich nicht nur für die freundliche Übernahme des Zweitgutachtens dieser Dissertation, sondern auch für die Einarbeitung in die Kristallographie und deren Faszination dafür, die ich nun mehr als nur nachvollziehen kann.

Der Prüfungskommission, bestehend aus Prof. Dr. T. M. Klapötke, Prof. Dr. K. Karaghiosoff, Prof. Dr. F. Bracher, Prof. Dr. J. Evers, Prof. Dr. Beck und Prof. Dr. A. Kornath, danke ich für Ihre Zeit und der Bereitschaft zur Bildung der selbigen.

Die Erstellung dieser Arbeit wurde durch ein Promotionsstipendium der Hanns-Seidel-Stiftung gefördert. Mein Dank richtet sich daher an die Hanns-Seidel-Stiftung für die finanzielle, aber auch für die ideelle Förderung. Im Besonderen werden mir die tollen Besuche und Seminare in Wildbad Kreuth und Kloster Banz im Gedächtnis bleiben. Vielen Dank dafür!

Herrn Dr. Burkhard Krumm danke ich für die gute Betreuung, den zahllosen Anregungen, Diskussionen und Hilfestellungen sowie für die Aufnahme zahlreicher NMR Spektren. Des Weiteren möchte ich Ihm für die immer sehr akribische Korrektur jeglicher Schriftstücke danken.

Dr. Jörg Stierstorfer danke ich für Hilfestellungen und Anregungen aller Art, sowie seinen teambildenden Maßnahmen im Arbeitskreis.

Frau Irene Scheckenbach danke ich für Ihr organisatorisches Multitalent und Ihre Unterstützung in verschiedensten und alltäglichen bürokratischen Aufgaben.

Dr. Sebastian F. Rest und Dr. Richard Moll danke ich für die Einführung in die nicht immer einfache Chemie der hochenergetischen Materialien und ihre psychologische Unterstützung bei einigen Geräuserscheinungen.

Allen während meiner Promotion anwesenden Laborkollegen im Arbeitskreis danke ich für die stets sehr gute freundschaftliche Arbeitsatmosphäre. Besonderer Dank geht hier an alle Doktoranten des Labors D.3.100 Regina Scharf, Carolin Pflüger, Michael Weyrauther, Richard

Moll, Sebastian Rest, Camilla Evangelisti und Thomas Reith, für alle fachlichen und weltanschaulichen Diskussionen.

Regina Scharf und Carolin Pflüger danke ich für die Korrektur und für die besonders gute Zusammenarbeit jeweils in dem Bereich der hochenergetischen Treibstoff-Oxydatoren und im Bereich der Kristallographie.

Besonderer Dank geht auch an all meine Praktikanten die alle mit viel Engagement einen erheblichen Beitrag zum Gelingen dieser Arbeit beigetragen haben.

Meinen sehr lieben Freunden Max, Babsi, Sabine, Simone, Simon, Julia, Peter 2×, Katharina, Christian 2×, Susi, Stefan 2×, Marina, Berny, Eva, Florian, Kathi, Karl, Roland danke ich für Eure Unterstützung in der nicht immer sehr einfachen Zeit. Danke auch an all die großartigen Ablenkungen!

Nicht zuletzt geht mein Dank an meine Familie, im Besonderen meinen Eltern Brigitte und Josef die mir durch Ihre unaufhörliche Unterstützung und Liebe dies alles erst ermöglicht haben. Meinen großartigen Schwestern Brigitte und Barbara danke ich dafür, dass ich mich immer auf Euch verlassen kann und Ihr mit Euren Familien (Mathias und Johanna, Tom und Gregor) ein einzigartiger Rückhalt seid.

Table of Contents

List of Schemes	VI
List of Figures	VIII
List of Tables	XI
I	General Introduction..... 1
1	Classification of Energetic Materials.....1
2	New Oxidizers for Solid Rocket Composite Propellants.....4
3	The Chemistry of Carbamates and Nitrocarbamates8
4	Objective Target.....10
5	References11
II	Summary..... 13
1	The Nitrocarbamate of Trinitroethanol.....14
2	Carbamates and Nitrocarbamates from Polynitro Alcohols.....14
3	The Polyvalent Nitrocarbamate of Pentaerythritol.....16
4	The Nitrocarbamate Relatives of Nitroglycerine and Co.....17
5	Nitrocarbamates of Polyvalent Sugar Alcohols.....18
6	The 1,1,1-Trinitroprop-2-yl Moiety.....18
7	Michael Addition of Nitroform19
8	The 3,3,3-Trinitropropyl Unit20
9	New FOX-7 Derivatives21
III	Results and Discussion 23
1	The Nitrocarbamate of Trinitroethanol..... 25
1.1	Abstract26
1.2	Introduction.....26
1.3	Results and Discussion.....27
1.3.1	Synthesis27
1.3.2	NMR Spectroscopy.....28
1.3.3	Single Crystal Structure Analysis.....30
1.3.4	Vibrational Spectroscopy32
1.3.5	Thermal Stabilities and Energetic Properties.....33
1.4	Conclusion36
1.5	Experimental Section.....36
1.5.1	General Procedures36

1.5.2	Computational Details.....	37
1.5.3	X-ray Crystallography.....	38
1.5.4	Synthesis.....	38
1.6	References.....	41
2	Carbamates and Nitrocarbamates from Polynitro Alcohols.....	43
2.1	Abstract.....	44
2.2	Introduction.....	44
2.3	Results and Discussion.....	45
2.3.1	Synthesis and Characterization.....	45
2.3.2	NMR Spectroscopy.....	46
2.3.3	Single Crystal X-ray Diffraction.....	47
2.3.4	Energetic Properties.....	53
2.4	Conclusion.....	54
2.5	Experimental Section.....	55
2.5.1	General Information.....	55
2.5.2	X-ray Crystallography.....	55
2.5.3	Energetic Properties and Computational Calculation.....	55
2.5.4	Synthesis.....	56
2.6	References.....	63
3	The Polyvalent Nitrocarbamate of Pentaerythritol.....	65
3.1	Press Release on the LMU Homepage.....	66
3.2	Cover Picture.....	68
3.3	Abstract.....	69
3.4	Introduction.....	69
3.5	Results and Discussion.....	69
3.5.1	Synthesis.....	69
3.5.2	NMR and vibrational Spectroscopy.....	70
3.5.3	Single Crystal Structure Analysis.....	72
3.5.4	Energetic Properties.....	75
3.5.5	SSRT-Performance Test.....	76
3.6	Conclusions.....	77
3.7	Experimental Section.....	78
3.7.1	General Information.....	78
3.7.2	X-ray Crystallography.....	78
3.7.3	Energetic Properties and Computational Calculation.....	79
3.7.4	Small scale shock reactivity test (SSRT).....	79
3.7.5	Synthesis.....	80

3.8	References	82
4	The Nitrocarbamate Relatives of Nitroglycerine and Co.....	85
4.1	Abstract	86
4.2	Introduction.....	86
4.3	Results and Discussion.....	87
4.3.1	Synthesis	87
4.3.2	NMR Spectroscopy.....	88
4.3.3	Vibrational Spectroscopy	88
4.3.4	Single Crystal Structure Analysis.....	89
4.3.5	Thermal Stabilities and Energetic Properties.....	92
4.4	Conclusion	94
4.5	Experimental Section.....	94
4.5.1	General Procedures	94
4.5.2	Computational Details.....	95
4.5.3	X-ray Crystallography.....	95
4.5.4	Calculation of Energetic Performance.....	96
4.5.5	Synthesis	96
4.6	References	101
5	Nitrocarbamates of Polyvalent Sugar Alcohols	103
5.1	Abstract	104
5.2	Introduction.....	104
5.3	Results and Discussion.....	105
5.3.1	Synthesis	105
5.3.2	NMR Spectroscopy and Vibrational Spectroscopy	107
5.3.3	Single Crystal Structure Analysis.....	108
5.3.4	Thermal Stabilities and Energetic Properties.....	111
5.4	Conclusion	113
5.5	Experimental Section.....	113
5.5.1	General Procedures	113
5.5.2	Computational Details.....	113
5.5.3	X-ray Crystallography.....	114
5.5.4	Synthesis	114
5.6	References	121
6	The 1,1,1-Trinitroprop-2-yl Moiety.....	123
6.1	Abstract	124
6.2	Introduction.....	124

6.3	Results and Discussion	125
6.3.1	Synthesis	125
6.3.2	NMR Spectroscopy and Vibrational Spectroscopy	126
6.3.3	Single Crystal Structure Analysis	129
6.3.4	Thermal Stabilities and Energetic Properties	131
6.4	Conclusion.....	135
6.5	Experimental Section.....	136
6.5.1	General Procedures.....	136
6.5.2	Computational Details.....	136
6.5.3	X-ray Crystallography	137
6.5.4	Synthesis	138
6.6	References.....	141
7	Michael Addition of Nitroform.....	143
7.1	Abstract.....	144
7.2	Introduction	144
7.3	Results and Discussion	145
7.3.1	Synthesis	145
7.3.2	NMR Spectroscopy.....	147
7.3.3	Vibrational Spectroscopy	147
7.3.4	Single Crystal Structure Analysis	148
7.3.5	Thermal Stabilities and Energetic Properties	152
7.4	Conclusion.....	155
7.5	Experimental Section.....	156
7.5.1	General Procedures.....	156
7.5.2	Computational Details.....	156
7.5.3	X-ray Crystallography	157
7.5.4	Synthesis	158
7.6	References.....	163
8	The 3,3,3-Trinitropropyl Unit	165
8.1	Abstract.....	166
8.2	Introduction	166
8.3	Results and Discussion	167
8.3.1	Synthesis	167
8.3.2	NMR Spectroscopy.....	169
8.3.3	Vibrational Spectroscopy	170
8.3.4	Single Crystal Structure Analysis	171
8.3.5	Thermal and Energetic Properties	177

8.4	Conclusion	180
8.5	Experimental Section.....	181
8.5.1	General Procedures	181
8.5.2	X-ray Crystallography.....	181
1.5.3	Computational Details.....	182
8.5.4	Synthesis	183
8.6	References	189
9	New FOX-7 Derivatives	191
9.1	Abstract	192
9.2	Introduction.....	192
9.3	Results and Discussion.....	194
9.3.1	Synthesis	194
9.3.2	NMR Spectroscopy and Vibrational Spectroscopy	197
9.3.3	Single Crystal Structure Analysis.....	201
9.3.4	Thermal Stabilities, Sensitivity and Energetic Properties.....	209
9.4	Conclusion	212
9.5	Experimental Section.....	214
9.5.1	General Procedures	214
9.5.2	Computational Details.....	214
9.5.3	X-ray Crystallography.....	215
9.5.4	Synthesis	215
9.6	References	220
IV	Appendix	223
1	Appendix A.1.....	223
2	Appendix A.2.....	226
3	Appendix A.3.....	233
4	Appendix A.4.....	235
5	Appendix A.5.....	238
6	Appendix A.6.....	247
7	Appendix A.7.....	248
8	Appendix A.8.....	252
9	Appendix A.9.....	260
10	Curriculum Vitae	268
11.	Bibliography.....	269

List of Schemes

Scheme I.1: Classification of energetic materials based on their use.....	1
Scheme I.2: Molecular structure of MF, LS, DDNP and tetrazene.....	2
Scheme I.3: Molecular structure of TNT, RDX, PETN, FOX-7 and CL-20.	2
Scheme I.4: Classification of rocket propellants.....	3
Scheme I.5: Molecular structures of hydrazinium nitroformate (HNF), triaminoguanidinium nitroformate (TAGNF) and ammonium dinitramide (ADN).	6
Scheme I.6: Chemical structure of substituted carbamates (A) and of a primary carbamate (B).....	8
Scheme I.7: Chemical structure of a primary nitrocarbamate (C).....	9
Scheme S.1: Synthesis of 2,2,2-trinitroethyl carbamate (B) and 2,2,2-trinitroethyl nitrocarbamate (C).	14
Scheme S.2: Synthesis of carbamates (E) and nitrocarbamates (F) starting from nitro alcohols (D)	15
Scheme S.3: Synthesis of carbamates (I) and nitrocarbamates (J) from simple alcohols (H).....	17
Scheme S.4: Overview of molecules containing the 1,1,1-trinitroprop-2-yl (L), the 2,2,2-trinitroethyl (M) and the 3,3,3-trinitropropyl (N) moieties.....	19
Scheme S.5: Synthetic overview of reaction of 1,1-diamino-2,2-dinitroethene (FOX-7) and chlorosulfonyl isocyanate (CSI).	21
Scheme 1-1: Synthesis of 2,2,2-trinitroethyl chloroformate (1).....	27
Scheme 1-2: Synthesis of 2,2,2-trinitroethyl carbamate (2) and 2,2,2-trinitroethyl nitrocarbamate (3).	27
Scheme 2-1: Synthesis of carbamates (2) and nitrocarbamates (3) from nitro alcohols (1).....	45
Scheme 3-1: Synthesis of pentaerythritol tetracarbamate (1).....	70
Scheme 3-2: Synthesis of pentaerythritol tetranitrocarbamate (2) and tetraammonium salt (3).....	70
Scheme 4-1: Synthesis of carbamates (2a–d) and nitrocarbamates (3a–d) from simple multivalent alcohols (1a–d).	87
Scheme 5-1: Concept of the manufacture of energetic materials based on renewable sugar alcohols.....	104
Scheme 5-2: The sugar alcohol selection.	106
Scheme 5-3: Synthesis of carbamates 2 and nitrocarbamates 3 from sugar alcohols 1	106
Scheme 6-1: Synthesis of 1,3-bis(1,1,1-trinitropropan-2-yl)urea (1).....	125
Scheme 6-2: Synthesis of 1,1,1-trinitropropan-2-yl nitrocarbamate (4) starting from nitroform	126

Scheme 6-3: Overview of molecules containing the 1,1,1-trinitroprop-2-yl, the 2,2,2-trinitroethyl and the 3,3,3-trinitropropyl moieties.....	131
Scheme 7-1: Synthesis of energetic compounds and intermediates starting from nitroform and acrylamide.....	145
Scheme 7-2: Synthesis of the hydrochloride 6 and nitrate 7 salt of 3,3,3-trinitropropan-1-amine.	146
Scheme 7-3: Synthesis of 4,4,4-trinitro- <i>N</i> -(2,2,2-trinitroethyl)-butanamide (8).....	146
Scheme 7-4: Synthesis of 2,2,2-trinitroethyl-4,4,4-trinitrobutanoate (9).....	146
Scheme 8-1: Synthetic overview of 3,3,3-trinitropropyl based compounds Part I.	167
Scheme 8-2: Synthetic overview of 3,3,3-trinitropropyl based compounds Part II.....	168
Scheme 8-3: Synthetic overview of 3,3,3-trinitropropyl based compounds Part III.	168
Scheme 9-1: Resonance hybrid structures of FOX-7.....	193
Scheme 9-2: Synthesis of 1-(1-amino-2,2-dinitrovinyl)urea (1) and its potassium salt (2).	194
Scheme 9-3: Synthesis overview of reaction of 1-amino-1-hydrazino-2,2-dinitroethene (HFOX) and chlorosulfonyl isocyanate (CSI).	195
Scheme 9-4: Tautomerization of 2-(2,2-dinitro-1-ureidoethylidene)hydrazine-1-carboxamide (5).	198
Scheme 9-5: Possible further reactions for better energetic properties.	213
Scheme A.5-1: General isodesmic reaction for the calculation of the heats of formation of polyvalent nitrocarbmates.	239

List of Figures

Figure I.1: Maximum reported perchlorate contamination in the United States (2004).....	5
Figure I.2: The effect of the perchlorate anion in the human body.	6
Figure S.1: X-ray molecular structure of 2,2,2-trinitroethyl nitrocarbamate (C).....	14
Figure S.2: Specific impulse I_{sp} and the nitrogen/hydrogen chloride content (Mol%) of the decomposition products of B , C and AP.....	15
Figure S.5: X-ray molecular structure of pentaerythritol tetranitrocarbamate (G).	16
Figure S.4: Small scale reactivity test (SSRT) of pentaerythritol tetranitrocarbamate (G).....	16
Figure S.5: X-ray structure of <i>meso</i> -erythritol tetranitrocarbamate (K) and packing along the <i>a</i> axis.	18
Figure S.8: X-ray molecular structure of 3,3,3-trinitropropan-1-amine nitrate (O).....	19
Figure S.9: X-ray molecular structure of <i>N</i> -(2,2,2-trinitroethyl)- <i>N</i> -(3,3,3-trinitropropyl) nitramine (P).....	20
Figure S.10: X-ray molecular structure of 1-(1-amino-2,2-dinitrovinyl)urea (Q) and packing along the <i>b</i> axis.	22
Figure 1-1: ^1H NMR resonance of the NH_2 group of 2 at variable temperatures in $[\text{D}_6]\text{DMSO}$..	29
Figure 1-2: X-ray molecular structure of 2,2,2-trinitroethyl carbamate (2).....	30
Figure 1-3: X-ray molecular structure of 2,2,2-trinitroethyl nitrocarbamate (3).....	31
Figure 1-4: Burning test of a compressed mixture of 2,2,2-trinitroethyl nitrocarbamate (3) (85%) and aluminum (15%).	35
Figure 2-1: X-ray molecular structure of 2-fluoro-2,2-dinitroethyl nitrocarbamate (3b).	48
Figure 2-2: X-ray molecular structure of 2,2-dinitropropane-1,3-diyl dicarbamate (2c).....	48
Figure 2-3: X-ray molecular structure of 2,2-dinitropropane-1,3-diyl bis(nitrocarbamate) (3c).....	49
Figure 2-4: X-ray molecular structure of 2,2-dinitropropyl carbamate (2d).....	50
Figure 2-5: X-ray molecular structure of 2,2-dinitropropyl nitrocarbamate (3d).	50
Figure 2-6: X-ray molecular structure of 4,4,4-trinitrobutyl carbamate (2e).	51
Figure 2-7: X-ray molecular structure of 4,4,4-trinitrobutyl nitrocarbamate (3e).....	51
Figure 2-8: Specific impulse I_{sp} and the nitrogen/hydrogen chloride content (Mol%) of the decomposition products calculated with EXPLO5 V.6.02.	54
Figure 3-1: ^{15}N NMR spectrum of pentaerythritol tetranitrocarbamate (2) and tetraammonium salt 3 in $[\text{D}_6]\text{DMSO}$	71
Figure 3-2: X-ray molecular structure of pentaerythritol tetranitrocarbamate (2).....	73

Figure 3-3: View of the crystal structure 2 along <i>c</i> axis (left) and <i>a</i> axis (right).	74
Figure 3-4: X-ray molecular structure of tetraammonium pentaerythritol tetranitrocarbamate (3).	75
Figure 3-5: DTA of pentaerythritol tetranitrocarbamate (2) (red) and pentaerythritol tetranitrate (PETN) (blue), with a heating rate of 5 °/min.	75
Figure 3-6: Small scale reactivity test (SSRT) of 2 . a) schematic set-up b) set-up before initiation c) aluminum block after the test d) measuring the volume with sand.....	77
Figure 4-1: X-ray molecular structure of ethane-1,2-diyl dicarbamate (2a).....	89
Figure 4-2: X-ray molecular structure of ethane-1,2-diyl bis(nitrocarbamate) (3a).....	90
Figure 4-3: X-ray molecular structure of propane-1,2,3-triyl tris(nitrocarbamate) (3b).	90
Figure 4-4: X-ray molecular structure of one unique molecule of nitroisobutylglycerol trinitrocarbamate (3c).	91
Figure 4-5: X-ray molecular structure of but-2-yne-1,4-diyl bis(nitrocarbamate) (3d).	91
Figure 5-1: X-ray molecular structure of <i>myo</i> -inositol hexacarbamate (2b).....	109
Figure 5-2: X-ray molecular structure of <i>meso</i> -erythritol tetranitrocarbamate 3a a), along <i>a</i> axis b), along <i>c</i> axis c).....	110
Figure 5-3: Deflagration and burning test of anhydrous nitrocarbamate 3a	112
Figure 6-1: ¹⁵ N NMR spectrum of 1,1,1-trinitropropan-2-yl carbamate (3) in CDCl ₃	127
Figure 6-2: X-ray molecular structure of 1,3-bis(1,1,1-trinitropropan-2-yl)urea (1).....	129
Figure 6-3: Disorder of the trinitromethyl group in the X-ray molecular structure of 1,3-bis(1,1,1- trinitropropan-2-yl)urea (1).....	130
Figure 6-4: X-ray molecular structure of 1,1,1-trinitropropan-2-yl carbamate (3).	131
Figure 7-1: X-ray molecular structure of 4,4,4-trinitrobutanamide (1).....	148
Figure 7-2: X-ray molecular structure of 4,4,4-trinitrobutanoic acid (2).	149
Figure 7-3: X-ray molecular structure of 4,4,4-trinitrobutanoyl azide (4).	150
Figure 7-4: X-ray molecular structure of 3,3,3-trinitropropan-1-amine hydrochloride (6).	150
Figure 7-5: X-ray molecular structure of 3,3,3-trinitropropan-1-amine nitrate (7).	151
Figure 7-6: X-ray molecular structure of 2,2,2-trinitroethyl-4,4,4-trinitrobutanoate (9).	152
Figure 8-1: ¹⁵ N NMR spectrum of <i>N</i> -(2,2,2-trinitroethyl)- <i>N</i> -(3,3,3-trinitropropyl) nitramine (10) in CD ₃ CN.	169
Figure 8-2: X-ray molecular structure of bis(3,3,3-trinitropropyl) urea (4).	171
Figure 8-3: Disorder of the C(NO ₂) ₃ moiety in the molecular structure of bis(3,3,3-trinitropropyl) urea (4).	172
Figure 8-4: X-ray molecular structure of bis(3,3,3-trinitropropyl) oxamide (5).	173

Figure 8-5: X-ray molecular structure of bis(3,3,3-trinitropropyl) oxalate (6).....	173
Figure 8-6: X-ray molecular structure of two molecules of 3,3,3-trinitropropyl carbamate (7)...	174
Figure 8-7: X-ray molecular structure of 3,3,3-trinitropropyl nitrocarbamate (8).	175
Figure 8-8: X-ray molecular structure of 3,3,3-trinitro- <i>N</i> -(2,2,2-trinitroethyl) propan-1-amine (9) showing a C/N disorder.	175
Figure 8-9: X-ray molecular structure of 3,3,3-trinitro- <i>N</i> -(2,2,2-trinitroethyl) propan-1-amine (9).	176
Figure 8-10: X-ray molecular structure of <i>N</i> -(2,2,2-trinitroethyl)- <i>N</i> -(3,3,3-trinitropropyl) nitramine (10).....	176
Figure 9-1: ¹³ C NMR spectra of 2-(2,2-dinitro-1-ureidoethylidene)hydrazine-1-carboxamide (5) in CD ₃ CN (red) and [D ₆]DMSO (blue).....	198
Figure 9-2: ¹⁵ N NMR spectrum of 1 (blue), 3 (orange) and 6_K (green) in [D ₆]DMSO.	200
Figure 9-3: X-ray molecular structure of 1-(1-amino-2,2-dinitrovinyl)urea (1).	201
Figure 9-4: Representation of the layered structure of compound 1	202
Figure 9-5: X-ray molecular structure of potassium 2-amino-2-(carbamoylimino)-1,1-dinitroethan- 1-ide (2).....	203
Figure 9-6: X-ray molecular structure of 1-amino-1-hydrazino-2,2-dinitroethene (HFOX).	204
Figure 9-7: X-ray molecular structure of 2-(1-amino-2,2-dinitrovinyl)hydrazine-1-carboxamide (3).	205
Figure 9-8: X-ray molecular structure of potassium 2-amino-2-(2-carbamoylhydrazono)-1,1- dinitroethan-1-ide (4).....	205
Figure 9-9: X-ray molecular structure of 2-(2,2-dinitro-1-ureidoethylidene)hydrazine-1- carboxamide (5).....	206
Figure 9-10: X-ray molecular structure of potassium (1-carbamoyl-5-oxo-1,2,4-triazol-3- yl)dinitromethanide (6_K).	207
Figure 9-11: X-ray molecular structure of ammonium (1-carbamoyl-5-oxo-1,2,4-triazol-3- yl)dinitromethanide (6_NH₄).....	208
Figure 9-12: Representation of the wave-layered structure of 6_NH₄ , view along the <i>a</i> axis.....	209
Figure 9-13: Comparison of DTA measurements (5 °C min ⁻¹) of FOX-7 (green), HFOX (blue), 1 (yellow) and 3 (red).....	209

List of Tables

Table 1-1: Multinuclear NMR resonances [ppm] of 1–3 in [D ₆]acetone.	28
Table 1-2: Characteristic IR and RAMAN vibrations of 1–3 in [cm ⁻¹]	32
Table 1-3: Physical and chemical properties of 2 and 3	33
Table 1-4: Predicted detonation, combustion parameters and sensitivity data for 2 and 3	34
Table 1-5: Predicted specific impulse I_{sp} of mixtures with aluminum and sensitivity data for 2 and 3	35
Table 2-1: Physical Properties of Carbamates 2a–e and Nitrocarbamates 3a–e	47
Table 2-2: Calculated detonation, combustion parameters and sensitivity data of the energetic carbamates 2a–e and nitrocarbamates 3a–e	52
Table 3-1: Multinuclear NMR resonances (in ppm, solvent [D ₆]DMSO) and characteristic Raman/IR vibrations bands (in cm ⁻¹ , ATR).	72
Table 3-2: Physical and energetic properties of 2 , 3 and pentaerythritol tetranitrate (PETN).	76
Table 4-1: Physical and chemical properties of 3a–3d	92
Table 4-2: Calculated heats of formation, predicted detonation and combustion parameters for 3a–3d	93
Table 5-1: Multinuclear NMR resonances (ppm) and characteristic Raman/IR vibrations (cm ⁻¹) of the carbamate 2a and the nitrocarbamate 3a of <i>meso</i> -erythritol.	107
Table 5-2: Physical properties and calculated detonation parameters of water free compounds 3a , 3b , 3c in comparison to PETN (Pentaerythritol tetranitrate) and ETN (<i>meso</i> -Erythritol tetranitrate).	111
Table 5-3: Calculated detonation parameters of 3a , 3b and 3c in comparison to PETN (Pentaerythritol tetranitrate) and ETN (<i>meso</i> -Erythritol tetranitrate).	112
Table 5-4: Experimental scales and yields for the synthesis of carbamates 2a–f from sugar alcohols 1a–f	115
Table 5-5: Experimental scales and yields for the synthesis of nitrocarbamates 3a–f by nitration of carbamates 2a–f	115
Table 6-1: Multinuclear NMR resonances (ppm) of 1 , 3 and 4 in CDCl ₃	127
Table 6-2: Selected IR and Raman bands of the compounds 1 , 3 and 4	128
Table 6-3: Physical and sensitivity data of 1A , 3A and 4A and the corresponding 2,2,2-trinitroethyl (B) and 3,3,3-trinitropropyl (C) derivatives.	132
Table 6-4: Calculated heats of formation and calculated detonation and propulsion parameters using EXPLO5 (V6.02) of 1A , 3A and 4A compared to the corresponding 2,2,2-trinitroethyl (B) and 3,3,3-trinitropropyl (C) derivatives and AP.	134

Table 7-1: Physical properties of the compounds 1 , 2 , 4 , 6 , 7 , 8 and 9 in comparison to ammonium perchlorate (AP).....	153
Table 7-2: Calculated detonation and combustion parameters in comparison to ammonium perchlorate (AP).....	154
Table 8-1: Selected IR and Raman bands for 1–10	170
Table 8-2: Physical and chemical properties of 3–10	178
Table 8-3: Calculated heat of formation, predicted detonation and combustion parameters for 4–10	180
Table 9-1: Multinuclear NMR resonances (^1H , ^{13}C , ^{15}N) of 1 , 3 , 5 and 6_K in ppm (number of hydrogens/multiplicity).....	197
Table 9-2: Measured bond lengths and torsion angles from FOX-7 derivatives all measured at 173 K.....	201
Table 9-3: Physical properties of 1–5 , 6_K and 6_NH₄ in comparison of the starting materials FOX-7 and HFOX.	210
Table 9-4: Calculated heat of formation and predicted detonation parameters for 1 , 3 , 5 and 6_NH₄ in comparison of the starting material FOX-7 and HFOX.	211
Table A.1-1: Cell parameters of 2 and 3 at 25 °C.....	223
Table A.1-2: Crystallographic data for 2 and 3	224
Table A.1-3: Hydrogen bonds of 2,2,2-trinitroethyl carbamate (2).	225
Table A.1-4: Hydrogen bonds of 2,2,2-trinitroethyl nitrocarbamate (3).....	225
Table A.2-1: Crystallographic data for 3b , 2c and 3c	226
Table A.2-2: Crystallographic data for 2d , 3d and 2e	227
Table A.2-3: Crystallographic data for 3e	228
Table A.2-4: Halogen and hydrogen bonds of 2-fluoro-2,2-dinitroethyl nitrocarbamate (3b).....	229
Table A.2-5: Hydrogen bonds of 2,2-dinitropropane-1,3-diyl dicarbamate (2c).....	229
Table A.2-6: Hydrogen bonds of 2,2-dinitropropane-1,3-diyl bis(nitrocarbamate) (3c).	229
Table A.2-7: Hydrogen bonds of 2,2-dinitropropyl carbamate (2d).	230
Table A.2-8: Hydrogen bonds of 2,2-dinitropropyl nitrocarbamate (3d).....	230
Table A.2-9: Hydrogen bonds of 4,4,4-trinitrobutyl carbamate (2e).....	231
Table A.2-10: Hydrogen bonds of compound 4,4,4-trinitrobutyl nitrocarbamate (3e).....	231
Table A.2-11: Further calculated detonation and combustion parameters.....	232
Table A.3-1: Crystallographic data for 2 and 3	233
Table A.3-2: Hydrogen bonds of pentaerythritol tetranitrocarbamate (2).....	234

Table A.3-3: Hydrogen bonds of tetraammonium salt of pentaerythritol tetranitrocarbamate (3).	234
Table A.4-1: Crystallographic data for 2a , 3a and 3b	235
Table A.4-2: Crystallographic data for 3c and 3d	236
Table A.4-3: Calculated heat of formation, predicted detonation and combustion parameters for 3a–3d and ethylene glycol dinitrate EGDN and nitroglycerin NG.	237
Table A.5-1: Crystallographic data for 2b and 3a	238
Table A.5-2: Results from GAUSSIAN 09 calculation.	241
Table A.5-3: Heat of formation in the gas phase $\Delta_f H^\circ_{\text{gas}}$ of the isodesmic reactions.	242
Table A.5-4: Results from GAUSSIAN 09 calculation.	243
Table A.5-5: Heat of formation in the gas phase $\Delta_f H^\circ_{\text{gas}}$ of the isodesmic reactions.	243
Table A.5-6: Results from GAUSSIAN 09 calculation.	244
Table A.5-7: Heat of formation in the gas phase $\Delta_f H^\circ_{\text{gas}}$ of the isodesmic reactions.	245
Table A.6-1: Crystallographic data for 2 and 4	247
Table A.7-1: Crystallographic data for 1 , 2 and 4	248
Table A.7-2: Crystallographic data for 6 , 7 and 9	249
Table A.7-3: Hydrogen bonds of 4,4,4-trinitrobutanamide (1).	250
Table A.7-4: Hydrogen bonds of 4,4,4-trinitrobutanoic acid (2).	250
Table A.7-5: Hydrogen bonds of 4,4,4-trinitrobutanoyl azide (4).	250
Table A.7-6: Hydrogen bonds of 3,3,3-trinitropropan-1-amine hydrochloride (6).....	250
Table A.7-7: Hydrogen bonds of 3,3,3-trinitropropan-1-amine nitrate (7).....	251
Table A.7-8: Hydrogen bonds of compound 2,2,2-trinitroethyl-4,4,4-trinitrobutanoate (9).....	251
Table A.8-1: Crystallographic data for 4 , 5 and 6	252
Table A.8-2: Crystallographic data for 7 , 8 and 9	253
Table A.8-3: Crystallographic data for 10	254
Table A.8-4: Hydrogen bonds of bis(3,3,3-trinitropropyl) urea (4).	255
Table A.8-5: Hydrogen bonds of bis(3,3,3-trinitropropyl) oxalamide (5).	255
Table A.8-6: Hydrogen bonds of bis(3,3,3-trinitropropyl) oxalate (6).	256
Table A.8-7: Hydrogen bonds of 3,3,3-trinitropropyl carbamate (7).	256
Table A.8-8: Hydrogen bonds of 3,3,3-trinitropropyl nitrocarbamate (8).	256
Table A.8-9: Hydrogen bonds of 3,3,3-trinitro- <i>N</i> -(2,2,2-trinitroethyl)propan-1-amine (9).....	257
Table A.8-10: Hydrogen bonds of <i>N</i> -(2,2,2-trinitroethyl)- <i>N</i> -(3,3,3-trinitropropyl) nitramide (10).	257

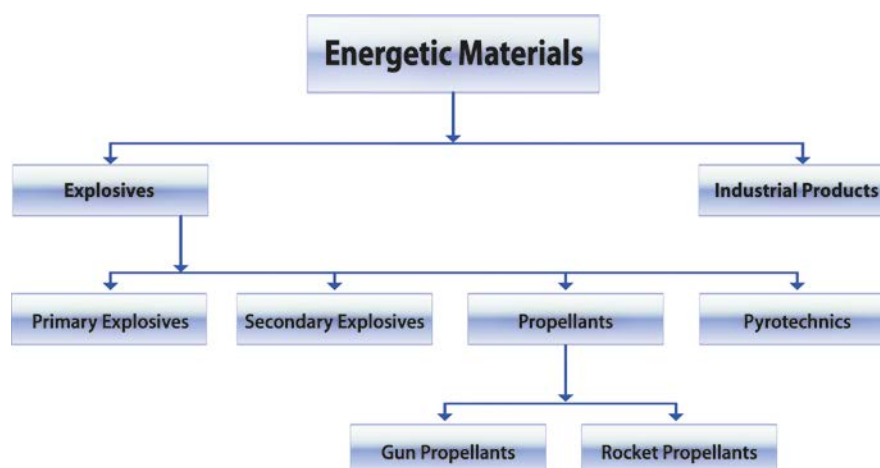
Table A.8-11: Further calculated detonation and combustion parameters.....	258
Table A.8-12: Comparison of physical and chemical properties of the 3,3,3-trinitropropyl and 2,2,2-trinitroethyl group with different moieties.	259
Table A.9-1: Crystallographic data for HFOX, 1 and 2	260
Table A.9-2: Crystallographic data for 3 , 4 and 5	261
Table A.9-3: Crystallographic data for 6_K and 6_NH₄	262
Table A.9-4: Hydrogen bonds of 1-(1-amino-2,2-dinitrovinyl)urea (1).....	263
Table A.9-5: Hydrogen bonds of potassium 2-amino-2-(carbamoylimino)-1,1-dinitroethan-1-ide (2).....	264
Table A.9-6: Hydrogen bonds of compound 1-amino-1-hydrazino-2,2-dinitroethene (HFOX).	264
Table A.9-7: Hydrogen bonds of 2-(1-amino-2,2-dinitrovinyl)hydrazine-1-carboxamide (3).	265
Table A.9-8: Hydrogen bonds of potassium 2-amino-2-(2-carbamoylhydrazono)-1,1-dinitroethan-1-ide (4).....	266
Table A.9-9: Hydrogen bonds of 2-(2,2-dinitro-1-ureidoethylidene)hydrazine-1-carboxamide (5).	266
Table A.9-10: Hydrogen bonds of potassium (1-carbamoyl-5-oxo-1,2,4-triazol-3-yl)dinitromethanide (6_K).....	267
Table A.9-11: Hydrogen bonds of ammonium (1-carbamoyl-5-oxo-1,2,4-triazol-3-yl)dinitromethanide (6_NH₄).....	267

I General Introduction

1 Classification of Energetic Materials

An energetic material is defined as a compound or a mixture of substances, which decomposes readily under release of enormous volume of gaseous products and a large amount of energy.^[1]

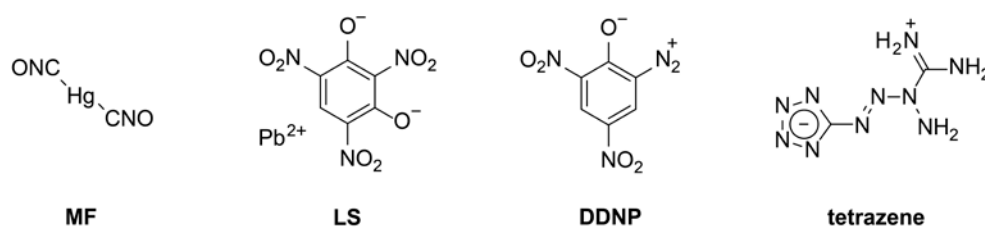
The earliest energetic material was “Greek Fire” and consisted of petroleum distillate, natural resin and other combustible materials. It was developed by the Byzantines but the exact composition is unknown.^[2] The development of energetic materials began with the accidental discovery of black powder/gun powder in China about 220 BC. This important discovery remained dormant until the 13th century, when in Europe the research on the properties of black powder started.^[1] Black powder is a mixture of fuel, charcoal and sulfur which is mixed with potassium nitrate as oxidizer and was introduced into the military at the end of the 13th century. It was used mainly as propellant charge for smaller and later also for large caliber artillery guns.^[1] Later ammonium nitrate was added as oxidizer in the black powder mixture but this was until the 19th century the only development on explosives and propellants. At the beginning of the 19th century the nitration of many compounds were realized which contains both the fuel and the oxidizer within the same molecule. This modern explosive design increased the power of the prepared energetic materials enormously. The first compound of this group was nitroglycerine (NG), which was prepared by the Italian chemist Ascanio Sobrero in 1846.^[2-3] Later in the 19th century and during the World War I and II there has been enormous growth in the field of explosives.



Scheme I.1: Classification of energetic materials based on their use.

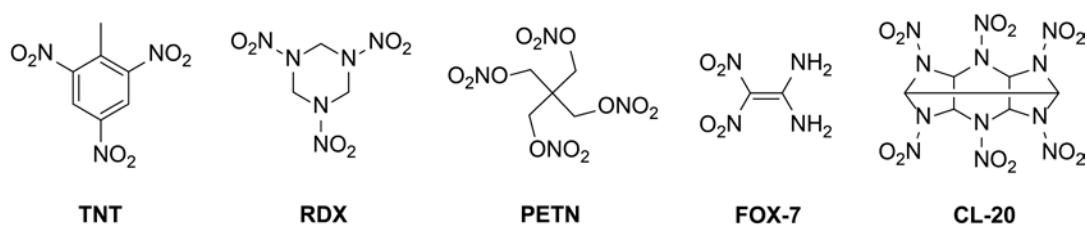
Energetic materials were divided into two major groups, explosives and industrial chemical products for non-explosive purpose. Industrial energetic chemical products are materials such as organic peroxides, nitrate esters, fertilizers or fine powdered metals. Explosives are best subdivided according to their use, into primary explosives, secondary/high explosives, propellants and pyrotechnics (Scheme I.1).

Primary Explosives are the most sensitive and most easily initiated energetic materials. Unlike secondary explosives, they are able to detonate upon mechanical or thermal stimulation.^[1] The decomposition is the result of a fast deflagration-to-detonation transition. The impact sensitivity (IS) of primary compounds is typically less than 4 J, the friction sensitivity (FS) is less than 10 N and the detonation velocity is quite low within the range of 3500 to 5000 m s⁻¹. Typical representatives of this group are mercury fulminate (MF), lead styphnate (LS), 2-diazo-4,6-dinitrophenol (DDNP) and the latest development tetrazene.



Scheme I.2: Molecular structure of MF, LS, DDNP and tetrazene.

Secondary Explosives show in contrast to primary explosives a much lower sensitivity to shock, friction, electrical discharge and heat contrary. The performance data as detonation pressure, detonation velocity and heat of explosion of secondary explosives are also significantly higher. The usual range for the detonation velocities is between 7000 to 9500 m s⁻¹, with sensitivities higher than 5 J towards impact and 60 N towards friction.^[1] The oldest secondary explosive is 2,4,6-trinitrotoluene (TNT) which was mainly used only during the two World Wars. The currently most employed secondary explosive which also serves as benchmark for new developed secondary explosives is 1,3,5-trinitro-1,3,5-triazinane (RDX).

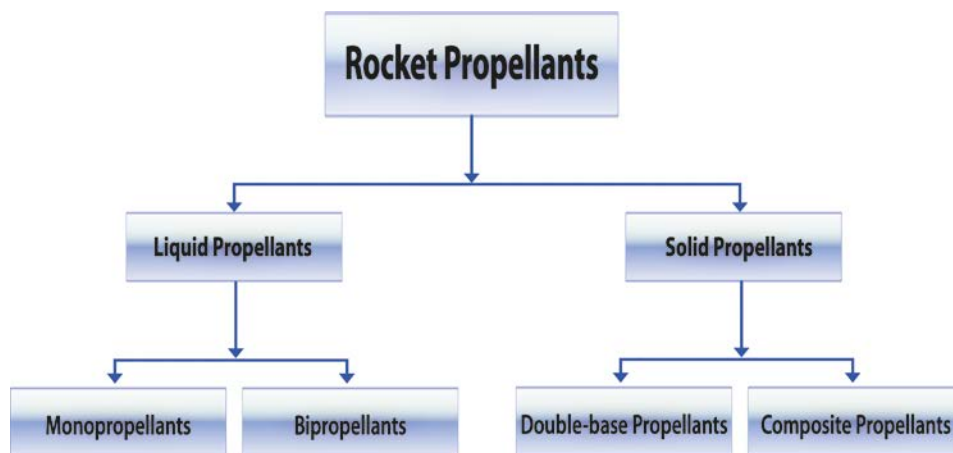


Scheme I.3: Molecular structure of TNT, RDX, PETN, FOX-7 and CL-20.

Other important examples are pentaerythritol tetranitrate (PETN) which is used as booster explosive, due to its easy initiation and 1,1-diamino-2,2-dinitroethene (FOX-7) which is a relatively new high energetic material. FOX-7 shows good explosive performances while the sensitivity against mechanical stimuli and thermal stress is very low. The most powerful secondary explosive currently in use is the cage-like 2,4,6,8,10,12-hexanitrohexaazaisowurtzitane (CL-20).

Pyrotechnic energetic material which is mostly known due to fireworks and signal flares. Contrary to primary and secondary explosives, which contain the oxidizer and the fuel in a single molecule, pyrotechnics are physical mixtures of different substances.^[1] Due to solid phase reactions and the higher activation energies the decomposition and burning rates are very slow. They often contain additionally additives for the generation of light, noise and smoke. Typical oxidizers are potassium perchlorate and nitrate, while typical fuels are carbon, boron or metals like magnesium.

Propellants are characterized by a controlled burn-off or deflagration, which does not pass into a detonation. Upon decomposition, large quantities of hot gasses are produced, which are used for the acceleration of projectiles, rockets or missiles. A further distinction is made between Gun Propellants and Rocket Propellants. Gun Propellants differs from Rocket propellants in the much higher burning rate and in the associated higher pressure in the combustion chamber or in the gun barrel. Rocket Propellant charges deliver a pressure of about 70 bar in the combustion chamber, whereas Gun Propellant charges work at 4000 bar.^[1] The oldest Gun Propellant is black powder, which is largely replaced due to its low efficiency by single, double and triple base gun propellants on the basis of nitroglycerine (NG), nitrocellulose (NC) and nitroguanidine (NQ).^[1,4]



Scheme I.4: Classification of rocket propellants.

Rocket Propellants on the other hand do not accelerate a separate projectile but act as the propulsion system for missiles or rockets. In general Rocket Propellants were categorized into

those for solid propellants and those for liquid propellants (Figure I.5). The liquid propellants can be further separated into mono- and bipropellants. Monopropellants are endothermic liquids (e.g. hydrazine N_2H_4), which decomposes exothermically mainly due to a catalyst, into nitrogen and hydrogen in the absence of oxygen.^[1] Although the energy content and performance of the monopropellants is relatively small they are long-term storable and therefore are used in small missiles and satellites e.g. for the correction of the orbit. The bipropellant systems show a better performance since oxidizer and fuel are transported in two different tanks. For acceleration both compounds were injected into the combustion chamber. The bipropellants are further separated into two different classes, either in cryogenic bipropellants, which are handled only at very low temperatures and therefore are unsuitable for military applications (e.g. liquid H_2 (LH2) and liquid O_2 (LOX)) and storable bipropellants (e.g. monomethylhydrazine (MMH)/red fuming nitric acid (DFNA)).^[2]

The solid propellants are categorized into double-base (homogeneous) and composite propellants (heterogeneous). Double-base propellants generally base on nitrocellulose (NC) and are often used in homogeneous formulations with nitroglycerine (NG) and nitroguanidine (NQ). The heterogeneous propellants generally base on heterogenic physical mixtures of crystalline oxidizer (e.g. ammonium perchlorate (AP)), fuel as propellant (e.g. aluminum) and a polymeric binder (e.g. hydroxyl-terminated polybutadiene (HTPB)) which has been cured with isocyanates (e.g. di- or poly-isocyanate).^[1]

2 New Oxidizers for Solid Rocket Composite Propellants

Ammonium perchlorate (AP) is the most used and most important oxidizer for solid rocket composite propellants for decades. AP has several advantages like its completely convertibility to gaseous decomposition products, has a very high oxygen balance of $\Omega_{\text{CO}} = 34\%$, is easily producible and is stable against mechanical stimuli. The physical drawback is that AP undergoes low-temperature autocatalytic decomposition reaction at temperatures greater than $150\text{ }^\circ\text{C}$.^[5] At temperatures above $300\text{ }^\circ\text{C}$ complete non-autocatalytical high-temperature decomposition occurs.^[5b] Another disadvantage of AP propellant formulations are inadequate properties which are shown in slow cook-off tests.^[6] It is expected that in formulations AP slowly decomposes and acidic side-products are formed. These acidic side-products further react with the binder-system causing cracks und cavities in the composite charge, which consequently negatively affects the performance and sensitivity. Another drawback of AP are the toxic decomposition products like hydrogen chloride which provokes further environmental problems and generates easy visible and

detectable expulsions leading to tactical disadvantages.^[7] However, the considerably biggest problem is the toxicity and the related environmental issues of the perchlorate anion.^[8] As a result of the utilization of ammonium perchlorate as solid rocket composite propellant and due to its high solubility, chemical stability, and persistence it has become widely distributed in surface and ground water systems (Figure I.1).^[9] Perchlorate is found in groundwater and drinking water throughout the United States and alone there the costs for remediation are estimated to be several billion dollars.^[1, 8a]

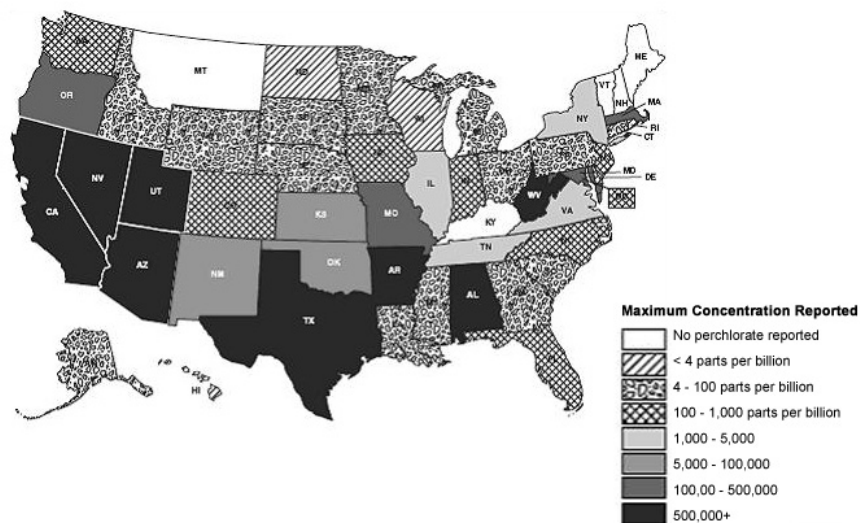


Figure I.1: Maximum reported perchlorate contamination in the United States (2004).^[10]

Perchlorate occurs both naturally and as a manufactured compound. At this time, most naturally occurring sources of perchlorate appear to be geographically limited to arid environments. These deposits tend to be of low concentration, except for the relatively high natural perchlorate concentrations found in Chilean caliche and potash ores.^[8a, 9, 11] In contrast, man-made perchlorate sources can be many times more concentrated than most natural sources. This synthetic perchlorate contamination is attributed to the use of AP in fireworks, signal flares and primarily on the use in solid composite propellants of rockets and missiles.^[9] In the United States, approximately 90% of the industrial synthesized perchlorate is used as the ammonium salt as an oxidizing agent for solid propellant.^[11] The main contamination is caused by improper disposal of solid propellants in the past, the frequent use of weapon systems containing perchlorate on the various training and testing ranges and the manufacture of compounds for the preparation of energetic materials (e.g. production of nitric acid, perchlorates and chlorates).^[9, 11]

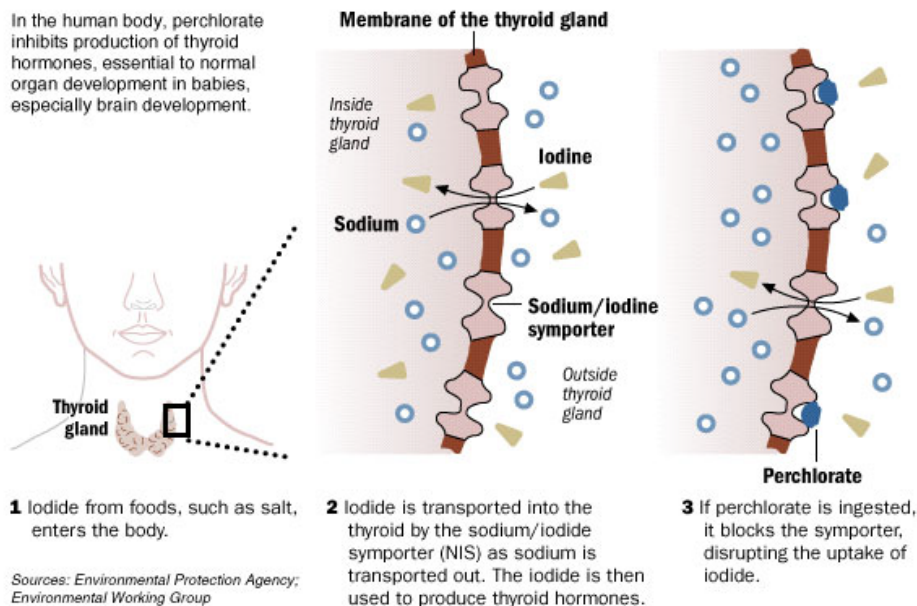
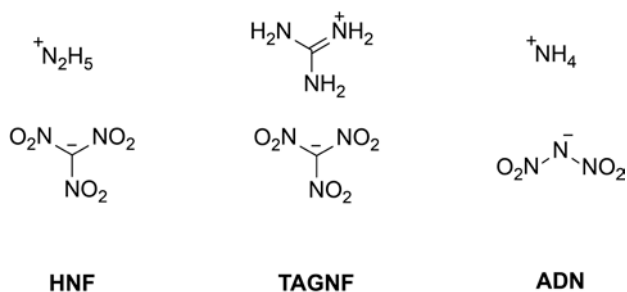


Figure I.2: The effect of the perchlorate anion in the human body.^[10]

The concern with perchlorate is that it competes with iodine for uptake into the thyroid gland (Figure I.2). This results in an iodine deficiency which disturbs the thyroid's ability to produce hormones needed for normal growth and development in vertebrates.^[12] Furthermore, scientific research indicates that perchlorate contaminated water effects the aquatic life and causes uncommon pigmentation of amphibian embryos and other marine organisms.^[13]



Scheme I.5: Molecular structures of hydrazinium nitroformate (HNF), triaminoguanidinium nitroformate (TAGNF) and ammonium dinitramide (ADN).

Possible alternatives for AP are ammonium nitrate (AN), ammonium dinitramide (ADN), hydrazinium nitroformate (HNF) and triaminoguanidinium nitroformate (TAGNF). However, they all cause other problems, such as low thermal stability, phase transition, hygroscopicity and binder compatibility.

Ammonium dinitramide (ADN), $\text{NH}_4\text{N}(\text{NO}_2)_2$, is one of the most promising oxidizers of future solid propellant formulations. It is eco-friendly, energetic and has no plume signature since there is no chlorine in its molecular structure. Problems of ADN are its hygroscopicity and its low thermal stability (melts at 93 °C and already decomposes at 135 °C).^[14] Other chemicals under research are the nitroformate salts HNF and TAGNF. Both compounds suffer from low thermal stabilities (HNF = 128 °C, TAGNF = 105 °C), and quite high sensitivities.^[15] Furthermore, the use of the hydrazinium cation may be problematic due to the potential release of highly hazardous hydrazine caused by thermal stress or alkaline conditions. Alternatively, AN propellants are discussed. However AN starts to decompose at its melting point (170 °) and is completely decomposed at 210 °C.^[1] Furthermore, AN is hygroscopic and shows several phase transitions from one polymorph to another. These both problems can be overcome by coating and phase stabilization.^[16] However, in general AN based propellants cannot provide the high energy output produced by AP.

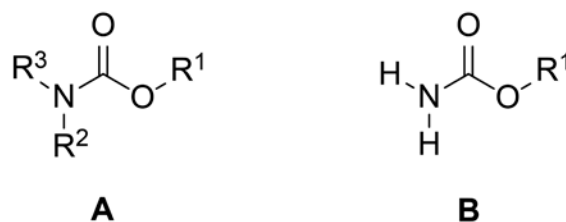
Further research work is absolutely necessary in order to find better oxidizers for solid propellants. In this context, the following requirements must be fulfilled:

The general requirements for a novel advanced HEDOS's are the following:^[1]

- High oxygen content $\Omega_{\text{CO}} > 25\%$
- High density, best close to 2 g cm^{-3}
- High thermal stability, at least 150 °C
- Sensitivities not higher than PETN (IS 4 J, FS 80 N)
- Low vapor pressure
- High enthalpy of formation
- Compatibility with fuel and binders
- Facile synthesis with minimum number of synthesis steps and economic starting materials

3 The Chemistry of Carbamates and Nitrocarbamates

Carbamates can be considered as carbonic acid derivatives containing a carbonyl function directly connected to an alkoxy and an amino function.^[17] Therefore, they exhibit some of the characteristic properties of amides and some of esters. Accordingly, the reactions of this class of esters of carbamic acid are those of amides and esters.

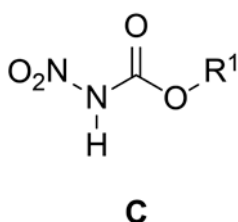


Scheme I.4: Chemical structure of substituted carbamates (**A**) and of a primary carbamate (**B**).

According to IUPAC, carbamates are named as salts or esters of the carbamic acid, or of the *N*-substituted carbamic acids, $R^2R^3NCO_2R^1$, where R^1 = alkyl, aryl or a cation ($R^2 = R^3 = H$, alkyl, aryl).^[17a] The esters are often called urethanes, a usage that is not correct only for the ethyl esters, but widely used in general sense. In the term alkyl carbamates, the alkyl refers to the *O*-alkyl ester in this way, the compound $EtOCONH_2$ is named as ethyl carbamate, while the substituents on the nitrogen atom are considered part of the carbamate.^[17a] Organic carbamates represent an important class of compounds and are utilized in various areas as pharmaceuticals, cosmetics, agrochemicals (fungicides, pesticides, herbicides, insecticides, etc.), intermediates in organic synthesis, protection of amino groups in synthetic organic chemistry, as linkers in the peptide chemistry and so on.^[17a, 18] Since *N*-unsubstituted carbamates are often stable crystalline solids having high melting points which are always higher than the corresponding acetates and alcohols this is also a particularly interesting group for the use in the field of energetic materials.^[17b, 19]

Classical synthesis of carbamates involves the use of harmful reagents such as phosgene and its derivatives. Especially the synthesis of primary carbamates (**B**) is very limited to several options. The standard synthesis of primary carbamates is a two step synthesis, starting from the corresponding alcohol and an excess of phosgene or phosgene derivatives. In the second step the carbamate is formed by treatment with ammonia.^[20] Another method is the addition of alcohols to urethanes or the nucleophilic attack to in situ prepared isocyanic acid.^[21] However all these routes have serious difficulties like the use of the highly toxic gas phosgene, the low reactivity of $HNCO$ or the possibility of multiple addition.

An alternative one step synthesis is the reagent chlorosulfonyl isocyanate (CSI).^[22] CSI is prepared by the reaction of sulfur trioxide and cyanogen chloride and was first reported by Graf in 1956. CSI, is commercially available and is one of the most reactive isocyanates.^[23] Its high reactive nature is due to polarization of the cumulated π -system by the electronegative chlorosulfonyl and isocyanate group. The reaction with alcohols is very fast and already proceeds at low temperatures, and without possible multi-addition which is prevented by the formation of a chlorosulfonylamide intermediate. This SO_2Cl group can easily be removed by aqueous work-up, leaving the pure primary carbamate. In summary, the advantages of CSI are monosubstitution, fast reaction times, simple isolation and nearly quantitative yields.^[23b]



Scheme I.5: Chemical structure of a primary nitrocarbamate (C).

The first article where *N*-nitrocarbamates (**C**) were mentioned, was of Thiele and Lachman in 1895 in Munich, who synthesized the nitrocarbamate of ethyl carbamate by nitration with ethyl nitrate.^[24] The related nitrocarbamates are more stable to acid hydrolysis due to resonance effects which lead to a reduction in the electrophilicity of the carbonyl group.^[25] The better stability allows also the synthesis of nitrocarbamates by nitration of carbamates using not only ethyl nitrate but nitric acid and nitrate salts in sulfuric acid. The nitration of the amine group also causes an increase of the acidity of the hydrogen atom of the $-\text{NHNO}_2$ group due to the electron withdrawing nitro group. Therefore salt formation of nitrocarbamates is also possible.^[25a, 26]

4 Objective Target

The objective of this thesis is the synthesis and investigation of new environmentally benign molecules, which contain a high amount of oxygen and therefore qualify themselves as oxidizers. This objective supports the goal of reducing future perchlorate contamination in groundwater by lower the need for production and use of perchlorate salts as an oxidizer in solid rocket motor and further energetic applications. These compounds should meet the challenge to combine different specifications like excellent performance, and good physical and chemical properties, and should additionally fulfill the requirements for new advanced oxidizers.

The general concept for the achievement of the main objective is the implementation of carbamate and nitrocarbamate moieties in the chemistry of high energetic materials. The connection of carbamates and nitrocarbamates with various moieties accomplish a high oxygen content of the resulting compounds. Moreover, the discovery of suitable precursors and building blocks for the synthesis of these compounds is of interest, as well as the understanding of their chemistry. Another target is the investigation of the less known high oxygen containing building blocks 3,3,3-trinitropropyl and 1,1,1-trinitropropyl moieties, with the aim to increase the stability compared to the 2,2,2-trinitroethyl group. In a side project the insensitive explosive and highly stable molecule FOX-7 is examined for the use as starting material for high oxygen-containing molecules.

Beside the development of strategies for syntheses also the chemical characterization of the resulting compounds is performed. This includes the molecular structure and investigations of interactions in and between the molecules, which are often present in nitrocarbamates, ureas and polynitro compounds and have a general influence on the chemical and physical properties. In addition to the chemical characterization, the physical properties of the materials are of interest, including the thermal stability and sensitivities to external stimuli. Finally, their energetic performance is examined to evaluate their suitability for energetic material applications, particularly as oxidizers for solid rocket composite propellants and explosives.

5 References

- [1] T. M. Klapötke, *Chemistry of High-Energy Materials*, 3rd ed., deGruyter, Berlin, **2015**.
- [2] J. P. Agrawal, *High Energy Materials*, Wiley-VCH, Weinheim, **2010**.
- [3] J. P. Agrawal, R. D. Hodgson, *Organic Chemistry of Explosives*, Wiley-VCH, Weinheim, **2007**.
- [4] T. Altenburg, T. M. Klapötke, A. Penger, J. Stierstorfer, *Z. Anorg. Allg. Chem.* **2010**, *636*, 463–471.
- [5] a) D. Majda, A. Korobov, U. Filek, B. Sulikowski, P. Midgley, D. Vowles, J. Klinowski, *Chem. Phys. Lett.* **2008**, *454*, 233–236; b) R. J. Brechner, G. D. Parkhurst, W. O. Humble, M. B. Brown, W. H. Herman, *J. Occup. Environ. Med.* **2000**, *42*, 777–782.
- [6] a) W. H. Beck, *Combust. Flame* **1987**, *70*, 171–190; b) S. Chaturvedi, P. N. Dave, *Arabian J. Chem.*, doi:10.1016/j.arabjc.2014.1012.1033.
- [7] A. M. Mebel, M. C. Lin, K. Morokuma, C. F. Melius, *J. Phys. Chem.* **1995**, *99*, 6842–6848.
- [8] a) C. Hogue, *Chem. Eng. News* **2011**, *89*, 6; b) P. Waldman, in *The Wall Street Journal, Perchlorate Runoff Flows To Water Supply of Millions*, New York, **2002**.
- [9] B. Gu, J. D. Coates, *Perchlorate: Environmental Occurrence, Interactions and Treatment*, Springer Science, New York, **2006**.
- [10] EPA - United States Environmental Protection Agency, EPA-HQ-OW-2009-0297, Drinking Water Contaminants – Standards and Regulations, **2009**.
- [11] C. W. Trumpolt, M. Crain, G. D. Cullison, S. J. P. Flanagan, L. Siegel, S. Lathrop, *Remediation* **2005**, *16*, 65–89.
- [12] a) E. D. McLanahan, M. E. Andersen, J. L. Campbell, J. W. Fisher, *Environ. Health Perspect.* **2009**, *117*, 731–738; b) J. W. Fisher, J. Campbell, S. Muralidhara, J. V. Bruckner, D. Ferguson, M. Mumtaz, B. Harmon, J. M. Hedge, K. M. Crofton, H. Kim, T. L. Almekinder, *Toxicol. Sci.* **2006**, *90*, 87–95; c) E. D. McLanahan, J. L. Campbell, D. C. Ferguson, B. Harmon, J. M. Hedge, K. M. Crofton, D. R. Mattie, L. Braverman, D. A. Keys, M. Mumtaz, J. W. Fisher, *Toxicol. Sci.* **2007**, *97*, 308–317.
- [13] J. Dumont, The Effects of Ammonium Perchlorate on Reproduction and Development of Amphibians, <http://www.dtic.mil/cgi-bin/GetTRDoc?Location=U2&doc=GetTRDoc.pdf&AD=ADA495519> (12/2015), **2008**.
- [14] J. Cui, J. Han, J. Wang, R. Huang, *J. Chem. Eng. Data* **2010**, *55*, 3229–3234.
- [15] a) M. Göbel, T. M. Klapötke, *Z. Anorg. Allg. Chem.* **2007**, *633*, 1006–1017; b) H. F. R. Schoeyer, A. J. Schnorhk, P. A. O. G. Korting, P. J. van Lit, J. M. Mul, G. M. H. J. L. Gadiot, J. J. Meulenbrugge, *J. Propul. Power* **1995**, *11*, 856–869.
- [16] K. Menke, J. Bohnlein-Mauss, H. Schmid, K. M. Bucerius, W. Engel **1997**, US 5596168A.
- [17] a) M. L. Birsa, S. Braverman, Y. Charalambides, M. Cherkinsky, C. Diaper, *Science of Synthesis: Houben-Weyl Methods of Molecular Transformations Vol. 18: Four Carbon-Heteroatom Bonds*, Thieme, Stuttgart, **2014**; b) P. Kočovský, *Tetrahedron Lett.* **1986**, *27*, 5521–5524.

- [18] R. L. Metcalf, *Insect Control*, Wiley-VCH, New York, **2000**.
- [19] a) N. Hen, M. Bialer, B. Yagen, *J. Med. Chem.* **2012**, *55*, 2835–2845; b) D. Chaturvedi, *Tetrahedron* **2012**, *68*, 15–45.
- [20] a) L. Cotarca, H. Eckert, *Phosgenations — A Handbook*, Wiley-VCH, Weinheim, **2005**; b) Q. J. Axthammer, T. M. Klapötke, B. Krumm, R. Moll, S. F. Rest, *Z. Anorg. Allg. Chem.* **2014**, *640*, 76–83.
- [21] a) W. M. Kraft, *J. Am. Chem. Soc.* **1948**, *70*, 3569–3571; b) B. Loev, M. F. Kormendy, *J. Org. Chem.* **1963**, *28*, 3421–3426.
- [22] J. K. Rasmussen, A. Hassner, *Chem. Rev. (Washington, DC, U. S.)* **1976**, *76*, 389–408.
- [23] a) R. Graf, *Chem. Ber.* **1956**, *89*, 1071–1079; b) D. N. Dhar, P. Dhar, *The Chemistry of Chlorosulfonyl Isocyanate*, World Scientific, Singapore, **2002**.
- [24] J. Thiele, A. Lachman, *Justus Liebigs Ann. Chem.* **1895**, *288*, 267–311.
- [25] a) G. Gattow, W. K. Knoth, *Z. Anorg. Allg. Chem.* **1983**, *499*, 194–204; b) H. M. Curry, J. P. Mason, *J. Am. Chem. Soc.* **1951**, *73*, 5449–5450.
- [26] a) D. S. Bohle, Z. Chua, *Inorg. Chem.* **2014**, *53*, 11160–11172; b) D. S. Bohle, Z. Chua, *Organometallics* **2015**, *34*, 1074–1084.

II Summary

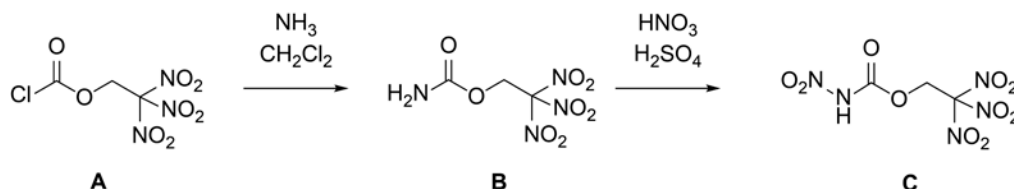
In the course of this thesis, various new energetic materials mainly based on carbamates and nitrocarbamates were synthesized and comprehensively investigated. Most of the compounds have a high oxygen content aiming to a positive oxygen balance. Therefore, these materials belong to the general class of high energy dense oxidizers (HEDO) and may be used in solid rocket composite propellants.

The main part of this thesis is section *III RESULTS AND DISCUSSION* which contains nine chapters, whereas each is an enclosed research project including its own abstract, introduction, results and discussion, experimental section and conclusion. Most chapters deal with the development of the nitrocarbamate implementation in the chemistry of high energetic materials.

In the first two chapters the concept of connecting molecules containing polynitro functionalities by the carbamate and nitrocarbamate moiety was investigated. Especially in Chapter 2 the use of the reagent chlorosulfonyl isocyanate (CSI) was introduced for a sophisticated preparation of carbamates. In Chapter 3 the nitrate ester groups of the well known and widely used explosive PETN (Pentaerythritol tetranitrate) were substituted with the nitrocarbamate unit. The tetravalent pentaerythritol tetranitrocarbamate (PETNC) reaches excellent physical properties (e.g. low sensitivities, good thermal stability). Furthermore, the stability of nitrocarbamates against alkaline conditions was demonstrated in principle by the preparation of the tetraammonium salt of PETNC. Due to the promising results this concept was further transformed to small molecules like glycerine (Chapter 4) and to polyvalent sugar alcohols (Chapter 5). In Chapter 6 the quite rare moiety 1,1,1-trinitropropan-2-yl was studied, including those of the 1,1,1-trinitropropan-2-yl nitrocarbamate. The Michael reaction of nitroform ($\text{HC}(\text{NO}_2)_3$) was introduced in Chapter 7 for the formation of precursor as well as the preparation of compounds owing a positive oxygen balance and being excellent potential high energetic dense oxidizers. In Chapter 8 the properties of the 3,3,3-trinitropropyl group was studied in combinations with further functionalities. In the last chapter the concept of adding a carbamoyl group to improve the properties of a given molecule was transferred to amines, in particular to the relatively new explosive 1,1-diamino-2,2-dinitroethene (FOX-7).

1 The Nitrocarbamate of Trinitroethanol

In the first chapter the carbamate (**B**) and nitrocarbamate (**C**) of the energetic alcohol 2,2,2-trinitroethanol were synthesized and fully characterized (Scheme S.1). As starting material for the synthesis of the carbamate the 2,2,2-trinitroethyl chloroformate (**A**) was prepared by a challenging synthesis method via chloroformylation of 2,2,2-trinitroethanol and phosgene.



Scheme S.1: Synthesis of 2,2,2-trinitroethyl carbamate (**B**) and 2,2,2-trinitroethyl nitrocarbamate (**C**).

The nitrocarbamate **C** shows a high positive oxygen balance with $\Omega_{CO} = +32.7\%$ which is quite close to ammonium perchlorate ($\Omega_{CO} = 34.0\%$). Along with the oxygen balance, the moderate sensitivities and high performance properties ($I_{sp} = 261$ s) this compound is a promising candidate for future use as high energy dense oxidizer. Moreover, the crystal structure of **C**, the first primary nitrocarbamate, was investigated (Figure S.1).

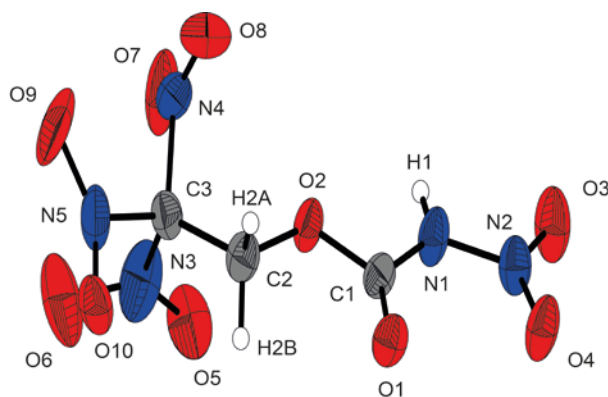
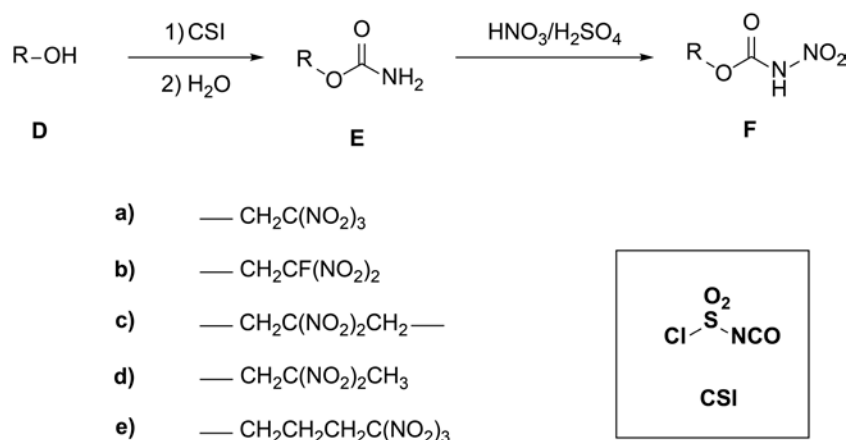


Figure S.1: X-ray molecular structure of 2,2,2-trinitroethyl nitrocarbamate (**C**).

2 Carbamates and Nitrocarbamates from Polynitro Alcohols

In Chapter 2 a more advanced synthesis strategy for the preparation of energetic carbamates (**E**) and nitrocarbamates (**F**) starting from the readily available polynitro alcohols (**D**) was introduced. The efficient synthesis of carbamates was performed with the reactive chlorosulfonyl isocyanate

(CSI) reagent (Scheme S.2). The carbamate-forming reaction with CSI has several advantages such as fast reaction times, simple manageable starting materials and high yields. For example the 2,2,2-trinitroethyl carbamate (**B**) of Chapter 1 was now synthesized in a one-step synthesis with a yield of 96% compared to a 71% yield in the two-step phosgene route. The nitration to form the nitrocarbamates (**F**) was realized in all cases in a mixture of anhydrous nitric and sulfuric acid (Scheme S.2).



Scheme S.2: Synthesis of carbamates (**E**) and nitrocarbamates (**F**) starting from nitro alcohols (**D**).

All new compounds were comprehensively characterized, including the X-ray molecular structure. The specific impulse I_{sp} of **F_a** in compositions with aluminum and binder are comparable with the standard compositions using the harmful ammonium perchlorate (AP) as oxidizer. Beside the high specific impulse I_{sp} only non toxic burning and combustion products like carbon monoxide, hydrogen and nitrogen are formed instead of corrosive HCl (Figure S.2).

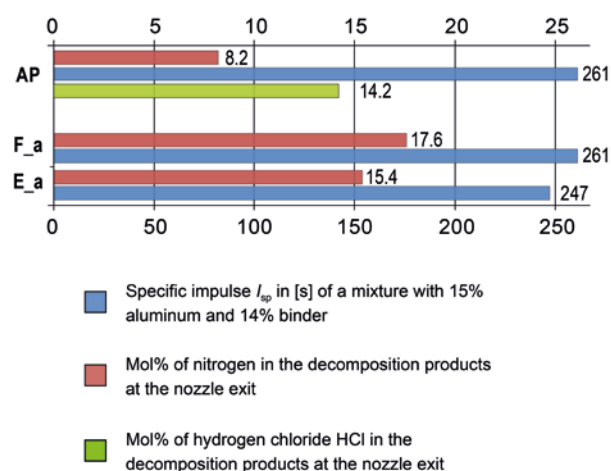


Figure S.2: Specific impulse I_{sp} and the nitrogen/hydrogen chloride content (Mol%) of the decomposition products of E_a, F_a and AP (calculated with EXPLO5 V6.02).

3 The Polyvalent Nitrocarbamate of Pentaerythritol

In Chapter 3 the four nitrate ester groups of the widely used explosive PETN (Pentaerythritol tetranitrate) were substituted with four nitrocarbamate units.

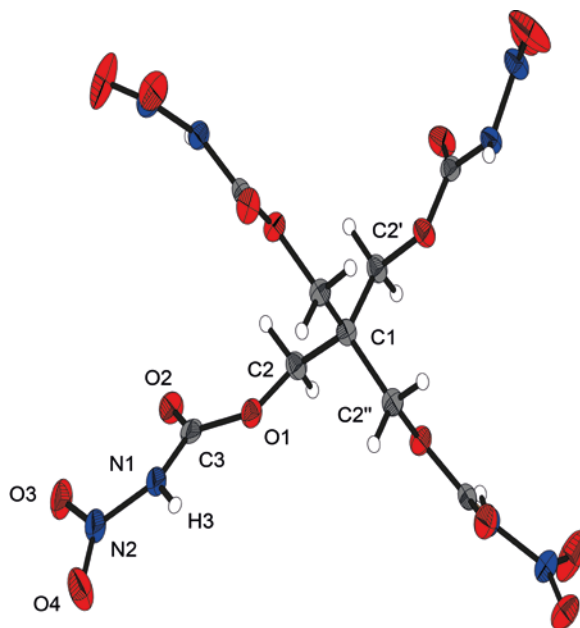


Figure S.3: X-ray molecular structure of pentaerythritol tetranitrocarbamate (**G**).

The pentaerythritol tetranitrocarbamate (**G**) reaches excellent physical properties, such as a higher decomposition point and a much lower impact sensitivity (8 J) than pentaerythritol tetranitrate (3 J). Furthermore, the stability against alkaline conditions of nitrocarbamates was demonstrated by the formation of the tetraammonium salt of **G**.

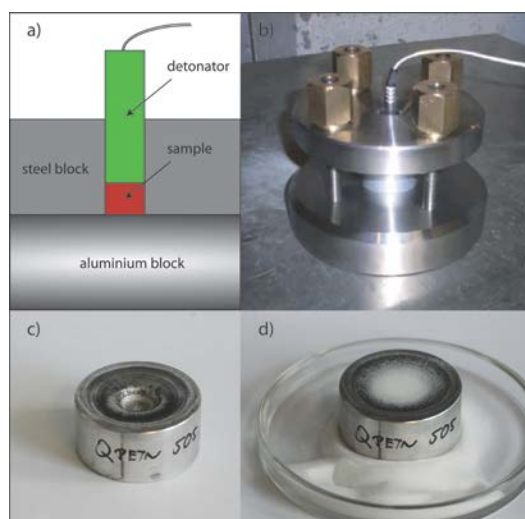
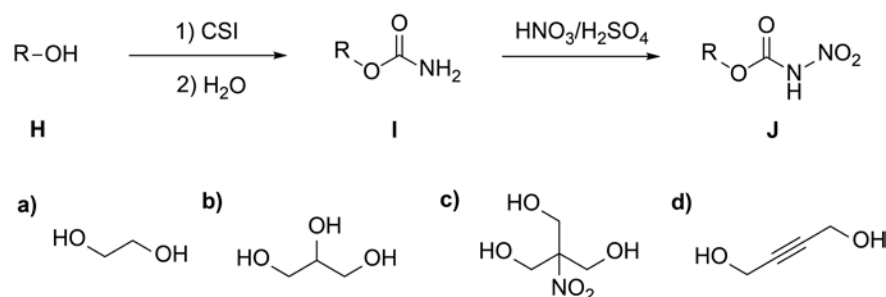


Figure S.4: Small scale reactivity test (SSRT) of pentaerythritol tetranitrocarbamate (**G**).

In order to assess the detonation performance of **G** a small scale reactivity test (SSRT) was performed (Figure S.4). For this test, a defined volume of the explosive is pressed into a perforated steel block, which is topped with a commercially available detonator. After ignition the volume of the dent in the aluminum block was measured. **G** shows only a slightly lower performance than PETN. From measuring the volume of the dent in the aluminum block, it can be concluded that the ignition of **G** was successful and **G** shows good energetic properties with a slightly lower performance than PETN.

4 The Nitrocarbamate Relatives of Nitroglycerine and Co.

Due to the promising results of the nitrocarbamate concept, it was further transformed to the small multivalent alcohols **H** glycol, glycerine, tris(hydroxymethyl) nitromethane and but-2-yne-1,4-diol (Scheme S.3).



Scheme S.3: Syntheses of carbamates (I) and nitrocarbamates (J) from simple alcohols (H).

All carbamates **I** and nitrocarbamates **J** were completely characterized, including the investigation and calculation of the energetic properties. In addition, the molecular structures were discussed by single X-ray diffraction. The nitrocarbamates of glycol exhibit improved detonation performances, in comparison to the corresponding nitrate ester ethylene glycol dinitrate (EGDN). The sensitivities towards impact (IS) of the herein presented nitrocarbamates **J** were classified as sensitive (8–15 J). Nevertheless, compared to the nitrate esters EGDN and nitroglycerine they can be handled without the risk of spontaneous detonation. The simple synthesis route, the good physical properties of the nitrocarbamates **J**, especially those of glycol and but-2-yne-1,4-diol, suggest potential application as energetic material.

5 Nitrocarbamates of Polyvalent Sugar Alcohols

In Chapter 5 the synthesis of various nitrocarbamates of polyvalent sugar alcohols were accomplished. These sugar alcohols are easily accessible from renewable biomass and are used mainly in the food and cosmetic industry. The concept of using renewable material for the preparation of explosives is well known.

The *meso*-erythritol tetranitrocarbamate (**K**) shows the best energetic properties, with a higher decomposition point and a much lower sensitivity than the related nitrate ester *meso*-erythritol tetranitrate (Figure S.5). Particularly noteworthy is the difference towards impact stimuli. Compared to the nitrate ester which has an impact sensitivity of 2 J and therefore is classified as very sensitive to impact, the nitrocarbamate **K** is less sensitive (6 J).

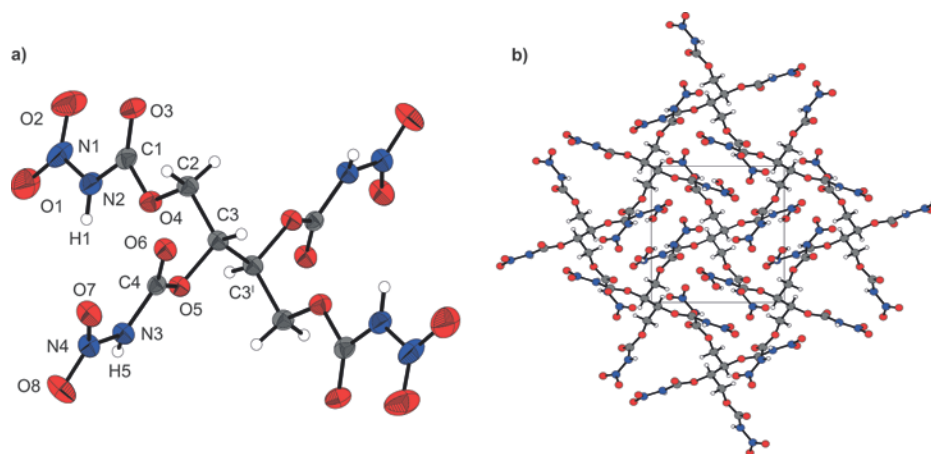
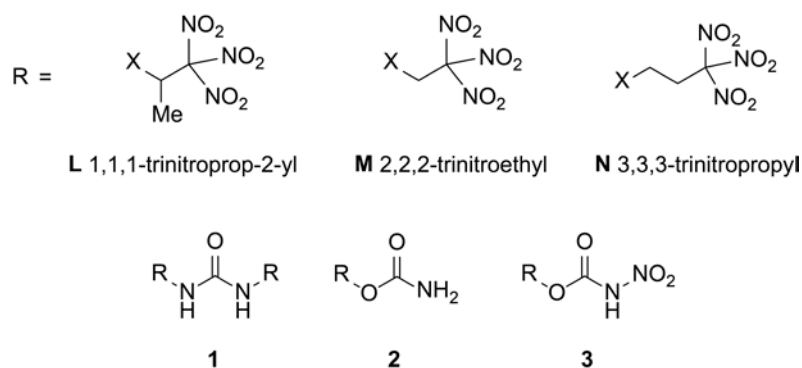


Figure S.5: X-ray structure of *meso*-erythritol tetranitrocarbamate (**K**) and packing along the *a* axis.

6 The 1,1,1-Trinitroprop-2-yl Moiety

Potential high energetic dense oxidizers with the 1,1,1-trinitropropan-2-yl moiety are described in this study. The 1,3-bis(1,1,1-trinitropropan-2-yl) urea (**L1**), was synthesized by a one-pot reaction from urea, acetaldehyde and nitroform ($\text{HC}(\text{NO}_2)_3$). The 1,1,1-trinitropropan-2-ol was also reacted with chlorosulfonyl isocyanate (CSI) resulting in 1,1,1-trinitroprop-2-yl carbamate (**L2**) which was further nitrated to the nitrocarbamate **L3** (Scheme S.4).



Scheme S.4: Overview of molecules containing the 1,1,1-trinitroprop-2-yl (**L**), the 2,2,2-trinitroethyl (**M**) and the 3,3,3-trinitropropyl (**N**) moieties.

Furthermore, the energetic properties, the sensitivities towards impact, friction and electrostatic discharge were tested. These values were similar to the corresponding 2,2,2-trinitroethyl (**M**) and 3,3,3-trinitropropyl (**N**) derivatives. **L1** exhibits the highest specific impulse I_{sp} of 267 s within a mixture of 15% aluminum of these compounds, which is even higher than the standard mixture composed of ammonium perchlorate and 15% aluminum.

7 Michael Addition of Nitroform

For the preparation of compounds owing a positive oxygen balance the addition of nitroform ($\text{HC}(\text{NO}_2)_3$) via a Michael reaction is a very useful and a straightforward synthesis step.

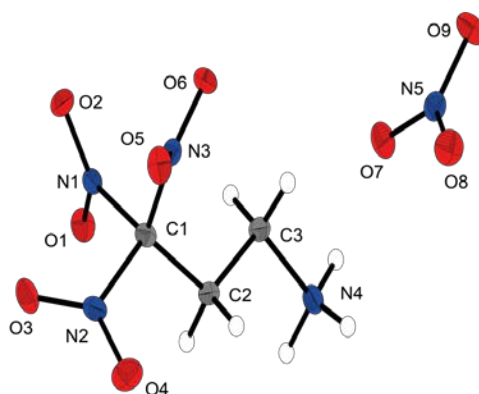


Figure S.6: X-ray molecular structure of 3,3,3-trinitropropan-1-amine nitrate (**O**).

The best compound in this chapter, with excellent detonation parameters, is the salt 3,3,3-trinitropropylamine nitrate (**O**) (Figure S.6), which has a very high detonation velocity (8838 m s^{-1}), significantly above those of TNT and PETN. Additionally, **O** seems to serve as a

good oxidizer candidate for composite rocket propellants with a specific impulse I_{sp} of 270 s within a mixture of 15% aluminum as fuel and 14% binder. However, the synthesis of materials containing the 3,3,3-trinitropropylamine group is of minimum five steps, albeit only common chemicals are needed.

8 The 3,3,3-Trinitropropyl Unit

In Chapter 8 the 3,3,3-trinitropropyl group was thoroughly studied. For this the 3,3,3-trinitropropyl group was introduced to the following functionalities: urea, oxamide, oxalate, carbamate, nitrocarbamate, nitrocarbamate, amine and nitramine.

The molecule with the highest oxygen (56%) and nitrogen content (28%) and a very high positive oxygen balance Ω_{CO} of +23.9% is the *N*-(2,2,2-trinitroethyl)-*N*-(3,3,3-trinitropropyl) nitramine (**P**) (Figure S.7). It is prepared by the Mannich condensation of 3,3,3-trinitropropylamine hydrochloride, formaldehyde and trinitromethane and subsequent nitration with nitric acid.

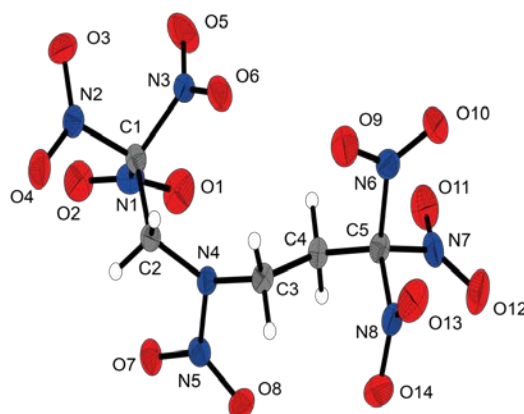


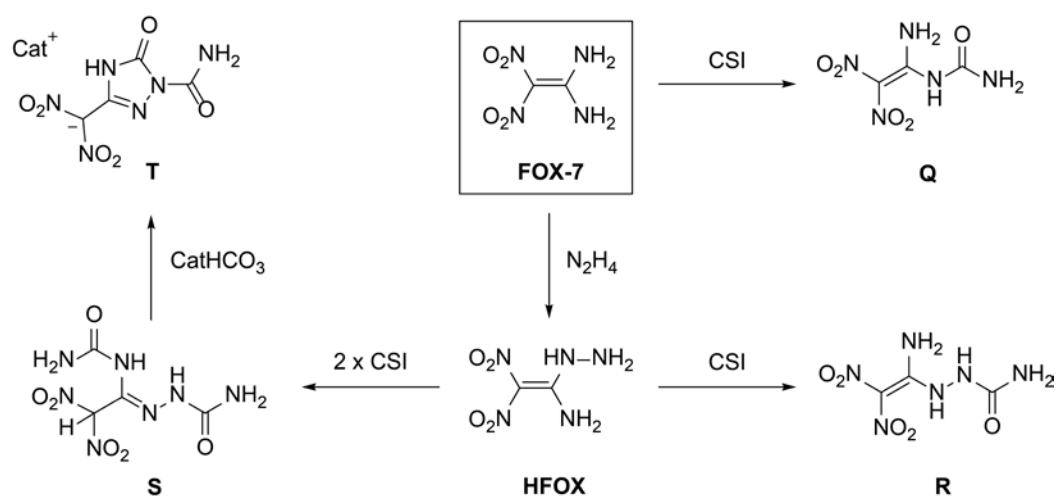
Figure S.7: X-ray molecular structure of *N*-(2,2,2-trinitroethyl)-*N*-(3,3,3-trinitropropyl) nitramine (**P**).

With respect to an application as high energy dense oxidizer in composite solid rocket propellants, several energetic performance data were computed. The best compound with excellent detonation parameters is the nitramine **P** (Figure S.7), with a detonation velocity of 9119 m s^{-1} and additionally a high detonation pressure. Both values the velocity and the detonation pressure are significantly above those of TNT, RDX and PETN. Apart from this, the nitramine **P** seems to serve as a good oxidizer candidate for composite rocket propellants. The specific impulse I_{sp} reaches 269 s within a mixture of 15% aluminum as fuel. However, the

synthesis of such 3,3,3-trinitropropyl containing materials is more elaborate compared to compounds containing the 2,2,2-trinitroethyl group.

9 New FOX-7 Derivatives

In the last Chapter the concept of adding a carbamoyl group to a molecule for improving the properties were transferred to amines, in particular to the explosive 1,1-diamino-2,2-dinitroethene (FOX-7). Several new energetic compounds based on the FOX-7 molecule were synthesized by reaction with chlorosulfonyl isocyanate (CSI) (Scheme S.5).



Scheme S.5: Synthetic overview of reaction of 1,1-diamino-2,2-dinitroethene (FOX-7) and chlorosulfonyl isocyanate (CSI).

Especially the neutral compounds **Q** and **R** show good energetic properties with detonation velocities V_{det} above 8500 m s^{-1} which are slightly lower than the one of FOX-7 (8852 m s^{-1}). This high performance is even more impressive considering the low sensitivity toward external mechanical stimuli.

Compound **Q** and **R** also show the same type of molecular packing as FOX-7. In both cases infinite two dimensional layers are formed (Figure S.10) with extensive intra- and intermolecular hydrogen bonds within the layers and weaker van der Waals interactions between the layers. The good physical-chemical properties of FOX-7, like the low sensitivity, are explained by this molecular packing structure with strong hydrogen bonds.

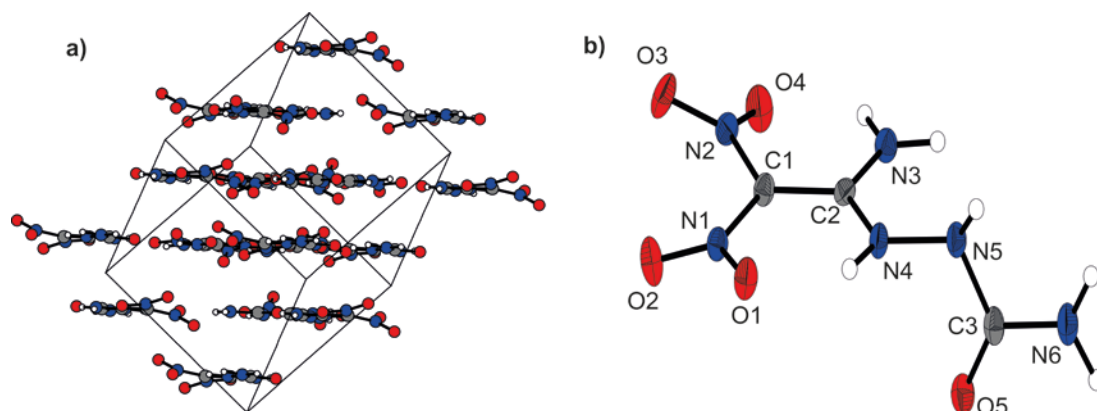


Figure S.8: X-ray structure of 1-(1-amino-2,2-dinitrovinyl)urea (**Q**) and packing along the *b* axis.

Furthermore, the possibility of salt formation was demonstrated by the synthesis of the corresponding potassium salts. Whereas the FOX-7 molecule reacts only once with the reagent CSI, the more reactive HFOX molecule was reacted twice at both ends the amino group and the hydrazino group to form the 2-(2,2-dinitro-1-ureidoethylidene)hydrazine-1-carboxamide (**S**). When **S** was stirred in a slight alkaline aqueous solution the heterocycle (1-carbamoyl-5-oxo-1,2,3-triazol-3-yl)dinitromethanide (**T**) was formed. This intermolecular cyclization reaction is very fast and takes place via a nucleophilic attack by the neighboring hydrazino group whereupon ammonia is eliminated. The ammonium salt of **T** shows a high thermal stability, with low sensitivity towards impact (20 J) and pleasing detonation properties (8359 m s^{-1}). These new synthesis route for the formation of 1,2,4-triazol-5-on heterocycles may be transferred to other starting materials.

III Results and Discussion

- 1 The Nitrocarbamate of Trinitroethanol
- 2 Carbamates and Nitrocarbamates from Polynitro Alcohols
- 3 The Polyvalent Nitrocarbamate of Pentaerythritol
- 4 The Nitrocarbamate Relatives of Nitroglycerine and Co.
- 5 Nitrocarbamates of Polyvalent Sugar Alcohols
- 6 The 1,1,1-Trinitroprop-2-yl Moiety
- 7 Michael Addition of Nitroform
- 8 The 3,3,3-Trinitropropyl Unit
- 9 New FOX-7 Derivatives

1 The Nitrocarbamate of Trinitroethanol

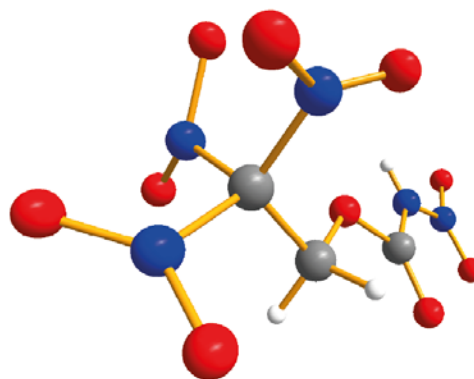
As published in *Z. Anorg. Allg. Chem.* **2014**, 640, 76–83.

THE ENERGETIC NITROCARBAMATE



DERIVED FROM PHOSGENE

PHOSGENE



1.1 Abstract

A new simple synthesis route for 2,2,2-trinitroethyl chloroformate (**1**), from easily available starting materials 2,2,2-trinitroethanol and phosgene is presented. 2,2,2-trinitroethyl carbamate (**2**) was obtained by the reaction of **1** with aqueous ammonia. The nitration of **2** with anhydrous nitric and sulfuric acid yields 2,2,2-trinitroethyl nitrocarbamate (**3**), which has potential as a perchlorate free high energetic dense oxidizer (HEDO) with a high oxygen balance of $\Omega(\text{CO}_2) = +14.9\%$. The thermal stability was studied using differential scanning calorimetry and the energies of formation were calculated on the CBS-4M level of theory, as well as several detonation parameters and propulsion properties were determined. In addition to full spectroscopic characterization, X-ray diffraction studies were performed for **2** and **3**.

1.2 Introduction

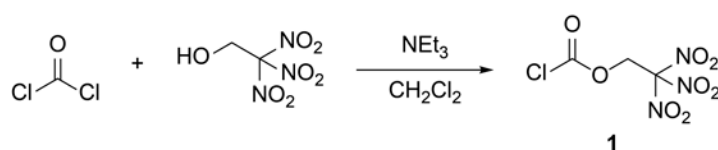
The 2,2,2-trinitroethyl moiety is a widely used building block in the chemistry of high energetic explosives, especially if performing as a high energy dense oxidizer (HEDO).^[1] Such compounds can be used as high performance, halogen-free propellants. These might overcome the environmental problems of hydrogen chloride formation during the use of ammonium perchlorate as oxidizer in rocket propellant formulations.^[2] Furthermore, the perchlorate anion has negative health effects, scientific research indicates that perchlorate contaminated water can disrupt the thyroid's ability to produce hormones needed for normal growth and development.^[3]

There are three synthesis routes for the chemical transfer of a 2,2,2-trinitroethyl functionality known. The most common way is the nucleophilic substitution of halogen atoms in reactive organic compounds like haloalkanes, acid halides and esters of the formic acid with the easy available alcohol 2,2,2-trinitroethanol.^[4] An alternative to this is the widespread Mannich reaction, which is a multi component condensation between a nitroalkane, an aldehyde and a primary or secondary amine. The mechanism of the reaction starts with the formation of an iminium ion from the amine and formaldehyde. This cationic intermediate can be attacked from the trinitromethanide anion to form the 2,2,2-trinitroethylamine unit.^[1b, 5] The third and less applied route, is the transfer of the 2,2,2-trinitroethyl moiety by a chloroformate.^[6]

1.3 Results and Discussion

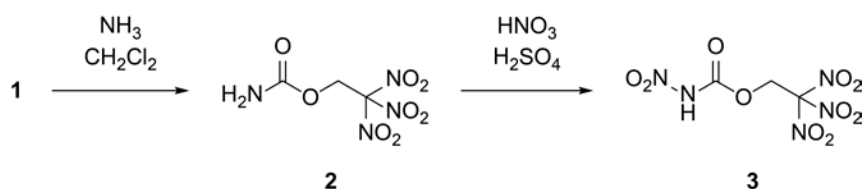
1.3.1 Synthesis

The standard synthesis of chloroformates is the reaction between alcohols and an excess of phosgene with a base as acid acceptor.^[7] Pure 2,2,2-trinitroethyl chloroformate (**1**) was first prepared in 1979 in a three step synthesis via *S*-ethyl chloroformate as starting material and claimed that a direct chloroformylation of β -nitro alcohols such as 2,2,2-trinitroethanol does not work properly.^[6] This was explained by the very fast reaction to the by-product bis(2,2,2-trinitroethyl) carbonate and a reverse Henry reaction with a decomposition of the alcohol to the corresponding aldehyde and nitroalkane introduced by the required base.^[4c, 6] Therefore, for the synthesis of **1** was used the phosgene analogue *S*-ethyl chlorothioformate with a subsequent replacement of the ethylthio group by chlorine with sulfur chloride.^[6]



Scheme 1-1: Synthesis of 2,2,2-trinitroethyl chloroformate (**1**).

In contrast to the literature prediction, the direct chloroformylation with phosgene and 2,2,2-trinitroethanol was successful (Scheme 1-1). The reaction works best with an excess of phosgene and the aid of one equivalent of non-nucleophilic bases, such as triethylamine. The product can easily be removed from the reaction mixture and was obtained as a colorless liquid in very good yields of around 86%. The described one-pot reaction procedure has several advantages such as a reduced consumption of chemicals and reduced reaction time.



Scheme 1-2: Synthesis of 2,2,2-trinitroethyl carbamate (**2**) and 2,2,2-trinitroethyl nitrocarbamate (**3**).

In the 1990ies it was briefly mentioned, that 2,2,2-trinitroethyl carbamate (**2**) could be synthesized by the reaction of 2,2,2-trinitroethanol and carbamoyl chloride.^[8] However, the

synthesis of **2** via the chloroformate **1** and aqueous ammonia in methylene chloride is the more preferred route of choice (Scheme 1-2). The nitration of the carbamate **2** with a mixture of sulfuric (95%) and nitric acid (100%) (1:1) leads to the formation of 2,2,2-trinitroethyl nitrocarbamate (**3**). Recrystallization from tetrachloromethane yielded almost quantitatively pure colorless product **3** as fine needles.

1.3.2 NMR Spectroscopy

All compounds were characterized by ^1H , ^{13}C and ^{14}N NMR spectroscopy (Table 1-1). In the ^1H NMR spectra of **1–3** the CH_2 group is observed at 5.68–5.51 ppm. The ^1H NMR spectrum of the carbamate **2** shows an interesting temperature dependent dynamic behavior of the NH_2 resonance of the amide group, which splits at 25 °C into two different signals. This is due to a restricted rotation along the C–NH_2 bond of the amide **2**. Temperature dependent ^1H NMR spectra were recorded in $[\text{D}_6]\text{DMSO}$ in the range of +25 to +60 °C (Figure 1-1). From these measurements, a coalescence temperature T_c of 42.5 °C and the corresponding chemical shift difference $\Delta\nu$ ($= 42.5$ °C) of 75.2 Hz, are determined. With these data, the free enthalpy of activation ΔG^\ddagger ($15.3 \text{ kcal mol}^{-1}$) is calculated by applying the Eyring equation.^[9] This activation barrier of rotation is within the range of other values obtained for amides.^[10] Furthermore, a diamagnetic shift of the amine resonance with increasing temperature is observed. This temperature dependence is the result of weakening the hydrogen bond and therefore lessening the electron withdrawing effect of the hydrogen bond acceptor on the proton. As a result the proton becomes more shielded and its resonance is shifted upfield.^[11]

Table 1-1: Multinuclear NMR resonances [ppm] of 1–3 in $[\text{D}_6]$ acetone.

	1	2	3
^1H		6.77 (s, NH)	10.70 (s, NH)
	5.51 (CH_2)	6.49 (s, NH)	5.53 (CH_2)
		5.68 (CH_2)	
^{13}C	149.5 (CO_2Cl)	154.5 (CO_2N)	145.2 (CO_2N)
	121.4 ($\text{C}(\text{NO}_2)_3$)	125.7 ($\text{C}(\text{NO}_2)_3$)	122.2 ($\text{C}(\text{NO}_2)_3$)
	63.3 (CH_2)	61.8 (CH_2)	62.1 (CH_2)
^{14}N	–36 (NO_2)	–33 (NO_2)	–36 (NO_2)
		–310 (NH_2)	–55 (NNO_2)
			–192 (NNO_2)

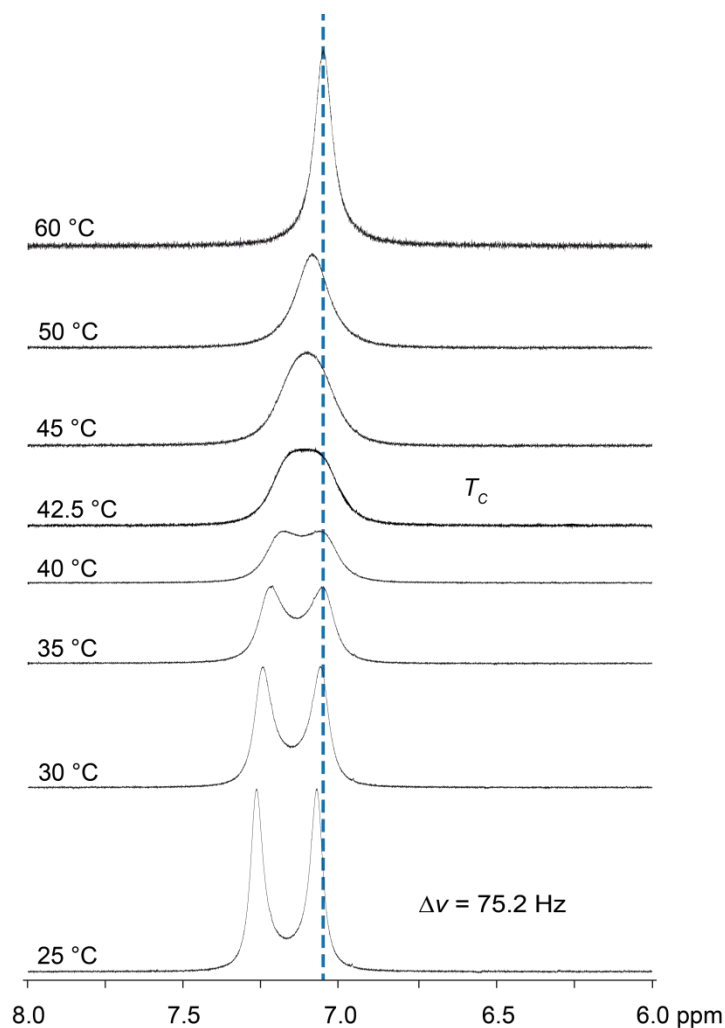


Figure 1-1: ^1H NMR resonance of the NH_2 group of **2** at variable temperatures in $[\text{D}_6]\text{DMSO}$.

The NH resonance of the nitrocarbamate **3** compared to the NH_2 of **2** is shifted downfield to 10.70 ppm. In the $^{13}\text{C}\{^1\text{H}\}$ NMR spectra the resonances of the carbon atoms of the methylene groups were observed at 63.3–61.8 ppm, those of the trinitromethyl groups broadened at 125.7–121.4 ppm and the carbonyl groups at 149.5 (**1**), 154.5 (**2**) and 145.2 ppm (**3**). The nitro resonances in the ^{14}N NMR of the trinitromethane moiety were found for **1–3** between –33 and –36 ppm and in addition, that of the nitrocarbamate of **3** was observed at –55 ppm. For compounds **2** and **3** a very broad resonance for the amide nitrogen atom was detected at –310 (**2**) and –192 ppm (**3**).

1.3.3 Single Crystal Structure Analysis

Single crystals of **2** and **3** were obtained from tetrachloromethane at ambient temperature. A full list of the crystallographic structure and refinement data are shown in Appendix A.1. Both compounds crystallize in the monoclinic space group $P2_1/c$ with four formula units per unit cell. The asymmetric unit with selected bond lengths and angles are shown in Figure 1-2 (**2**) and Figure 1-3 (**3**).

The molecular structure of the carbamate **2** shows a large part with nearly planar arrangement. This planar range comprised the carbamate, the C2 carbon of the methylene group and C3 of the trinitromethyl moiety. The conformation of the substituents at C2 and C3 is nearly staggered (N2-C3-C2-H3A $43.3(1)^\circ$, N3-C3-C2-H3B $42.6(1)^\circ$, N4-C3-C2-O2 $42.7(1)^\circ$). The C–N bond lengths of the trinitromethyl moiety are in the range of 1.52 \AA , which is significantly longer than a regular C–N bond (1.47 \AA).^[12] This is typical for molecules with the trinitromethyl moiety and is due to steric repulsion effects.^[1b, 4a] The three nitro groups arrange in a propeller like constitution, which optimize the non-bonded intramolecular attractions (partial charge distribution of nitrogen (δ^+) and oxygen (δ^-) atom in the nitro group) and electrostatic repulsion of two neighboring nitro groups.

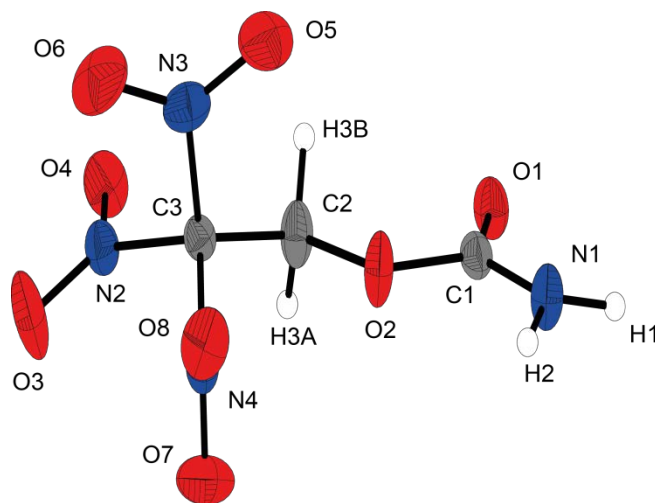


Figure 1-2: X-ray molecular structure of 2,2,2-trinitroethyl carbamate (2).

Atom distance (\AA) and angles (deg): O1–C1 1.210(2), O3–N2 1.212(2), O7–N4 1.206(2), O2–C2 1.425(2), O2–C1 1.362(2), O6–N3 1.207(2), O8–N4 1.211(2), N2–O4 1.206(2), N2–C3 1.519(2), C2–C3 1.509(2), N4–C3 1.521(2), N3–O5 1.212(2), N3–C3 1.528(2), N1–C1 1.333(2), N1–H1 0.91(2), N1–H2 0.87(2), C1–O2–C2 114.8(1), C2–C3–N2 111.8(1), N2–C3–N4 108.0(1), C2–C3–N3 113.8(1), N2–C3–N3 106.4(1), C1–N1–H1 118.1(11), C1–N1–H2 119.2(12), H1–N1–H2 119.1(16), O1–C1–N1 127.8(2), O1–C1–O2 122.1(1), N1–C1–O2 110.1(1), N1–C1–O2–C2 176.8(1), O1–C1–O2–C2 $-4.7(2)$, C1–O2–C2–C3 $-172.4(1)$, H1–N1–C1–O1 $-170.1(14)$, H2–N1–C1–O1 169.5(14).

The N \cdots O attractions (N2 \cdots O6, N3 \cdots O8, N4 \cdots O3) are found in **2** with distances in the range of 2.55–2.67 Å, which are much shorter than the sum of the van der Waals radii for nitrogen and oxygen (3.07 Å).^[13] In addition, another strong attractive intramolecular N \cdots O interaction with 2.60 Å is observed between the nitrogen atom N4 of the trinitromethyl functionality and the oxygen O2. The carbamate group with a short C–NH₂ bond (1.333 Å) and shortened N–H bonds (0.87 and 0.91 Å) shows typical values for carbamates.^[14] The molecules of **2** are cross-linked three dimensional via hydrogen bonds. The intermolecular hydrogen-bond lengths and angles are shown in the Appendix A.1. In the structure can be found three classical NH \cdots O hydrogen bonds with the carbonyl and the nitro group as acceptors. The two hydrogen interactions with the carbonyl (O1), can be classified as strong, while the interaction with the nitro group (O5) is moderate on the basis of the distance and angle of the hydrogen bond.^[15] Also an unusual hydrogen bond with carbon as donor (CH \cdots O) can be observed in **2**, between the methylene (C2–H3A) and one nitro group (O7), which is only weak.^[16]

The data collection of **3** had to be performed at higher temperature, because the compound showed a phase transition at about –62 °C. This phase transition leads to microfracture of the single crystal, which made a measurement impossible. Thus, the data collection was carried out at –30 °C, causing much greater thermal vibrations of the atoms, especially of the trinitromethyl group. In the literature only one single crystal X-ray structure of a nitrocarbamate, alkylated at the carbamate nitrogen, is known.^[17]

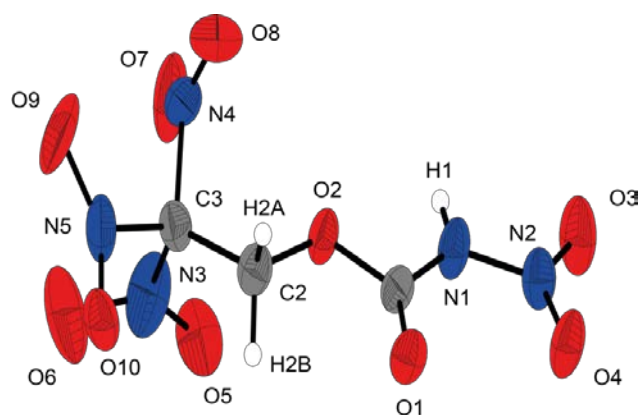


Figure 1-3: X-ray molecular structure of 2,2,2-trinitroethyl nitrocarbamate (3).

Atomic distances (Å) and angles (deg): O1–C1 1.182(5), O2–C1 1.333(4), O2–C2 1.437(6), O3–N2 1.201(6), O4–N2 1.213(5), O5–N3 1.15(1), O6–N3 1.31(1), O7–N4 1.40(1), O8–N4 1.16(1), O9–N5 1.267(7), O10–N5 1.238(8), N1–N2 1.373(5), N1–C1 1.358(6), N1–H1 0.82(5), N3–C3 1.49(1), N4–C3 1.473(8), N5–C3 1.529(8), C2–C3 1.472(6), O3–N2–N1 126.4(4), N1–N2–O4 114.7(4), O4–N2–O3 118.9(4), N2–N1–H1 112(3), H1–N1–C1 123(3), C1–N1–N2 124.6(4), O4–N2–N1–C1 –2.0(6), O4–N2–N1–H1 –177(3), O3–N2–N1–C1 –177.9(4), N2–N1–C1–O2 177.8(4), N2–N1–C1–O1 –1.4(7), N1–C1–O2–C2 –179.8(3), C1–O2–C2–C3 –166.7(3).

The nitrocarbamate moiety of compound **3** shows a perfect planarity as shown by the sum of the angles around the C1 and the two nitrogen atoms N1/N2, where the angle sum is 360.0° each. The N1–N2 bond of the nitramine moiety is 1.373 Å, which indicates a substantial of a double bond character, achieved by delocalization of the nitrogen lone pair. This is also evidenced by a shortened N–H bond (0.82 Å) compared with the carbamate structure of **2**. The carbonyl group, *cis* orientated to the nitro group, shows also a slight shortening (1.182 Å). The trinitroethyl moiety has the same propeller like configuration compared to **2**, which is stabilized with short strong attractive interactions of N···O atoms (N3···O7, N4···O9, N4···O2, N5···O6). The nitrocarbamate **3** shows two classical hydrogen bonds, which links the hydrogen attached to N1 to two oxygen atoms (O1^{*i*}, O4^{*j*}), of symmetry related nitrocarbamate functionality. Here, the interaction between the carbonyl (O1) and the NH group is significantly the strongest. Also an improper hydrogen bond with carbon as donor (CH···O) can be observed, between the methylene (C2–H2A/B) and neighboring nitro groups.^[16] This extensive hydrogen-bonding may help to explain the good thermal stability.^[17]

1.3.4 Vibrational Spectroscopy

The vibrational analysis of **1–3** showed the characteristic asymmetric NO₂ stretching vibrations in the range of 1615 to 1588 cm⁻¹ and the symmetric stretching vibrations at 1304 to 1271 cm⁻¹ (Table 1-2). All vibrations of the nitro groups for **1–3** are in a close range, explained by the similarity of the functional groups. The carbonyl stretching vibration was observed in the typical range between 1785 and 1721 cm⁻¹. The N–H stretching vibrations for **2** and **3** were found in the range of 3447–3062 cm⁻¹.

Table 1-2: Characteristic IR and RAMAN vibrations of **1–3** in [cm⁻¹]

	1		2		3	
	<i>RAMAN</i>	<i>IR</i>	<i>RAMAN</i>	<i>IR</i>	<i>RAMAN</i>	<i>IR</i>
νNH			3300 (4)	3447 w 3352 m 3302 w	3170 (9)	3168 w 3062 w
νCO	1785 (14)	1777 m	1721 (17)	1729 m	1768 (49)	1772 m
ν_{as} NO₂	1615 (26)	1598 s	1622 (31)	1590 s	1609 (46)	1588 s
ν_s NO₂	1301 (32)	1293 m	1304 (31)	1300 m	1303 (55)	1271 w

RAMAN intensities in brackets; IR intensities: s = strong, m = medium, w = weak.

1.3.5 Thermal Stabilities and Energetic Properties

2,2,2-trinitroethyl carbamate (**2**) melts at 91 °C (onset) and is thermally stable up to 169 °C (onset). It burns residue-free with a smokeless flame due to a balanced amount of oxygen and shows no sensitivity towards impact, but it is sensitive to friction.

By a low temperature DSC measurement of 2,2,2-trinitroethyl nitrocarbamate (**3**) an endothermic solid phase transformation can be observed at -62 °C (onset). Upon further heating, the compound showed a melting point at 109 °C (onset) and decomposition starts at 153 °C (onset). The sensitivities of **3** are in the range of RDX, and therefore it is sensitive to friction, impact and electrostatic discharge. For the calculation of the performance parameters using the EXPLO5 V6.02^[18] program, the cell parameters of **2** and **3** were determined at 25 °C in order to obtain the density of the substances at standard conditions (see Appendix A.1). The performance data of **2** and **3** are summarized in Table 1-4.

Table 1-3: Physical and chemical properties of 2 and 3.

	2	3
formula	C ₃ H ₄ N ₄ O ₈	C ₃ H ₃ N ₅ O ₁₀
FW /g mol ⁻¹	224.09	269.08
T _m /°C (onset) ^{a)}	91	109
T _{dec} /°C (onset) ^{b)}	169	153
N /% ^{c)}	25.00	26.03
N + O /% ^{d)}	82.12	85.49
Ω _{CO} /% ^{e)}	+21.42	+32.70
Ω _{CO₂} /% ^{f)}	+0.00	+14.87
ρ /g cm ⁻³ ^{g)}	1.839 (173 K)	1.725 (243 K)
Δ _f H° /kJ mol ⁻¹ ^{h)}	-459	-366
Δ _f U° /kJ kg ⁻¹ ⁱ⁾	-1960	-1278

a) Melting (T_m) and b) decomposition (T_d) point from DSC measurement carried out at a heating rate of 5 °C min⁻¹. c) Nitrogen content. d) Combined nitrogen and oxygen content. e) Oxygen balance assuming the formation of CO. f) Oxygen balance assuming the formation of CO₂. g) Room temperature density calculated from X-ray measurement. h) Energy of formation and i) Heat of formation calculated with CBS-4M method.

The determining parameter for high energy dense oxidizers (HEDO) is the specific impulse I_{sp} . It is used to evaluate the performance of solid rocket propellants and the used high energy dense oxidizers. An expression for I_{sp} is given in Equation 1, where γ is the ratio of specific heats for the combustion gases, R the ideal gas constant, T_c the burning temperature in the combustion chamber and M the molecular weight of the gaseous combustion products at the nozzle.^[1a] I_{sp} is therefore dependent on the burning temperature proportional and the molecular weight of the combustion products reciprocal. The heat of combustion can be increased by adding a high performing fuel, which has an increased heat of combustion ΔH_c .

$$I_s^* = \frac{1}{g} \sqrt{\frac{2 \gamma R T_c}{(\gamma - 1)M}} \quad \gamma = \frac{C_p}{C_v} \quad \text{Eq. 1}$$

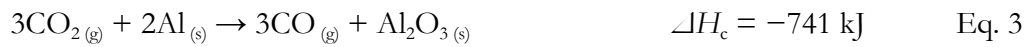


Table 1-4: Predicted detonation, combustion parameters (using EXPLO5 V6.02) and sensitivity data for 2 and 3.

	2	3
Q_v /kJ kg ⁻¹ a)	-5286	-4456
T_{ex} /K b)	3780	3618
V_0 /L kg ⁻¹ c)	761	750
P_{CJ} /kbar d)	302	232
V_{det} /m s ⁻¹ e)	8530	7704
IS /J f)	>40	10
FS /N g)	64	96
ESD /J h)	0.15	0.10
grain size / μm i)	<500	500–1000

a) Heat of detonation b) Temperature of the combustion gases. c) Volume of the explosion gases. d) Detonation pressure. e) Detonation velocity. f) Impact and g) Friction sensitivities. h) Sensitivity towards electrostatic discharge. i) Grain size of the samples used for sensitivity tests.



Figure 1-4: Burning test of a compressed mixture of 2,2,2-trinitroethyl nitrocarbamate (**3**) (85%) and aluminum (15%).

Aluminum has a very high heat of combustion ΔH_c and the combustion products (Al_2O_3) are not harmful to the environment. The oxidation of aluminum with oxygen is highly exothermic and produces a lot of heat (Eq. 2^[19]), which increases T_c . In the case of an oxygen deficit, the aluminum reacts further with the gaseous products water and carbon dioxide, to form hydrogen and carbon monoxide. Also, these two reactions in an oxygen-deficient composition produce a great amount of heat (Eq. 3 and Eq. 4^[19]) and no change in the volume of produced gas.

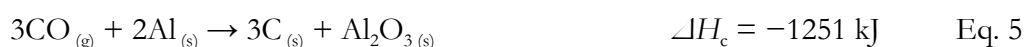


Table 1-5: Predicted specific impulse I_{sp} of mixtures with aluminum (using EXPLO5 V6.02) and sensitivity data for **2** and **3**.

	2	3	AP
I_{sp} / s^a	246	232	157
I_{sp} / s (30% Al) ^b	251	251	247
I_{sp} / s (25% Al) ^b	255	252	247
I_{sp} / s (20% Al) ^b	255	256	244
I_{sp} / s (15% Al) ^b	254	251	235
I_{sp} / s (10% Al) ^b	253	248	224
I_{sp} / s (5% Al) ^b	250	244	198
I_{sp} / s (15% Al, 14% binder) ^c	247	261	261
I_{sp} / s (10% Al, 14% binder) ^c	239	256	257
I_{sp} / s (5% Al, 14% binder) ^c	228	252	250

a) Specific impulse. b) Specific impulse for mixtures with the compound **2**, **3** and ammonium perchlorate (AP) as oxidizer with different values of aluminum. c) Specific impulse for mixtures with different values of aluminum and binder (6% polybutadiene acrylic acid, 6% polybutadiene acrylonitrile and 2% bisphenol A ether) at 70.0 kbar chamber pressure, equilibrium expansion and isobaric combustion condition (1 bar).

However, there is a limit to the amount of aluminum that can be added, because aluminum can also react with carbon monoxide to form carbon and alumina. This reaction also causes an increase of heat but the gas volume decreases radically from 3 to 0 moles for this reaction (Eq. 5^[19]). An increase of the value for I_{sp} by 20 s leads empirically to a doubling of the usual payload.^[1a] Therefore, the development of new energetic oxidizers based on CHNO compounds decomposing into small gasses molecules is a promising way to increase the specific impulse of solid rocket boosters. The specific impulse I_{sp} of **2** in a mixture of 20% of aluminum as fuel is 255 s. The specific impulse of **3** achieved with an admixture of 15% aluminum in the binder system (14%) 261 s and is therefore in the range of the standard mixture of ammonium perchlorate (Table 1-5).

1.4 Conclusion

The facile synthesis route of choice for 2,2,2-trinitroethyl chloroformate (**1**) is a direct chloroformulation of 2,2,2-trinitroethanol with phosgene. This route has compared to the known route several advantages. The reaction with aqueous ammonia gives 2,2,2-trinitroethyl carbamate (**2**) and nitration furnishes 2,2,2-trinitroethyl nitrocarbamate (**3**). By a low temperature DSC measurement an endothermic solid phase transformation of **3** was observed at $-62\text{ }^{\circ}\text{C}$. On further heating melting occurs at $109\text{ }^{\circ}\text{C}$ and decomposing at $153\text{ }^{\circ}\text{C}$. The nitrocarbamate **3** has a very high positive oxygen balance $\Omega(\text{CO}_2)$ of $+14.9\%$. Thus, the molecule consists of 59.5% of oxygen and 26.0% of nitrogen. These examples demonstrate that the 2,2,2-trinitroethylformate group is a very promising energetic moiety, which combines very high oxygen content and relative high stability. The specific impulse I_{sp} of compositions with **3** is comparable with compositions using ammonium perchlorate as oxidizer. Advantageously, the burning of **3** with aluminum produces no toxic substances such as hydrogen chloride.

1.5 Experimental Section

1.5.1 General Procedures

Raman spectra were recorded with a Bruker MultiRAM FT-Raman instrument fitted with a liquid nitrogen cooled germanium detector and a Nd:YAG laser ($\lambda = 1057\text{ nm}$, 500 mW). Infrared spectra were measured with a Perkin–Elmer Spectrum BX-FTIR spectrometer equipped with a

Smiths DuraSAMPLIR II ATR device. All spectra were recorded at ambient temperature. NMR spectra were recorded with a JEOL Eclipse 400 instrument and chemical shifts were determined with respect to external Me₄Si (¹H, 399.8 MHz; ¹³C, 100.5 MHz) and MeNO₂ (¹⁴N, 28.9 MHz). Mass spectrometric data were obtained with a JEOL MStation JMS 700 spectrometer (DCI+, DEI+). Elemental Analysis of C/H/N were performed with an Elementar Vario EL analyzer. Melting points were measured with a Linseis DSC-PT10 apparatus, using a heating rate of 5 °C min⁻¹ and checked by a Büchi Melting Point B-540 apparatus and are not corrected. The sensitivity data (impact, friction, and electrostatic discharge) were performed with a drophammer, friction tester, and electrostatic discharge device conform to the directive of the Federal Institute for Materials Research and Testing (BAM).^[1b]

1.5.2 Computational Details

All ab initio calculations were carried out using the program package Gaussian 03 (Revision B.03)^[20] and visualized by GaussView 5.08.^[21] Structure optimizations and frequency analyses were performed with Becke's B3 three parameter hybrid functional using the LYP correlation functional (B3LYP). For C, H, N and O a correlation consistent polarized double-zeta basis set was used (cc-pVDZ). The structures were optimized without symmetry constraints and the energy is corrected with the zero point vibrational energy.^[22] The enthalpies (*H*) and free energies (*G*) were calculated using the complete basis set (CBS) method in order to obtain accurate values.^[22a] The CBS models use the known asymptotic convergence of pair natural orbital expressions to extrapolate from calculations using a finite basis set to the estimated complete basis set limit. CBS-4 starts with a HF/3-21G(d) geometry optimization, which is the initial guess for the following SCF calculation as a base energy and a final MP2/6-31+G calculation with a CBS extrapolation to correct the energy in second order. The used CBS-4M method additionally implements a MP4(SDQ)/6-31+(d,p) calculation to approximate higher order contributions and also includes some additional empirical corrections.^[23] The enthalpies of the gas-phase species were estimated according to the atomization energy method.^[24]

All calculations affecting the detonation parameters were carried out using the program package EXPLO5 V6.02.^[18] The detonation parameters were calculated at the Chapman-Jouguet (CJ) point with the aid of the steady-state detonation model using a modified Becker-Kistiakowski-Wilson equation of state for modeling the system. The CJ point is found from the Hugoniot curve of the system by its first derivative. The specific impulses I_{sp} were also calculated with the EXPLO5 V6.02 program, assuming an isobaric combustion of a composition of **2** and **3**

as oxidizer, aluminum as fuel, 6% polybutadiene acrylic acid, 6% polybutadiene acrylonitrile as binder and 2% bisphenol-A as epoxy curing agent. A chamber pressure of 70.0 bar and an ambient pressure of 1.0 bar with equilibrium expansion conditions were estimated for the calculations. The best dues of oxidizer and fuel were determined empirically under constant amounts of binder and epoxy curing agent.

1.5.3 X-ray Crystallography

For all compounds, an Oxford Xcalibur3 diffractometer with a CCD area detector was employed for data collection using Mo- K_{α} radiation ($\lambda = 0.71073 \text{ \AA}$). The structures were solved by direct methods (SIR97)^[25] and refined by full-matrix least-squares on F^2 (SHELXL).^[26] All non-hydrogen atoms were refined anisotropically. The hydrogen atom positions were calculated, except for the N-terminal hydrogen which were located in a difference Fourier map and then refined freely. Crystallographic data (excluding structure factors) for the structures reported in this paper have been deposited with the Cambridge Crystallographic Data Centre as supplementary publication no. CCDC-923988 (**2**) and CCDC-923989 (**3**). Copies of the data can be obtained free of charge on application to CCDC, 12 Union Road, Cambridge CB2 1EZ, UK [fax.: (internat.) + 44 1223/336-033; e-mail: deposit@ccdc.cam.ac.uk].

1.5.4 Synthesis

Caution! *All of the described compounds are energetic with sensitivities towards heat, impact and friction. Although no hazards occurred during preparation and manipulation, additional proper protective precautions (face shield, leather coat, earthened equipment and shoes, Kevlar[®] gloves and ear plugs) should be used when undertaking work with these compounds.*

Caution! *Phosgene is a highly toxic, irritating and corrosive gas. Inhalation can cause fatal respiratory damage. Phosgene reacts violently and decomposes to toxic compounds on contact with moisture, including chlorine and carbon monoxide.*

2,2,2-Trinitroethyl chloroformate (1): In a four-necked, 250 mL round-bottomed flask cooled in a dry-ice/ethanol bath and equipped with a magnetic stirrer, gas inlet, septum, dry-ice/ethanol cooled reflux condenser with gas outlet, and a thermometer, phosgene (14.0 g, 13.9 mmol) was condensed at $-70 \text{ }^{\circ}\text{C}$. A solution of 2,2,2-trinitroethanol (5.0 g, 27.6 mmol) in dichloromethane (100 mL) was added, while the temperature was maintained below $-50 \text{ }^{\circ}\text{C}$. A solution of

triethylamine (2.9 g, 4.0 mL, 29.0 mmol) diluted in dichloromethane (50 mL) was added dropwise within 1 h, still maintaining the temperature below $-50\text{ }^{\circ}\text{C}$. Afterwards, the mixture and the reflux condenser were allowed to warm up and were stirred for 12 h at ambient temperature. The organic solvent was removed and the light yellow residue was extracted with diethyl ether ($3 \times 50\text{ mL}$). The insoluble triethylammonium chloride was filtered off and the combined organic phase was washed with ice-cold water (200 mL) and dried with magnesium sulfate. All volatiles were removed *in vacuo* and the residue was distilled (oil bath $65\text{ }^{\circ}\text{C}$, 0.03 mbar) yielding 8.9 g of **1** (86%) as a colorless liquid.

IR: (ATR): $\nu = 3024$ (w), 2974 (w), 2893 (w), 1777 (m), 1598 (s), 1438 (w), 1384 (w), 1347 (w), 1293 (m), 1124 (s), 1088 (s), 979 (w), 853 (w), 826 (w), 796 (s), 778 (m), 721 (w), 676 (m) cm^{-1} . Raman: (200 mW): $\nu = 3020$ (16), 2972 (56), 1785 (14), 1615 (26), 1439 (14), 1384 (25), 1349 (42), 1301 (32), 1170 (6), 1091 (8), 1034 (24), 892 (21), 856 (100), 827 (10), 800 (16), 777 (9), 723 (7), 641 (8), 549 (14), 531 (14), 501 (55), 462 (14), 398 (45), 374 (75), 338 (17), 285 (46), 234 (31) cm^{-1} . ^1H NMR (acetone- D_6) $\delta = 5.51$ (s, 2H, CH_2) ppm. $^{13}\text{C}\{^1\text{H}\}$ NMR (acetone- D_6) $\delta = 149.5$ (CO_2Cl), 121.4 ($\text{C}(\text{NO}_2)_3$), 63.3 (CH_2) ppm. ^{14}N NMR (acetone- D_6) $\delta = -36$ ($\text{C}(\text{NO}_2)_3$) ppm. EA ($\text{C}_3\text{H}_2\text{N}_3\text{O}_8\text{Cl}$, 243.52) calc.: C 14.80, H 0.83, N 17.26, Cl 14.56 %; found: C 15.01, H 0.73, N 17.01, Cl 14.16 %.

2,2,2-Trinitroethyl carbamate (2): Into a stirring solution of **1** (0.50 g, 2.1 mmol) in dichloromethane (5 mL), chilled to $-30\text{ }^{\circ}\text{C}$, concentrated ammonia (30%, 0.5 mL, 8.0 mmol) was added dropwise. The mixture was stirred for 1 h at $-30\text{ }^{\circ}\text{C}$. The precipitate formed was filtered off and recrystallized from hot water, to obtain 0.38 g (83%) colorless needles of the carbamate **2**.

DSC ($5\text{ }^{\circ}\text{C min}^{-1}$): $91\text{ }^{\circ}\text{C}$ (onset mp.) (Lit.^[8] $92\text{-}93\text{ }^{\circ}\text{C}$), $169\text{ }^{\circ}\text{C}$ (onset dec.). IR: (ATR): $\nu = 3447$ (w), 3352 (w), 3302 (w), 2962 (m), 1729 (m), 1590 (s), 1441 (w), 1399 (m), 1367 (w), 1325 (m), 1300 (m), 1248 (w), 1167 (w), 1138 (w), 1105 (m), 1027 (w), 910 (w), 873 (w), 858 (w), 804 (m), 784 (m), 772 (m), 741 (w), 673 (w), 646 (w), 606 (w), 546 (m), 527 (m) cm^{-1} . Raman: (200 mW): $\nu = 3300$ (4), 3004 (23), 2964 (51), 2828 (3), 1721 (17), 1622 (31), 1608 (28), 1587 (18), 1445 (17), 1404 (8), 1369 (54), 1304 (31), 1250 (15), 1171 (10), 1145 (10), 1112 (9), 1091 (9), 1027 (17), 910 (19), 878 (10), 859 (100), 802 (14), 786 (12), 745 (10), 674 (10), 647 (12), 549 (18), 524 (9), 426 (55), 397 (46), 377 (72), 305 (53), 265 (17), 212 (30) cm^{-1} . ^1H NMR (acetone- D_6) $\delta = 6.77$ (s, 1H, NH_2), 6.49 (s, 1H, NH_2), 5.68 (s, 2H, CH_2) ppm. $^{13}\text{C}\{^1\text{H}\}$ NMR (acetone- D_6) $\delta = 154.5$ (CO_2N), 125.7 ($\text{C}(\text{NO}_2)_3$), 61.8 (CH_2) ppm. ^{14}N NMR (acetone- D_6) $\delta = -33$ ($\text{C}(\text{NO}_2)_3$), -310 (NH_2) ppm. MS (DEI+) m/z (%): 225 (15) $[(\text{M} + \text{H})^+]$, 59 (13) $[\text{CHNO}_2^+]$, 46 (59) $[\text{NO}_2^+]$, 44 (100) $[(\text{M} - \text{OCH}_2(\text{NO}_2)_3)^+, \text{CONH}_2^+]$, 43 (31) $[\text{CHNO}^+]$, 30 (71) $[\text{NO}^+]$. EA ($\text{C}_3\text{H}_4\text{N}_4\text{O}_8$, 224.09) calc.:

C 16.08, H 1.80, N 25.00 %; found: C 15.89, H 1.78, N 24.50 %. BAM drophammer: >40 J; friction tester: 64 N; ESD: 0.15 J (grain size <500 μm).

2,2,2-Trinitroethyl nitrocarbamate (3): Into concentrated sulfuric acid (1 mL) was dropped red fuming nitric acid (>99.5%, 1 mL) at 0 °C. To this chilled nitration mixture, 2,2,2-trinitroethyl carbamate (**2**) (0.25 g, 1.1 mmol) was added in small portions. The solution was stirred for 2 h at 0 °C and for 2 h at ambient temperature. The mixture was poured onto ice-water (200 mL), extracted with ethyl acetate (3 x 50 mL) and the combined organic phase was dried with magnesium sulfate. The solvent was removed under reduced pressure and the crude solid product was recrystallized from carbon tetrachloride to obtain 0.30 g (99%) colorless needles of **3**.

DSC (5 °C min⁻¹): 109 °C (onset mp.), 153 °C (onset dec.). IR: (ATR): ν = 3168 (w), 3062 (w), 3013 (w), 2900 (w), 1772 (m), 1588 (s), 1466 (m), 1444 (w), 1390 (w), 1351 (w), 1326 (m), 1398 (s), 1271 (w), 1170 (s), 990 (m), 972 (s), 882 (w), 856 (w), 826 (m), 792 (m), 777 (m), 760 (m), 745 (m), 710 (w), 668 (w) cm⁻¹. Raman: (200 mW): ν = 3170 (9), 3013 (33), 2966 (48), 2868 (9), 1768 (49), 1609 (46), 1468 (23), 1442 (23), 1393 (32), 1353 (46), 1324 (75), 1303 (55), 1272 (26), 1183 (19), 1095 (16), 1050 (51), 998 (62), 883 (21), 859 (100), 794 (17), 781 (18), 761 (19), 657 (18), 542 (25), 461 (58), 377 (72), 407 (85), 376 (92), 271 (69) cm⁻¹. ¹H NMR (acetone-D₆) δ = 10.70 (s, 1H, NH), 5.53 (s, 2H, CH₂) ppm. ¹³C {¹H} NMR (acetone-D₆) δ = 145.2 (CO₂N), 122.2 (C(NO₂)₃), 62.1 (CH₂) ppm. ¹⁴N NMR (acetone-D₆) δ = -36 (C(NO₂)₃), -55 (NNO₂), -192 (NNO₂) ppm. MS (DCI+) m/z (%): 270 (1) [(M + H)⁺], 225 (2) [(M - NO₂)⁺]. EA (C₃H₃N₅O₁₀, 269.08) calc.: C 13.39, H 1.12, N 26.03 %; found: C 13.54, H 1.09, N 25.70 %. BAM drophammer: 10 J; friction tester: 96 N; ESD: 0.10 J (grain size 500-1000 μm).

1.6 References

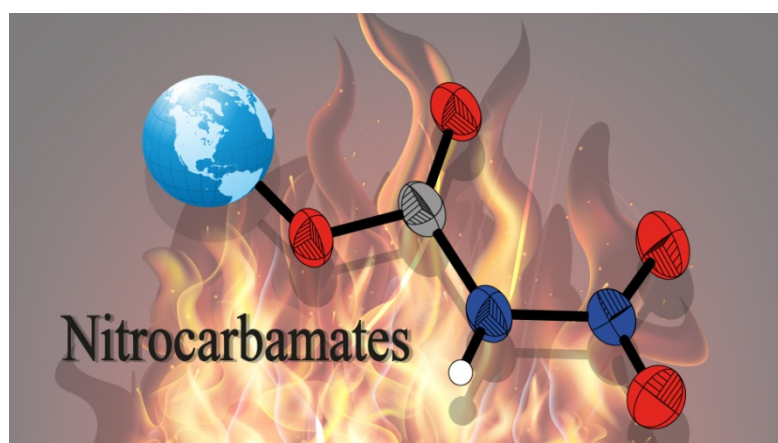
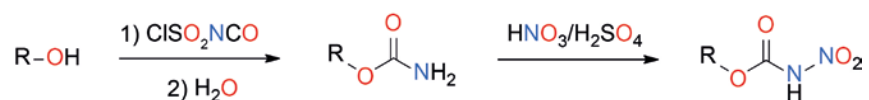
- [1] a) T. M. Klapötke, *Chemistry of High-Energy Materials*, 2nd ed., deGruyter, Berlin, **2012**; b) M. Göbel, T. M. Klapötke, *Adv. Funct. Mater.* **2009**, *19*, 347–365.
- [2] M. Göbel, T. M. Klapötke, *Z. Anorg. Allg. Chem.* **2007**, *633*, 1006–1017.
- [3] C. Hogue, *Chem. Eng. News* **2011**, *89*, 6.
- [4] a) T. M. Klapötke, B. Krumm, R. Moll, S. F. Rest, *Z. Anorg. Allg. Chem.* **2011**, *637*, 2103–2110; b) T. M. Klapötke, B. Krumm, R. Moll, in *New Trends Res. Energ. Mater., Proc. Semin., 13th, Vol. 2*, **2010**, pp. 523–527; c) H. Feuer, T. Kucera, *J. Org. Chem.* **1960**, *25*, 2069–2070; d) M. Göbel, T. M. Klapötke, *Acta Crystallogr., Sect. C: Cryst. Struct. Commun.* **2007**, *63*, 562–564.
- [5] S. V. Lieberman, E. C. Wagner, *J. Org. Chem.* **1949**, *14*, 1001–1012.
- [6] W. H. Gilligan, S. L. Stafford, *Synthesis* **1979**, 600–602.
- [7] L. Cotarca, H. Eckert, *Phosgenations — A Handbook*, Wiley-VCH, Weinheim, **2005**.
- [8] O. A. Luk'yanov, G. V. Pokhvisneva, *Russ. Chem. Bull.* **1992**, *41*, 1286–1288.
- [9] a) M. Oki, *Applications of Dynamic NMR Spectroscopy to Organic Chemistry*, Wiley-VCH, Deerfield Beach, **1985**; b) T. M. Klapötke, B. Krumm, P. Mayer, K. Polborn, O. P. Ruscitti, *Inorg. Chem.* **2001**, *40*, 5169–5176.
- [10] K. B. Wiberg, P. R. Rablen, *J. Am. Chem. Soc.* **1995**, *117*, 2201–2209.
- [11] D. S. Raiford, C. L. Fisk, E. D. Becker, *Anal. Chem.* **1979**, *51*, 2050–2051.
- [12] A. F. Holleman, E. Wiberg, N. Wiberg, *Lehrbuch der Anorganischen Chemie*, 102nd ed., deGruyter, Berlin, **2008**.
- [13] A. Bondi, *J. Phys. Chem.* **1964**, *68*, 441–451.
- [14] B. Sepehrnia, J. R. Ruble, G. A. Jeffrey, *Acta Crystallogr.* **1987**, *43*, 249–251.
- [15] T. Steiner, *Angew. Chem., Int. Ed.* **2002**, *41*, 48–76.
- [16] Y. Gu, T. Kar, S. Scheiner, *J. Am. Chem. Soc.* **1999**, *121*, 9411–9422.
- [17] R. Butcher, R. Gilardi, C. George, J. Flippen-Anderson, *J. Chem. Crystallogr.* **1996**, *26*, 381–388.
- [18] M. Sućeska, *EXPLO5 V.6.02*, Zagreb (Croatia), **2013**.
- [19] J. Akhavan, *The Chemistry of Explosives*, 2nd ed., Royal Soc. of Chemistry, Cambridge, **2004**.
- [20] M. J. Frisch, G. W. Trucks, H. B. Schlegel, G. E. Scuseria, M. A. Rob, J. R. Cheeseman, J. A. Montgomery, T. Vreven, K. N. Kudin, J. C. Burant, J. M. Millam, S. S. Iyengar, J. Tomasi, V. Barone, B. Mennucci, M. Cossi, G. Scalmani, N. Rega, G. A. Petersson, H. Nakatsuji, M. Hada, M. Ehara, K. Toyota, R. Fukuda, J. Hasegawa, M. Ishida, T. Nakajima, Y. Honda, O. Kitao, H. Nakai, M. Klene, X. Li, J. E. Knox, H. P. Hratchian, J. B. Cross, V. Bakken, C. Adamo, J. Jaramillo, R. Gomperts, R. E. Stratmann, O. Yazyev, A. J. Austin, R. Cammi, C. Pomelli, J. W. Ochterski, P. Y. Ayala, K. Morokuma, G. A.

- Voth, P. Salvador, J. J. Dannenberg, V. G. Zakrzewski, S. Dapprich, A. D. Daniels, M. C. Strain, O. Farkas, D. K. Malick, A. D. Rabuck, K. Raghavachari, J. B. Foresman, J. V. Ortiz, Q. Cui, A. G. Baboul, S. Clifford, J. Cioslowski, B. B. Stefanov, G. Liu, A. Liashenko, P. Piskorz, I. Komaromi, R. L. Martin, D. J. Fox, T. Keith, M. A. Al-Laham, C. Y. Peng, A. Nanayakkara, M. Challacombe, P. M. W. Gill, B. Johnson, W. Chen, M. W. Wong, C. Gonzalez, J. A. Pople, Rev. B.03 ed., Gaussian, Inc., Wallingford CT, **2003**.
- [21] R. D. Dennington, T. A. Keith, J. M. Millam, *GaussView*, Ver. 5.08 ed., Semichem, Inc., Wallingford CT, **2009**.
- [22] a) T. M. Klapötke, J. Stierstorfer, *Phys. Chem. Chem. Phys.* **2008**, *10*, 4340–4346; b) J. A. Montgomery, M. J. Frisch, J. W. Ochterski, G. A. Petersson, *J. Chem. Phys.* **2000**, *112*, 6532–6542.
- [23] J. W. Ochterski, G. A. Petersson, J. A. Montgomery, *J. Chem. Phys.* **1996**, *104*, 2598–2619.
- [24] a) E. F. C. Byrd, B. M. Rice, *J. Phys. Chem.* **2005**, *110*, 1005–1013; b) L. A. Curtiss, K. Raghavachari, P. C. Redfern, J. A. Pople, *J. Chem. Phys.* **1997**, *106*, 1063–1079.
- [25] a) A. Altomare, M. C. Burla, M. Camalli, G. L. Cascarano, C. Giacovazzo, A. Guagliardi, A. G. G. Moliterni, G. Polidori, R. Spagna, *J. Appl. Crystallogr.* **1999**, *32*, 115–119; b) A. Altomare, G. Cascarano, C. Giacovazzo, A. Guagliardi, A. G. G. Moliterni, M. C. Burla, G. Polidori, M. Camalli, R. Spagna, *SIR97*, **1997**.
- [26] G. M. Sheldrick, *SHELX-97*, **1997**.

2 Carbamates and Nitrocarbamates from Polynitro Alcohols

As published in *J. Org. Chem.* **2015**, 80, 6329–6335.

SYNTHESIS OF ENERGETIC NITROCARBAMATES FROM POLYNITRO ALCOHOLS AND THEIR POTENTIAL AS HIGH ENERGETIC OXIDIZERS



2.1 Abstract

A new synthesis strategy for the preparation of energetic carbamates and nitrocarbamates starting from readily available polynitro alcohols is introduced. The efficient synthesis of mainly new carbamates was performed with the reactive chlorosulfonyl isocyanate (CSI) reagent. The carbamates were nitrated using mixed acid to form the corresponding primary nitrocarbamates. The thermal stability of all synthesized compounds was studied using differential scanning calorimetry, and the energies of formation were calculated on the CBS-4 M level of theory. Detonation parameters and propulsion properties were determined with the software package EXPLO5 V6.02. Furthermore, for all new substances single crystal X-ray diffraction studies were performed and are presented and discussed.

2.2 Introduction

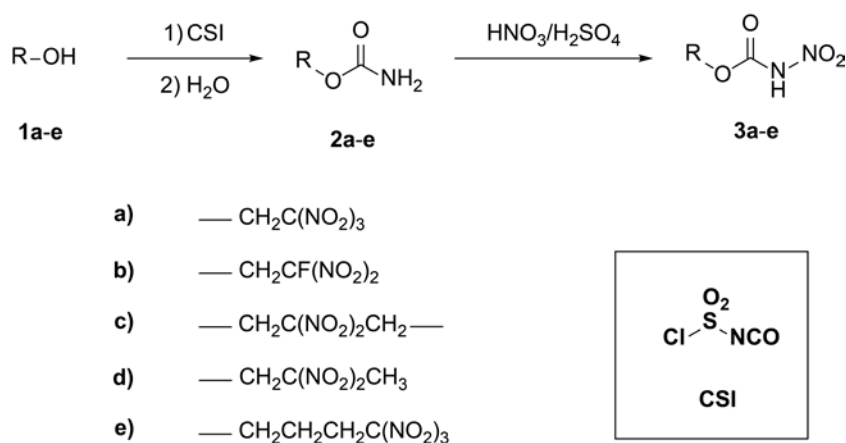
The chemistry of highly energetic materials is still a very active research topic, especially the issue of high energy dense oxidizers (HEDOs), which have been investigated intensively in the recent years.^[1] Oxidizers are compounds that release an excess of oxygen, which reacts with fuel and produce large amounts of hot gases for propulsion. An interesting but sparsely investigated energetic functionality which emerged, is the primary nitrocarbamate.^[1e, 2] This energetic chemical moiety can be synthesized starting from polynitro alcohols. The previously described synthesis of carbamates starts with the reaction of the corresponding alcohol with phosgene to form the chloroformate, which is then further treated with ammonia; the carbamate is nitrated subsequently to the nitrocarbamate.^[2a, 3] In the case of 2,2,2-trinitroethanol, this synthesis route proceeds quite satisfactorily but has still some disadvantages.^[1e] The hazardous handling with the highly toxic gas phosgene needs to be addressed, and the use of alkaline reagents is problematic because of the instability of polynitro alcohols in basic media.^[3-4] It has been found that a much advanced versatile synthesis route of the carbamate moiety is a one step synthesis with the reagent chlorosulfonyl isocyanate (CSI). CSI is a commercially available reagent and was discovered in Germany in 1956.^[5] It consists of a sulfonyl center with two electron-withdrawing components, the chloro atom and the isocyanate group, which results in one of the most reactive isocyanates.^[5a, 6] The reaction with alcohols is very fast and already proceeds at low temperatures and without possible multiaddition prevented by the formation of a chlorosulfonylamide intermediate. This SO₂Cl group is removed by aqueous workup to form chlorosulfonate and the

pure carbamate. In summary, the advantages of CSI are monosubstitution, fast reaction times, simple workup and often nearly quantitative yields.

2.3 Results and Discussion

2.3.1 Synthesis and Characterization

The carbamate of 2,2,2-trinitroethanol (**1a**) was first synthesized via the chloroformate-ammonia route.^[1e] With the new methodology using the reagent chlorosulfonyl isocyanate (CSI), the 2,2,2-trinitroethyl carbamate (**2a**) is now conveniently synthesized in a one-step synthesis with a yield of 96% compared to previously 71%.^[1e] Further advantages are the faster reaction time, the handling of the starting materials, and the simple work up, which leaves pure product without further purification. CSI also reacts effectively with less reactive alcohols such as 2-fluoro-2,2-dinitroethanol (**1b**). The corresponding carbamate **2b** was isolated in an almost quantitative yield of 98%; however, the synthesis of the corresponding chloroformate is quite complicated and time-consuming and can be synthesized with only 40% yield.^[7] CSI works very well with multivalent alcohols such as 2,2-dinitropropane-1,3-diol (**1c**). Scheme 2-1 displays the synthesis and the involved nitro alcohols. In all carbamate forming reactions with CSI, the -carbamates were isolated as colorless pure products in high yields, often practically quantitative (see Experimental Section).



Scheme 2-1: Synthesis of carbamates (**2**) and nitrocarbamates (**3**) from nitro alcohols (**1**).

The carbamates **2a–e** were converted into the nitrocarbamates **3a–e** by a mixture of concentrated sulfuric (96%) and fuming nitric acid (100%) (1:1). After the reaction mixture is

quenched with water, it is crucial that it is immediately extracted with ethyl acetate. Subsequent recrystallization is important to obtain pure products.

2.3.2 NMR Spectroscopy

All carbamates and nitrocarbamates were characterized with multinuclear NMR, vibrational (IR, Raman) spectroscopy, and mass spectrometry. Furthermore, all compounds were evaluated for their thermal stabilities with differential scanning calorimetry (DSC), and the purity grade was checked with CHN elemental analysis.

In the NMR spectra clear trends are visible. In the ^1H NMR spectra of all carbamates, the NH_2 resonance is found in the region between 7 and 5 ppm as very broad signals because of the keto-enol delocalization of the nitrogen lone pair and the restricted rotation.^[1e, 8] In the case of the nitrocarbamates, this NH resonance is significantly downfield shifted below 13 ppm due to increased acidity. In the ^{13}C NMR spectra, the most obvious feature is the resonance of the carbamate carbonyl group, which changes to higher field from the carbamates **2** around 155 ppm to 149 ppm for the nitrocarbamates **3** due to increased shielding by the presence of adjacent nitro groups. The $^{14/15}\text{N}$ carbamate resonances are detected around -300 ppm (broadened in ^{14}N). Upon nitration to **3**, this resonance is significantly shifted downfield to around -200 ppm. Relatively sharp signals are present for the nitro groups, and those of the nitramine units are detected at -45 to -57 ppm.

In the vibrational spectra, the characteristic strong carbonyl stretching vibration of the carbamates are found in the range of 1744 to 1712 cm^{-1} and that of the nitrocarbamates shifted to slightly higher wave numbers at 1745 to 1772 cm^{-1} . The stretching vibrations of the NH_2 and NH groups are all above 3000 cm^{-1} showing multiple peaks, whereas only one peak remains for the nitrocarbamates.^[9]

The physical properties of the carbamates **2** and nitrocarbamates **3** are summarized in Table 2-1. The melting points of the carbamates show a trend, namely that it decreases with the increasing of the carbon backbone. The exceptions are the bivalent carbamate **2c** with the higher possibility of hydrogen bonding of the two carbamate moieties and the fluoro compound **2b**, which is a liquid and has a relatively high decomposition point of $219\text{ }^\circ\text{C}$. This tendency toward high decomposition points of 2-fluoro-2,2-dinitroethanol (**1b**) derivatives compared to those of 2,2,2-trinitroethanol (**1a**) was confirmed elsewhere,^[10] except for the nitrocarbamate **3b**. The decomposition points of the nitrocarbamates are all in the same range. The doubly functionalized compound **3c** shows the highest melting ($152\text{ }^\circ\text{C}$) and decomposition point of $158\text{ }^\circ\text{C}$. Some

nitrocarbamates possess an high combined nitrogen/oxygen content, such as **3a** (85.5%) and the bivalent **3c** (80.7%).

Table 2-1: Physical Properties of Carbamates 2a–e and Nitrocarbamates 3a–e.

	2a	2b	2c	2d	2e
formula	C ₃ H ₄ N ₄ O ₈	C ₃ H ₄ N ₃ O ₆ F	C ₅ H ₈ N ₄ O ₈	C ₄ H ₇ N ₃ O ₆	C ₅ H ₈ N ₄ O ₈
FW /g mol ⁻¹	224.09	197.08	252.14	193.11	252.14
T _m /°C (onset) ^{a)}	91	(liquid)	136	68	53
T _{dec} /°C (onset) ^{b)}	169	219	182	192	156
N /% ^{c)}	25.0	21.3	22.2	21.8	22.2
O /% ^{d)}	57.1	48.7	47.8	49.7	47.8
N+O /% ^{e)}	82.1	70.0	73.0	71.5	73.0
Ω _{CO} /% ^{f)}	+21.4	+12.2	-6.4	+12.4	-6.4
	3a	3b	3c	3d	3e
formula	C ₃ H ₃ N ₅ O ₁₀	C ₃ H ₃ N ₄ O ₈ F	C ₅ H ₆ N ₆ O ₁₂	C ₄ H ₆ N ₄ O ₈	C ₅ H ₇ N ₅ O ₁₀
FW /g mol ⁻¹	269.08	242.08	342.13	238.11	297.14
T _m /°C (onset) ^{a)}	109	80	152	76	82
T _{dec} /°C (onset) ^{b)}	153	145	158	140	145
N /% ^{c)}	26.0	23.1	24.6	23.5	23.6
O /% ^{d)}	59.5	52.9	56.1	53.8	53.8
N+O /% ^{e)}	85.5	76.0	80.7	77.3	77.4
Ω _{CO} /% ^{f)}	+32.7	+26.4	+18.7	+20.2	+8.1

a) Onset melting (T_m) point from DSC measurement carried out at a heating rate of 5 °C min⁻¹. b) Onset decomposition (T_{dec}) point from DSC measurements carried out at a heating rate of 5 °C min⁻¹. c) Nitrogen content. d) Oxygen content. e) Combined nitrogen and oxygen content. f) Oxygen balance assuming the formation of CO, H₂O, N₂, and HF. g) Liquid at room temperature.

2.3.3 Single Crystal X-ray Diffraction

Single crystals suitable for X-ray diffraction measurements were obtained by crystallization at room temperature from acetonitrile (**2c**, **2d** and **2e**) and tetrachloromethane (**3b**, **3c**, **3d** and **3e**). A full list of the crystallographic structure and refinement data are shown in Appendix A.2.

The nitrocarbamate **3b** crystallizes in the monoclinic space group $P2_1/c$ with four formula units per unit cell and a relatively high density of 1.94 g cm⁻³ (see Figure 2-1). The nitrocarbamate moiety inclusively the atom O5 and C2 of the backbone shows an almost perfect planarity as

shown by the torsion angles. Remarkable is the short nitramine bond N3–N4 with 1.38 Å, indicating a double bond character, caused by the delocalization of the nitrogen lone pair. The C–N bond lengths of the fluorodinitromethyl moiety are both in the range of 1.53 Å. They are elongated compared to regular C–N bonds (1.47 Å), which has steric reasons and is typical for this type of compounds.^[1b, 10b] The N1–C1–N2 angle is 104.8 °, the N1–C1–F1 angle 107.6 ° and N2–C1–F1 angle 107.3 °; therefore the much smaller fluorine atom claims more space in the crystal. The high density is likely caused by the presence of several hydrogen bridge-bondings.

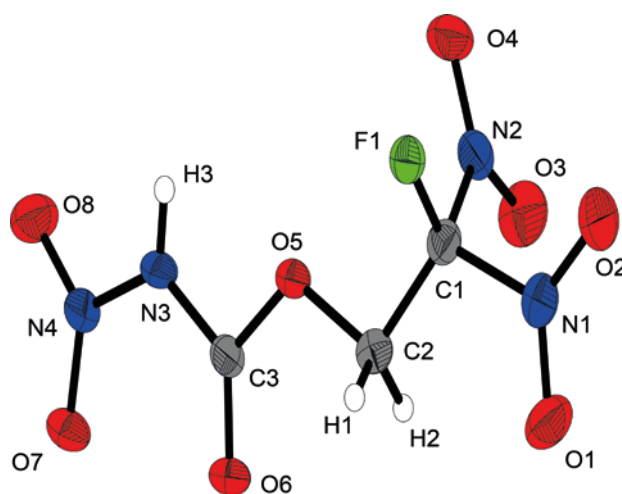


Figure 2-1: X-ray molecular structure of 2-fluoro-2,2-dinitroethyl nitrocarbamate (3b).

Atom distances (Å) and angles (deg): C1–N1 1.525(2), C1–N2 1.533(2), C1–F1 1.323(2), C3–O6 1.193(2), N3–N4 1.376(2), N3–H3 0.80(2), N2–C1–N1 104.8(1), N1–C1–F1 107.6(1), N2–C1–F1 107.3(1), O7–N4–N3–C3 4.8(2), H3–N3–C3–O6 –179(2), O6–C3–O5–C2 3.6(2), N3–C3–O5–C2 –176.0(1).

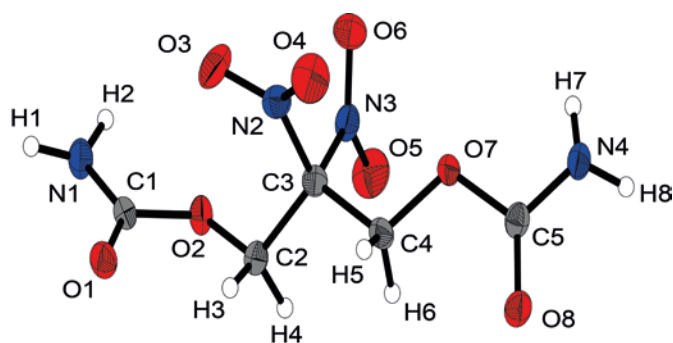


Figure 2-2: X-ray molecular structure of 2,2-dinitropropane-1,3-diyl dicarbamate (2c).

Selected atom distances (Å) and angles (deg): C1–N1 1.325(3), C1–O1 1.216(2), C1–O2 1.369(2), C3–N2 1.525(3), C3–N3 1.527(2), H1–N1–C1–O1 13(2), H2–N1–C1–O1 168(2), H7–N4–C5–O8 166(2), H8–N4–C5–O7 –170(2).

The carbamate **2c** of the bivalent alcohol crystallizes in the orthorhombic space group $Pna2_1$ with four formulas per unit cell and a density of 1.71 g cm⁻³ (see Figure 2-2). The two

crystallographic different arms of the molecule can be regarded as nearly identical. On both sides of the carbamate structure all hydrogen of the NH_2 group are turned out in the same direction of more than 10° from the expected planarity of this moiety. A reason for this could be the strength and the large number of hydrogen bonding. Characteristic in this structure are also the longer geminal $\text{C}-\text{NO}_2$ (1.53 Å) bonds of the carbon bonded nitro groups. The orthogonal arrangement of these nitro groups generates in the crystal also quite strong non-bonded intermolecular attractions between partial charged distribution of nitrogen (δ^+) and oxygen (δ^-). The $\text{N}\cdots\text{O}$ electrostatic attractions ($\text{N}2\cdots\text{O}6$, $\text{N}3\cdots\text{O}2$, $\text{N}3\cdots\text{O}7$) can be found with distances of 2.56, 2.64 and 2.80 Å, which is much shorter than the sum of the van der Waals radii of oxygen and nitrogen (3.07 Å).

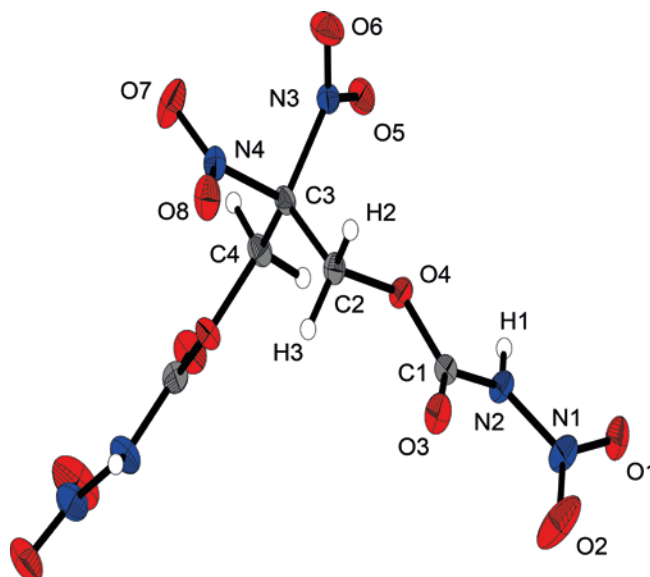


Figure 2-3: X-ray molecular structure of 2,2-dinitropropane-1,3-diyl bis(nitrocarbamate) (3c).

Selected atom distances (Å) and angles (deg): $\text{N}2-\text{N}1$ 1.381(2), $\text{H}1-\text{N}2$ 0.81(2), $\text{N}2-\text{C}1$ 1.378(2), $\text{O}4-\text{C}1$ 1.345(2), $\text{O}3-\text{C}1$ 1.200(2), $\text{C}3-\text{N}4$ 1.525(2), $\text{C}3-\text{N}3$ 1.534(2), $\text{N}1-\text{N}2-\text{C}1$ 124.1(1), $\text{O}2-\text{N}1-\text{N}2-\text{C}1$ $-21.3(2)$.

The nitrocarbamate **3c** crystallizes in the orthorhombic space group $Pbca$ with eight formulas per unit cell and a density of 1.78 g cm^{-3} (see Figure 2-3). Compared to the non-nitrated form the molecular structure is nearly identical. An exception is the longer bond lengths of $\text{C}1-\text{N}2$ (1.38 Å) of the nitrocarbamate compared to the carbamate. The reason for this is the lower electronic density on the nitrogen $\text{N}2$, resulting in less ability for resonance-stabilization to the carbonyl moiety.

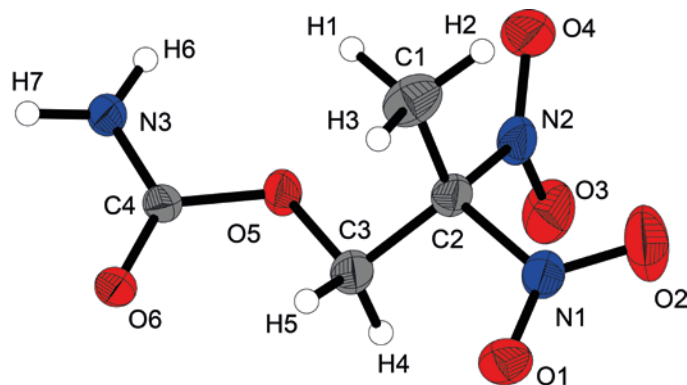


Figure 2-4: X-ray molecular structure of 2,2-dinitropropyl carbamate (**2d**).

Selected atom distances (Å) and angles (deg): C2–N1 1.518(3), C2–N2 1.528(3), C4–N3 1.326(3), O6–C4–N3–H7 8(2), H7–N3–C4–O5 –173(2).

The carbamate **2d** (Figure 2-4) and the nitrocarbamate **3d** (Figure 2-5) with the 2,2-dinitropropyl moiety both crystallize in the monoclinic space group $P2_1/c$ with four units per cell. The carbamate **2d** crystallizes with a significantly lower density of 1.59 g cm^{-3} compared to the nitrocarbamate **3d**, which has a density of 1.75 g cm^{-3} . The two compounds **2d** and **3d** show the same structural properties as the previously discussed, such as long C–NO₂ bonds and the planarity of the carbamate/nitrocarbamate moiety

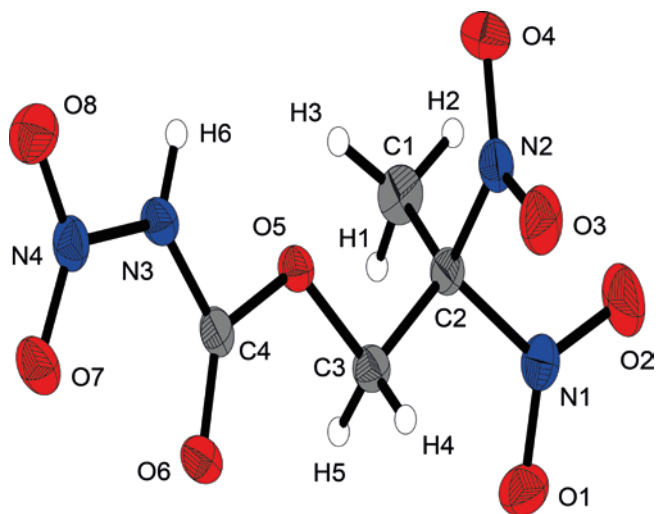


Figure 2-5: X-ray molecular structure of 2,2-dinitropropyl nitrocarbamate (**3d**).

Selected atom distances (Å) and angles (deg): H6–N3 0.84(2), C4–N3 1.379(2), N3–N4 1.382(2), C1–C2–C3 115.1(1), C3–C2–N1 108.6(1), C3–C2–N2 107.5(1), O8–N4–N3–C4 177.5(1), N4–N3–C4–O6 –0.4(2), N4–N3–C4–O5 179.9(1).

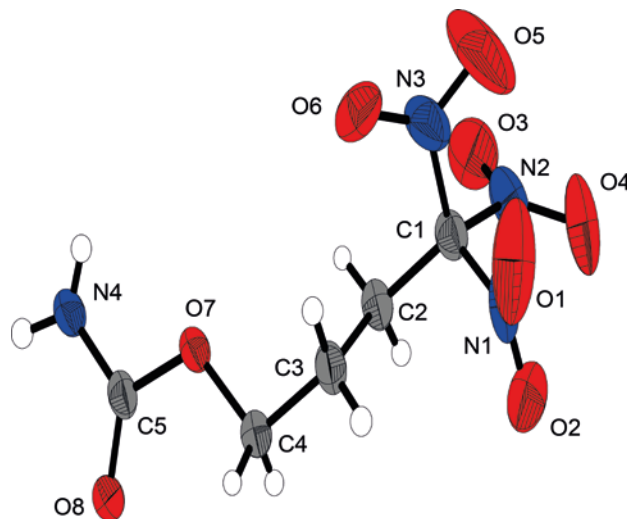


Figure 2-6: X-ray molecular structure of 4,4,4-trinitrobutyl carbamate (2e).

Selected atom distances (Å) and angles (deg): C1–C2 1.511(4), C1–N1 1.534(4), C1–N2 1.513(3), C1–N3 1.515(4), C4–O7 1.442(3), C5–O8 1.215(3), N1–C1–N3 106.6(2), N1–C1–C2 110.9(2), N4–C5–O7–C4 $-178.9(2)$, H7–N4–C5–O8 $5(2)$.

The crystal growing, the data collection, the solution and refinement of the carbamate **2e** and the nitrocarbamate **3e** of 4,4,4-trinitrobutanol were difficult, as illustrated by the quite high refinement values. The carbamate **2e** crystallizes in the monoclinic space group $P2_1/c$ with the same structural properties as the other described carbamates. Particularly striking in this structure is the angle around the C1 atom (Figure 2-6). It can be observed that the angles N–C1–N are around 8° smaller than the angles C2–C1–N. That indicates that the big three nitro groups take up less space due to optimized propeller structure than the neighboring small methylene group.

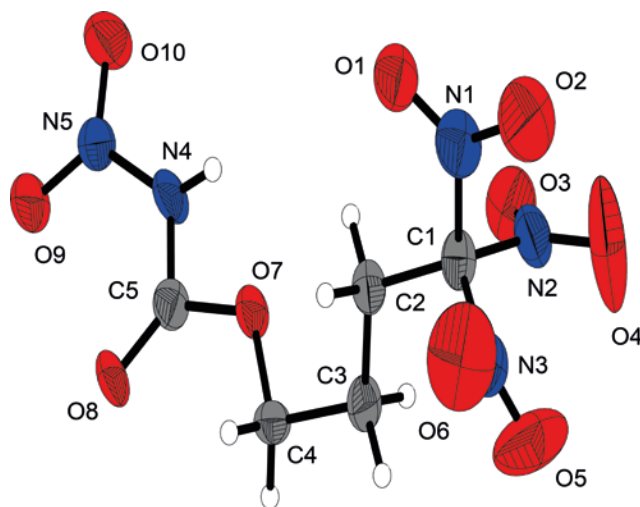


Figure 2-7: X-ray molecular structure of 4,4,4-trinitrobutyl nitrocarbamate (3e).

Selected atom distances (Å) and angles (deg): O8–C5 1.202(5), N4–N5 1.372(5), N4–C5 1.384(6), C8–H11 0.990, C8–C9 1.504(6), C2–C1–N1 111.1(4), N1–C1–N2 102.9(4), C5–N4–N5–O10 $-161.5(4)$.

Table 2-2: Calculated detonation, combustion parameters (Using EXPLO5 V6.02 EOS BKWG-S) and sensitivity data of the energetic carbamates 2a–e and nitrocarbamates 3a–e.

	2a	2b	2c	2d	2e	AP
density (RT) ^{a)}	1.82	1.58	1.69	1.57	1.63	1.95
$\Delta_f H^\circ$ /kJ mol ⁻¹ ^{b)}	-459	-659	-902	-553	-523	-296
$\Delta_f U^\circ$ /kJ kg ⁻¹ ^{c)}	-1961	-3257	-3480	-2759	-1977	-2433
IS /J ^{d)}	40	40	30	40	40	15
FS /N ^{e)}	64	360	360	360	360	>360
ESD /J ^{f)}	0.15	(liquid)	0.20	0.20	0.20	>1.50
Q_v /kJ kg ⁻¹ ^{g)}	-5286	-3922	-3260	-3779	-4547	-1422
P_{CJ} /kbar ^{h)}	302	211	196	186	221	158
V_{det} /m s ⁻¹ ⁱ⁾	8530	7273	7256	7130	7524	6368
I_{sp} /s ^{j)}	246	227	182	196	220	157
I_{sp} /s (15%Al) ^{k)}	254	248	228	238	253	235
I_{sp} /s (15%Al+binder) ^{l)}	247	233	214	225	237	261
	3a	3b	3c	3d	3e	AP
density (RT) ^{a)}	1.72	1.92	1.76	1.73	1.66	1.95
$\Delta_f H^\circ$ /kJ mol ⁻¹ ^{b)}	-366	-573	-709	-455	-428	-296
$\Delta_f U^\circ$ /kJ kg ⁻¹ ^{c)}	-1277	-2284	-1986	-1816	-1347	-2433
IS /J ^{d)}	10	10	4	20	20	15
FS /N ^{e)}	96	360	240	360	360	>360
ESD /J ^{f)}	0.10	0.15	0.10	0.20	0.20	>1.5
Q_v /kJ kg ⁻¹ ^{g)}	-4456	-4342	-5088	-4839	-5184	-1422
P_{CJ} /kbar ^{h)}	232	338	275	271	262	158
V_{det} /m s ⁻¹ ⁱ⁾	7704	8526	8157	7945	7858	6368
I_{sp} /s ^{j)}	232	237	245	242	251	157
I_{sp} /s (15%Al) ^{k)}	251	252	254	259	265	235
I_{sp} /s (15%Al+binder) ^{l)}	261	248	244	243	249	261

a) RT densities are recalculated from X-ray densities. b) Heat and c) energy of formation calculated with ab initio calculations on the CBS-4M level. d) Sensitivity toward impact. e) Friction. f) Electrostatic discharge. g) Heat of detonation. h) Detonation pressure. i) Detonation velocity. j) Specific impulse I_{sp} . j) Specific impulse I_{sp} with aluminum. k) Specific impulse I_{sp} with aluminum and binder (6% polybutadiene acrylic acid, 6% polybutadiene acrylonitrile and 2% bisphenol A ether) at 70.0 kbar chamber pressure and isobaric combustion condition (1 bar).

2.3.4 Energetic Properties

For the manipulation of energetic materials the sensitivity is very important. The sensitiveness to impact (IS) of a solid or liquid material is tested by the action of a falling mass on the sample for its decompose or explosion. The friction sensitivity (FS) is determined by rubbing a small amount between porcelain with different contact pressures.^[11] All compounds show no sensitivity against friction, except the compounds with the 2,2,2-trinitroethyl unit **2a** and **3a** which are classified as friction sensitive. The nitrocarbamate of the diol **3c** shows the highest sensitivity of 4 J (very sensitive) against impact and is therefore just as sensitive as the common explosive pentaerythritol tetranitrate (PETN).^[11] All other nitrocarbamates can be ranked as sensitive and all carbamates as less sensitive to impact (Table 2-2).

The most important performance parameter for rocket propellants is the specific impulse I_{sp} , which is defined as the impulse change per mass unit (kg) of the propellant mixture.^[1a] The I_{sp} depends mainly on the burning temperature in the combustion chamber and reciprocal to the average molar mass of the gaseous decomposition products (For more information, see the Appendix A.2). To achieve a high combustion temperature a fuel is added to the oxidizer. As fuel is used mainly aluminum which has a very high heat of combustion $\Delta_c H$, is cheap, and its combustion (Al_2O_3) products are not harmful to the environment.^[12] The best specific impulse I_{sp} with an admixture of 15% aluminum were achieved with **3e** (265 s) and is therefore much higher as the standard oxidizer ammonium perchlorate (**AP**) (235 s) (see Table 2-2). The standard mixture consists of **AP** (76%), aluminum (15%) and a polymeric binder (14%) results in a value for the I_{sp} of 261 s. The compound that best compares is the nitrocarbamate **3a** with an identical value of 261 s. However, not only the absolute performance of the propellant mixture is essential, other properties such as the ecological and toxicological point of view of the used compounds and the decomposition products are important.^[13]

AP produces the toxic gas hydrogen chloride when burned, which is generated in a significant amount of 14.2% (see Figure 2-8).^[13] If nitrocarbamate **3a** is compared with **AP**, the nitrogen content is more than doubled, and in addition, no halogenated products were produced, which makes RADAR detection of the rocket emission more difficult.^[1a]

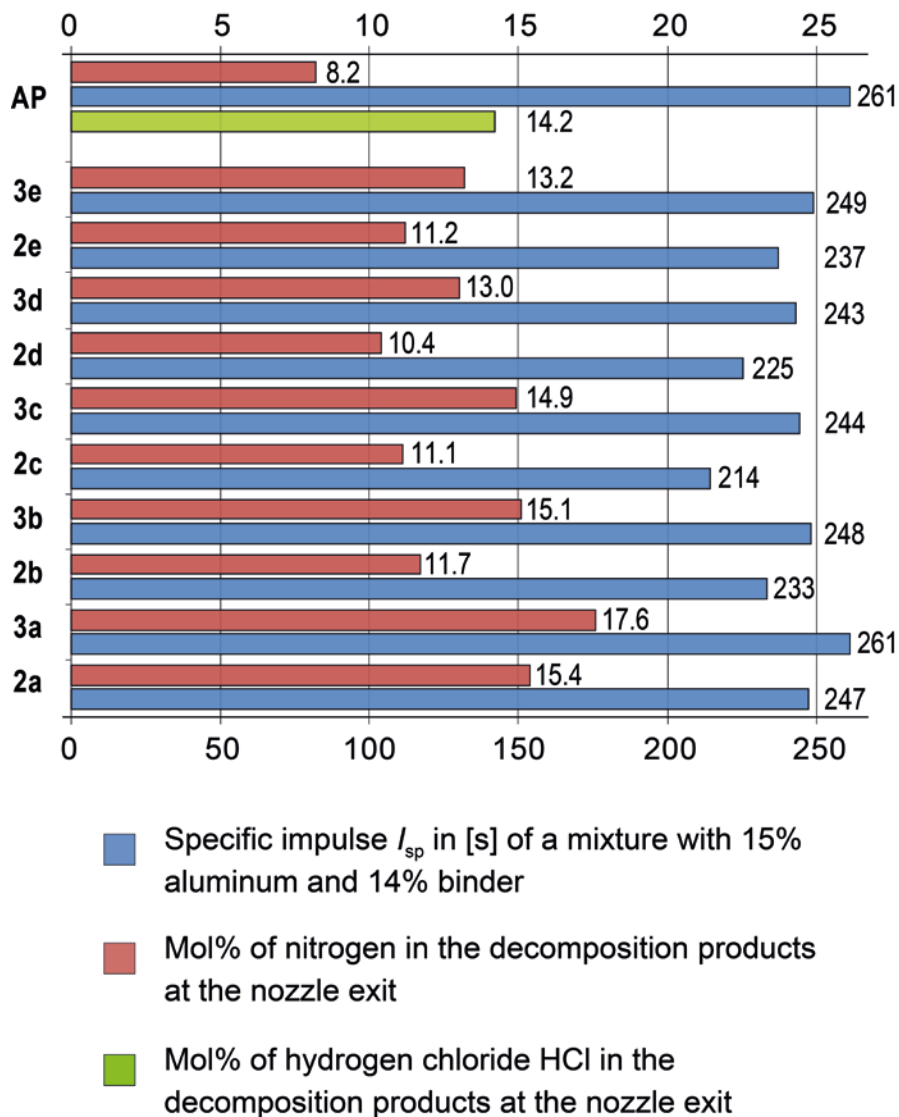


Figure 2-8: Specific impulse I_{sp} and the nitrogen/hydrogen chloride content (Mol%) of the decomposition products calculated with EXPLO5 V.6.02.

2.4 Conclusion

A facile, two-step synthesis route for nitrocarbamates is presented by the reaction of polynitro alcohols with chlorosulfonyl isocyanate (CSI) and subsequent nitration. The carbamate-forming reaction with CSI has several advantages such as fast reaction times, simple manageable starting materials, and very high yields. The nitration to the nitrocarbamate proceeds in all cases with a mixture of nitric and sulfuric acid. All new compounds were fully characterized, including the X-ray molecular structure. The specific impulse I_{sp} of compositions are comparable with compositions using ammonium perchlorate (AP) as oxidizer. Favorably, the burning and combustion of these compounds produces no toxic substances such as hydrogen chloride.

2.5 Experimental Section

2.5.1 General Information

All chemicals were used as supplied. The nitro alcohols 2,2,2-trinitroethanol,^[4a] 2-fluoro-2,2-dinitroethanol,^[1b] 2,2-dinitropropan-1,3-diol,^[14] 2,2-dinitropropanol^[15], and 4,4,4-trinitrobutanol^[16] were synthesized according to the literature. Raman spectra were recorded in a glass tube with Nd:YAG laser excitation up to 1000 mW (at 1064 nm) in the range between 400 and 4000 cm^{-1} . Infrared spectra were measured with an ATR device. All spectra were recorded at ambient temperature. NMR spectra were recorded with a 400 Hz instrument, and chemical shifts were determined with respect to external standard (Me_4Si ^1H and ^{13}C , MeNO_2 ^{14}N , and ^{15}N). Melting and decomposition points were measured with a DSC with a heating rate of 5 $^\circ\text{C min}^{-1}$ in a temperature range of 15–300 $^\circ\text{C}$. The melting points were checked by a melting point apparatus (not corrected).

2.5.2 X-ray Crystallography

The low-temperature (173 K) single-crystal X-ray diffraction were performed with $\text{MoK}\alpha$ radiation ($\lambda = 0.71073 \text{ \AA}$). Data collection was performed using CRYSA LIS CCD software.^[17] The data reduction was carried out using CRYSA LIS RED software.^[18] The solution of the structure was performed by direct methods (SIR97),^[19] refined by the full-matrix least-squares on F2 (SHELXL)^[20] implemented in the WINGX software package,^[21] and finally checked with the PLATON software^[22]. All non-hydrogen atoms were refined anisotropically. The hydrogen atom positions were located in a difference Fourier map. ORTEP plots are shown with thermal ellipsoids at the 50% probability level.

2.5.3 Energetic Properties and Computational Calculation

The sensitivity data were performed using a BAM drophammer and a BAM friction tester.^[23] All *ab initio* calculations were carried out using the program package Gaussian 09 (Rev. A.03)^[24] and visualized by GaussView 5.08.^[25] Structure optimizations and frequency analyses were performed with Becke's B3 three-parameter hybrid functional using the LYP correlation functional (B3LYP). For C, H, N, and O, a correlation consistent polarized double- ξ basis set was used (cc-pVDZ). The structures were optimized with symmetry constraints, and the energy is corrected with the

zero-point vibrational energy.^[26] The enthalpies (H) and free energies (G) were calculated using the complete basis set (CBS) method in order to obtain accurate values. The CBS models use the known asymptotic convergence of pair natural orbital expressions to extrapolate from calculations using a finite basis set to the estimated complete basis set limit. CBS-4 starts with a HF/3-21G(d) geometry optimization, which is the initial guess for the following SCF calculation as a base energy and a final MP2/6-31+G calculation with a CBS extrapolation to correct the energy in second order. The used CBS-4 M method additionally implements a MP4(SDQ)/6-31+(d,p) calculation to approximate higher order contributions and also includes some additional empirical corrections.^[27] The enthalpies of the gas-phase species were estimated according to the atomization energy method.^[28] All calculations affecting the detonation parameters were carried out using the program package EXPLO5 V6.02 (EOS BKWG-S).^[29] The detonation parameters were calculated at the Chapman-Jouguet (CJ) point with the aid of the steady-state detonation model using a modified Becker–Kistiakowski–Wilson equation of state for modeling the system. The CJ point is found from the Hugoniot curve of the system by its first derivative. The specific impulses I_{sp} were also calculated with the program package EXPLO5 V6.02 program, assuming an isobaric combustion of a composition of an oxidizer, aluminum as fuel, 6% polybutadiene acrylic acid, 6% polybutadiene acrylonitrile as binder and 2% bisphenol A as epoxy curing agent.^[29b] A chamber pressure of 70.0 bar, an initial temperature of 3300 K and an ambient pressure of 1.0 bar with equilibrium expansion conditions were estimated for the calculations.

2.5.4 Synthesis

CAUTION! All compounds are energetic materials with sensitivity toward heat, impact, and friction. No hazards occurred during preparation and manipulation; additional proper protective precautions (face shield, leather coat, earthened equipment and shoes, Kevlar® gloves and ear plugs) should be used when undertaking work with these compounds.

2,2,2-Trinitroethyl carbamate (2a): 2,2,2-Trinitroethanol (**1a**) (0.76 g, 4.2 mmol) was dissolved in dry acetonitrile (10 mL) and placed in an ice bath. Chlorosulfonyl isocyanate (CSI) (0.64 g, 4.5 mmol) was added very slowly at 0 °C. The ice bath was removed, and stirring at room temperature was continued for 1.5 h. The reaction mixture was again cooled with an ice bath, water (50 mL) was added with caution, and the mixture was stirred for 10 min at room

temperature. The precipitate was filtered to obtain 0.90 g (96%) colorless 2,2,2-trinitroethyl carbamate (**2a**).

DSC (5 °C min⁻¹): 91–92 °C (mp. range), 169 °C (onset dec.). IR: (ATR, cm⁻¹): ν = 3447 (w), 3354 (w), 3302 (w), 2963 (m), 1729 (m), 1590 (s), 1441 (w), 1399 (m), 1367 (w), 1325 (m), 1300 (m), 1248 (w), 1166 (w), 1138 (w), 1105 (m), 1027 (w), 910 (w), 873 (w), 858 (w), 804 (m), 784 (m), 771 (m), 746 (w), 673 (w), 646 (w), 606 (w), 544 (m). Raman: (400 mW, cm⁻¹): ν = 3301 (4), 3003 (23), 2962 (51), 2828 (4), 1719 (17), 1629 (31), 1609 (28), 1587 (18), 1445 (17), 1404 (8), 1369 (54), 1304 (31), 1250 (15), 1171 (10), 1145 (10), 1112 (9), 1091 (9), 1027 (17), 911 (21), 878 (13), 860 (100), 802 (14), 786 (12), 745 (10), 681 (10), 646 (12), 550 (18), 426 (55), 397 (46), 378 (72), 307 (48), 266 (21), 212 (33). ¹H NMR (acetone-D₆, 399.8 MHz) δ = 6.76 (s, 1H, NH₂), 6.47 (s, 1H, NH₂), 5.68 (s, 2H, CH₂) ppm. ¹³C{¹H} NMR (acetone-D₆, 100.5 MHz) δ = 154.5 (CO₂N), 125.7 (C(NO₂)₃), 61.8 (CH₂) ppm. ¹⁴N NMR (acetone-D₆, 28.9 MHz) δ = -33 (C(NO₂)₃), -310 (br, NH₂) ppm. MS (DEI+) *m/e* (%): 225 (15) [(M + H)⁺]. EA (C₃H₄N₄O₈): C, 16.08; H, 1.80; N, 25.00. Found: C, 15.89; H, 1.78; N, 25.12. BAM drophammer: >40 J. Friction tester: 64 N. ESD: 0.15 J (grain size <500 μ m).

2,2,2-Trinitroethyl nitrocarbamate (3a): Prepared according ref^[1e].

2-Fluoro-2,2-dinitroethyl carbamate (2b): 2-Fluoro-2,2-dinitroethanol (**2a**) (1.70 g, 11.0 mmol) was dissolved in dry acetonitrile (25 mL) and placed in an ice bath. Chlorosulfonyl isocyanate CSI (1.84 g, 13.0 mmol) was added very slowly at 0 °C. The ice bath was removed, and stirring at room temperature was continued for 1 h. The reaction mixture was again cooled with an ice bath, water (10 mL) was added with caution, and the mixture was stirred for 10 min at room temperature. The organic solvent was removed on the rotary evaporator. The aqueous solution was extracted with dichloromethane (5 x 50 mL). The combined organic phases were washed with brine (2 x 80 mL) and dried with magnesium sulfate. The solvent was removed under reduced pressure to obtain a slightly yellow oil 2.12 g (98%) of 2-fluoro-2,2-dinitroethanol carbamate (**2b**).

DSC (5 °C min⁻¹): 212 °C (boil.), 219 °C (onset dec.). IR: (ATR, cm⁻¹): ν = 3357 (w), 2924 (w), 2260 (w), 1744 (m), 1587 (vs), 1445 (w), 1402 (w), 1352 (w), 1314 (m), 1230 (w), 1082 (m), 1003 (w), 918 (w), 878 (w), 850 (m), 798 (s), 759 (w). Raman (1064 nm, 500 mW, cm⁻¹): ν = 3353 (5), 3313 (4), 3190 (4), 3026 (13), 2971 (40), 2258 (4), 1733 (9), 1595 (24), 1435 (11), 1370 (56), 1324 (22), 1247 (8), 1127 (20), 1027 (14), 923 (10), 852 (100), 796 (8), 760 (5), 676 (7), 569 (12), 504 (14), 423 (27), 378 (26), 352 (34), 237 (20). ¹H NMR (CDCl₃, 399.8 MHz) δ : 5.42 (br, 1H, NH₂), 5.27 (br, 1H, NH₂), 5.15 (d, ³J (H,F) = 15.9 Hz, 2H; CH₂) ppm. ¹³C {¹H} NMR (CDCl₃, 100.5

MHz) δ : 154.2 (CO), 119.2 (d, 1J (C,F) = 294.3 Hz; $C(NO_2)_2F$), 60.9 (d, 2J (C,F) = 19.2 Hz; CH_2) ppm. ^{14}N NMR ($CDCl_3$, 28.9 MHz) δ : -25 (NO_2), -311 (NH_2) ppm. ^{19}F NMR ($CDCl_3$, 376.3 MHz) δ : -111.8 (t, br) ppm. EA ($C_3H_4N_3O_6F$): C, 18.28; H, 2.05; N, 21.32. Found: C, 18.52; H, 2.17; N, 20.98. MS m/e (EI) 198.1 $[(M + H)^+]$. BAM drophammer: 40 J. Friction tester: 360 N (liquid).

2-Fluoro-2,2-dinitroethyl nitrocarbamate (3b): Into concentrated sulfuric acid (2 mL) was dropped fuming nitric acid (>99.5%, 2 mL) at 0 °C. To this chilled nitration mixture 2-fluoro-2,2-dinitroethyl carbamate (**2b**) (0.39 mg, 2.0 mmol) in small portions was added. The solution was stirred for 10 min at this temperature and 1 h at ambient temperature. The mixture was poured onto ice-water (200 mL) and extracted with ethyl acetate (3 x 75 mL). The combined organic phases were washed with water (2 x 100 mL), brine (1 x 80 mL) and dried with magnesium sulfate. The solvent was removed under reduced pressure to get a crude oily solid, which solidified after drying. After recrystallization from carbon tetrachloride 0.33 mg (98%) of colorless pure 2-fluoro-2,2-dinitroethyl nitrocarbamate (**3b**) was obtained.

DSC (5 °C min^{-1}): 80–81 °C (mp. range), 145 °C (onset dec.). IR (ATR, cm^{-1}): ν = 3244 (w), 3021 (w), 2976 (w), 1768 (s), 1611 (s), 1595 (s), 1453 (m), 1444 (s), 1351 (m), 1305 (s), 1244 (m), 1179 (s), 1128 (s), 1114 (m), 1041 (w), 1007 (w), 973 (s), 930 (m), 849 (w), 826 (m), 773 (s), 748 (m), 734 (m), 660 (w). Raman (1064 nm, 700 mW, cm^{-1}): ν = 3223 (25), 3126 (24), 3022 (48), 2979 (88), 2869 (9), 2816 (25), 1830 (24), 1769 (73), 1698 (25), 1642 (29), 1612 (55), 1603 (52), 1588 (49), 1534 (26), 1470 (34), 1447 (56), 1390 (46), 1362 (75), 1318 (97), 1276 (27), 1246 (35), 1206 (32), 1127 (41), 1112 (31), 1043 (96), 1007 (100), 973 (34), 932 (30), 853 (81), 778 (32), 733 (27), 576 (35), 492 (56), 459 (76), 416 (75), 369 (89), 333 (74), 282 (51), 223 (84). 1H NMR (acetone- D_6 , 399.8 MHz) δ : 13.58 (br, 1H, NH), 5.67 (d, 3J (H,F) = 15.9 Hz, 2H; CH_2) ppm. ^{13}C $\{^1H\}$ NMR (acetone- D_6 , 100.5 MHz) δ : 146.7 (CO), 119.5 (d, 1J (C,F) = 294.4 Hz; $C(NO_2)_2F$), 61.9 (d, 2J (C,F) = 20.0 Hz; CH_2) ppm. ^{15}N NMR (acetone- D_6 , 40.6 MHz) δ = -24.8 (CNO_2), -47.8 ($NHNO_2$), -190.5 ($NHNO_2$) ppm. ^{19}F NMR (acetone- D_6 , 376.3 MHz) δ = -111.7 (br) ppm. EA ($C_3H_3N_4O_8F$): C, 14.88; H, 1.25; N, 23.14. Found: C, 15.08; H, 1.28; N, 22.81. MS m/e (DEI+) 243.1 $[(M + H)^+]$. BAM drophammer: 10 J. Friction tester 360 N, ESD: 0.15 J (grain size 100 - 500 μm).

2,2-Dinitropropane-1,3-diyl dicarbamate (2c): 2,2-Dinitropropane-1,3-diol (1.66 g, 10.0 mmol) was dissolved in dry acetonitrile (20 mL) and placed in an ice bath, and chlorosulfonyl isocyanate CSI (3.26 g, 23 mmol) was added very slowly at 0 °C. The ice bath was removed, and stirring at room temperature was continued for 2 h. The reaction mixture was again cooled with an ice bath,

water (5 mL) was added with caution, and the mixture was stirred for 10 min at room temperature. Upon cooling, a white precipitate formed that was filtered and washed with cold water. The solid was dried under high vacuum to obtain 2.43 g (96%) of colorless pure 2,2-dinitropropane-1,3-diyl dicarbamate (**2c**).

DSC (5 °C min⁻¹): 136–137 °C (mp. range), 182 °C (onset. dec.). IR (ATR, cm⁻¹): ν = 3414 (m), 3337 (m) 3286 (m), 2959 (w), 1766 (w), 1713 (s), 1613 (m), 1584 (vs), 1568 (s), 1452 (m), 1442 (m), 1393 (s), 1334 (vs), 1299 (s), 1256 (m), 1151 (m), 1126 (m), 1066 (vs), 932 (m), 886 (m), 853 (s), 785 (m), 775 (s), 760 (m), 741 (m), 680 (m). Raman (1064 nm, 1000 mW, cm⁻¹): ν = 3008 (39), 2972 (73), 1712 (40), 1611 (7), 1583 (34), 1456 (31), 1444 (7), 1376 (41), 1330 (25), 1303 (19), 1259 (25), 1143 (31), 1104 (10), 984 (9), 933 (58), 888 (30), 858 (95), 762 (12), 683 (33), 582 (14), 557 (10), 522 (27), 506 (11), 409 (81), 360 (42), 292 (28), 225 (19). ¹H NMR (acetone-D₆, 399.8 MHz) δ : 6.53 (br, 2H, NH₂), 6.28 (br, 2H, NH₂), 5.00 (s, 4H, CH₂) ppm. ¹³C{¹H} NMR (acetone-D₆, 100.5 MHz) δ : 154.4 (CO(NH₂)OR), 115.2 (C(NO₂)₂), 60.9 (CH₂) ppm. ¹⁴N NMR (acetone-D₆, 28.9 MHz) δ : -16 (NO₂), -309 (NH₂) ppm. EA (C₅H₈N₄O₈): C, 23.82; H, 3.20; N, 22.22. Found: C, 23.90; H, 3.18; N, 22.22. MS m/e (DEI⁺): 254.1 [(M + 2H)⁺], 253 [(M + H)⁺], BAM drophammer: 30 J. Friction tester: 360 N. ESD: >0.2 J (grain size 100 - 250 μ m).

2,2-Dinitropropane-1,3-diyl bis(nitrocarbamate) (3c): Fuming nitric acid (>99.5%, 4 mL) was dropped into concentrated sulfuric acid (4 mL) at 0 °C. To this nitration mixture chilled in an ice bath was 2,2-dinitropropane-1,3-diyl dicarbamate **3b** (504 mg, 2.0 mmol) in small portions, and the mixture was stirred for 10 min at 0 °C and 1 h at ambient temperature. The nitration mixture was poured onto ice-water (200 mL) and extracted immediately with ethyl acetate (3 x 50 mL). The combined organic phases were washed with water (3 x 100 mL) and brine (1 x 100 mL) and dried with magnesium sulfate. The solvent was removed under reduced pressure to get crude slight yellow oily product. A colorless precipitate could be obtained by treating the slurry with chloroform and was recrystallized from 1,1-dichloroethane to obtain 540 mg (79%) of colorless pure 2,2-dinitropropane-1,3-diyl bis(nitrocarbamate) (**3c**).

DSC (5 °C min⁻¹): 152 - 153 °C (mp. range), 158 °C (onset dec.). IR (ATR, cm⁻¹): ν = 3240 (w), 3198 (w), 3055 (w), 2897 (w), 1773 (m), 1617 (m), 1597 (m), 1564 (m), 1446 (m), 1363 (w), 1322 (m), 1291 (w), 1185 (s), 1169 (s), 1104 (w), 1010 (w), 974 (m), 880 (w), 866 (w), 822 (m), 746 (m), 724 (w), 675 (w). Raman (1064 nm, 800 mW, cm⁻¹): ν = 3211 (7), 3038 (16), 3021 (17), 2993 (33), 2976 (32), 2888 (7), 1769 (39), 1604 (18), 1593 (24), 1566 (10), 1454 (35), 1400 (14), 1365 (20), 1323 (61), 1273 (20), 1196 (16), 1177 (10), 1133 (12), 1081 (22), 1025 (100), 980 (16), 949 (12), 869

(47), 828 (11), 763 (12), 725 (9), 590 (11), 459 (37), 419 (42), 332 (34), 287 (20), 256 (33), 225 (20). ^1H NMR (acetone- D_6 , 399.8 MHz) δ : 13.75 (br, 2H; NH), 5.35 (s, 4H; CH_2) ppm. ^{13}C $\{^1\text{H}\}$ NMR (acetone- D_6 , 100.5 MHz) δ : 147.5 (CO), 114.6 ($\text{C}(\text{NO}_2)_2$), 62.9 (CH_2) ppm. ^{14}N NMR (acetone- D_6 , 28.9 MHz) δ : -20 (NO_2), -48 (NO_2NH), -206 (NHNO_2) ppm. EA ($\text{C}_5\text{H}_6\text{N}_6\text{O}_{12}$): C, 17.55; H, 1.77; N, 24.56. Found: C, 17.85; H, 1.76; N, 24.39. MS m/e (DEI+) 343.1 $[(\text{M} + \text{H})^+]$. BAM drophammer: 4 J. Friction tester: 240 N, ESD: 0.10 J (grain size 100 - 500 μm).

2,2-Dinitropropyl carbamate (2d): 2,2-Dinitropropanol (1.50 g, 10.0 mmol) was dissolved in dry acetonitrile (15 mL) and placed in an ice bath and chlorosulfonyl isocyanate CSI (1.70 g, 12 mmol) was added very slowly at 0 °C. The ice bath was removed, and stirring at room temperature was continued for 1 h. The reaction mixture was again cooled with an ice bath, water (10 mL) was added with caution, and the mixture was stirred for 10 min at room temperature. The organic solvent was removed on the rotary evaporator. The residue crystallized on cooling, was filtered, and was washed with cold water. The precipitate was recrystallized from a hot mixture of water (25 mL) and ethanol (5 mL) and afterward dried under high vacuum to obtain 1.71 g (90%) of colorless pure 2,2-dinitropropyl carbamate (**2d**).

DSC (5 °C min^{-1}): 68 - 70 °C (mp. range), 192 °C (onset dec.). IR (ATR, cm^{-1}): ν = 3437 (w), 3343 (w), 3291 (w), 2897 (w), 1712 (s), 1615 (w), 1583 (s), 1561 (s), 1459 (w), 1447 (w), 1400 (s), 1383 (m), 1325 (s), 1274 (w), 1224 (w), 1157 (w), 1122 (w), 1086 (s), 977 (w), 946 (w), 901 (w), 870 (m), 847 (m), 777 (m), 769 (m), 726 (w), 692 (w), 660 (w). Raman (1064 nm, 500 mW, cm^{-1}): ν = 3031 (48), 3021 (32), 2986 (41), 2956 (58), 2929 (6), 1710 (18), 1596 (9), 1575 (29), 1447 (25), 1391 (29), 1366 (26), 1331 (22), 1277 (10), 1229 (7), 1127 (17), 1103 (11), 979 (14), 948 (18), 904 (16), 873 (10), 849 (100), 770 (11), 728 (8), 693 (14), 661 (6), 567 (19), 504 (21), 469 (10), 414 (43), 365 (15), 338 (42), 248 (17), 211 (26). ^1H NMR (acetone- D_6 , 399.8 MHz) δ : 6.41 (br, 1H; NH_2), 6.25 (br, 1H; NH_2), 4.96 (s, 2H; CH_2O), 2.28 (s, 3H; CH_3) ppm. ^{13}C $\{^1\text{H}\}$ NMR (acetone- D_6 , 100.5 MHz) δ : 155.6 (CO), 117.7 ($\text{C}(\text{NO}_2)_2$), 64.5 (CH_2), 20.7 (CH_3) ppm. ^{14}N NMR (acetone- D_6 , 28.9 MHz) δ : = -10 (NO_2), -310 (NH_2) ppm. EA ($\text{C}_4\text{H}_7\text{N}_3\text{O}_6$): C, 24.88; H, 3.65; N, 21.76. Found: C, 24.95; H, 3.79; N, 21.61. MS m/e (DEI+) 194.1 $[(\text{M} + \text{H})^+]$. BAM drophammer: 40 J. Friction tester: 360 N. ESD: 0.20 J (grain size < 100 μm).

2,2-Dinitropropyl nitrocarbamate (3d): Fuming nitric acid (>99.5%, 2 mL) was dropped into concentrated sulfuric acid (2 mL) at 0 °C. To this nitration mixture chilled in an ice bath was added the 2,2-dinitropropyl carbamate **2d** (0.38 g, 2.0 mmol) in small portions. The mixture was stirred for a further 60 min at this temperature and poured onto ice-water (200 mL). The aqueous solution was extracted with ethyl acetate (3 x 75 mL). The combined organic phases were washed

with water (2 x 100 mL) and brine (1 x 80 mL) and dried with magnesium sulfate. The solvent was removed under reduced pressure to give a pale yellow oil, which solidified after drying after 2 days. After recrystallization from carbon tetrachloride 0.41 g (85%) of colorless pure 2,2-dinitropropyl nitrocarbamate (**2d**) was obtained.

DSC (5 °C min⁻¹): 76 - 77 °C (mp. range), 140 °C (onset dec.). IR (ATR, cm⁻¹): ν = 3264 (w), 2982 (w), 1762 (s), 1611 (s), 1589 (s), 1565 (s), 1447 (s), 1397 (m), 1348 (m), 1326 (m), 1274 (w), 1181 (s), 1152 (s), 1124 (m), 1017 (w), 976 (s), 876 (w), 849 (m), 822 (m), 760 (w), 750 (m), 739 (m), 729 (w), 669 (w). Raman (1064 nm, 700 mW, cm⁻¹): ν = 3040 (58), 2985 (68), 2958 (88), 2925 (14), 1763 (45), 1639 (13), 1609 (23), 1580 (38), 1566 (19), 1450 (52), 1400 (37), 1360 (39), 1332 (41), 1319 (53), 1275 (18), 1237 (13), 1203 (18), 1128 (28), 1108 (18), 1017 (100), 978 (26), 947 (20), 878 (22), 851 (87), 826 (15), 760 (14), 731 (23), 671 (18), 572 (34), 503 (39), 458 (57), 412 (63), 357 (41), 319 (44), 234 (55). ¹H NMR (acetone-D₆, 399.8 MHz) δ : 13.56 (br, 1H; NH), 5.21 (s, 2H; CH₂O), 2.34 (s, 3H; CH₃) ppm. ¹³C {¹H} NMR (acetone-D₆, 100.5 MHz) δ : 147.1 (CO), 116.1 (C(NO₂)₂), 64.8 (CH₂), 19.7 (CH₃) ppm. ¹⁴N NMR (acetone-D₆, 28.9 MHz) δ : -11 (CNO₂), -47 (NHNO₂), -201 (NHNO₂) ppm. EA (C₄H₆N₄O₈): C, 20.18; H, 2.54; N, 23.53. Found: C, 20.43; H, 2.65; N, 23.12. MS m/e (DEI+) [(M + H)⁺]. BAM drophammer: 20 J. Friction tester: 360 N, ESD: 0.20 J (grain size < 100 μ m).

4,4,4-Trinitrobutyl carbamate (2e): 4,4,4-Trinitrobutanol (1.04 g, 5.0 mmol) was dissolved in dry acetonitrile (20 mL) and placed in an ice bath, and chlorosulfonyl isocyanate CSI (0.72 g, 5.1 mmol) was added very slowly at 0 °C. The ice bath was removed, and stirring at room temperature was continued for 1 h. The reaction mixture was again cooled with an ice bath, water (10 mL) was added with caution, and the mixture was stirred for 10 min at room temperature. The organic solvent was removed on the rotary evaporator. The yellow oily residue was recrystallized from a hot mixture of water (90 mL) and ethanol (10 mL), filtered, and washed with cold water. The solid was dried under high vacuum to obtain 1.22 g (96%) of colorless pure 4,4,4-trinitrobutanol carbamate (**2e**).

DSC (5 °C min⁻¹): 53 - 54 °C (mp. range), 156 °C (onset dec.). IR (ATR, cm⁻¹): ν = 3485 (w), 3322 (w), 3252 (w), 2983 (w), 2358 (w), 1731 (w), 1698 (m), 1574 (s), 1474 (w), 1441 (w), 1410 (m), 1383 (w), 1333 (m), 1301 (s), 1252 (w), 1225 (w), 1141 (w), 1114 (w), 1089 (m), 1074 (s), 1024 (w), 940 (w), 870 (w), 854 (m), 805 (m), 791 (s), 784 (s), 743 (w), 708 (w), 680 (w). Raman (1064 nm, 500 mW, cm⁻¹): ν = 2983 (39), 2971 (39), 2946 (57), 2915 (21), 1687 (12), 1603 (29), 1476 (18), 1445 (9), 1428 (20), 1364 (35), 1307 (39), 1256 (10), 1228 (10), 1118 (20), 1090 (18), 1024 (9), 970 (14), 941 (13), 872 (26), 857 (100), 797 (11), 723 (9), 675 (14), 562 (16), 505 (19), 415 (35), 375

(70), 334 (21), 279 (25). ^1H NMR (acetone- D_6 , 399.8 MHz) δ : 5.92 (br, 2H; NH_2), 4.15–4.12 (m, 2H; CH_2O), 3.46–3.42 (m, 2H; CH_2), 2.09–2.01 (m, 2H; $\text{CH}_2\text{CH}_2\text{CH}_2\text{O}$) ppm. ^{13}C $\{^1\text{H}\}$ NMR (acetone- D_6 , 100.5 MHz) δ : 156.5 (CO), 131.1 ($\text{C}(\text{NO}_2)_3$), 62.0 (CH_2O), 31.0 ($\text{CH}_2\text{C}(\text{NO}_2)_3$), 24.0 ($\text{CH}_2\text{CH}_2\text{O}$) ppm. ^{14}N NMR (acetone- D_6 , 28.9 MHz) δ : -28 (CNO_2), -314 (NH_2) ppm. EA ($\text{C}_5\text{H}_8\text{N}_4\text{O}_8$): C, 23.82; H, 3.20; N, 22.22. Found: C, 23.87; H, 3.31; N, 22.05. MS m/e (FAB+) 253.1 $[(\text{M} + \text{H})^+]$. BAM drophammer: 40 J. Friction tester: 360 N. ESD: 0.20 J (grain size 100 - 500 μm).

4,4,4-Trinitrobutyl nitrocarbamate (3e): Fuming nitric acid (>99.5%, 2 mL) was dropped into concentrated sulfuric acid (2 mL) at 0 °C. To this nitration mixture chilled in an ice bath was added the 4,4,4-trinitrobutyl carbamate **2e** (504 mg, 2.0 mmol) in small portions. The mixture was stirred for a further 60 min at this temperature and poured onto ice-water (200 mL). The aqueous solution extracted with ethyl acetate (3 x 75 mL). The combined organic phases were washed with water (2 x 100 mL), brine (1 x 80 mL) and was dried with magnesium sulfate. The solvent was removed under reduced pressure to obtain a pale yellow oil, which solidified after several hours under high vacuum. After recrystallization from a mixture of water/ethanol (10:1) 172 mg (29%) of colorless pure 4,4,4-trinitrobutyl nitrocarbamate was obtained (**3e**).

DSC (5 °C min^{-1}): 82 - 84 °C (mp. range), 145 °C (onset dec.). IR (ATR, cm^{-1}): $\nu = 3167$ (w), 3047 (w), 1745 (s), 1616 (m), 1594 (m), 1578 (s), 1469 (w), 1443 (m), 1389 (w), 1371 (w), 1307 (m), 1253 (w), 1228 (w), 1186 (s), 1144 (m), 1118 (w), 1083 (w), 1030 (w), 996 (w), 966 (w), 942 (m), 903 (w), 882 (m), 856 (w), 822 (w), 799 (m), 758 (w), 732 (w). Raman (1064 nm, 500 mW, cm^{-1}): $\nu = 3159$ (6), 2981 (49), 2947 (64), 2876 (9), 2831 (6), 2739 (6), 1756 (26), 1612 (45), 1473 (19), 1447 (24), 1423 (24), 1362 (44), 1331 (42), 1309 (39), 1256 (16), 1228 (12), 1195 (10), 1119 (14), 1084 (20), 1007 (51), 962 (10), 885 (12), 856 (100), 793 (10), 729 (10), 565 (15), 471 (19), 450 (28), 374 (55), 332 (18), 296 (25). ^1H NMR (acetone- D_6 , 399.8 MHz) δ : 13.33 (br, 1H; NH), 4.46–4.43 (m, 2H; CH_2O), 3.56–3.52 (m, CH_2), 2.22–2.12 (m, 2H; $\text{CH}_2\text{CH}_2\text{CH}_2\text{O}$) ppm. ^{13}C $\{^1\text{H}\}$ NMR (acetone- D_6 , 100.5 MHz) δ : 148.3 (CO), 130.9 ($\text{C}(\text{NO}_2)_3$), 64.6 (CH_2O), 30.8 ($\text{CH}_2\text{C}(\text{NO}_2)_3$), 23.3 ($\text{CH}_2\text{CH}_2\text{O}$) ppm. ^{14}N NMR (acetone- D_6 , 28.9 MHz) δ : -28 (CNO_2), -45 (NHNO_2), -204 (NHNO_2) ppm. EA ($\text{C}_5\text{H}_7\text{N}_5\text{O}_{10}$): C, 20.21; H, 2.37; N, 23.57. Found: C, 20.33; H, 2.39; N, 23.36. MS m/e (DEI+): 298.1 $[(\text{M} + \text{H})^+]$. BAM drophammer: 20 J. Friction tester: 360 N. ESD: 0.20 J (grain size < 100 μm).

2.6 References

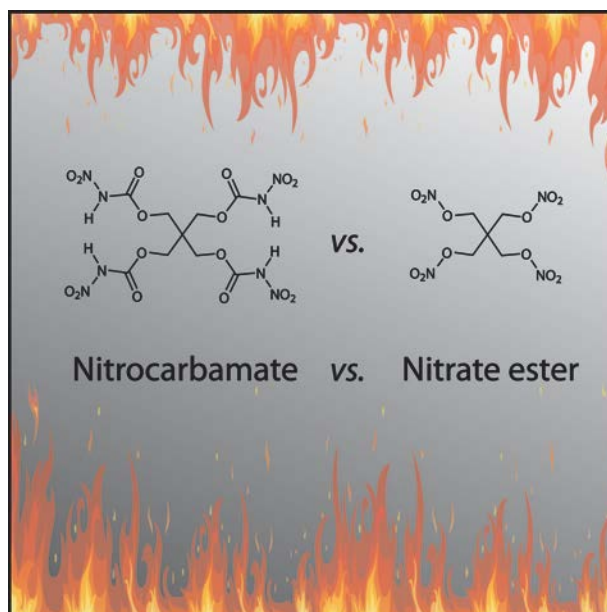
- [1] a) T. M. Klapötke, *Chemistry of High-Energy Materials*, 2nd ed., deGruyter, Berlin, **2012**; b) T. M. Klapötke, B. Krumm, R. Moll, *Chem. – Eur. J.* **2013**, *19*, 12113–12123; c) T. M. Klapötke, B. Krumm, S. F. Rest, M. Sućeska, *Z. Anorg. Allg. Chem.* **2014**, *640*, 84–92; d) T. T. Vo, D. A. Parrish, J. M. Shreeve, *J. Am. Chem. Soc.* **2014**, *136*, 11934–11937; e) Q. J. Axthammer, T. M. Klapötke, B. Krumm, R. Moll, S. F. Rest, *Z. Anorg. Allg. Chem.* **2014**, *640*, 76–83.
- [2] a) G. Gattow, W. K. Knoth, *Z. Anorg. Allg. Chem.* **1983**, *499*, 194–204; b) Q. J. Axthammer, B. Krumm, T. M. Klapötke, *Eur. J. Org. Chem.* **2015**, *2015*, 723–729.
- [3] L. Cotarca, H. Eckert, *Phosgenations – A Handbook*, Wiley-VCH, Weinheim, **2005**.
- [4] a) H. Feuer, T. Kucera, *J. Org. Chem.* **1960**, *25*, 2069–2070; b) W. H. Gilligan, S. L. Stafford, *Synthesis* **1979**, 600–602.
- [5] a) D. N. Dhar, P. Dhar, *The Chemistry of Chlorosulfonyl Isocyanate*, World Scientific, Singapore, **2002**; b) R. Graf, *Chem. Ber.* **1956**, *89*, 1071–1079; c) D. N. Dhar, K. S. K. Murthy, *Synthesis* **1986**, *1986*, 437–449.
- [6] J. K. Rasmussen, A. Hassner, *Chem. Rev. (Washington, DC, U. S.)* **1976**, *76*, 389–408.
- [7] J. P. Senet, C. Ucciani **1977**, FR 2327228.
- [8] C. R. Kemnitz, M. J. Loewen, *J. Am. Chem. Soc.* **2007**, *129*, 2521–2528.
- [9] G. Socrates, *Infrared and Raman Characteristic Group Frequencies: Tables and Charts*, 3rd ed., John Wiley & Sons, Chichester, **2004**.
- [10] a) Q. J. Axthammer, M. A. Kettner, T. M. Klapötke, R. Moll, S. F. Rest, *New Trends Res. Energ. Mater., Proc. Semin., 16th* **2013**, pp. 29–39; b) T. M. Klapötke, B. Krumm, R. Moll, in *New Trends Res. Energ. Mater., Proc. Semin., 13th, Vol. 2*, **2010**, pp. 523–527.
- [11] R. Meyer, J. Köhler, A. Homburg, *Explosives*, Wiley-VCH, Weinheim, **2007**.
- [12] J. Akhavan, *The Chemistry of Explosives*, 2nd ed., Royal Soc. of Chemistry, Cambridge, **2004**.
- [13] J. Dumont, The Effects of Ammonium Perchlorate on Reproduction and Development of Amphibians, <http://www.dtic.mil/cgi-bin/GetTRDoc?Location=U2&doc=GetTRDoc.pdf&AD=ADA495519> (12/2015), **2008**.
- [14] M. H. Gold, E. E. Hamel, K. Klager, *J. Org. Chem.* **1957**, *22*, 1665–1667.
- [15] L. Garver, V. Grakauskas, K. Baum, *J. Org. Chem.* **1985**, *50*, 1699–1702.
- [16] J. F. Weber, M. B. Frankel, *Propellants, Explos., Pyrotech.* **1990**, *15*, 26–29.
- [17] Oxford Diffraction Ltd., *CrysAlis CCD*, Version 1.171.35. (release 16-05-2011 CrysAlis 171.Net), Abingdon, Oxford, **2011**.
- [18] Oxford Diffraction Ltd., *CrysAlis RED*, Version 1.171.35.11 (release 16-05-2011 CrysAlis 171.NET), Abingdon, Oxford, **2011**.

- [19] A. Altomare, M. C. Burla, M. Camalli, G. L. Cascarano, C. Giacovazzo, A. Guagliardi, A. G. G. Moliterni, G. Polidori, R. Spagna, *J. Appl. Crystallogr.* **1999**, *32*, 115–119.
- [20] a) G. M. Sheldrick, *SHELX-97, Programs for Crystal Structure Determination*, **1997**; b) G. M. Sheldrick, *Acta Crystallogr., Sect. A: Found. Crystallogr.* **2008**, *A64*, 112–122.
- [21] L. Farrugia, *J. Appl. Crystallogr.* **1999**, *32*, 837–838.
- [22] A. Spek, *Acta Crystallogr., Sect. D: Biol. Crystallogr.* **2009**, *65*, 148–155.
- [23] M. Göbel, T. M. Klapötke, *Adv. Funct. Mater.* **2009**, *19*, 347–365.
- [24] M. J. Frisch, G. W. Trucks, H. B. Schlegel, G. E. Scuseria, M. A. Robb, J. R. Cheeseman, V. B. G. Scalmani, B. Mennucci, G. A. Petersson, H. Nakatsuji, M. Caricato, X. Li, H. P. Hratchian, A. F. Izmaylov, J. Bloino, G. Zheng, J. L. Sonnenberg, M. Hada, M. Ehara, K. Toyota, R. Fukuda, J. Hasegawa, M. Ishida, T. Nakajima, Y. Honda, O. Kitao, H. Nakai, T. Vreven, J. J. A. Montgomery, J. E. Peralta, F. Ogliaro, M. Bearpark, J. J. Heyd, E. Brothers, K. N. Kudin, V. N. Staroverov, R. Kobayashi, J. Normand, K. Raghavachari, A. Rendell, J. C. Burant, S. S. Iyengar, J. Tomasi, M. Cossi, N. Rega, J. M. Millam, M. Klene, J. E. Knox, J. B. Cross, V. Bakken, C. Adamo, J. Jaramillo, R. Gomperts, R. E. Stratmann, O. Yazyev, A. J. Austin, R. Cammi, C. Pomelli, J. W. Ochterski, R. L. Martin, K. Morokuma, V. G. Zakrzewski, G. A. Voth, P. Salvador, J. J. Dannenberg, S. Dapprich, A. D. Daniels, Ö. Farkas, J. B. Foresman, J. V. Ortiz, J. Cioslowski, D. J. Fox, *Gaussian 09*, Rev. A.02 ed., Gaussian, Inc., Wallingford CT, **2009**.
- [25] R. D. Dennington, T. A. Keith, J. M. Millam, *GaussView*, Ver. 5.08 ed., Semichem, Inc., Wallingford CT, **2009**.
- [26] J. A. Montgomery, M. J. Frisch, J. W. Ochterski, G. A. Petersson, *J. Chem. Phys.* **2000**, *112*, 6532–6542.
- [27] J. W. Ochterski, G. A. Petersson, J. A. Montgomery, *J. Chem. Phys.* **1996**, *104*, 2598–2619.
- [28] E. F. C. Byrd, B. M. Rice, *J. Phys. Chem.* **2005**, *110*, 1005–1013.
- [29] a) M. Sućeska, *Propellants, Explos., Pyrotech.* **1991**, *16*, 197–202; b) M. Sućeska, *EXPLO5 V.6.02*, Zagreb, **2013**.

3 The Polyvalent Nitrocarbamate of Pentaerythritol

As published in *Eur. J. Org. Chem.* **2015**, 2015, 723–729.

NEW PENTAERYTHRITOL BASED ENERGETIC MATERIALS RELATED TO NITROPENTA (PETN)



3.1 Press Release on the LMU Homepage

www.en.uni-muenchen.de/news/newsarchiv/2014/klapoetke.html

High-energy materials

Safer, more stable, easier to store

München, 12/01/2014

LMU chemists have developed a new secondary explosive which has a significantly higher thermal stability than the commonly used pentaerythritol tetranitrate (PETN) and is therefore easier and safer to handle.

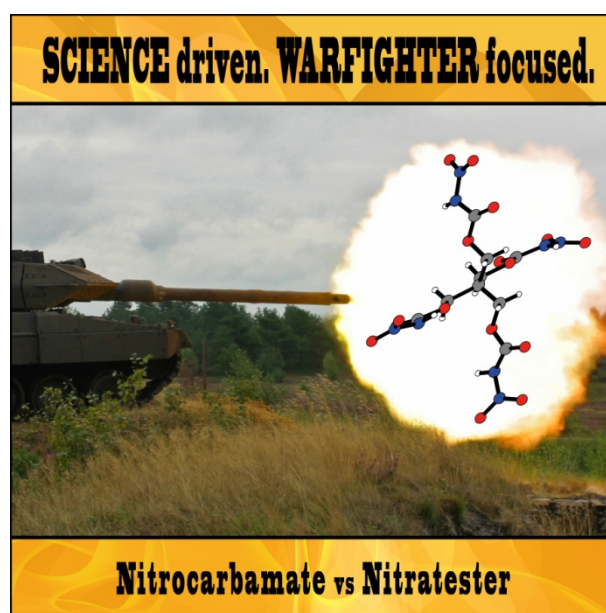
The figure depicts the crystal structure of the new compound pentaerythritol tetranitrocarbamate.

Explosive chemicals are designed to store large amounts of energy and release it instantaneously on demand. Yet they must also be sufficiently stable, both to adventitious detonation and to decomposition, to permit long-term storage with minimal risk to the security of personnel. PETN (pentaerythritol tetranitrate), a so-called nitrate ester, is a widely utilized explosive compound, but its sensitivity to friction and impact leaves a lot to be desired. A research group led by Professor Thomas M. Klapötke in the Department of Chemistry at LMU Munich has now developed a new derivative of PETN that is thermally more stable than its parent. Synthesis and characterization of the new compound is described in the latest issue of the “European Journal of Organic Chemistry”.

Unlike PETN, the new material does not belong to the nitrate esters, and was synthesized by nitration of a so-called carbamate in a two-step scheme. The reaction product, pentaerythritol tetranitrocarbamate (PETNC for short), is thus classified as a nitrocarbamate. The primary carbamate itself was synthesized from the corresponding alcohol under mild conditions, using chlorosulfonyl isocyanate (CSI) as a catalyst. “This method has a number of advantages – the

reaction is very rapid, for one thing – and it could provide a synthetic route to a whole range of new materials,” says Professor Klapötke.

Like PETN, PETNC is a secondary explosive, and requires the use of a primary explosive as a detonator. Indeed, the laboratory tests carried out by the LMU researchers revealed that PETNC has a higher thermal stability than PETN. While the latter melts at 141°C and begins to decompose at 165°C, PETNC remains stable up to a temperature of 196°C.



“PETNC is not only less susceptible to heat, it is also significantly less sensitive to impact than PETN, and not at all sensitive to friction. So it should be much easier and safer to handle in practice,” Klapötke adds. In order to test its performance as an explosive, the new compound was packed into a steel ring bolted to an aluminum block, and a commercially available detonator was used to set it off. By measuring the degree of deformation of the underlying aluminum block, the researchers determined that PETNC’s detonation parameters are only slightly less favorable than those of PETN, in good agreement with theoretical calculations based on its chemical structure.

3.2 Cover Picture

1st February Issue in *Eur. J. Org. Chem.* 4/2015

[4]

Eur. J. Org. Chem., 2015, 661–896

D 6093

4/2015
1st February Issue

www.eurjoc.org

Cover Picture
Thomas M. Klapötke et al.
Pentaerythritol-Based Energetic Materials

Microreview
Łukasz Albrecht et al.
Optically Active Organophosphorus Compounds

A sister journal of Asian Journal of Organic Chemistry
EJOCHF (4) 661–896 (2015) · ISSN 1434-193X · No. 4/2015

A Journal of
ChemPubSoc
Europe
Supported by
ACES
WILEY-VCH

3.3 Abstract

The synthesis of new tetravalent pentaerythritol tetranitrocarbamate and its tetraammonium salt was performed by efficient two step synthesis, starting from the cheap and readily commercially available pentaerythritol. Apart from full spectroscopic characterization, the thermal stabilities were examined using differential thermal analysis, as well as the energies of formation calculated. Furthermore, X-ray diffraction studies were performed and are presented.

3.4 Introduction

The combination of diverse chemical functional groups makes chemistry what it is, a never ending story. As a matter of course, this concept could also be used in the synthesis of energetic materials. However, in the field of developing new energetic materials it is indispensable, that the synthesis is as simple as inexpensive. On the basis of the neopentane derivative pentaerythritol there are only few energetic compounds known. The most common and popular explosive is pentaerythritol tetranitrate $C(CH_2ONO_2)_4$ (Nitropenta, PETN).^[1] More recently, the first silicon based pentaerythritol derivative $Si(CH_2ONO_2)_4$, has been synthesized and was shown to be extraordinarily sensitive and therefore not suitable for further applications.^[2] The precursor for PETN and for this study as well is the common and commercially available pentaerythritol.

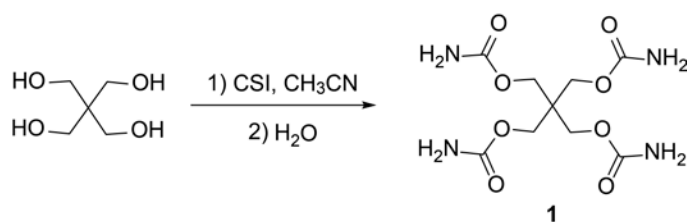
Primary nitrocarbamates as energetic materials are sparsely reported.^[3] Nitrocarbamates can be synthesized in high yields by nitration of unsubstituted carbamates employing various nitration mixtures. For the preparation of carbamates several routes are possible.

3.5 Results and Discussion

3.5.1 Synthesis

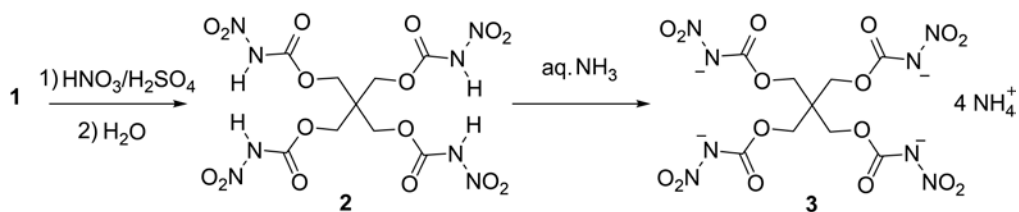
The standard synthesis of primary carbamates is a two step synthesis, starting from the corresponding alcohol and reaction with an excess of phosgene or phosgene derivatives. In the second step the carbamate is formed by treatment with ammonia.^[4] Another method is the addition of alcohols to urethanes or the nucleophilic attack to in situ prepared isocyanic acid.^[5] However the latter route is problematic with polyvalent alcohols, because of an in general less reactive reagent and potential multiple additions. An alternative one step synthesis starting from

the alcohol is the reaction with the reagent chlorosulfonyl isocyanate (CSI).^[6] CSI, a commercially available reagent, was discovered in 1956 and is one of the most reactive isocyanates.^[7] The reaction with alcohols is very fast and already proceeds at low temperatures, and without possible multi-addition prevented by the formation of an chlorosulfonylamide intermediate. This SO₂Cl group can easily be removed by aqueous work-up, leaving the pure carbamate. In summary, the advantages of CSI are monosubstitution, fast reaction times, simple isolation and nearly quantitative yields.^[7b] This reagent was also adopted for the synthesis of pentaerythritol tetracarbamate (**1**),^[8] as outlined in Scheme 3-1.



Scheme 3-1: Synthesis of pentaerythritol tetracarbamate (**1**).

The nitration of the carbamate **1** with a mixture of sulfuric and nitric acid leads to the four-fold *sym*-nitrated pentaerythritol tetranitrocarbamate (**2**). Further treatment with aqueous ammonia (alternatively gaseous ammonia into solutions in organic solvents) leads quantitatively to the tetraammonium salt **3** (Scheme 3-2).



Scheme 3-2: Synthesis of pentaerythritol tetranitrocarbamate (**2**) and tetraammonium salt (**3**).

3.5.2 NMR and vibrational Spectroscopy

The CH₂ resonance of the nitrocarbamate **2** shows a slight downfield shift in the ¹H NMR spectrum to 4.15 ppm compared to the carbamate **1** at 3.97 ppm, whereas the NH resonance suffers a strong downfield shift to 12.64 ppm from 6.58 ppm because of acidification, due to the nitration of the amino nitrogen, as well as increased broadening. In the ammonium salt **3** the CH₂-group is shifted back upfield to 3.88 ppm due to deprotonation. In the ¹³C{¹H} NMR the

largest change is observed on the carbonyl carbon atom. After nitration the carbamate carbon resonance is shifted upfield from 157.0 ppm to 148.9 ppm, and upon deprotonation shifted back downfield to 160.4 ppm. The methylene carbon resonances were observed at 62.6–64.3 ppm, those of the quaternary carbon are found obviously in a quite narrow range of 42.8–42.5 ppm (Table 3-1).

In the ^{15}N NMR spectrum of the carbamate **1** a triplet is observed at -306.1 ppm for the amide, caused by a hydrogen 1J coupling of 90.1 Hz. In the spectra of the nitrocarbamate **2** the nitro group is found at -42.2 ppm and the NH group at -185.2 ppm (no coupling to hydrogen due to exchange with solvent $[\text{D}_6]\text{DMSO}$ because of high acidity). Upon deprotonation to **3** both resonances suffer a significant low field shift to -137.4 ppm and -9.2 ppm, respectively. Furthermore, the resonance for the ammonium cation is observed at -360.2 ppm (Figure 3-1).

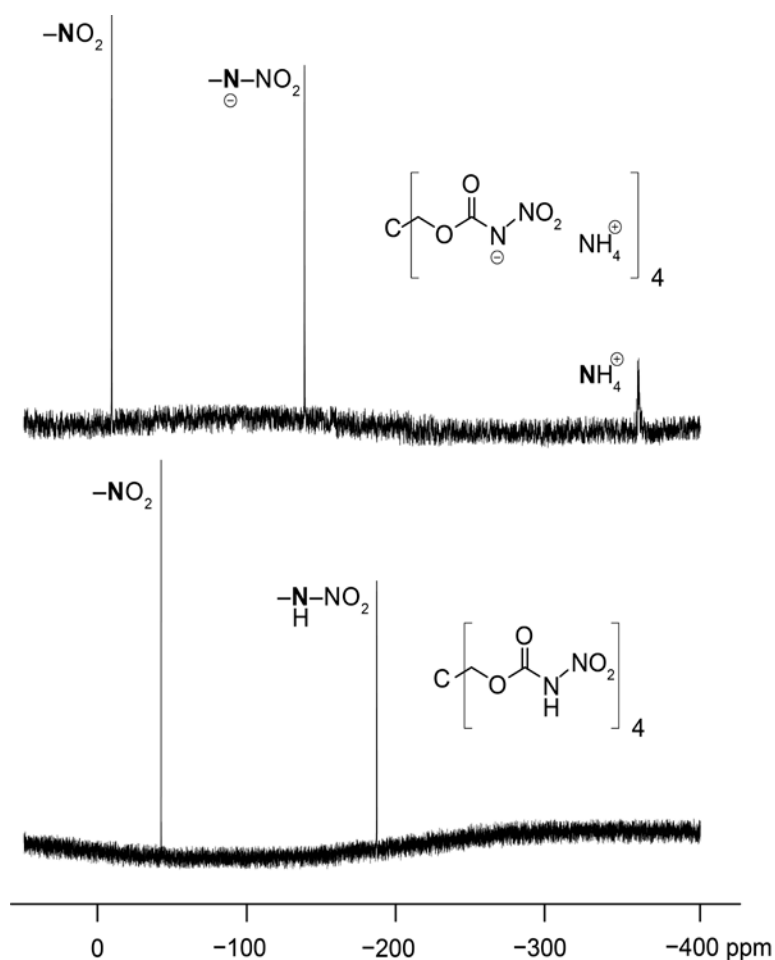


Figure 3-1: ^{15}N NMR spectrum of pentaerythritol tetranitrocarbamate (**2**) and tetraammonium salt **3** in $[\text{D}_6]\text{DMSO}$.

Table 3-1: Multinuclear NMR resonances (in ppm, solvent [D₆]DMSO) and characteristic Raman/IR vibrations bands (in cm⁻¹, ATR).

	1		2		3	
¹ H	6.58 (NH ₂)		12.64 (NH)		7.24 (NH ₄)	
	3.97 (CH ₂)		4.15 (CH ₂)		3.88 (CH ₂)	
¹³ C{ ¹ H}	157.0 (CO)		148.9 (CO)		160.4 (CO)	
	62.6 (CH ₂)		64.3 (CH ₂)		63.3 (CH ₂)	
	42.8 (C)		42.7 (C)		42.5 (C)	
¹⁵ N	-306.1(NH ₂)		-42.2 (NO ₂)		-9.2 (NO ₂)	
			-185.2 (NH)		-137.4 (NNO ₂)	
					-360.2 (NH ₄)	
	RAMAN	IR	RAMAN	IR	RAMAN	IR
νNH	3354 (9)	3437 m	3174 (5)	3233 w	3150 (18)	3476 br
	3326 (8)	3331 w		3169 m		3190 br
		3279 w		3044 w		3060 br
		3194 w				
νCO	1698 (38)	1687 s	1778 (31)	1778 m	1691 (37)	1659 m
ν_{as}NO₂	-	-	1612 (13)	1609 s	1682 (35)	1659 m
ν_sNO₂	-	-	1263 (20)	1322 m	1304 (47)	1301 w

In the vibrational spectra a significant shift of the carbonyl stretching frequency to higher wave numbers is observed after nitration of **1**, which is again lowered when deprotonated to the ammonium salt **3** (Table 3-1). In contrast to the carbonyl vibration, the asymmetric stretching vibration of the nitro group in **3** is found at a higher wave number compared to the neutral nitrocarbamate **2**, which causes some overlapping with the carbonyl vibration in the infrared spectrum.

3.5.3 Single Crystal Structure Analysis

A full list of the crystallographic structure and refinement data are shown in Appendix A.3. Single crystals of the nitrocarbamate **2** were obtained from acetone at ambient temperature. It crystallizes in the tetragonal space group $P-42_1c$ with two formula units per unit cell and a density of 1.77 g/cm⁻³ at -173 °C. The asymmetric unit consists only of one arm and the center quaternary carbon (Figure 3-2). This is due to the tetragonal space group which causes a 4-fold

rotoinversion axis and two glide planes perpendicular to one another through the quaternary central carbon atom C1.

The nitrocarbamate unit of **2** does not show a perfect planarity as would be expected. The nitro group is rotated more than 30° out of plane of the carbamate moiety, which is demonstrated by the torsion angle O3–N2–N1–C3 (-30.4°). This differs from the only literature known crystal structure of a primary nitrocarbamate, which shows nearly perfect planarity of the whole nitrocarbamate unit.^[3] The N1–N2 bond of the nitramine moiety is 1.379 Å, which indicates a substantial double bond character, achieved by delocalization of the nitrogen lone pair of N1. This is also evidenced by a shortened N–H bond (0.86 Å). The carbonyl group is *cis* oriented to the nitro group and with 1.191 Å shortened as well. The C3–N1 distance of 1.386 Å is also shortened and thus between a single (1.47 Å) and a double (1.27 Å) bond.

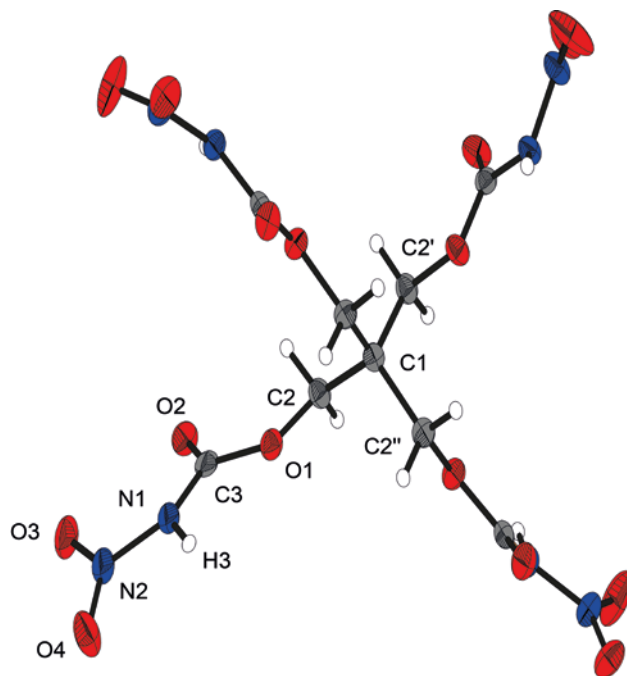


Figure 3-2: X-ray molecular structure of pentaerythritol tetranitrocarbamate (2).

Selected atom distances (Å) and angles (deg.): H3–N1 0.86(2), C2–O1 1.450(2), C3–N1 1.386(2), C3–O1 1.333(2), C3–O2 1.191(2), N1–N2 1.379(2), N2–O3 1.210(2), N2–O4 1.220(2), C2–C1–C2' 105.2(1), C2–C1–C2'' 111.6(1), C1–C2–O1 107.3(1), O1–C3–O2 127.0(2), O1–C3–N1 106.3(1), O2–C3–N1 126.7(2), C3–N1–H3 121(1), C3–N1–N2 121.7(2), H3–N1–N2 111(1), N1–N2–O4 114.6(2), O4–N2–O3 126.0(2), O3–N2–N1 119.4(2), C2–O1–C3–O2 $-4.4(3)$, O1–C3–N1–N2 $-165.8(2)$, O1–C3–N1–H3 $-16(2)$, O2–C3–N1–H3 165(2), O3–N2–N1–C3 $-30.4(2)$, O4–N2–N1–C3 151.8(2), H3–N1–N2–O3 177(1), H3–N1–N2–O4 $-1(1)$.

In the structure of **2** one quite strong classical hydrogen bond is present, which links the hydrogen H3 of the amine to an oxygen atom of a symmetry related carbonyl functionality (O2).

Furthermore, two improper hydrogen bonds with carbon as donor are observed, between the methylene group (C2–H1/2) and the oxygens (O3/O4) of two different symmetry related nitro groups (for details see Appendix A.3). These extensive hydrogen bonds connect and stabilize the layer structure which is visible along the crystallographic axis *a* (Figure 3-3, right) and could explain the better thermal stability compared to pentaerythritol tetranitrate (PETN).

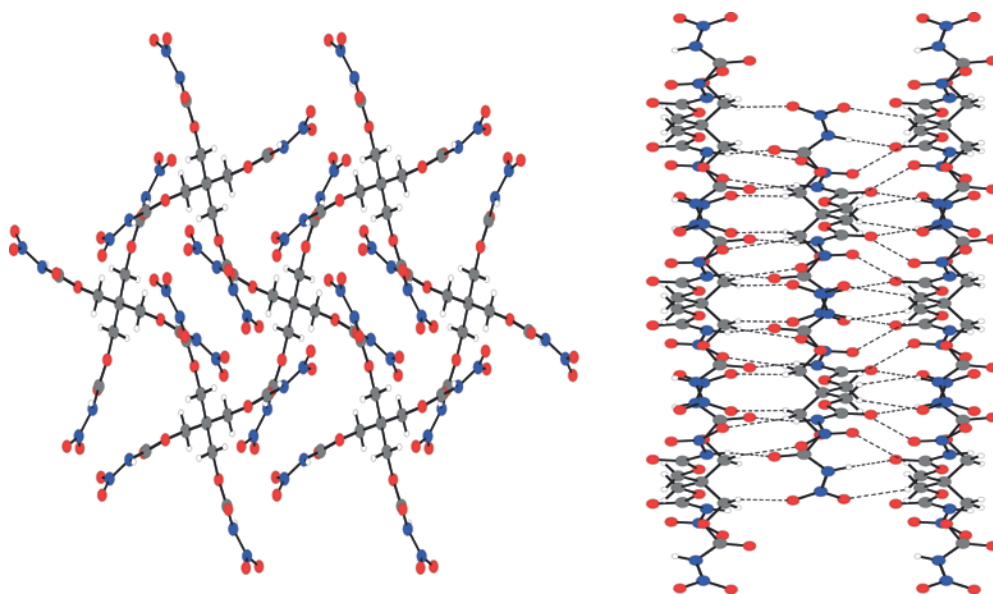


Figure 3-3: View of the crystal structure **2** along *c* axis (left) and *a* axis (right).

Single crystals of the tetraammonium salt **3** were obtained from aqueous solution and crystallize in the orthorhombic space group *Pbca* with eight formula units per unit cell and a density of 1.64 g/cm³ at –100 °C. Here, only one glide plane intersects through the central quaternary carbon of the anion, which leads to all four different side arms. Otherwise, the molecular structure of the salt **3** is similar to the neutral compound **2**. A noticeable change is only observed at the elongation of the N–N (0.05 Å) and the N–O (0.03 Å) bonds, which is due to the increased negative charge of the anions. The nitro groups are also out of plane of the carbamate moiety in a range from 5.4 to 22.0 ° (torsion angle C–N–N–O). The C–N–N angle shows a reduction compared to the neutral compound of more than 6 ° to 16 ° due to the greater negative charge on the nitrogen carbamate moiety. The salt **3** shows classical and non classical hydrogen bonds, which links the hydrogens of the CH₂ and the ammonium ions with oxygen donors of the nitro and carbonyl groups. The ammonium cations take a special position, where they are linked with a chelating nitrocarbamate anion (Figure 3-4). Each cation forms hydrogen bridges to the oxygen atom of the ester moiety plus to the anionic nitrogen of the nitramine unit (for more details see Appendix A.3).

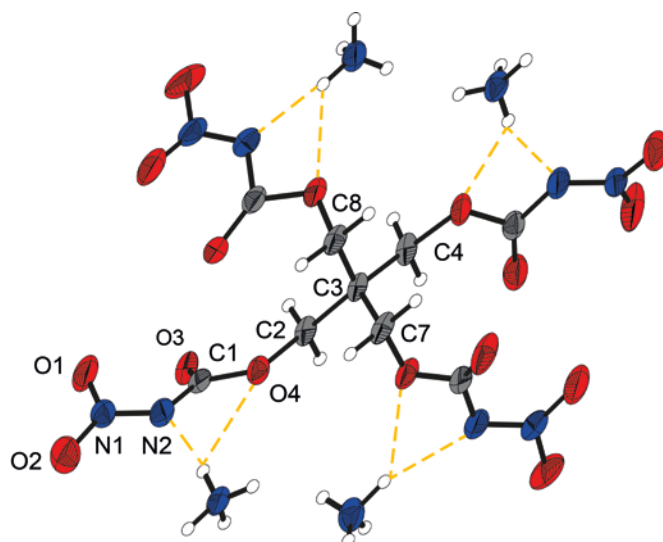


Figure 3-4: X-ray molecular structure of tetraammonium pentaerythritol tetranitrocarbamate (3).

Selected bond lengths (Å) and angles (deg.): C1–N2 1.381(3), C1–O3 1.220(3), C1–O4 1.347(2), C2–C3 1.533(3), C2–O4 1.447(3), C2–H1 0.96(4), C2–H2 0.97(4), N1–N2 1.332(3), N1–O1 1.250(3), N1–O2 1.247(3), N2–C1–O3 130.0(2), N2–C1–O4 106.7(2), O3–C1–O4 123.1(2), C3–C2–O4 108.5(2), C3–C2–H1 112(2), C3–C2–H2 110(2), O4–C2–H1 109(2), O4–C2–H2 109(2), H1–C2–H2 108(3), N2–N1–O1 123.3(2), N2–N1–O2 116.9(2), O1–N1–O2 119.7(2), C1–N2–N1 116.0(2), C1–O4–C2 115.7(2), C1–N2–N1–O1 –22.0(3), O3–C1–N2–N1 –20.8(3).

3.5.4 Energetic Properties

The tetranitrocarbamate **2** shows no melting point and is thermally stable up to a temperature of 196 °C (onset) (Figure 3-5). Therefore, the thermal stability of **2** is higher than that of PETN which melts at 141 °C and begins already to decompose at 165 °C or lower.^[9]

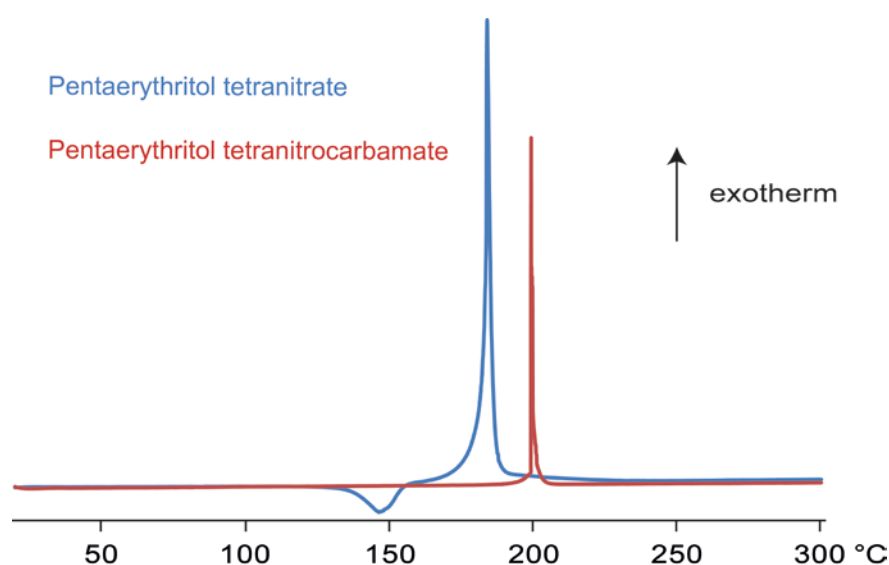


Figure 3-5: DTA of pentaerythritol tetranitrocarbamate (2) (red) and pentaerythritol tetranitrate (PETN) (blue), with a heating rate of 5 °/min.

The nitrocarbamate **2** also shows a lower sensitivity towards impact with a value of 8 J and no sensitivity to friction. The nitrogen content of 23% in **2** is more than 5% higher compared to that of PETN, however the oxygen balance Ω and the detonation velocity is lower compared to those of PETN (Table 3-2). Unexpectedly, the ammonium salt **3** starts to decompose earlier at 136 °C compared to the molecular compound **2**, which is in contrast to the observed values for the corresponding ethyl nitrocarbamates.^[3d]

Table 3-2: Physical and energetic properties of 2, 3 and pentaerythritol tetranitrate (PETN).

	2	3	PETN
formula	C ₉ H ₁₂ N ₈ O ₁₆	C ₉ H ₂₄ N ₁₂ O ₁₆	C ₅ H ₈ N ₄ O ₁₂
IS / J ^[a]	8	>40	3
FS / N ^[b]	360	>360	60
ESD / J ^[c]	0.75	>1.0	0.5
$N / \%$	23.0	30.2	17.7
$\Omega_{CO} / \%$ ^[d]	+3.28	-14.38	+15.18
$T_{dec.} / ^\circ C$	196	136	165
$\rho / g\ cm^{-3}$ (RT)	1.76	1.64	1.78
$\Delta_f H_m^\circ / kJ\ mol^{-1}$ ^[e]	-1311	-2378	-561
$\Delta_{Ex} U^\circ / kJ\ kg^{-1}$ ^[f]	-4034	-2364	-5980
$P_{CJ} / kbar$ ^[f]	248	163	319
$V_{det.} / m\ s^{-1}$ ^[f]	7742	6914	8405
$V_o / L\ kg^{-1}$ ^[f]	727	880	743

[a] impact sensitivity, [b] friction sensitivity, [c] sensitivity towards electrostatic discharge, [d] oxygen balance assuming the formation of CO, [e] enthalpy and energy of formation calculated with the CBS-4M method with Gaussian09,^[10] [f] predicted heat of combustion, temperature of gaseous products, detonation pressure detonation velocity and volume of gaseous products calculated with the program package EXPLO5 Version 6.02.^[11]

3.5.5 SSRT-Performance Test

In order to assess the explosive performance of **2** on a small laboratory scale, a small scale reactivity test (SSRT) was performed.^[12] Here, a defined volume of the explosive is pressed into a perforated steel block, which is topped with a commercially available detonator (Orica-DYNADET-C2-0ms). Initiation of the tested explosive results in denting a separate aluminum block, which is placed right underneath the steel block (Figure 3-6). From measuring the volumes of the dent, it can be concluded that the small scale explosive performance of **2** (605 mg sand) is

slightly lower than the performance of PETN (917 mg sand), thus also confirming the calculated values with EXPLO5. However, the test clearly indicated that the nitrocarbamate **2** can be detonated.

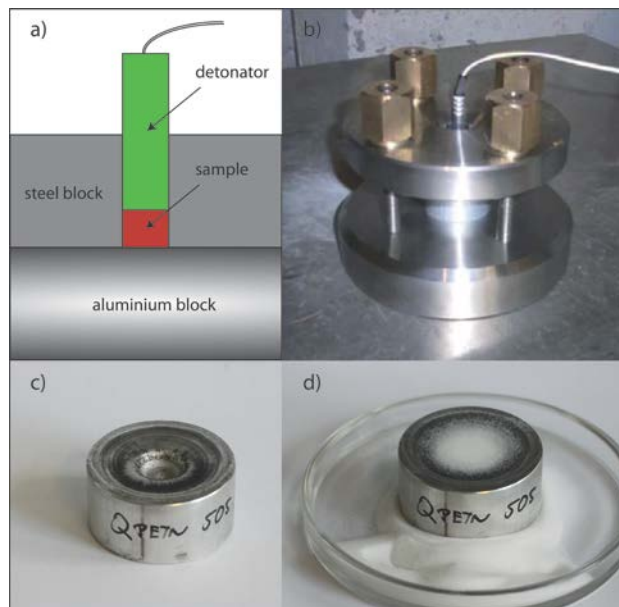


Figure 3-6: Small scale reactivity test (SSRT) of **2**. a) schematic set-up b) set-up before initiation c) aluminum block after the test d) measuring the volume with sand.

3.6 Conclusions

The facile synthesis of choice for pentaerythritol tetracarbamate (**1**) is a one step synthesis from pentaerythritol, which is inexpensive and commercially available. The synthesis has compared to previously known routes several advantages, like fast reaction time and high yield of pure product. The nitration to the new material pentaerythritol tetranitrocarbamate (**2**) proceeds in high yields. Thermally stable **2** decomposes at 196 °C and thus shows a higher heat stability and lower sensitivity against friction and impact compared to the well-known pentaerythritol tetranitrate (PETN).

The ability to form salts of the nitrocarbamate, i.e. tetraammonium salt **3**, demonstrates the stability of the nitrocarbamate moiety against bases and nucleophiles. This concept of a nitrocarbamate synthesis could likely be transferred to other types of mono- and polyvalent alcohols and open the door to a variety of new materials.

3.7 Experimental Section

3.7.1 General Information

All chemicals were used as supplied. Raman spectra were recorded in a glass tube with a Bruker MultiRAM FT-Raman spectrometer with Nd:YAG laser excitation up to 1000 mW (at 1064 nm) in the range between 400 and 4000 cm^{-1} . Infrared spectra were measured with a Perkin–Elmer Spectrum BX-FTIR spectrometer equipped with a Smiths DuraSamplIR II ATR device. All spectra were recorded at ambient (20 °C) temperature. NMR spectra were recorded with a JEOL Eclipse 400 instrument and chemical shifts were determined with respect to external Me_4Si (^1H , 399.8 MHz; ^{13}C , 100.5 MHz) and MeNO_2 (^{15}N , 40.6 MHz). Mass spectrometric data were obtained with a JEOL MStation JMS 700 spectrometer (DCI+, DEI+). Analysis of C/H/N were performed with an Elemental Vario EL Analyzer. Melting and decomposition points were measured with a Perkin-Elmer Pyris6 DSC and an OZM Research DTA 552-Ex with a heating rate of 5 °C min^{-1} in a temperature range of 15 to 400 °C and checked by a Büchi Melting Point B-540 apparatus (not corrected).

3.7.2 X-ray Crystallography

The low-temperature single-crystal X-ray diffraction of were performed on an Oxford XCalibur3 diffractometer equipped with a Spellman generator (voltage 50 kV, current 40 mA) and a KappaCCD detector operating with $\text{MoK}\alpha$ radiation ($\lambda = 0.7107 \text{ \AA}$). Data collection was performed using the CRYSLIS CCD software.^[13] The data reduction was carried out using the CRYSLIS RED software.^[14] The solution of the structure was performed by direct methods (SIR97)^[15] and refined by full-matrix least-squares on F2 (SHELXL)^[16] implemented in the WINGX software package^[17] and finally checked with the PLATON software^[18]. All non-hydrogen atoms were refined anisotropically. The hydrogen atom positions were located in a difference Fourier map. ORTEP plots are shown with thermal ellipsoids at the 50% probability level. Crystallographic data (excluding structure factors) for the structures reported in this paper have been deposited at the Cambridge Crystallographic Data Centre (CCDC-1003442 (2) and CCDC-1003443 (3)).

3.7.3 Energetic Properties and Computational Calculation

The sensitivity data were performed using a BAM drophammer and a BAM friction tester.^[19] All *ab initio* calculations were carried out using the program package Gaussian 09 (Rev. A.02)^[10] and visualized by GaussView 5.08.^[20] Structure optimizations and frequency analyses were performed with Becke's B3 three parameter hybrid functional using the LYP correlation functional (B3LYP). For C, H, N and O a correlation consistent polarized double-zeta basis set was used (cc-pVDZ). The structures were optimized with symmetry constraints and the energy is corrected with the zero point vibrational energy.^[21] The enthalpies (H) and free energies (G) were calculated using the complete basis set (CBS) method in order to obtain accurate values. The CBS models use the known asymptotic convergence of pair natural orbital expressions to extrapolate from calculations using a finite basis set to the estimated complete basis set limit. CBS-4 starts with a HF/3-21G(d) geometry optimization, which is the initial guess for the following SCF calculation as a base energy and a final MP2/6-31+G calculation with a CBS extrapolation to correct the energy in second order. The used CBS-4M method additionally implements a MP4(SDQ)/6-31+(d,p) calculation to approximate higher order contributions and also includes some additional empirical corrections.^[22] The enthalpies of the gas-phase species were estimated according to the atomization energy method.^[23] All calculations affecting the detonation parameters were carried out using the program package EXPLO5 V6.02.^[11, 24] The detonation parameters were calculated at the Chapman-Jouguet (CJ) point with the aid of the steady-state detonation model using a modified Becker-Kistiakowski-Wilson equation of state for modeling the system. The CJ point is found from the Hugoniot curve of the system by its first derivative.

3.7.4 Small scale shock reactivity test (SSRT)

The SSRT test was introduced by the Indian Head Division and the Naval Surface Warfare Center. The SSRT measures the shock reactivity of energetic materials, without requiring a transition to detonation. The test setup has the benefits that only a small amount of sample (~500 mg) is needed compared to a lead block test and a gap test. The sample volume V_s is recommended to be 0.284 mL. For the test setup no possible attenuator (between detonator and sample) and air gap (between sample and aluminum block) was used. The sample weight was calculated using the formula density of the material at room temperature. The dent, which was generated by the detonation, was measured by filling with powdered SiO₂ and measuring the resulting weight.

3.7.5 Synthesis

CAUTION! Compounds **2** and **3** are energetic materials with sensitivity towards heat, impact and friction. No hazards occurred during preparation and manipulation, additional proper protective precautions (face shield, leather coat, earthened equipment and shoes, Kevlar® gloves and ear plugs) should be used when undertaking work with these compounds.

Pentaerythritol tetracarbamate (1): Pentaerythritol (0.55 g, 4 mmol) was suspended in dry acetonitrile (20 mL) and placed in an ice bath and chlorosulfonyl isocyanate CSI (2.83 g, 20 mmol) was added very slowly at 0 °C. During the addition the alcohol dissolved and at the end of the addition a colorless precipitate appeared. The ice bath was removed and stirring at room temperature was continued for 1 h. The reaction mixture was again cooled with an ice bath and water (10 mL) was added with caution. The organic solvent was removed in vacuum after phase separation and the formed precipitate was filtered. The precipitate was further washed thoroughly with cold water and dried under high vacuum to obtain 1.22 g (99%) of colorless pure pentaerythritol tetracarbamate (**1**).

DSC (5 °C min⁻¹): 235 °C (onset mp.); IR: (cm⁻¹): ν = 3436 (m), 3330 (w), 3276 (w), 2986 (w), 2921 (w), 1687 (s), 1595 (m), 1478 (w), 1408 (s), 1353 (s), 1277 (m), 1177 (w), 1077 (vs), 930 (w), 785 (w), 673 (w). Raman: (500 mW, cm⁻¹): ν = 3326 (9), 3281 (8), 3195 (5), 3004 (58), 2927 (34), 2261 (5), 1698 (38), 1584 (15), 1484 (39), 1424 (6), 1363 (9), 1252 (36), 1106 (42), 1067 (10), 977 (100), 934 (19), 920 (26), 676 (10), 654 (18), 582 (10), 554 (9), 501 (8), 370 (8), 269 (27), 245 (26), 222 (44). ¹H NMR (DMSO-D₆) δ = 6.58 (br, 8H, NH₂), 3.97 (s, 8H, CH₂) ppm. ¹³C{¹H} NMR (DMSO-D₆) δ = 157.0 (CO), 62.6 (CH₂), 42.8 (C) ppm. ¹⁵N NMR (DMSO-D₆) δ = -306.1 (t, ¹J(N,H) = 90.1 Hz, NH₂) ppm. EA (C₉H₁₆N₄O₈, 308.25) calc.: C 35.07, H 5.23; N 18.18 %; found: C 34.97; H 5.36; N 18.15 %. MS (DEI+) *m/z* (%): 309 (1) [M + H]⁺, 248 (81) [M - O₂CNH₂]⁺, 44 (100) [CO₂]⁺. BAM drophammer: >40 J; friction tester: >360 N; ESD: >1.0 J (at grain size <100 μm).

Pentaerythritol tetranitrocarbamate (2): Red fuming nitric acid (>99.5%, 4 mL) was dropped into concentrated sulfuric acid (4 mL) at 0 °C. To this nitration mixture chilled in an ice bath, the tetracarbamate **1** (310 mg, 1.0 mmol) was added in small portions. The suspension was stirred 10 minutes at 0 °C and one hour at ambient temperature. The nitration mixture was poured onto ice-water (200 mL) and the precipitate was filtered off. The precipitate was washed three times with water and dried under high vacuum to obtain 460 mg (94%) colorless pentaerythritol

tetranitrocarbamate (**2**). For further purification the product **2** is dissolved in basic aqueous solution and precipitates in quantitative yield upon acidification.

DSC (5 °C min⁻¹): 196 °C (onset dec.); IR: (cm⁻¹): $\nu = 3233$ (w), 3166 (w), 3041 (w), 1768 (m), 1648 (w), 1608 (s), 1482 (w), 1441 (m), 1397 (w), 1379 (w), 1322 (m), 1299 (w), 1190 (s), 1173 (s), 1023 (w), 1006 (w), 977 (w), 951 (s), 915 (w), 811 (w), 748 (m), 729 (w), 657 (w). Raman: (500 mW, cm⁻¹): $\nu = 3174$ (5), 2998 (19), 2984 (23), 2918 (12), 1778 (31), 1612 (13), 1473 (19), 1450 (10), 1385 (5), 1333 (38), 1300 (7), 1263 (19), 1201 (12), 1176 (8), 1104 (7), 1035 (100), 985 (10), 916 (6), 885 (6), 790 (5), 751 (5), 716 (7), 513 (8), 490 (10), 470 (23), 287 (7). ¹H NMR (DMSO-D₆) $\delta = 12.64$ (br, 4H, NH), 4.15 (s, 8H, CH₂) ppm. ¹³C{¹H} NMR (DMSO-D₆) $\delta = 148.9$ (CO), 64.3 (CH₂), 42.7 (C) ppm. ¹⁵N NMR (DMSO-D₆) $\delta = -42.2$ (NO₂), -185.2 (NHNO₂) ppm. EA (C₉H₁₂N₈O₁₆, 488.24) calc.: C 22.14, H 2.48; N 22.95 %; found: C 22.01; H 2.68; N 21.50 %. MS (DEI+) m/z (%): 489 (1) [M + H]⁺, 383 (1) [M - CO₂]⁺, 44 (100) [CO₂]⁺. BAM drophammer: 8 J; friction tester: 360 N; ESD: 0.25 J (at grain size <100 μm).

Tetraammonium pentaerythritol tetranitrocarbamate (3): The tetranitrocarbamate **2** (488 mg, 1.0 mmol) was suspended in water (20 mL) and aqueous ammonia (~0.5 mL) was added slowly, while no precipitation remained. The solvent was evaporated at standard pressure at room temperature. The colorless product was dried, to obtain pure tetraammonium pentaerythritol tetranitrocarbamate (**3**) in quantitative yield.

DSC (5 °C min⁻¹): 136 °C (onset mp.); IR: (cm⁻¹): $\nu = 3175$ (w), 3038 (w), 1643 (m), 1421 (m), 1365 (m), 1291 (m), 1203 (s), 1165 (s), 1068 (s), 962 (m), 888 (w), 780 (m), 753 (w), 729 (w). Raman: (500 mW, cm⁻¹): $\nu = 3151$ (17), 3122 (18), 2972 (41), 2903 (25), 1691 (37), 1682 (36), 1462 (34), 1390 (30), 1304 (47), 1260 (31), 1218 (34), 1124 (41), 977 (100), 855 (22), 794 (33), 495 (32), 409 (21), 306 (32). ¹H NMR (DMSO-D₆) $\delta = 7.24$ (s, 16H, NH₄), 3.88 (s, 8H, CH₂) ppm. ¹³C{¹H} NMR (DMSO-D₆) $\delta = 160.4$ (CO), 63.3 (CH₂), 42.5 (C) ppm. ¹⁵N NMR (DMSO-D₆) $\delta = -9.2$ (NO₂), -137.4 (NNO₂), -360.2 (NH₄) ppm. EA (C₉H₂₄N₁₂O₁₆, 556.36) calc.: C 19.43, H 4.35; N 30.21 %; found: C 19.20; H 4.52; N 28.94 %. BAM drophammer: 40 J; friction tester: 360 N; ESD: 0.25 J (at grain size 100-500 μm).

3.8 References

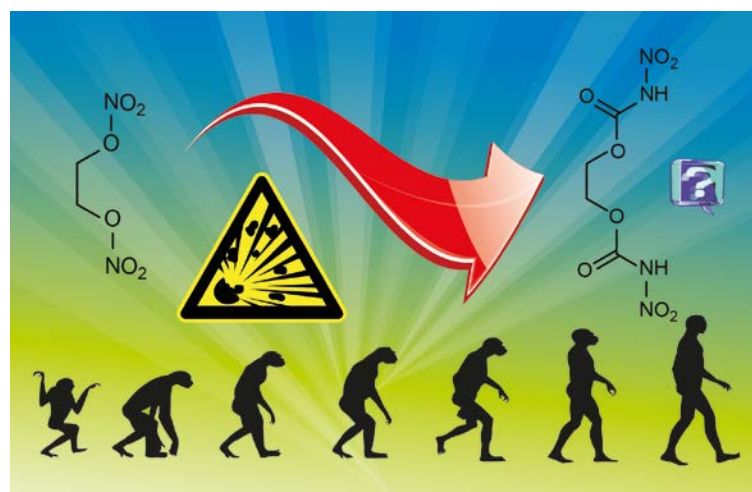
- [1] a) T. J. Dunn, W. L. Neumann, M. M. Rogic, S. R. Woulfe, *J. Org. Chem.* **1990**, *55*, 6368–6373; b) W. S. Anderson, H. J. Hyer, J. E. Sundberg, T. P. Rudy, *Ind. Eng. Chem. Res.* **2000**, *39*, 4011–4013; c) J. Köhler, R. Meyer, A. Homburg, *Explosivstoffe*, Wiley-VCH, Weinheim, **2008**; d) J. P. Agrawal, *High Energy Materials*, Wiley-VCH, Weinheim, **2010**; e) T. Klapötke, *Chemistry of High-Energy Materials*, 2nd ed., deGruyter, Berlin, **2012**.
- [2] a) T. M. Klapötke, B. Krumm, R. Ilg, D. Troegel, R. Tacke, *J. Am. Chem. Soc.* **2007**, *129*, 6908–6915; b) J. S. Murray, P. Lane, A. Nieder, T. M. Klapötke, P. Politzer, *Theor. Chem. Acc.* **2010**, *127*, 345–354.
- [3] Q. J. Axthammer, T. M. Klapötke, B. Krumm, R. Moll, S. F. Rest, *Z. Anorg. Allg. Chem.* **2014**, *640*, 76–83.
- [4] L. Cotarca, H. Eckert, *Phosgenations — A Handbook*, Wiley-VCH, Weinheim, **2005**.
- [5] a) W. M. Kraft, *J. Am. Chem. Soc.* **1948**, *70*, 3569–3571; b) B. Loev, M. F. Kormendy, *J. Org. Chem.* **1963**, *28*, 3421–3426.
- [6] J. K. Rasmussen, A. Hassner, *Chem. Rev. (Washington, DC, U. S.)* **1976**, *76*, 389–408.
- [7] a) R. Graf, *Chem. Ber.* **1956**, *89*, 1071–1079; b) D. N. Dhar, P. Dhar, *The Chemistry of Chlorosulfonyl Isocyanate*, World Scientific, Singapore, **2002**.
- [8] a) L. E. Sydney **1954**, GB 704851; b) M. G. Kim, *J. Appl. Polym. Sci.* **2011**, *122*, 2209–2220.
- [9] R. Meyer, J. Köhler, A. Homburg, *Explosives*, Wiley-VCH, Weinheim, **2007**.
- [10] M. J. Frisch, G. W. Trucks, H. B. Schlegel, G. E. Scuseria, M. A. Robb, J. R. Cheeseman, V. B. G. Scalmani, B. Mennucci, G. A. Petersson, H. Nakatsuji, M. Caricato, X. Li, H. P. Hratchian, A. F. Izmaylov, J. Bloino, G. Zheng, J. L. Sonnenberg, M. Hada, M. Ehara, K. Toyota, R. Fukuda, J. Hasegawa, M. Ishida, T. Nakajima, Y. Honda, O. Kitao, H. Nakai, T. Vreven, J. J. A. Montgomery, J. E. Peralta, F. Ogliaro, M. Bearpark, J. J. Heyd, E. Brothers, K. N. Kudin, V. N. Staroverov, R. Kobayashi, J. Normand, K. Raghavachari, A. Rendell, J. C. Burant, S. S. Iyengar, J. Tomasi, M. Cossi, N. Rega, J. M. Millam, M. Klene, J. E. Knox, J. B. Cross, V. Bakken, C. Adamo, J. Jaramillo, R. Gomperts, R. E. Stratmann, O. Yazyev, A. J. Austin, R. Cammi, C. Pomelli, J. W. Ochterski, R. L. Martin, K. Morokuma, V. G. Zakrzewski, G. A. Voth, P. Salvador, J. J. Dannenberg, S. Dapprich, A. D. Daniels, Ö. Farkas, J. B. Foresman, J. V. Ortiz, J. Cioslowski, D. J. Fox, *Gaussian 09*, Rev. A.02 ed., Gaussian, Inc., Wallingford CT, **2009**.
- [11] M. Sućeska, *EXPLO5 V.6.02*, Zagreb, **2013**.
- [12] N. Fischer, D. Fischer, T. M. Klapötke, D. G. Piercey, J. Stierstorfer, *J. Mater. Chem.* **2012**, *22*, 20418–20422.
- [13] Oxford Diffraction Ltd., *CrysAlis CCD*, Version 1.171.35. (release 16-05-2011 CrysAlis 171.Net), Abingdon, Oxford, **2011**.
- [14] Oxford Diffraction Ltd., *CrysAlis RED*, Version 1.171.35.11 (release 16-05-2011 CrysAlis 171.NET), Abingdon, Oxford, **2011**.

- [15] A. Altomare, M. C. Burla, M. Camalli, G. L. Cascarano, C. Giacovazzo, A. Guagliardi, A. G. G. Moliterni, G. Polidori, R. Spagna, *J. Appl. Crystallogr.* **1999**, *32*, 115–119.
- [16] a) G. M. Sheldrick, *SHELX-97, Programs for Crystal Structure Determination*, **1997**; b) G. M. Sheldrick, *Acta Crystallogr., Sect. A: Found. Crystallogr.* **2008**, *A64*, 112–122.
- [17] L. Farrugia, *J. Appl. Crystallogr.* **1999**, *32*, 837–838.
- [18] A. Spek, *Acta Crystallogr., Sect. D: Biol. Crystallogr.* **2009**, *65*, 148–155.
- [19] M. Göbel, T. M. Klapötke, *Adv. Funct. Mater.* **2009**, *19*, 347–365.
- [20] R. D. Dennington, T. A. Keith, J. M. Millam, *GaussView*, Ver. 5.08 ed., Semichem, Inc., Wallingford CT, **2009**.
- [21] J. A. Montgomery, M. J. Frisch, J. W. Ochterski, G. A. Petersson, *J. Chem. Phys.* **2000**, *112*, 6532–6542.
- [22] J. W. Ochterski, G. A. Petersson, J. A. Montgomery, *J. Chem. Phys.* **1996**, *104*, 2598–2619.
- [23] E. F. C. Byrd, B. M. Rice, *J. Phys. Chem.* **2005**, *110*, 1005–1013.
- [24] M. Sućeska, *Propellants, Explos., Pyrotech.* **1991**, *16*, 197–202.

4 The Nitrocarbamate Relatives of Nitroglycerine and Co.

As published in *Z. Anorg. Allg. Chem.* **2016**, 642, 211–218.

SELECTED NITROCARBAMATES OF GLYCERINE AND CO. AND THE FIRST ACETYLENE DERIVATIVE



4.1 Abstract

A simple two step synthesis route for the preparation of several energetic multivalent nitrocarbamates of easily available alcohols is presented. The carbamates were obtained by the reaction of the alcohols and the reactive reagent chlorosulfonyl isocyanate (CSI) with subsequent aqueous work-up. The nitration of the carbamates was performed with mixed acid (nitric and sulfuric acid). The thermal stabilities were explored by using differential scanning calorimetry and the energies of formation were calculated on the CBS-4M level of theory, as well as several detonation and propulsion parameters for the application as energetic materials. All compounds were fully characterized and discussed in addition with single X-ray diffraction.

4.2 Introduction

The first article where nitrocarbamates were mentioned, was of THIELE and LACHMAN in 1895, who synthesized a nitrocarbamate from ethyl carbamate by nitration with ethyl nitrate.^[1] After that, nitrocarbamates have received little to almost no attention. Recently, this class of compounds regained interest in respect of energetic materials. Several primary nitrocarbamates from various polynitroalcohols have been synthesized, as well as a tetravalent nitrocarbamate of pentaerythritol, which is also the starting material for the well known explosive PETN (Pentaerythritol).^[2] These new nitrocarbamates exhibit good physical and energetic properties with higher decomposition points and lower sensitivities against mechanical stimuli compared to the related nitrate esters.

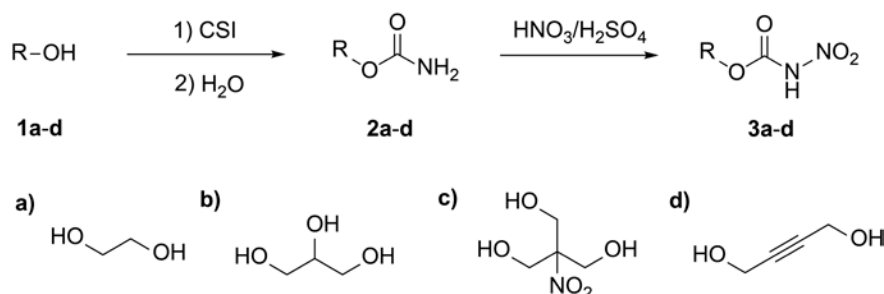
The nitrate esters of glycerine and ethylene glycol, nitroglycerine (NG) and ethylene glycol dinitrate (EGDN), were both invented in the 19th century and are both extremely sensitive to impact.^[3] Nevertheless, they are still in use in various applications, such as blasting gelatin, gun and double based propellants with a high oxygen content and good detonation parameters. Their corresponding primary nitrocarbamates of these easy available multivalent alcohols are unknown, and should show a higher stability due to the possibility of hydrogen bonding of the nitrocarbamate moiety. Tris(hydroxymethyl)nitromethane is a cheap commercially available industrial product and therefore became of interest to our research. In addition, a diol containing an acetylene moiety was selected, because nitrocarbamates with alkyne functionalities are unknown.

4.3 Results and Discussion

4.3.1 Synthesis

The most applied method to convert alcohols into the corresponding carbamates is performed by the reaction of urea or isocyanic acid.^[4] In the case of polyols a two-step synthesis is necessary, due to a lowered reactivity, potential multiaddition and polymerization is possible. First, the alcohol is reacted with phosgene or phosgene substitutes such as phenyl chloroformate, followed by treatment with ammonia to generate the carbamate.^[5] The carbamates of glycol **1a** and glycerine **1b** were previously prepared via this two-step phenyl chloroformate route.^[5]

In our study now, we report the synthesis of the carbamates **2a–d** from four readily commercially available polyols ethylene glycol (**1a**), glycerine (**1b**), tris(hydroxymethyl) nitromethane (**1c**) and but-2-yne-1,4-diol (**1d**) in a one-step procedure with the reagent chlorosulfonyl isocyanate (CSI) (Scheme 4-1). CSI has also the advantage to form a chlorosulfonylamide intermediate preventing multi-addition, which is destroyed by the aqueous work-up.^[6]



Scheme 4-1: Synthesis of carbamates (**2a–d**) and nitrocarbamates (**3a–d**) from simple multivalent alcohols (**1a–d**).

In contrast to the aforementioned two-step synthesis with phenyl chloroformate, the CSI route has the advantage of a simple and faster procedure and higher yields (86% to 93%). The nitration of the carbamates **2a–d** was performed in a mixture of anhydrous nitric acid and concentrated sulfuric acid. The conversion to the primary nitrocarbamates **3a–d** can also be achieved by the use of anhydrous nitric acid on its own as nitrating agent, but only with a large excess of anhydrous nitric acid for a complete nitration. The nitrocarbamates of ethylene glycol **3a** and but-2-yne-1,4-diol **3d** were separated by filtration after quenching the reaction mixture with ice-water. However, the carbamate **2a** was nitrated at room temperature, the temperature for **2d** has to be lower than 4 °C, since the alkyne moiety tends to be unstable in the nitration mixture, and gaseous

decomposition products were formed accompanied with decreasing yields. The nitrocarbamates **3b** and **3c** are highly water-soluble, and therefore require extraction with ethyl acetate after quenching with ice-water. All four nitrocarbamates **3a–d** were obtained anhydrous, but **3b** and **3c** were shown to be rather hygroscopic, visible by melting and resolidification. On the other hand, **3a** and **3d** are recrystallized from water without inclusion of crystal water. In general, the nitrocarbamates are better soluble in water compared to their carbamate analogues.

4.3.2 NMR Spectroscopy

In the ^1H NMR spectrum of the carbamates the resonance of the methylene groups is found at 4.61–4.01 ppm. This low field shift is typical for attached carbamate units compared to those of the corresponding alcohols (around 2 ppm). In the spectra of the nitrocarbamates this effect is further enhanced because of the electron withdrawing nature of the nitro group, resulting in an additional downfield shift of approximately 0.5 ppm for the methylene groups. A similar but weaker trend is observed for the CH_2 moiety in the ^{13}C NMR spectra. The resonance of the carbamate carbonyl carbon atom is found near 156 ppm, whereas for the nitrocarbamates a significant upfield shift to around 148 ppm occurs, due to the presence of the electron withdrawing nitro group.

The NH_2 resonance in the ^1H NMR spectrum of the carbamates is quite broad as a result of the restricted rotation around the C–N bond, and located around 6.5 ppm.^[7] The line-widths of the NH resonances of the nitrocarbamates are smaller but shifted to lower field beyond 13 ppm, caused by the acidification due to the neighboring nitro group. For the carbamate **2a** and the corresponding nitrocarbamate **3a** exemplary the ^{15}N NMR spectrum was recorded, showing the NH_2 resonance at –310.0 ppm and the NHNO_2 shifted downfield to –196.2 ppm. The resonances of the nitro groups are found at –46.3 ppm, in a typical range for nitrocarbamates.^[2b]

4.3.3 Vibrational Spectroscopy

In the vibrational spectra, the characteristic bands of the carbonyl groups of the carbamates are located in the range of 1685–1613 cm^{-1} . For the nitrocarbamates these stretching frequencies are shifted to 1784–1743 cm^{-1} . Further, for all nitrocarbamates the typical asymmetric and symmetric stretching vibration of the NO_2 groups can be observed around 1600 and 1200 cm^{-1} . An additional intense peak in the Raman in the region of 1001–1031 cm^{-1} vibration can be assigned according the literature to the N–N stretching vibration of the nitrocarbamate moiety.^[8]

4.3.4 Single Crystal Structure Analysis

Single crystals suitable for X-ray diffraction studies were obtained by crystallization at room temperature from water (**2a**, **3a**, **3d**) and from acetonitrile (**3b**, **3c**). A full list of the crystallographic structure and refinement data are shown in Appendix A.4.

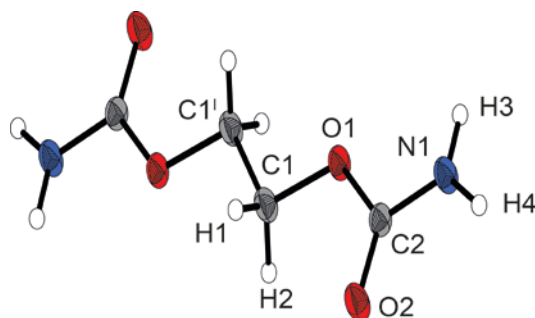


Figure 4-1: X-ray molecular structure of ethane-1,2-diyl dicarbamate (2a).

Selected atom distance (Å) and angles (deg): C1–O1 1.439(2), C2–N1 1.321(2), C2–O1 1.357(2), C2–O2 1.224(2), N1–H3 0.91(2), N1–H4 0.93(3), C2–O1–C1 114.8(1), O2–C2–O1–C1 2.3(2), H4–N1–C2–O2 –2(2).

For the purpose of a discussion and comparison of the energetic nitrocarbamates also a crystal structure of the carbamate **2a** was determined. The dicarbamate **2a** (Figure 4-1) crystallizes in the monoclinic space group $P2_1/c$ and the asymmetric unit consists of a half molecule, due to an inversion center in the center of the glycol structure. The carbamate moiety and in addition the complete carbon backbone is nearly perfectly planar which is displayed by the two torsion angles O2–C2–O1–C1 2.3 ° and H4–N1–C2–O2 –2.0 °. However, this is not the case in the corresponding nitrocarbamate **3a**.

Compound **3a** crystallizes in the orthorhombic space group $Pdd2$ with one molecule as asymmetric unit (Figure 4-2). Compared to the carbamate, both nitrocarbamate ends are non-planar and the nitro groups are turned out more than 10 °, which was observed earlier in structures of nitrocarbamates.^[8b] The short N–N bond lengths of the nitramines with 1.38 Å indicate significant double bond character and are achieved by delocalization of the nitrogen lone pair on N2 and N3. Furthermore, the distance of the C–O in the carbonyl groups and N–H bonds show compared to the carbamate structure of **2a** a slight shortening as a result of the electron withdrawing nitro group.

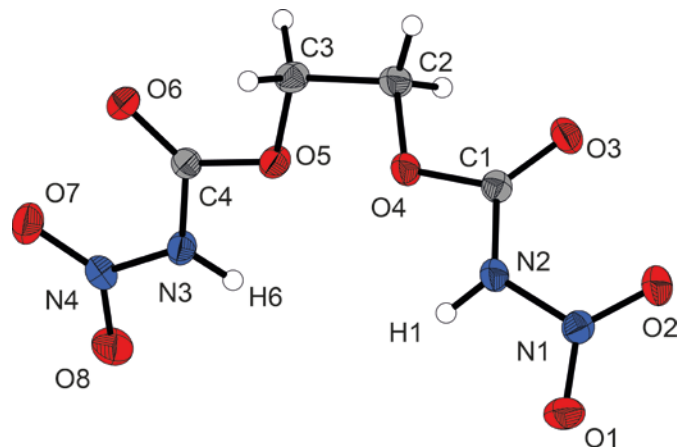


Figure 4-2: X-ray molecular structure of ethane-1,2-diyl bis(nitrocarbamate) (3a).

Selected atom distances (Å) and angles (deg): C1–N2 1.390(1), C1–O3 1.195(1), C1–O4 1.332(1), C2–O4 1.461(1), N2–H1 0.84(2), N1–N2 1.377(1), N1–N2–H1 111(1), H1–N2–C1 121(1), N1–N2–C1 122.44(9), N1–N2–C1–O3 –15.0(2), O1–N1–N2–C1 160.75(2).

The nitrocarbamate **3b** with the glycerine backbone crystallizes in the triclinic space group $P\bar{1}$ with one water and two acetonitrile molecules (Figure 4-3). Similar geometric features are present, although here just two of the three nitrocarbamates moieties are turned significantly out of planarity.

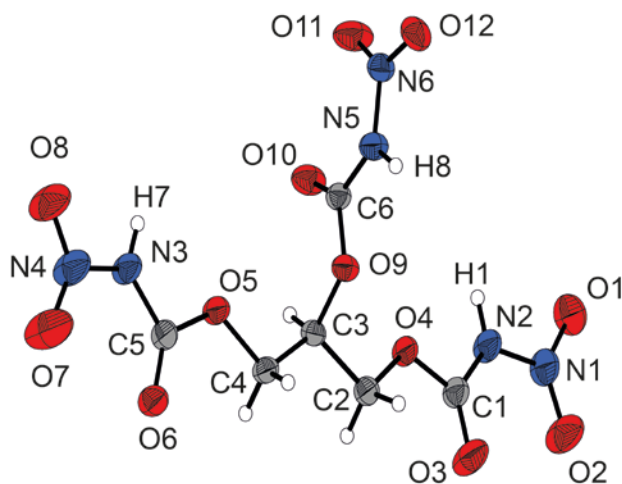


Figure 4-3: X-ray molecular structure of propane-1,2,3-triyl tris(nitrocarbamate) (3b).

Selected atom distances (Å) and angles (deg): C1–N2 1.379(3), C1–O3 1.189(2), C1–O4 1.328(2), N1–N2 1.376(2), N2–H1 0.85(2), C6–N5–N6–O12 –177.5(2), O1–N1–N2–C1 –170.5(2).

The nitrocarbamate **3c** of the alcohol tris(hydroxymethyl) nitromethane crystallizes in the space group $P2_1/c$ with a large unit cell and with two unique molecules and two solvent (acetonitrile)

molecules (Figure 4-4). Here, the dihedral angles C–N–N–O of the nitrocarbamates moieties are all turned out of the plane more than 10° and show the same structure characteristics.

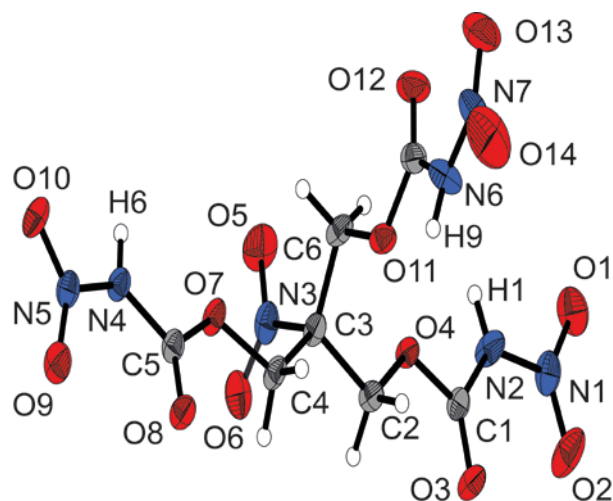


Figure 4-4: X-ray molecular structure of one unique molecule of nitroisobutylglycerol trinitrocarbamate (3c). Selected atom distances (Å) and angles (deg): N2–C1 1.376(3), N2–H1 0.86(3), N3–C3–C6 106.6(2), N3–C3–C4 107.6(2), N3–C3–C2 107.6(2), N1–N2–C1–O4 175.2(2), O1–N1–N2–C1 $-172.3(2)$.

The nitrocarbamate **3d** with the alkyne group crystallizes in the monoclinic space group $P2_1/c$ with half of the molecule as asymmetric unit (Figure 4-5). In this case, the nitro group is rotated away to a large degree of 24.2° out of the plane and thus represents a maximum value so far observed. A reason for this observation could be the result of competing conjugation requirements of the alkyne, the carbamate and the nitro functional group. In the literature is also discussed, that with increasing alkyl chain length of the alkoxy group a decrease in planarity of the nitrocarbamate moiety seems to occur.^[8b]

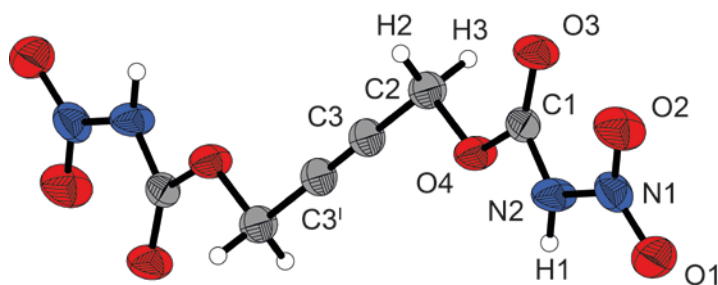


Figure 4-5: X-ray molecular structure of but-2-yne-1,4-diyl bis(nitrocarbamate) (3d).

Selected atom distances (Å) and angles (deg): C1–N2 1.381(2), C1–O3 1.187(2), C1–O4 1.322(2), C2–C3 1.458(2), C3–C3' 1.183(2), C2–O4 1.452(2), O4–C2–C3 105.8(1), O3–C1–O4–C2 7.5(2), N1–N2–C1–O3 7.4(3), O1–N1–N2–C1 155.8(2).

4.3.5 Thermal Stabilities and Energetic Properties

The nitrate esters of the four alcohols glycol, glycerine, tris(hydroxymethyl) nitromethane and but-2-yne-1,4-diol are reported and the first two are well established. The nitrate ester of tris(hydroxymethyl) nitromethane is reported to be fairly unstable and impossible to stabilize;^[3] whereas that of but-2-yne-1,4-diol has been mentioned previously, but remains questionable as no details of the compound are available.^[9] The four here presented nitrocarbamates are all solids compared to their nitrate ester analogues, which are oily liquids partially with high vapor pressures. Another advantage of the nitrocarbamates is the higher nitrogen content of approximately 5%, whereas the oxygen balance Ω is lower. The sensitivity against mechanical stimuli is very important for a safe handling and use of energetic materials. The sensitivity against friction (FS) is determined by rubbing a small amount between a porcelain plate and a pin with different contact pressures. No significant differences in the comparison of the nitrate esters **EGDN** and **NG** and the nitrocarbamates **3a** and **3b** were observed (Table 4-1); both groups of materials show only slight sensitivity to friction (≥ 360 N insensitive, 360–80 N sensitive, 80–10 N very sensitive, ≤ 10 N extremely sensitive).

Table 4-1: Physical and chemical properties of 3a–3d.

	3a	3b	3c	3d
$T_m / ^\circ\text{C}$ [a]	151	-	-	-
$T_{\text{dec}} / ^\circ\text{C}$ [b]	157	152	148	149
ρ (RT) / g cm^{-3} [c]	1.82	1.78	1.72	1.68
IS / J [d]	15	10	15	8
FS / N [e]	360	240	360	240
ESD / J [f]	0.20	0.15	0.15	0.15
N / % [g]	23.5	23.6	23.6	21.4
O / % [h]	53.8	53.9	54.0	48.8
$N+O$ / % [i]	77.3	77.5	77.6	70.2
Ω_{CO_2} / % [j]	-20.2	-18.0	-17.3	-42.7
Ω_{CO} / % [k]	+8.9	+9.0	+9.6	-6.1

[a] Onset melting T_m and [b] onset decomposition point T_{dec} from DSC measurement carried out at a heating rate of $5\text{ }^\circ\text{C min}^{-1}$. [c] Density at room temperature from pycnometer measurement. [d] Impact sensitivity. [e] Friction sensitivity. [f] Sensitivity towards electrostatic discharge. [g] Nitrogen content. [h] Oxygen content. [i] Sum of nitrogen and oxygen content. [j] Oxygen balance assuming the formation of CO and the formation of the formation of [k] CO₂ at the combustion.

The more important value is the sensitiveness towards impact (IS) of a compound which is tested by the action of a dropping weight on a sample.^[10] The nitrates **EGDN** and **NG** exhibit an extraordinarily high sensitivity of 0.2 J and must be classified in the most dangerous class (≥ 40 J insensitive, 40–35 J less sensitive, 35–4 J sensitive, ≤ 3 J very sensitive).^[3, 10] However, the nitrocarbamates **3a** and **3b** are much less sensitive; they have to be classified as sensitive (from 8 to 15 J) but can be handled without the risk of spontaneous detonation, which is not the case for **EGDN** and **NG**. The sensitivity values for the nitrocarbamates **3a/b/c** are fairly similar, except an impact sensitivity of 8 J for the alkyne derivative **3d** at the border to very sensitive.

The performance of energetic materials can be calculated by the computer code EXPLO5 (V.6.02).^[11] The major parameters are the detonation velocity V_{det} , heat of explosion Q_v and the detonation pressure P_{CJ} . These values depend in turn on the density and the energy of formation of the material at room temperature. The detonation and combustion parameters are summarized in Table 4-2 (for further values especially for the nitrate esters see Appendix A.4).

Table 4-2: Calculated heats of formation, predicted detonation and combustion parameters (using the EXPLO5 V6.02 code) for 3a–3d.

	3a	3b	3c	3d
$\Delta H_f^\circ / \text{kJ mol}^{-1}$ [a]	–685	–985	–1023	–339
$\Delta U_f^\circ / \text{kJ kg}^{-1}$ [b]	–2784	–2676	–2373	–1208
$Q_v / \text{kJ kg}^{-1}$ [c]	–4013	–4064	–4294	–4816
T_{ex} / K [d]	2944	3038	3216	3406
$V_0 / \text{L kg}^{-1}$ [e]	731	727	734	745
$P_{\text{CJ}} / \text{kbar}$ [f]	278	261	248	236
$V_{\text{det}} / \text{m s}^{-1}$ [g]	8014	7842	7703	7594
I_{sp} / s [h]	218	221	228	221
I_{sp} / s (5% Al) [i]	230	231	238	235
I_{sp} / s (10% Al) [i]	241	240	246	247
I_{sp} / s (15% Al) [i]	246	246	250	252
I_{sp} / s (20% Al) [i]	249	249	253	246
I_{sp} / s (15% Al, binder) [j]	236	236	237	238

[a] Enthalpy and [b] energy of formation calculated by the CBS-4 M method using Gaussian 09.^[17,18] [c] Heat of explosion. [d] Detonation temperature. [e] Volume of gaseous products. [f] Detonation pressure [g] Detonation velocity calculated by using the EXPLO5 (Version 6.02) program package.^[11] [h] Specific impulse of the neat compound using the EXPLO5 (Version 6.02) program package at 70.0 bar chamber pressure and with equilibrium expansion.^[11] [i] Specific impulse for compositions with different percentage of aluminum [j] and with binder (6% polybutadiene acrylic acid, 6% polybutadiene acrylonitrile and 2% bisphenol A ether).

The nitrocarbamate of glycol **3a** shows the highest detonation velocity in the here discussed selection of 8014 m s^{-1} . The corresponding nitrate ester, nitroglycol **EGDN**, has a significantly lower detonation velocity of 7502 m s^{-1} , due to the much lower density (1.59 g cm^{-3}) and in spite of the good oxygen balance Ω . Furthermore, all nitrocarbamates show an advantageously lower detonation temperature with still good detonation pressures. Moreover, the alkyne nitrocarbamate **3d** shows good properties, especially in propellant mixtures with aluminum as fuel, which achieves a specific impulse I_{sp} of 252 s with an admixture of 15% aluminum as the best ratio.

4.4 Conclusion

The synthesis route of choice for the preparation of multivalent nitrocarbamates is the two step synthesis starting with the carbamate preparation from alcohols with chlorosulfonyl isocyanate (CSI) and subsequent nitration. Full characterization of the materials including discussion of the energetic properties in addition with molecular structures of all nitrocarbamates were performed. The nitrocarbamates are solids with low sensitivity to mechanic stimuli and good thermal stabilities. The nitrocarbamate of glycol, ethane-1,2-diyl bis(nitrocarbamate) (**3a**), exhibits good detonation performances, which are much higher than values of the corresponding nitrate ester **EGDN**. The simple synthetic route, the good physical properties especially those of **3a** and the acetylene nitrocarbamate, but-2-yne-1,4-diyl bis(nitrocarbamate) (**3d**), suggest potential application as energetic materials.

4.5 Experimental Section

4.5.1 General Procedures

All chemicals were used as supplied. Raman spectra were recorded in a glass tube with Nd:YAG laser excitation up to 1000 mW (at 1064 nm). Infrared spectra were measured with an ATR device. All spectra were recorded at ambient temperature. NMR spectra were recorded with a JEOL/Bruker instrument, and chemical shifts were determined with respect to external Me_4Si (^1H , 399.8 MHz; ^{13}C , 100.5 MHz) and MeNO_2 (^{15}N , 40.6 MHz; ^{14}N , 28.9 MHz). Melting and decomposition points were measured with a DSC with a heating rate of $5 \text{ }^\circ\text{C min}^{-1}$ in a temperature range of 15–400 $^\circ\text{C}$. The melting points were checked by a melting point apparatus

(not corrected). The sensitivity data were performed using a BAM drophammer and a BAM friction tester.^[10, 12]

4.5.2 Computational Details

All ab initio calculations were carried out using the program package Gaussian 09 (Rev. A.02)^[13] and visualized by GaussView 5.08.^[14] Structure optimizations and frequency analyses were performed with Becke's B3 three parameter hybrid functional using the LYP correlation functional (B3LYP). For C, H, N and O a correlation consistent polarized double- ζ basis set cc-pVDZ was used. The structures were optimized with symmetry constraints and the energy is corrected with the zero point vibrational energy.^[15] The enthalpies (H) and free energies (G) were calculated using the complete basis set (CBS) method in order to obtain accurate values. The CBS models used the known asymptotic convergence of pair natural orbital expressions to extrapolate from calculations using a finite basis set to the estimated complete basis set limit. CBS-4 M starts with a HF/3-21G(d) structure optimization, which is the initial guess for the following SCF calculation as a base energy and a final MP2/6-31+G calculation with a CBS extrapolation to correct the energy in second order. The used CBS-4 M method additionally implements a MP4(SDQ)/6-31+(d,p) calculation to approximate higher order contributions and also includes some additional empirical corrections.^[16] The enthalpies of the gas-phase species were estimated according to the atomization energy method.^[17]

4.5.3 X-ray Crystallography

Crystals suitable for X-ray crystallography were selected by means of a polarization microscope and mounted on a glass fiber. The measurements were investigated with an Oxford XCalibur3 KappaCCD diffractometer. The diffractometer is equipped with a generator (voltage 50 kV, current 40 mA) and a KappaCCD detector operating with MoK α radiation ($\lambda = 0.7107 \text{ \AA}$). The solution of the structure was performed by direct methods (SIR97)^[18] and refined by full-matrix least-squares on F^2 (SHELXL)^[19] implemented in the WINGX software package^[20] and finally checked with the PLATON software^[21]. All non-hydrogen atoms were refined anisotropically. The hydrogen atom positions were located in a difference Fourier map. ORTEP plots are shown with thermal ellipsoids at the 50% probability level. Crystallographic data (excluding structure factors) for the structures reported in this paper have been deposited (1429437 (**2a**), 1429438 (**3a**),

1429439 (**3b**), 1429440 (**3d**), 1429441 (**3c**)) and can be obtained free of charge from the Cambridge Crystallographic Data Centre via www.ccdc.cam.ac.uk/data_request/cif.

4.5.4 Calculation of Energetic Performance

All calculations affecting the detonation parameters were carried out using the program package EXPLO5 V6.02.^[11, 22] The detonation parameters were calculated at the Chapman-Jouguet (CJ) condition point with the aid of the steady-state detonation model using a modified Becker-Kistiakowski-Wilson equation of state for modeling the system. The CJ point is found from the Hugoniot curve of the system by its first derivative. The specific impulses I_{sp} were also calculated with the EXPLO5 V6.02 program, assuming an isobaric combustion of a composition of oxidizer with different amounts of aluminum as fuel. A chamber pressure of 70.0 bar and an ambient pressure of 1.0 bar with equilibrium expansion conditions were estimated for the calculations.

4.5.5 Synthesis

CAUTION! Nitrocarbamates are potential energetic materials and are sensitive toward heat, impact, and friction. No hazards occurred during preparation and manipulation; additional proper protective precautions (face shield, leather coat, earthened equipment and shoes, Kevlar gloves, and ear plugs) should be used when handling these compounds.

Carbamates 2a–d: The alcohol (**1a–d**) (10 mmol) was diluted in fresh distilled acetonitrile (20 mL) and placed in an ice bath and chlorosulfonyl isocyanate (CSI) (1.05 per equivalent hydroxyl group) was added slowly. The ice bath was removed, and stirring at room temperature was continued for 1 h. The reaction mixture was again cooled with an ice bath, and quenched carefully with water (20 mL). The stirring was continued at room temperature for 0.5 h and the organic solvent was removed. The formed precipitate was filtered, washed thoroughly with water and dried under high vacuum to obtain colorless pure carbamate (**2a**, 72%; **2b**, 82%; **3c**, 62%; **2d**, 92%).

Nitrocarbamate 3a: Into cooled concentrated sulfuric acid (98.5%, 4 mL) was dropped fuming nitric acid (>99.5%, 4 mL) below 5 °C. Into this chilled mixed acid the carbamate **2a** 296 mg, 2 mmol) was added in small portions. The mixture was stirred 10 minutes at this temperature and 1.5 h at ambient temperature. The reaction mixture was poured onto ice-water (50 mL) and

stirred for further. The formed precipitate was filtered off and washed with water. After recrystallization from water, 357 mg (75%) of colorless pure product **3a** was obtained.

Nitrocarbamates 3b and 3c: Into concentrated sulfuric acid (98.5%, 3 mL) was dropped fuming nitric acid (>99.5%, 3 mL) at 0 °C. To this chilled nitration mixture the carbamate **2b** or **2c** (221 mg, 1 mmol or 280 mg, 1 mmol) in small portions was added. The suspension was stirred 15 minutes at this temperature and 1.5 h at ambient temperature. The mixture was poured onto ice-water (100 mL), and extracted with ethyl acetate (3 x 50 mL). The combined organic phases were washed with water and brine and dried sufficient with magnesium sulfate. The solvent was removed under reduced pressure to obtain a oily product, which turns into a colorless precipitate by treating the slurry with chloroform. After recrystallization from acetonitrile and drying under high vacuum pure colorless nitrocarbamate was obtained (**2b**, 281 mg, 79%; **2c**, 195 mg, 47%).

Nitrocarbamate 3d: Into concentrated sulfuric acid (98.5%, 4 mL) was dropped fuming nitric acid (>99.5%, 4 mL per equivalent) below 5 °C in an ice bath. Into this chilled mixed acid the carbamate **2d** (344 mg, 2 mmol) was added in small portions. The mixture was stirred 50 minutes below 4 °C and was poured onto ice-water (50 mL) and further stirred. The formed precipitate was filtered off and washed with water. After recrystallization from water, 278 mg (56%) of colorless pure product **3d** was obtained.

Ethane-1,2-diyl dicarbamate (2a): ^1H NMR ($[\text{D}_6]$ DMSO): δ 6.51 (s, 4H, NH_2), 4.01 (s, 4H, CH_2) ppm. $^{13}\text{C}\{^1\text{H}\}$ NMR ($[\text{D}_6]$ DMSO): δ 157.1 (CO), 62.7 (CH_2) ppm. $^{15}\text{N}\{^1\text{H}\}$ NMR ($[\text{D}_6]$ DMSO): δ -310.0 (NH_2) ppm. IR (ATR, cm^{-1}): ν 3422 (m), 3339 (w), 3266 (m), 3209 (m), 2990 (w), 2915 (w), 1643 (s), 1614 (s), 1483 (w), 1395 (s), 1308 (s), 1227 (w), 1090 (s), 894 (m), 776 (m), 696 (m). Raman (1064 nm, 500 mW, cm^{-1}): ν 3410 (6), 3267 (8), 3208 (14), 2975 (65), 2922 (40), 1694 (25), 1673 (15), 1646 (8), 1631 (16), 1483 (28), 1442 (9), 1374 (7), 1276 (26), 1123 (100), 1080 (19), 968 (56), 663 (50), 573 (13), 307 (32), 236 (18). MS (DEI+) m/e : 149.1 $[(\text{M}+\text{H})^+]$. Elemental analysis, calcd (%): $\text{C}_4\text{H}_8\text{N}_2\text{O}_4$ (148.12): C 32.44, H 5.44, N 18.91; found: C 32.42, H 5.62, N 18.78. DSC (5 °C min^{-1} , onset): 166 °C (melt.), 225 °C (dec.). BAM drophammer: >40 J. Friction tester: >360 N (grain size 100–500 μm).

Ethane-1,2-diyl bis(nitrocarbamate) (3a): ^1H NMR ($[\text{D}_6]$ acetone): δ 13.4 (br, 2H, NH), 4.51 (s, 4H, CH_2) ppm. $^{13}\text{C}\{^1\text{H}\}$ NMR ($[\text{D}_6]$ acetone): δ 148.4 (CO), 64.1 (CH_2) ppm. $^{15}\text{N}\{^1\text{H}\}$ NMR ($[\text{D}_6]$ acetone): δ -46.3 (NHNO_2), -196.2 (NHNO_2) ppm. IR (ATR, cm^{-1}): ν 3285 (w), 3147 (w), 3040 (w), 2968 (w), 1754 (m), 1741 (m), 1619 (m), 1600 (m), 1592 (m), 1551 (w), 1492 (w), 1465 (w), 1437 (m), 1366 (m), 1321 (m), 1278 (w), 1246 (w), 1195 (s), 1168 (s), 1048 (w), 1033 (m), 996

(m), 983 (m), 880 (s), 796 (m), 756 (m), 737 (m), 725 (w), 665 (w). Raman (1064 nm, 800 mW, cm^{-1}): ν 3020 (24), 3000 (35), 2977 (53), 2970 (72), 1745 (55), 1627 (29), 1595 (28), 1529 (24), 1464 (40), 1446 (38), 1406 (35), 1341 (59), 1325 (87), 1279 (57), 1249 (32), 1197 (31), 1181 (29), 1124 (29), 1099 (37), 1037 (55), 1001 (100), 891 (32), 806 (37), 764 (32), 726 (35), 463 (65), 454 (62), 401 (69), 299 (48), 279 (51). MS (DEI+) m/e : 239.1 $[(M+H)^+]$. Elemental analysis, calcd (%): $\text{C}_4\text{H}_6\text{N}_4\text{O}_8$ (238.11): C 20.18, H 2.54, N 23.53; found: C 20.17, H 2.61, N 23.40. DSC ($5\text{ }^\circ\text{C min}^{-1}$, onset): $151\text{ }^\circ\text{C}$ (melt.), $157\text{ }^\circ\text{C}$ (dec.). BAM drophammer: 40 J. Friction tester: 360 N (grain size 100–500 μm).

Propane-1,2,3-triyl tricarbamate (2b): ^1H NMR ($[\text{D}_6]\text{DMSO}$): δ 6.57 (s, 6H, NH_2), 4.87 (m, 1H, CH), 4.04 (m, 4H, CH_2) ppm. $^{13}\text{C}\{^1\text{H}\}$ NMR ($[\text{D}_6]\text{DMSO}$): δ 156.9 (CONH_2), 156.5 (CONH_2), 70.2 (CH), 62.9 (CH_2) ppm. ^{14}N NMR ($[\text{D}_6]\text{DMSO}$): δ -308 (NH_2) ppm. IR (ATR, cm^{-1}): ν 3431 (m), 3342 (m), 3279 (m), 3218 (m), 2966 (w), 2930 (w), 1710 (m), 1685 (s), 1616 (m), 1610 (m), 1470 (m), 1449 (m), 1409 (s), 1355 (m), 1344 (m), 1317 (s), 1247 (w), 1140 (s), 1070 (s), 1055 (s), 1041 (s), 978 (m), 939 (w), 928 (m), 868 (w), 829 (w), 780 (s), 751 (w), 762 (m). Raman (1064 nm, 500 mW, cm^{-1}): ν = 3413 (10), 3276 (13), 3249 (15), 3205 (27), 3020 (48), 2987 (57), 2968 (100), 2932 (57), 1696 (35), 1639 (25), 1630 (28), 1475 (21), 1456 (15), 1423 (22), 1299 (48), 1251 (25), 1128 (40), 1054 (18), 979 (29), 930 (68), 830 (67), 668 (36), 523 (22), 504 (60). MS (DEI+) m/e : 222.1 $[(M+H)^+]$. Elemental analysis, calcd (%): $\text{C}_6\text{H}_{11}\text{N}_3\text{O}_6$ (221.17): C 32.58, H 5.01, N 19.00; found: C 32.19, H 5.27, N 18.69. DSC ($5\text{ }^\circ\text{C min}^{-1}$, onset): $167\text{ }^\circ\text{C}$ (melt.). BAM drophammer: >40 J. Friction tester: >360 N (grain size $<100\text{ }\mu\text{m}$).

Propane-1,2,3-triyl tris(nitrocarbamate) (3b): ^1H NMR ($[\text{D}_6]\text{DMSO}$): δ 13.6 (br, 3H; NH), 5.47 (m, CH_2CHCH_2), 4.67 (m, 2H, CHHCHCHH), 4.50 (m, 2H, CHHCHCHH) ppm. $^{13}\text{C}\{^1\text{H}\}$ NMR ($[\text{D}_6]\text{DMSO}$): δ 148.1 ($\text{C}(\text{OCH}_2)$), 147.9 ($\text{C}(\text{OCH})$), 71.4 ($\text{OCH}(\text{CH}_2)_2$), 63.7 ($\text{OCH}_2(\text{CH})$) ppm. ^{14}N NMR ($[\text{D}_6]\text{DMSO}$): δ -46 (NHNO_2), -196 (br, NHNO_2) ppm. IR (ATR, cm^{-1}): ν 3513 (w), 3377 (w), 3145 (w), 3029 (w), 2869 (w), 2293 (w), 2261 (w), 1753 (s), 1608 (s), 1430 (m), 1404 (m), 1328 (m), 1283 (w), 1155 (vs), 1076 (m), 994 (m), 976 (m), 944 (m), 923 (m), 875 (m), 802 (m), 749 (m), 733 (m), 725 (m). Raman (1064 nm, 500 mW, cm^{-1}): ν 3130 (10), 2980 (71), 2945 (81), 2903 (14), 2294 (8), 2261 (38), 1791 (22), 1760 (34), 1611 (17), 1461 (31), 1360 (29), 1326 (61), 1286 (26), 1241 (14), 1208 (13), 1142 (20), 1108 (25), 1078 (21), 1014 (100), 923 (17), 881 (11), 803 (16), 743 (12), 643 (8), 460 (46), 389 (31), 287 (17). MS (DEI+) m/e : 357.2 $[(M+H)^+]$. Elemental analysis, calcd (%): $\text{C}_6\text{H}_8\text{N}_6\text{O}_{12}$ (356.16): C 20.23, H 2.26, N 23.60; found: C 22.22, H 2.33, N 23.09. DSC ($5\text{ }^\circ\text{C min}^{-1}$, onset): $152\text{ }^\circ\text{C}$ (dec.). BAM drophammer: 8 J. Friction tester: 120 N (grain size $<100\text{ }\mu\text{m}$).

Nitroisobutylglycerol tricarbamate (2c): ^1H NMR ($[\text{D}_6]$ acetone): δ 6.16 (s, 6H, NH_2), 4.49 (s, 6H, CH_2) ppm. $^{13}\text{C}\{^1\text{H}\}$ NMR ($[\text{D}_6]$ acetone): δ 155.5 (CO), 89.6 (CNO_2), 61.2 (CH_2) ppm. ^{14}N NMR ($[\text{D}_6]$ acetone): δ -5 (NO_2), -299 (NH_2) ppm. IR (ATR, cm^{-1}): ν 3447 (w), 3349 (w), 3290 (w), 3223 (w), 1719 (s), 1703 (m), 1613 (m), 1560 (m), 1546 (m), 1467 (m), 1459 (m), 1449 (m), 1430 (w), 1396 (m), 1358 (m), 1333 (s), 1312 (m), 1299 (m), 1163 (m), 1106 (m), 1079 (s), 964 (w), 922 (w), 904 (w), 859 (w), 836 (w), 776 (w), 769 (m), 689 (w), 678 (w). Raman (1064 nm, 700 mW, cm^{-1}): ν 3257 (13), 3202 (14), 3038 (38), 3002 (54), 2971 (100), 2900 (13), 1711 (37), 1648 (23), 1588 (12), 1549 (30), 1467 (40), 1439 (21), 1393 (17), 1362 (29), 1337 (22), 1317 (34), 1241 (28), 1202 (17), 1143 (37), 1110 (41), 1004 (19), 966 (17), 923 (94), 895 (35), 838 (65), 751 (17), 685 (29), 669 (24), 598 (27), 585 (32), 560 (31), 520 (27), 493 (28), 354 (46), 333 (29), 259 (51), 222 (26). MS (DEI+) m/e : 281.2 $[(\text{M}+\text{H})^+]$. Elemental analysis, calcd (%): $\text{C}_7\text{H}_{12}\text{N}_4\text{O}_8$ (280.19): C 30.01, H 4.32, N 20.00; found: C 30.00, H 4.25, N 19.92. DSC ($5\text{ }^\circ\text{C min}^{-1}$, onset): $188\text{ }^\circ\text{C}$ (mp.), $202\text{ }^\circ\text{C}$ (dec.). BAM drophammer: $>40\text{ J}$. Friction tester: $>360\text{ N}$ (grain size 100–500 μm).

Nitroisobutylglycerol tris(nitrocarbamate) (3c): ^1H NMR ($[\text{D}_6]$ acetone): δ 13.7 (br, 3H, NH), 4.88 (s, 6H, CH_2) ppm. $^{13}\text{C}\{^1\text{H}\}$ NMR ($[\text{D}_6]$ acetone): δ 147.2 (CO), 88.2 (CNO_2), 62.6 (CH_2) ppm. ^{14}N NMR ($[\text{D}_6]$ acetone): δ -8 (CNO_2), -46 (NHNO_2) ppm. IR (ATR, cm^{-1}): ν 3247 (w), 3197 (w), 3053 (w), 2360 (w), 1772 (s), 1614 (s), 1571 (w), 1553 (m), 1445 (m), 1387 (w), 1355 (w), 1329 (m), 1198 (s), 1174 (s), 1012 (w), 979 (m), 955 (m), 861 (w), 819 (w), 801 (w), 747 (w), 718 (w). Raman (1064 nm, 500 mW, cm^{-1}): ν 3198 (9), 3022 (18), 2983 (32), 2918 (10), 2708 (7), 1774 (43), 1619 (16), 1573 (10), 1555 (12), 1468 (33), 1357 (28), 1323 (42), 1268 (14), 1207 (14), 1180 (11), 1101 (12), 1031 (100), 981 (20), 862 (35), 816 (11), 732 (12), 647 (16), 464 (35), 350 (29), 234 (27). MS (DCI+) m/e : 416.2 $[(\text{M}+\text{H})^+]$. Elemental analysis, calcd (%): $\text{C}_7\text{H}_9\text{N}_7\text{O}_{14}$ (415.18): C 20.25, H 2.18, N 23.62; found: C 20.34, H 2.33, N 23.92. DSC ($5\text{ }^\circ\text{C min}^{-1}$, onset): $149\text{ }^\circ\text{C}$ (dec.). BAM drophammer: 15 J. Friction tester: 360 N (grain size $<100\text{ }\mu\text{m}$).

But-2-yne-1,4-diyl dicarbamate (2d): ^1H NMR ($[\text{D}_6]$ DMSO): δ 6.7 (br, 4H, NH_2), 4.61 (s, 4H, CH_2) ppm. $^{13}\text{C}\{^1\text{H}\}$ NMR ($[\text{D}_6]$ DMSO): δ 156.3 (CO), 82.0 (C_{sp}), 51.8 (CH_2) ppm. ^{14}N NMR ($[\text{D}_6]$ DMSO): δ -302 (NH_2) ppm. IR (ATR, cm^{-1}): ν 3445 (m), 3333 (w), 3251 (m), 3188 (w), 2954 (w), 1722 (s), 1601 (m), 1445 (m), 1406 (m), 1319 (s), 1225 (m), 1154 (m), 1121 (m), 1039 (s), 1003 (m), 927 (m), 773 (s), 723 (m), 686 (w). Raman (1064 nm, 500 mW, cm^{-1}): ν 3446 (3), 3247 (6), 3184 (6), 2980 (31), 2955 (100), 2903 (7), 2879 (9), 2327 (36), 2254 (79), 1714 (18), 1608 (13), 1454 (45), 1402 (22), 1335 (19), 1234 (24), 1136 (20), 1053 (20), 990 (13), 933 (37), 832 (15), 643 (33), 561 (38), 432 (26), 355 (73), 249 (18). MS (DEI+) m/e : 173.1 $[(\text{M}+\text{H})^+]$. Elemental analysis, calcd (%): $\text{C}_6\text{H}_8\text{N}_2\text{O}_4$ (172.14): C 41.86, H 4.68, N 16.27; found: C 41.69, H 4.67, N 16.49. DSC ($5\text{ }^\circ\text{C min}^{-1}$, onset): $149\text{ }^\circ\text{C}$ (dec.). BAM drophammer: 15 J. Friction tester: 360 N (grain size $<100\text{ }\mu\text{m}$).

min⁻¹, onset): 187 °C (melt.), 264 °C (dec.). BAM drophammer: >40 J. Friction tester: >360 N (grain size <100 μm).

But-2-yne-1,4-diyl bis(nitrocarbamate) (3d): ¹H NMR ([D₆]acetone): δ 13.5 (br, 2H, NH), 4.95 (s, 4H, CH₂) ppm. ¹³C{¹H} NMR ([D₆]acetone): δ 147.9 (CO), 81.0 (C_{sp}), 53.9 (CH₂) ppm. ¹⁴N NMR ([D₆]acetone): δ -46 (NO₂), -199 (NH) ppm. IR (ATR, cm⁻¹): ν 3168 (w), 3048 (w), 1737 (m), 1606 (m), 1442 (m), 1374 (m), 1319 (m), 1235 (m), 1189 (s), 1159 (s), 1011 (m), 995 (w), 936 (s), 816 (m), 754 (w), 731 (w), 662 (w). Raman (1064 nm, 500 mW, cm⁻¹): ν 3173 (5), 2998 (20), 2967 (71), 2885 (7), 2336 (21), 2271 (25), 2258 (30), 1738 (20), 1628 (15), 1458 (14), 1442 (10), 1375 (38), 1329 (42), 1239 (8), 1196 (21), 1013 (100), 992 (14), 949 (10), 935 (12), 783 (10), 532 (12), 467 (26), 346 (41), 287 (5). MS (DEI+) *m/e*: 263.1 [(M+H)⁺]. Elemental analysis, calcd (%): C₆H₆N₄O₈ (262.13): C 27.49, H 2.31, N 21.37; found: C 27.42, H 2.42, N 21.19. DSC (5 °C min⁻¹, onset): 148 °C (dec.). BAM drophammer: 8 J. Friction tester: 240 N (grain size 100–500 μm).

4.6 References

- [1] J. Thiele, A. Lachman, *Justus Liebigs Ann. Chem.* **1895**, 288, 267–311.
- [2] a) Q. J. Axthammer, B. Krumm, T. M. Klapötke, *J. Org. Chem.* **2015**, 80, 6329–6335; b) Q. J. Axthammer, B. Krumm, T. M. Klapötke, *Eur. J. Org. Chem.* **2015**, 2015, 723–729.
- [3] J. Köhler, R. Meyer, A. Homburg, *Explosivstoffe*, Wiley-VCH, Weinheim, **2008**.
- [4] A. R. Modarresi-Alam, F. Khamooshi, M. Nasrollahzadeh, H. A. Amirazizi, *Tetrahedron* **2007**, 63, 8723–8726.
- [5] M. G. Kim, *J. Appl. Polym. Sci.* **2011**, 122, 2209–2220.
- [6] a) R. Graf, *Chem. Ber.* **1956**, 89, 1071–1079; b) D. N. Dhar, K. S. K. Murthy, *Synthesis* **1986**, 1986, 437–449.
- [7] Q. J. Axthammer, T. M. Klapötke, B. Krumm, R. Moll, S. F. Rest, *Z. Anorg. Allg. Chem.* **2014**, 640, 76–83.
- [8] a) G. Gattow, W. K. Knoth, *Z. Anorg. Allg. Chem.* **1983**, 499, 194–204; b) D. S. Bohle, Z. Chua, *Inorg. Chem.* **2014**, 53, 11160–11172.
- [9] a) T. Urbanski, W. Tarantowicz, *Bull. Acad. Pol. Sci., Ser. Sci., Chim., Geol. Geogr.* **1958**, 6, 289–292; b) A. D. Nikolaeva, A. P. Kirsanov **1976**, SU 504749A1; c) S. Narasimhan, S. K. Srinivasan, N. Venkatasubramanian, *Magn. Reson. Chem.* **1987**, 25, 91–92.
- [10] T. M. Klapötke, *Chemistry of High-Energy Materials*, 2nd ed., deGruyter, Berlin, **2012**.
- [11] M. Sućeska, *EXPLO5 V.6.02*, Zagreb, **2013**.
- [12] M. Göbel, T. M. Klapötke, *Adv. Funct. Mater.* **2009**, 19, 347–365.
- [13] M. J. Frisch, G. W. Trucks, H. B. Schlegel, G. E. Scuseria, M. A. Robb, J. R. Cheeseman, V. B. G. Scalmani, B. Mennucci, G. A. Petersson, H. Nakatsuji, M. Caricato, X. Li, H. P. Hratchian, A. F. Izmaylov, J. Bloino, G. Zheng, J. L. Sonnenberg, M. Hada, M. Ehara, K. Toyota, R. Fukuda, J. Hasegawa, M. Ishida, T. Nakajima, Y. Honda, O. Kitao, H. Nakai, T. Vreven, J. J. A. Montgomery, J. E. Peralta, F. Ogliaro, M. Bearpark, J. J. Heyd, E. Brothers, K. N. Kudin, V. N. Staroverov, R. Kobayashi, J. Normand, K. Raghavachari, A. Rendell, J. C. Burant, S. S. Iyengar, J. Tomasi, M. Cossi, N. Rega, J. M. Millam, M. Klene, J. E. Knox, J. B. Cross, V. Bakken, C. Adamo, J. Jaramillo, R. Gomperts, R. E. Stratmann, O. Yazyev, A. J. Austin, R. Cammi, C. Pomelli, J. W. Ochterski, R. L. Martin, K. Morokuma, V. G. Zakrzewski, G. A. Voth, P. Salvador, J. J. Dannenberg, S. Dapprich, A. D. Daniels, Ö. Farkas, J. B. Foresman, J. V. Ortiz, J. Cioslowski, D. J. Fox, *Gaussian 09*, Rev. A.02 ed., Gaussian, Inc., Wallingford CT, **2009**.
- [14] R. D. Dennington, T. A. Keith, J. M. Millam, *GaussView*, Ver. 5.08 ed., Semichem, Inc., Wallingford CT, **2009**.
- [15] J. A. Montgomery, M. J. Frisch, J. W. Ochterski, G. A. Petersson, *J. Chem. Phys.* **2000**, 112, 6532–6542.
- [16] J. W. Ochterski, G. A. Petersson, J. A. Montgomery, *J. Chem. Phys.* **1996**, 104, 2598–2619.

- [17] E. F. C. Byrd, B. M. Rice, *J. Phys. Chem.* **2005**, *110*, 1005–1013.
- [18] A. Altomare, M. C. Burla, M. Camalli, G. L. Cascarano, C. Giacovazzo, A. Guagliardi, A. G. G. Moliterni, G. Polidori, R. Spagna, *J. Appl. Crystallogr.* **1999**, *32*, 115–119.
- [19] a) G. M. Sheldrick, *SHELX-97, Programs for Crystal Structure Determination*, **1997**; b) G. M. Sheldrick, *Acta Crystallogr., Sect. A: Found. Crystallogr.* **2008**, *A64*, 112–122.
- [20] L. Farrugia, *J. Appl. Crystallogr.* **1999**, *32*, 837–838.
- [21] A. Spek, *Acta Crystallogr., Sect. D: Biol. Crystallogr.* **2009**, *65*, 148–155.
- [22] M. Sućeska, *Propellants, Explos., Pyrotech.* **1991**, *16*, 197–202.

5 Nitrocarbamates of Polyvalent Sugar Alcohols

As published in *Chem. – Asian J.* **2015**, *11*, 568–575.

EFFICIENT SYNTHESIS OF PRIMARY NITROCARBAMATES OF SUGAR ALCOHOLS: FROM FOOD TO ENERGETIC MATERIALS



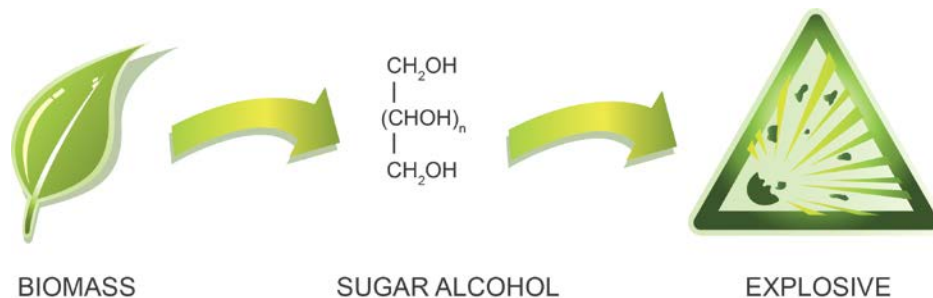
5.1 Abstract

The first nitrocarbamates derived from polyalcohols are synthesized and discussed. The precursor sugar alcohols with different chain lengths, acyclic and cyclic structures, are easily available from renewable biomass, used for food and cosmetic industry. A two-step procedure results in the formation of nitrocarbamate derivatives. Their energetic properties are in the range of the well-known explosive nitrate ester PETN.

The synthesis of various new polyvalent nitrocarbamates derived from sugar alcohols was accomplished by an economically benign two-step synthesis. The precursor carbamates were synthesized with the reagent chlorosulfonyl isocyanate (CSI) and further nitrated using mixed acid. The starting materials, sugar alcohols, are renewable biomass, mainly used in food and cosmetic industry. The structures of one carbamate and one nitrocarbamate were exemplary described by single-crystal X-ray analysis. The heat of formation is calculated by the use ofisodesmic reactions and the energetic performance data were estimated. All compounds were fully characterized by elemental analysis, vibrational spectroscopy, ^1H , ^{13}C , and $^{14/15}\text{N}$ NMR spectroscopy and thermal analysis (DSC). The nitrocarbamates exhibit good detonation performance and have significantly lower sensitivities compared to the commonly used nitrate ester explosive PETN.

5.2 Introduction

The research on Explosives and Energetic Materials is having great progress in the area of synthetic chemistry. In 2014, more than 900 publications with the concept or the keyword explosive were published. All around the world research teams have attracted large interest in the topics of synthesis, characterization, calculation and also the detection of such compounds.^[1]



Scheme 5-1: Concept of the manufacture of energetic materials based on renewable sugar alcohols.

The concept of using renewable material and food, as cellulose, starch or sugar alcohols for the manufacture of energetic materials is not new (Scheme 5-1).^[2] A well-known example is nitrocellulose, which after picric acid is the second earliest known organic explosive, and the first one which based on renewable resources.^[3] Sugar alcohols are a class of polyols with the general formula $\text{HOCH}_2(\text{CHOH})_n\text{CH}_2\text{OH}$. The production of such compounds is accomplished by the use of chemical or biochemical transformation starting from different carbohydrates like sugar, starch and also especially cellulose.^[4] The application area of such sugar alcohols is quite broad and mainly located towards the food industry, where they are used as sweetener and as a healthier substitute for sucrose.^[5]

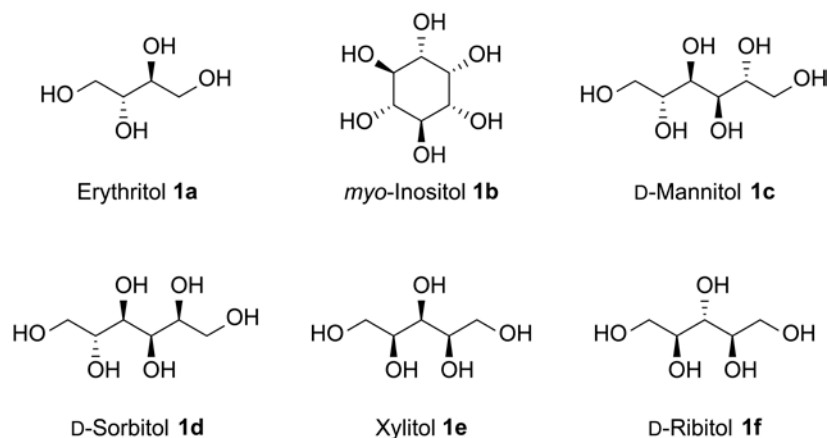
Primary nitrocarbamates are relatively sparsely reported so far and can chemically be described as nitrogen nitrated esters of the unstable carbamic acid.^[6] Very recently, these compounds became of interest and some derivatives with and without energetic properties were prepared.^[7] Another recent publication describes the synthesis of small primary nitrocarbamates and their use as nitrogen acids for the oxidative addition to metal centered complexes.^[8] The synthesis of such primary nitrocarbamates can be performed efficiently by the nitration of the corresponding carbamates. The carbamate precursors were prepared in the past by reaction of alcohols with phosgene. Phosgene has the drawback being a highly toxic gas with strong limitations on transportation and storage.^[9] In a second step the intermediate formed chloroformate is converted with ammonia into the carbamate.^[7b] Alternatives for phosgene are organic carbonates, activated carbon dioxide or phosgene substitutes, but which are not practicable, because these reagents can only produce *N*-substituted carbamates in good quality and yields.^[10] Another important, also an industrial route for *N*-unsubstituted carbamates, is the treatment of alcohols with in situ generated isocyanic acid.^[11] However, the reaction with the rather unstable isocyanic acid again is not practicable for polyvalent or multivalent alcohols, because of the low reactivity and the potential of multiple addition and polymerization.^[12]

5.3 Results and Discussion

5.3.1 Synthesis

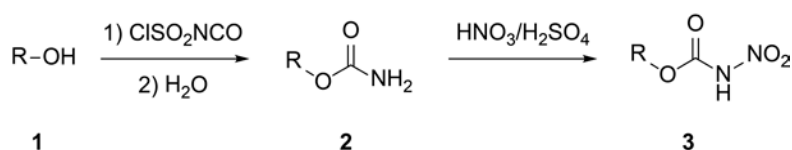
A further development of an isocyanic acid equivalent is introduced by the two highly activated isocyanates chlorosulfonyl isocyanate (CSI) and trichloroacetyl isocyanate (TAI).^[13] Both reagents are easy-to-handle liquids, which quickly react with alcohols already at low temperatures.^[14] Advantageously is the formation of a chlorosulfonyl, respectively trichloroacetyl, carbamate

intermediate, which prevent multiaddition during the reaction time. The carbamate is released by aqueous work-up of the reaction mixture, often in high yields. In this work, the CSI reagent was applied to the synthesis of multivalent carbamates (Scheme 5-3), including a good commercial availability and reasonable price.



Scheme 5-2: The sugar alcohol selection.

Selections of six sugar alcohols (Scheme 5-2) with different chain lengths, stereoisomerisms, acyclic and cyclic structures were tested for reactivity towards CSI and nitration. These particular alcohols were selected for their availability as well as being products from renewable sources. Erythritol **1a** is the smallest polyol with four carbons, which is produced by enzymatic reactions from monosaccharides and mostly consumed as a low-calory sweetener.^[15]



Scheme 5-3: Synthesis of carbamates **2** and nitrocarbamates **3** from sugar alcohols **1**.

The transformation of the polyols into the carbamates were performed in the solvent acetonitrile with equivalent amounts of CSI (Scheme 5-3). The conversion is complete within one to two hours at ambient temperature with yields of pure colorless carbamates **2a-f** above 85% after aqueous work-up. The carbamates **2a/b/c** were previously synthesized by the two step chloroformate-ammonia route in much lower yields from 41 to 71%.^[9a] Further advantages of the here presented one-step reaction with the CSI reagent are faster conversion rates and simplified work-up resulting in pure products. The nitration to the poly-nitrocarbamates **3a-f** was

performed in mixed acid in a well established fashion.^[7a, 7c] The nitrocarbamates **3a/b/c** are obtained after aqueous work-up, whereas **3d/e/f** are more water-soluble and require extraction with ethyl acetate. All compounds crystallize as hydrates with different water contents. In case of the less water-soluble **3a/b/c** all crystal water can be removed in vacuum at 70 °C, at which they are stable. The others can also be obtained anhydrous, but they exhibit a fairly high hygroscopicity.

5.3.2 NMR Spectroscopy and Vibrational Spectroscopy

The carbamates and nitrocarbamates were thoroughly characterized by multinuclear NMR, vibrational (IR, Raman) spectroscopy and mass spectrometry. In general, all carbamate and all nitrocarbamate compounds show nearly the same characteristics. A remarkable difference is observed in the solubility properties, i.e. the nitrocarbamates are better soluble compared to the corresponding carbamates. Therefore, the NMR spectra of the carbamates are recorded in [D₆]DMSO, while those of the nitrocarbamates are recorded in acetone.

Table 5-1: Multinuclear NMR resonances (ppm) and characteristic Raman/IR vibrations (cm⁻¹) of the carbamate **2a and the nitrocarbamate **3a** of *meso*-erythritol.**

		2a	3a	
¹ H	NH ₂ / NH	6.6	12.7	
	CH	4.93	5.44	
	CH ₂	4.13, 3.98	4.76, 4.47	
¹³ C	CO	156.7, 156.2	148.2, 147.6	
	CH	70.7	71.6	
	CH ₂	62.4	63.1	
¹⁵ N	NH ₂ / NHNO ₂	-307.6, -308.2	-189.7, -189.9	
	NO ₂	-	-45.8, -46.2	
		2a	3a	
		<i>IR</i>	<i>Raman</i>	
ν CO	1682, 1646	1674, 1641	1784, 1743	1780, 1751
ν_s NO ₂	-	-	1634, 1607	1631, 1610
ν_{as} NO ₂	-	-	1326	1357, 1330
ν N-N	-	-	999	1003
ν C-N	1110	1109	1166	1165

Exemplary, the data of the carbamate/nitrocarbamate of the simplest sugar alcohol *meso*-erythritol **1a** are displayed in Table 5-1. In the ^1H NMR spectrum of the carbamate **2a** the hydrogen atoms of the two similar NH_2 groups are chemically different, but cannot be distinguished, because there is one very broad resonance located around 6.6 ppm. Upon nitration to the nitrocarbamate **3a**, for the remaining hydrogen atom of the NHNO_2 group a significant downfield shift to 12.7 ppm occurs, due to the strong withdrawing effect of the attached nitro group. This resonance has now another increase in line width compared to **2a**. The trend of the downfield shift could be also observed in a similar fashion for the CH/CH_2 resonances.

In the ^{13}C NMR spectrum of carbamate **2a** the two different carbonyl groups are found, as to be expected, in close proximity at 156.7 and 156.2 ppm. For the nitrocarbamate **3a** this group suffers a high field shift by almost 9 ppm to 148.2 and 147.6 ppm, due to the increased shielding caused by the presence of the neighboring nitro group. Similar as the tendency in the ^1H NMR, the methylene and methine carbon resonances are shifted slightly downfield. The most significant shift can be observed in the ^{15}N NMR spectrum upon nitration. The resonance of the carbamate nitrogen detected at -307.6 and -308.2 ppm is shifted significantly to lower field in the nitrocarbamate to -189.7 and -189.9 ppm. The two different nitro groups in **3a** are observed at -45.8 and -46.2 ppm which is in a typical range for those type of compounds.^[7b, 7c] In the vibrational spectra, the characteristic bands of the carbonyl groups in the carbamate **2a** are located at 1682 and 1646 cm^{-1} . In the nitrocarbamate **3a** these stretching frequencies are shifted to much higher frequencies at 1784 and 1743 cm^{-1} and thus display a significantly stronger bonding.^[16] According to literature, the N–N stretching vibration in nitrocarbamates can be assigned to the region around 1000 cm^{-1} .^[8, 17]

5.3.3 Single Crystal Structure Analysis

Suitable crystals of **2b** and **3a** for X-ray single diffraction were grown from hot water. The structures are shown in Figures 5-1 and 5-2. The *myo*-inositol hexacarbamate **2b** crystallizes in the tetragonal space group *Pbca*. This isomer adopts a chair configuration, occupying the maximum number of the carbamates moieties in equatorial position (five from six, with maximum distance for steric reasons as in the starting alcohol *myo*-inositol).^[18] The six independent carbamate moieties have approximately the same dimensions and all show a nearly planar arrangement with typical values for carbamates.^[7c]

The nitrocarbamate **3a** crystallizes in the monoclinic space group $P2_1/n$ (Figure 5-1). The asymmetric unit is half of the molecule due to an inversion center in the center of the *meso*

molecule. The two independent nitrocarbamates units show the same steric geometry. In contrast to what would be expected, the nitro groups are twisted out in average of approximately 10° of the nitrocarbamate unit, which is demonstrated by the torsion angle C1–N2–N1–O2 (10.9°).

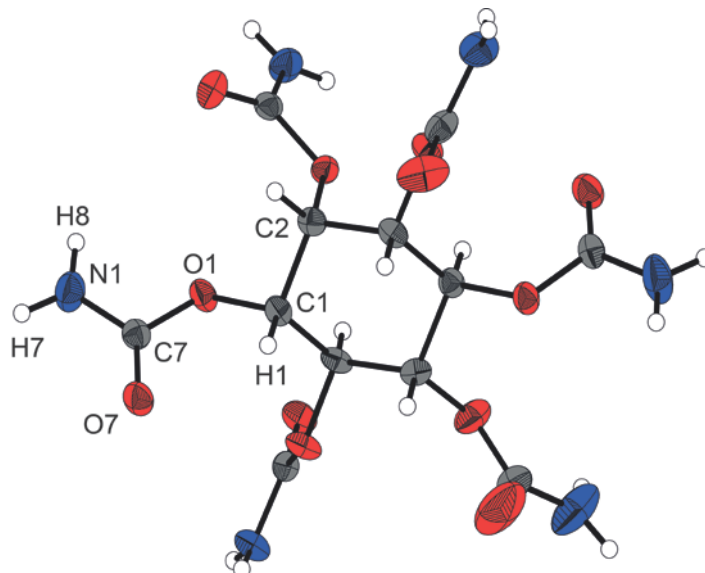


Figure 5-1: X-ray molecular structure of *myo*-inositol hexacarbamate (2b).

Selected atom distances (Å) and angles (deg.): C1–O1 1.431(3), O1–C7 1.357(2), C7–O7 1.215(2), C7–N1 1.331(3), N1–H7 0.89(4), N1–H8 0.84(3), C1–O1–C7 116.6(2), O1–C7–O7 123.6(2), O7–C7–N1 126.5(2), O1–C7–N1 109.9(2), H1–C1–O1–C7 $-4(1)$, O1–C7–N1–H8 $-14(2)$, O1–C7–N1–H7 177(2), O7–C7–N1–H7 3(2).

The atom distance of the nitramine moiety (N1–N2, N3–N4) is 1.36/1.37 Å, which indicates a substantial double bond character, achieved by delocalization of the nitrogen lone pair of N2/N3. Comparing the bond distances of the carbamate with those of the nitrocarbamate, the only main difference is the carbon-nitrogen bond. In the carbamate the already short C7–N1 bond (1.38 Å) is further shortened in the nitrocarbamate N1–N2 bond to 1.33 Å and thus closer to a double bond (1.27 Å) than a single carbon-nitrogen bond (1.47 Å). When compared with the corresponding nitrate ester, *meso*-erythritol tetranitrate (ETN), the nitrocarbamate **3a** shows less strained angles and no strong O···O closed shell interactions.^[19] Furthermore, the nitrocarbamate structure shows extensive hydrogen bonding which stabilize the layered structure (see Figure 5-2) and therefore lead to a significantly lower sensitivity against mechanic stimuli and a higher decomposition point (Table 5-2).

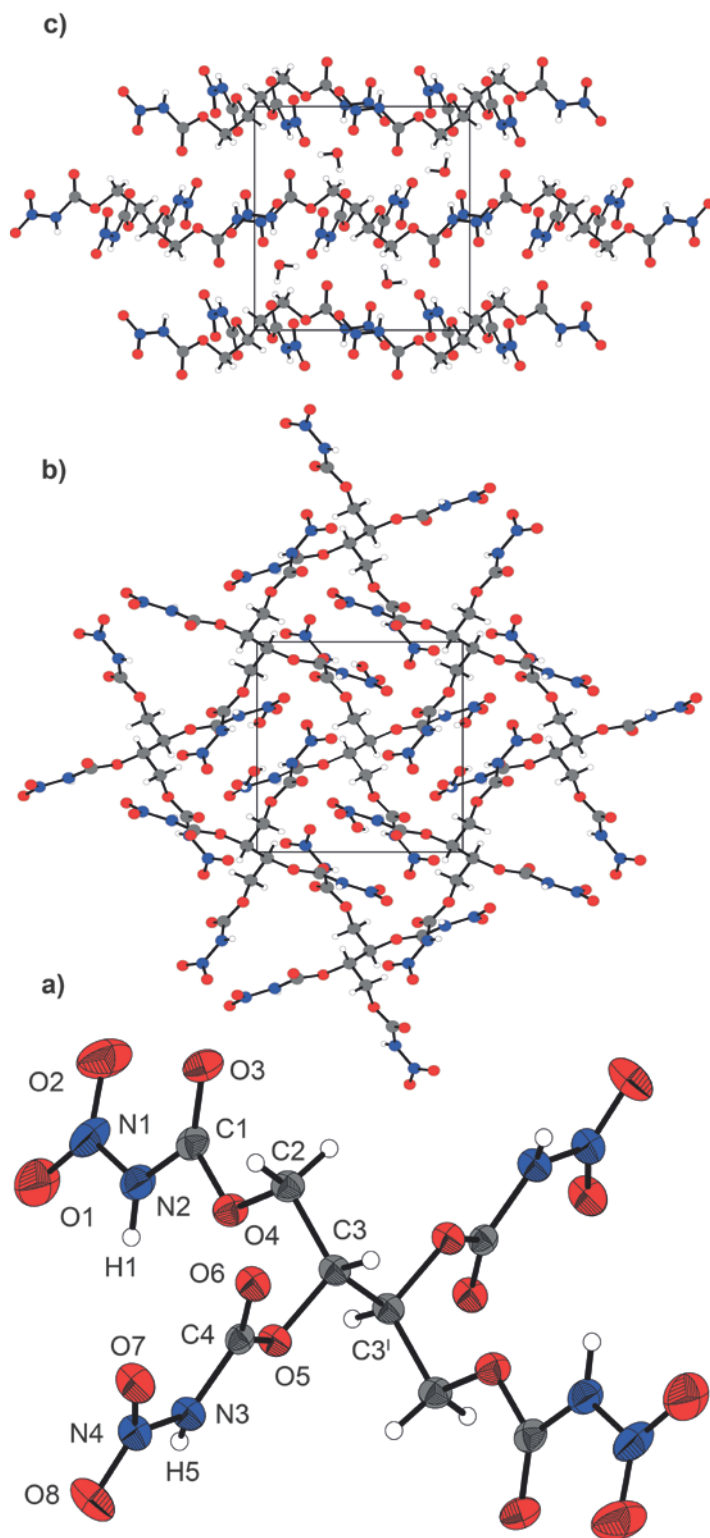


Figure 5-2: X-ray molecular structure of *meso*-erythritol tetranitrocarbamate 3a a), along *a* axis b), along *c* axis c).

Selected atom distances (Å) and angles (deg): C2–O4 1.445(2), O4–C1 1.319(2), C1–O3 1.192(2), C1–N2 1.378(3), N2–H1 0.83(3), N2–N1 1.372(3), N1–O1 1.211(3), N1–O2 1.213(3), C2–O4–C1 116.2(1), O4–C1–O3 126.4(2), O3–C1–N2 128.2(2), O4–C1–N2 105.4(2), C1–N2–N1 125.1(2), N1–N2–H1 114(2), C1–N2–H1 120(2), N2–N1–O2 118.6(2), N2–N1–O1 114.8(2), O1–N1–O2 126.6(2), O4–C1–N2–H1 –5(3), O3–C1–N2–N1 –6.3(3), O4–C1–N2–N1 175.5(2), C1–N2–N1–O2 –11.0(3), C1–N2–N1–O1 170.4(2).

5.3.4 Thermal Stabilities and Energetic Properties

The energetic properties (Table 5-2) are important for a safe handling of such materials. For this purpose, the anhydrous nitrocarbamates **3a–c** were used (dehydrated at 70 °C under vacuum). The sensitivity towards impact (IS) is tested by the action of a falling weight from different heights. The friction sensitivity (FS) is determined by rubbing a small amount between a porcelain plate and a pin with different contact pressures.^[20] As a result, **3a–c** all exhibit less friction sensitivity compared to the related explosives PETN (Pentaerythritol tetranitrate) and ETN (*meso*-Erythritol tetranitrate). Particularly noteworthy is the difference against impact stimuli. The nitrocarbamate **3a** is classified as sensitive to impact with a value of 6 J, whereas ETN is extremely sensitive to impact shock (2 J). ETN also explodes violently when burned,^[2b] and contrary, **3a** burns fast without any deflagration or detonation (Figure 5-3).

Table 5-2: Physical properties and calculated detonation parameters (using EXPLO5 V6.02) of water free compounds 3a, 3b, 3c in comparison to PETN (Pentaerythritol tetranitrate) and ETN (meso-Erythritol tetranitrate).

	3a	3b	3c	PETN ^[2b]	ETN ^[2b, 19]
density (RT) ^[a]	1.84	1.83	1.78	1.78	1.77
formula	C ₈ H ₁₀ N ₈ O ₁₆	C ₁₂ H ₁₂ N ₁₂ O ₂₄	C ₁₂ H ₁₄ N ₁₂ O ₂₄	C ₅ H ₈ N ₄ O ₁₂	C ₄ H ₆ N ₄ O ₁₂
$\Delta H_f^\circ / \text{kJ mol}^{-1}$ ^[b]	-1322	-1918	-1846	-561	-437
$\Delta U_f^\circ / \text{kJ kg}^{-1}$ ^[b]	-2700	-2623	-2511	-1594	-1356
$T_{\text{dec onset}}$ ^[c]	181	181	142	165	163
IS / J ^[d]	6	5	6	3	2
FS / N ^[e]	160	120	160	60	57
ESD / J ^[f]	0.15	0.15	0.20	0.06	0.06
$N / \%$ ^[g]	23.6	23.1	23.5	17.7	18.6
$\Omega_{\text{CO}} / \%$ ^[h]	+12.8	+13.6	+13.0	+15.2	+26.5

[a] Densities at RT measured by gas pycnometer. [b] Heat and energy of formation calculated with isodesmic reactions for further information see SI. [c] Onset decomposition point from DSC measurements carried out at a heating rate of 5 °C. [d] Sensitivity against impact. [e] Friction. [f] Electrostatic discharge. [g] Nitrogen content. [h] Oxygen balance for C_aH_bO_cN_d, 1600 (c-a-b/2)/M_w; M_w = molecular weight.

The thermal stabilities were investigated by differential scanning calorimetry (DSC) with a heating rate of 5 °C per minute. The two nitrocarbamates **3a** and **3b** have satisfying decomposition points of 181 °C both, which are higher than the nitrate esters ETN and PETN (163 °C/165 °C). On the other hand, the other four nitrocarbamates **3c–f** all show decomposition

points mostly before complete loss of crystal water as well as below the important benchmark of 150 °C.

The main criteria for the performance of energetic materials is the detonation velocity V_{det} (Table 5-3). The best V_{det} of the here presented nitrocarbamates shows the *meso*-erythritol tetranitrocarbamate (**3a**) with 8066 m s⁻¹ which is around 300 m s⁻¹ lower than the corresponding nitrate esters ETN. Another positive aspect of the nitrocarbamates is the higher nitrogen content by approximately five percent. This and the quite low decomposition temperature could protect a gun barrel, if used in propellant charges.^[21]

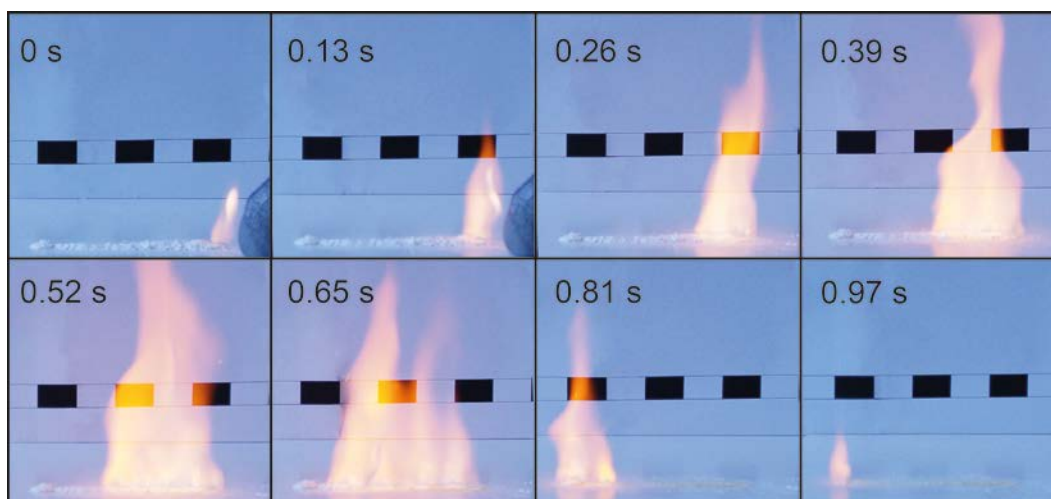


Figure 5-3: Deflagration and burning test of anhydrous nitrocarbamate 3a.

Table 5-3: Calculated detonation parameters (using EXPLO5 V6.02) of 3a, 3b and 3c in comparison to PETN (Pentaerythritol tetranitrate) and ETN (*meso*-Erythritol tetranitrate).

	3a	3b	3c	PETN ^[2b]	ETN ^[2b, 19]
$\Delta_{\text{ex}}U^{\circ}/\text{kJ kg}^{-1}$ ^[a]	-4031	-4046	-4167	-5980	-5960
T_{ex} / K ^[b]	2998	3094	3139	3970	4174
$P_{\text{Cj}} / \text{kbar}$ ^[c]	284	272	261	319	294
$V_{\text{det}} / \text{m s}^{-1}$ ^[d]	8066	7949	7843	8405	8409

[a] Heat of detonation. [b] Detonation temperature. [c] Detonation pressure. [d] Detonation velocity.

5.4 Conclusion

The facile synthesis of multivalent carbamates by the one step synthesis with the reagent chlorosulfonyl isocyanate and the corresponding alcohol works also good with the more complex sugar alcohol molecules. The synthesis has compared to the known routes several advantages, like fast reaction times and high yields of pure products. The nitration to the new polynitrocarbamates proceeds well in nitric and sulfuric acid. The nitrocarbamate of *meso*-erythritol **3a** in our selection shows the best energetic properties, with a higher decomposition point and a much lower sensitivity than the related nitrate ester ETN.

5.5 Experimental Section

5.5.1 General Procedures

All chemicals were used as supplied. Raman spectra were recorded in a glass tube with a Bruker MultiRAM FT-Raman spectrometer with Nd:YAG laser excitation up to 1000 mW (at 1064 nm). Infrared spectra were measured with a Perkin–Elmer Spectrum BX-FTIR spectrometer equipped with a Smiths DuraSamplIR II ATR device. All spectra were recorded at ambient (25 °C) temperature. NMR spectra were recorded with a JEOL/Bruker instrument and chemical shifts were determined with respect to external Me₄Si (¹H, 399.8 MHz; ¹³C, 100.5 MHz) and MeNO₂ (¹⁵N, 40.6 MHz; ¹⁴N, 28.9 MHz). Mass spectrometric data were obtained with a JEOL MStation JMS 700 spectrometer (DCI+, DEI+, FAB+, FAB–). Analysis of C/H/N were performed with an Elemental Vario EL Analyzer. Melting and decomposition points were measured with a Perkin-Elmer Pyris6 DSC and an OZM Research DTA 552-Ex with a heating rate of 5 °C min⁻¹ in a temperature range of 15 to 400 °C and checked by a Büchi Melting Point B-540 apparatus (not corrected). The sensitivity data were performed using a BAM drophammer and a BAM friction tester.^[21]

5.5.2 Computational Details

The heats of formations were calculated by the use of isodesmic reactions. This was necessary due to the high molecular weight and associated difficulties with complete basis set (CBS) calculation method. For further information see Appendix A.5. All calculations affecting the detonation parameters were carried out using the program package EXPLO5 V6.02.^[22]

5.5.3 X-ray Crystallography

The low-temperature single-crystal X-ray diffraction of were performed on an Oxford XCalibur3 diffractometer equipped with a Spellman generator (voltage 50 kV, current 40 mA) and a KappaCCD detector operating with MoK α radiation ($\lambda = 0.7107 \text{ \AA}$). Data collection was performed using the CRYSLIS CCD software.^[23] The data reduction was carried out using the CRYSLIS RED software.^[24] The solution of the structure was performed by direct methods (SIR97)^[25] and refined by full-matrix least-squares on F2 (SHELXL)^[26] implemented in the WINGX software package^[27] and finally checked with the PLATON software^[28]. All non-hydrogen atoms were refined anisotropically. The hydrogen atom positions were located in a difference Fourier map. ORTEP plots are shown with thermal ellipsoids at the 50% probability level. Additional crystallographic data and structure refinement parameters are listed in the Appendix A.5. Crystallographic data (excluding structure factors) for the structures reported in this paper have been deposited at the Cambridge Crystallographic Data Centre (1423039 (**2b**), 1423040 (**3a**)) and can be obtained free of charge from the Cambridge Crystallographic Data Centre via www.ccdc.cam.ac.uk/data_request/cif.

5.5.4 Synthesis

Safety Announcement: CAUTION! Chlorosulfonyl isocyanate (CSI) is a very corrosive liquid and reacts violently with water. Energetic materials are sensitive toward heat, impact and friction. No hazards occurred during preparation and manipulation; additional proper protective precautions (face shield, leather coat, earthened equipment and shoes, Kevlar gloves, and ear plugs) should be used when undertaking work with these compounds.

Carbamates 2a–f. The sugar alcohol (**1a–f**) (5 mmol) was suspended in dry acetonitrile (40 mL) and placed in an ice bath and chlorosulfonyl isocyanate (CSI) (1.10 equiv per OH-group) was added slowly. The ice bath was removed, and stirring at RT was continued for 1.5 h. The reaction mixture was again cooled with an ice bath, and quenched carefully with water (20 mL). The stirring was continued at RT for 1 h. The formed precipitate was filtered and washed thoroughly with water. The residue was suspended in a solution of sodium hydrogen carbonate (0.5%, 40 mL) and stirred for 1 h. The precipitate was filtered, washed with water and dried under high vacuum to obtain colorless pure carbamate (**2a–f**).

Table 5-4: Experimental scales and yields for the synthesis of carbamates 2a–f from sugar alcohols 1a–f.

Sugar alcohol	Equiv. of CSI	Yield
1a Erythritol (5 mmol, 0.61 g)	4.40 (22.0 mmol, 3.11 g)	92%
1b <i>myo</i> -Inositol (5 mmol, 0.90 g)	6.60 (33.0 mmol, 4.67 g)	90%
1c D-Mannitol (5 mmol, 0.91 g)	6.60 (33.0 mmol, 4.67 g)	96%
1d D-Sorbitol (5 mmol, 0.91 g)	6.60 (33.0 mmol, 4.67 g)	90%
1e Xylitol (5 mmol, 0.76 g)	5.50 (27.5 mmol, 3.89 g)	85%
1f D-Ribitol (5 mmol, 0.76 g)	5.50 (27.5 mmol, 3.89 g)	88%

Nitrocarbamates 3a–c. Into concentrated sulfuric acid (98.5%) was dropped fuming nitric acid (>99.5%) below 5 °C in an ice-bath. Into this chilled nitration mixture (mixed acid) the dried carbamate (**2a–c**) (1 mmol) was added in small portions. The suspension was stirred 10 minutes at this temperature and 1.5 h at ambient temperature. The reaction mixture was poured onto ice-water (100 mL) and stirred further. The formed precipitate was filtered off and washed with water. After recrystallization from water, colorless pure nitrocarbamates could be obtained. The water free nitrocarbamates were obtained by dehydration at 70 °C for 24 h under high vacuum.

Nitrocarbamates 3d–f. Into concentrated sulfuric acid (98.5%) was dropped fuming nitric acid (>99.5%) below 5 °C in an ice bath. To this chilled nitration mixture the dried carbamate (1 mmol) was added in small portions. The suspension was stirred 10 minutes at this temperature and 1.5 h at ambient temperature. The reaction mixture was poured onto ice-water (100 mL) and stirred for 15 minutes. The aqueous solution is extracted with ethyl acetate (3×50 mL). The combined organic phases were washed with water (1×100 mL) and brine (2×100 mL) and dried with magnesium sulfate. The solvent was removed under reduced pressure to obtain an oil which solidified under high vacuum. All three nitrocarbamates **3d–f** show a high hygroscopic behavior at ambient conditions.

Table 5-5: Experimental scales and yields for the synthesis of nitrocarbamates 3a–f by nitration of carbamates 2a–f.

Carbamates	Nitric acid 100%	Sulfuric acid 98.5%	Yield
2a (1 mmol, 294 mg)	4 mL	4 mL	71%
2b (1 mmol, 438 mg)	6 mL	6 mL	65%
2c (1 mmol, 440 mg)	6 mL	6 mL	70%
2d (1 mmol, 440 mg)	6 mL	6 mL	60%
2e (1 mmol, 367 mg)	5 mL	5 mL	55%
2f (1 mmol, 367 mg)	5 mL	5 mL	41%

meso-Erythritol tetracarbamate (2a): ^1H NMR ($[\text{D}_6]$ DMSO): $\delta = 6.60$ (br, 8H, NH_2), 4.93 (m, 2H, CH), 4.13 (m, 2H, CH_2), 3.98 (m, 2H, CH_2) ppm. $^{13}\text{C}\{^1\text{H}\}$ NMR ($[\text{D}_6]$ DMSO): $\delta = 156.7$ (CO), 156.2 (CO), 70.7 (CH), 62.4 (CH_2) ppm. $^{15}\text{N}\{^1\text{H}\}$ NMR ($[\text{D}_6]$ DMSO): $\delta = -307.6$ (NH_2), -308.2 (NH_2) ppm. IR (ATR, cm^{-1}): $\nu = 3432$ (m), 3353 (w), 3306 (w), 3215 (w), 2990 (w), 1682 (s), 1646 (s), 1613 (m), 1453 (w), 1414 (w), 1385 (m), 1333 (m), 1274 (w), 1234 (w), 1110 (m), 1079 (s), 1049 (s), 988 (w), 888 (w), 858 (w), 772 (m), 704 (w), 704 (w). Raman (1064 nm, 1000 mW, cm^{-1}): $\nu = 3431$ (7), 3311 (12), 3213 (16), 3005 (34), 2980 (100), 1674 (65), 1641 (26), 1469 (48), 1428 (19), 1380 (14), 1319 (12), 1264 (44), 1166 (16), 1109 (51), 1060 (15), 1033 (14), 996 (61), 883 (71), 850 (36), 714 (21). MS (DCI+) m/e : 295.2 $[(\text{M}+\text{H})^+]$, 252.2 $[(\text{M}-\text{HNCO})^+]$, 234.2 $[(\text{M}-\text{HOCONH}_2)^+]$. Elemental analysis, calcd (%): $\text{C}_8\text{H}_{14}\text{N}_4\text{O}_8$ (294.22): C 32.66, H 4.80, N 19.04; found: C 32.66, H 4.86, N 19.10. DSC ($5\text{ }^\circ\text{C min}^{-1}$, onset): 256°C (melt.).

myo-Inositol hexacarbamate (2b): ^1H NMR ($[\text{D}_6]$ DMSO): $\delta = 6.55$ (br m, 12H, NH_2), 5.32 (m, 1H, CH), 5.19 (m, 2H, CH), 4.86 (m, 3H, CH) ppm. $^{13}\text{C}\{^1\text{H}\}$ NMR ($[\text{D}_6]$ DMSO): $\delta = 156.0$ (CO), 155.9 (CO), 71.9 (CH), 69.9 (CH), 69.5 (CH), 69.1 (CH) ppm. IR (ATR, cm^{-1}): $\nu = 3450$ (w), 3344 (m), 3213 (w), 1705 (s), 1648 (w), 1600 (s), 1398 (w), 1336 (s), 1317 (s), 1181 (w), 1114 (m), 1079 (s), 1061 (s), 1007 (m), 984 (m), 974 (m), 935 (m), 917 (w), 879 (w), 771 (m). Raman (1064 nm, 1000 mW, cm^{-1}): $\nu = 3304$ (18), 3011 (16), 3010 (18), 2962 (64), 1698 (36), 1606 (22), 1403 (30), 1316 (31), 1285 (16), 1182 (27), 1118 (42), 975 (17), 936 (100), 906 (22), 884 (20), 672 (21), 584 (16). MS (FAB+) m/e : 877.1 $[(2\times\text{M}+\text{H})^+]$, 623.3 $[(\text{M}+\text{matrix}(2\times\text{glycerine})+\text{H})^+]$, 531.2 $[(\text{M}+\text{matrix}(\text{glycerine})+\text{H})^+]$, 439.2 $[(\text{M}+\text{H})^+]$. Elemental analysis, calcd (%): $\text{C}_{12}\text{H}_{18}\text{N}_6\text{O}_{12}\times 1\text{ H}_2\text{O}$ (456.32): C 31.58, H 4.42, N 18.42; found: C 31.92, H 4.53, N 18.63. DSC ($5\text{ }^\circ\text{C min}^{-1}$, onset): $255\text{ }^\circ\text{C}$ (melt.).

D-Mannitol hexacarbamate (2c): ^1H NMR ($[\text{D}_6]$ DMSO): $\delta = 6.54$ (br, 12H, NH_2), 5.13 (s, 2H, CH), 4.91 (s, 2H, CH), 4.08 (m, 4H, CH_2) ppm. $^{13}\text{C}\{^1\text{H}\}$ NMR ($[\text{D}_6]$ DMSO): $\delta = 156.8$ (CO), 156.2 (CO), 155.9 (CO), 70.6 (CH), 70.5 (CH), 62.3 (CH_2) ppm. IR (ATR, cm^{-1}): $\nu = 3428$ (m), 3356 (w), 3308 (w), 3214 (w), 1675 (s), 1652 (w), 1641 (m), 1612 (m), 1454 (w), 1398 (m), 1339 (m), 1318 (m), 1268 (w), 1235 (w), 1104 (m), 1054 (s), 1026 (m), 983 (w), 943 (w), 868 (w), 769 (w), 704 (w). Raman (1064 nm, 1000 mW, cm^{-1}): $\nu = 3429$ (10), 3313 (19), 3210 (32), 2999 (59), 2975 (84), 2954 (39), 2896 (9), 1683 (89), 1637 (20), 1461 (31), 1382 (18), 1351 (17), 1318 (16), 1278 (28), 1252 (31), 1163 (34), 1145 (28), 1109 (90), 1063 (22), 1033 (24), 1009 (68), 987 (21), 898 (39), 875 (100), 851 (30), 781 (14), 756 (22), 660 (60), 630 (21). MS (DCI+) m/e : 380.2 $[(\text{M}-\text{HOCONH}_2)^+]$, 337.2 $[(\text{M}-(\text{HOCONH}_2-\text{HNCO}))^+]$. Elemental analysis, calcd (%):

$C_{12}H_{20}N_6O_{12}$ (440.32): C 32.73, H 4.58, N 19.09; found: C 32.41, H 4.68, N 18.91. DSC (5 °C min^{-1} , onset): 274 °C (melt.).

D-Sorbitol hexacarbamate (2d): 1H NMR ($[D_6]DMSO$): δ = 6.49 (m br, 12H, NH_2), 5.12 (m, 2H, $2\times CH$), 4.98 (m, 1H, CH), 4.86 (m, 1H, CH), 4.14 (m, 2H, CH_2), 3.95 (m, 2H, CH_2) ppm. $^{13}C\{^1H\}$ NMR ($[D_6]DMSO$): δ = 156.8 (CO), 156.7 (CO), 156.2 (CO), 156.0 (CO), 156.0 (CO), 155.9 (CO), 70.3 (CH), 70.3 (CH), 70.2 (CH), 69.6 (CH), 63.0 (CH_2), 62.3 (CH_2) ppm. IR (ATR, cm^{-1}): ν = 3430 (s), 3348 (w), 3308 (w), 3214 (w), 1703 (s), 1682 (s), 1646 (m), 1614 (m), 1413 (m), 1343 (m), 1333 (m), 1316 (m), 1293 (w), 1268 (w), 1236 (w), 1114 (m), 1064 (s), 1036 (m), 1020 (m), 959 (w), 928 (w), 860 (w), 844 (w), 770 (w), 742 (w), 704 (w). Raman (1064 nm, 1000 mW, cm^{-1}): ν = 3425 (14), 3319 (18), 3263 (17), 3209 (28), 3005 (22), 2980 (100), 2859 (52), 2927 (35), 2898 (13), 1678 (62), 1642 (23), 1467 (38), 1435 (22), 1354 (20), 1335 (15), 1319 (23), 1272 (20), 1255 (40), 1160 (31), 1108 (88), 1038 (24), 1017 (48), 998 (35), 949 (35), 876 (46), 866 (48), 846 (41), 742 (19), 680 (26). MS (DCI+) m/e : 380.2 $[(M-HOCONH_2)^+]$, 337.2 $[(M-(HOCONH_2-HNCO))^+]$. Elemental analysis, calcd (%): $C_{12}H_{20}N_6O_{12}$ (440.32): C 32.73, H 4.58, N 19.09; found: C 32.73, H 4.58, N 18.96. DSC (5 °C min^{-1} , onset): 273 °C (melt.).

Xylitol pentacarbamate (2e): 1H NMR ($[D_6]DMSO$): δ = 6.57 (br, 10H, NH_2), 5.11 (m, 1H, CH), 5.00 (m, 2H, CH), 4.10 (m, 2H, CH_2), 3.96 (m, 2H, CH_2) ppm. $^{13}C\{^1H\}$ NMR ($[D_6]DMSO$): δ = 156.7 (CO), 156.4 (CO), 156.3 (CO), 70.0 (CH), 70.0 ($2\times CH$), 63.1 (CH_2) ppm. IR (ATR, cm^{-1}): ν = 3432 (m), 3344 (w), 3280 (w), 3217 (w), 1703 (s), 1644 (w), 1613 (s), 1462 (w), 1414 (s), 1391 (m), 1353 (m), 1317 (m), 1305 (m), 1252 (w), 1161 (w), 1139 (w), 1112 (w), 1074 (s), 1035 (s), 1024 (s), 985 (w), 968 (w), 882 (w), 844 (w), 774 (w). Raman (1064 nm, 1000 mW, cm^{-1}): ν = 3417 (19), 3248 (28), 3201 (39), 3021 (25), 2972 (100), 2930 (50), 1687 (51), 1640 (46), 1471 (46), 1309 (20), 1281 (22), 1254 (51), 1163 (37), 1113 (73), 1027 (42), 986 (25), 967 (40), 957 (58), 915 (38), 844 (82), 665 (53). MS (DCI+) m/e : 307.3 $[(M-HOCONH_2)^+]$. Elemental analysis, calcd (%): $C_{10}H_{17}N_5O_{10}$ (367.27): C 32.70, H 4.67, N 19.07; found: C 32.57, H 4.66, N 19.11. DSC (5 °C min^{-1} , onset): 234 °C (melt.).

D-Ribitol pentacarbamate (2f): 1H NMR ($[D_6]DMSO$): δ = 6.62 (br, 10H, NH_2), 4.96 (m, 3H, CH), 4.15 (m, 2H, CH_2), 3.97 (m, 2H, CH_2) ppm. $^{13}C\{^1H\}$ NMR ($[D_6]DMSO$): δ = 156.8 (CO), 156.1 (CO), 155.9 (CO), 71.1 (CH), 70.3 ($2\times CH$), 62.7 (CH_2) ppm. IR (ATR, cm^{-1}): ν = 3429 (m), 3342 (w), 3283 (w), 3216 (w), 1709 (s), 1610 (m), 1409 (m), 1388 (m), 1356 (s), 1337 (w), 1323 (m), 1298 (w), 1290 (w), 1150 (w), 1106 (m), 1089 (s), 1057 (m), 1036 (w), 998 (w), 962 (w), 924 (w), 900 (w), 877 (w), 858 (w), 768 (m), 704 (w). Raman (1064 nm, 1000 mW, cm^{-1}): ν = 3412 (10), 3254 (17), 3203 (23), 3010 (31), 2968 (50), 2953 (80), 2914 (10), 1709 (33), 1640 (32), 1475 (23),

1367 (13), 1321 (12), 1291 (11), 1161 (32), 1159 (57), 1129 (44), 1036 (22), 1000 (100), 925 (22), 878 (21), 857 (178), 681 (20). MS (DCI+) m/e : 307.2 [(M-HOCONH₂)⁺]. Elemental analysis, calcd (%): C₁₀H₁₇N₅O₁₀ (367.27): C 32.70, H 4.67, N 19.07; found: C 32.59, H 4.78, N 19.10. DSC (5 °C min⁻¹, onset): 236 °C (melt.).

meso-Erythritol tetranitrocarbamate (3a): ¹H NMR ([D₆]acetone): δ = 12.7 (br, 4H, NH), 5.44 (m, 2H, CH), 4.76 (m, 2H, CH₂), 4.47 (m, 2H, CH₂) ppm. ¹³C{¹H} NMR ([D₆]acetone): δ = 148.2 (CO), 147.6 (CO), 71.6 (CH), 63.1 (CH₂) ppm. ¹⁵N{¹H} NMR ([D₆]acetone): δ = -45.8 (NO₂), -46.2 (NO₂), -189.7 (NH), -189.9 (NH) ppm. IR (ATR, cm⁻¹): ν = 3629 (w), 3511 (w), 3180 (w), 1784 (m), 1743 (m), 1634 (w), 1607 (m), 1450 (m), 1326 (w), 1288 (w), 1236 (w), 1166 (s), 1060 (w), 1033 (m), 999 (m), 948 (m), 902 (w), 806 (m), 750 (s), 737 (s). Raman (1064 nm, 1000 mW, cm⁻¹): ν = 3025 (25), 2988 (54), 2961 (47), 2912 (8), 1780 (23), 1751 (42), 1631 (9), 1610 (12), 1468 (47), 1454 (19), 1390 (12), 1357 (32), 1330 (73), 1256 (35), 1220 (24), 1177 (18), 1165 (14), 1109 (16), 1079 (20), 1042 (36), 1003 (100), 924 (13), 889 (15), 835 (9), 813 (12), 732 (13). MS (FAB-) m/e : 473.1 [(M-H)⁻]. Elemental analysis, calcd (%): C₈H₁₀N₈O₁₆×2H₂O (510.24): C 18.83, H 2.77, N 21.97; found: C 18.85, H 2.70, N 21.92. DSC (5 °C min⁻¹, onset): 181 °C (dec.). BAM drophammer: 10 J. Friction tester: 240 N, ESD: 0.50 J (grain size 100–500 μm).

Dehydration under vacuum at 70 °C for 24 hours: IR (ATR, cm⁻¹): ν = 3305 (w), 1763 (s), 1605 (s), 1442 (s), 1336 (m), 1248 (w), 1168 (s), 1107 (w), 1056 (w), 1032 (m), 994 (m), 950 (m), 889 (w), 827 (w), 801 (m), 754 (m), 742 (m). Elemental analysis, calcd (%): C₈H₁₀N₈O₁₆ (474.02): C 20.26, H 2.13, N 23.63; found: C 20.36, H 2.28, N 23.59. BAM drophammer: 6 J. Friction tester: 216 N, ESD: 0.15 J (grain size 100–500 μm).

myo-Inositol hexanitrocarbamate (3b): ¹H NMR ([D₆]acetone): δ = 14.0, 13.9, 13.8 (br, 6H, NH), 5.94 (m, 1H, CH), 5.71 (m, 3H, CH), 5.48 (m, 2H, CH) ppm. ¹³C{¹H} NMR ([D₆]acetone): δ = 147.7 (CO), 147.7 (CO), 147.4 (CO), 147.2 (CO), 71.4 (CH), 71.0 (CH), 70.1 (CH), 70.0 (CH) ppm. ¹⁴N NMR ([D₆]acetone): δ = -47 (NO₂) ppm. IR (ATR, cm⁻¹): ν = 3592 (w), 3155 (m), 2984 (w), 1773 (m), 1619 (m), 1605 (m), 1441 (w), 1330 (s), 1266 (w), 1161 (s), 1131 (s), 986 (s), 951 (s), 896 (w), 823 (w), 726 (m). Raman (1064 nm, 1000 mW, cm⁻¹): ν = 2994 (25), 2962 (47), 1805 (31), 1788 (43), 1613 (19), 1443 (23), 1381 (35), 1367 (44), 1324 (100), 1227 (19), 1190 (16), 1164 (20), 1137 (27), 1097 (42), 1012 (86), 1004 (81), 802 (19), 906 (22), 745 (15). MS (FAB-) m/e : 860.2 [(M+matrix(glycerine)-H)⁻], 707.2 [(M-H)⁻], 619.3 [(M-CONHNO₂)⁻]. Elemental analysis, calcd (%): C₁₂H₁₂N₁₂O₂₄×2H₂O (744.32): C 19.36, H 2.17, N 22.56; found: C 19.44, H 2.17, N 22.58. DSC (5 °C min⁻¹, onset): 181 °C (dec.). BAM drophammer: 8 J. Friction tester: 360 N, ESD: 0.50 J (grain size 100–500 μm).

Dehydration under vacuum at 70 °C for 24 hours: IR (ATR, cm^{-1}): $\nu = 31800$ (w), 3034 (w), 2982 (w), 1777 (m), 1612 (s), 1434 (m), 1395 (w), 1330 (m), 1264 (w), 1163 (s), 987 (s), 951 (s), 894 (w), 825 (m), 738 (m), 728 (m). Elemental analysis, calcd (%): $\text{C}_{12}\text{H}_{12}\text{N}_{12}\text{O}_{24}$ (708.23): C 20.35, H 1.71, N 23.10; found: C 20.36, H 1.98, N 23.37. BAM drophammer: 4 J. Friction tester: 80 N, ESD: 0.15 J (grain size 100–500 μm).

D-Mannitol hexanitrocarbamate (3c): ^1H NMR ($[\text{D}_6]$ acetone): $\delta = 13.8$ (br, 6H, NH), 5.61 (m, 2H, CH), 5.45 (m, 2H, CH), 4.75 (m, 2H, CH_2), 4.45 (m, 2H, CH_2) ppm. $^{13}\text{C}\{^1\text{H}\}$ NMR ($[\text{D}_6]$ acetone): $\delta = 148.3$ (CO), 147.9 (CO), 147.8 (CO), 71.2 (CH), 70.3 (CH), 63.1 (CH_2) ppm. ^{14}N NMR ($[\text{D}_6]$ acetone): $\delta = -46$ (NO_2) ppm. IR (ATR, cm^{-1}): $\nu = 3613$ (m), 3527 (w), 3123 (w), 3009 (w), 2771 (w), 1764 (s), 1621 (s), 1455 (m), 1390 (w), 1330 (m), 1297 (w), 1284 (w), 1251 (w), 1175 (s), 1118 (s), 1105 (s), 1063 (w), 1035 (w), 999 (m), 972 (m), 918 (m), 903 (w), 794 (w), 732 (m). Raman (1064 nm, 1000 mW, cm^{-1}): $\nu = 3030$ (17), 3014 (23), 2987 (39), 1786 (55), 1612 (13), 1464 (23), 1402 (11), 1361 (28), 1330 (92), 1285 (12), 1266 (18), 1220 (19), 1157 (18), 1137 (18), 1101 (10), 1065 (10), 1003 (100), 895 (11), 812 (13), 723 (16). (FAB $^-$) m/e : 709.2 $[(\text{M}-\text{H})^-]$. Elemental analysis, calcd (%): $\text{C}_{12}\text{H}_{20}\text{N}_6\text{O}_{12} \times 6\text{H}_2\text{O}$ (818.40): C 17.61, H 3.20, N 20.54; found: C 17.41, H 3.20, N 20.11. DSC (5 $^\circ\text{C min}^{-1}$, onset): 142 $^\circ\text{C}$ (dec.). BAM drophammer: 30 J. Friction tester: 360 N, ESD: 0.50 J (grain size 100–500 μm).

Dehydration under vacuum at 70 °C for 24 hours: IR (ATR, cm^{-1}): $\nu = 3531$ (w), 3198 (w), 3034 (w), 2772 (w), 1766 (s), 1610 (s), 1435 (m), 1326 (m), 1255 (w), 1148 (s), 973 (m), 888 (w), 805 (m), 737 (m). Elemental analysis, calcd (%): $\text{C}_{12}\text{H}_{12}\text{N}_{12}\text{O}_{24}$ (710.31): C 20.29, H 1.99, N 23.66; found: C 20.33, H 2.08, N 23.48. BAM drophammer: 4 J. Friction tester: 60 N, ESD: 0.20 J (grain size 100–500 μm).

D-Sorbitol hexanitrocarbamate (3d): ^1H NMR ($[\text{D}_6]$ acetone): $\delta = 13.8$ (br, 6H, NH), 5.63 (m, 4H, CH), 4.74 (m, 2H, CH_2), 4.49 (m, 2H, CH_2) ppm. $^{13}\text{C}\{^1\text{H}\}$ NMR ($[\text{D}_6]$ acetone): $\delta = 148.1$ (CO), 148.0 (CO), 147.9 (CO), 147.8 (CO), 71.7 (CH), 71.3 (CH), 70.9 (CH), 70.4 (CH), 63.7 (CH_2), 62.9 (CH_2) ppm. ^{14}N NMR ($[\text{D}_6]$ acetone): $\delta = -47$ (NO_2) ppm. IR (ATR, cm^{-1}): $\nu = 3542$ (w), 3250 (w), 3183 (w), 2984 (w), 2827 (w), 2772 (w), 1767 (s), 1610 (s), 1443 (m), 1360 (m), 1260 (w), 1147 (s), 969 (m), 887 (w), 805 (w), 735 (m). Raman (1064 nm, 1000 mW, cm^{-1}): $\nu = 2983$ (46), 1787 (35), 1623 (29), 1453 (36), 1328 (99), 1224 (22), 1173 (21), 1104 (24), 1047 (40), 1005 (100), 743 (23). (FAB $^-$) m/e : 709.2 $[(\text{M}-\text{H})^-]$. Elemental analysis, calcd (%): $\text{C}_{12}\text{H}_{20}\text{N}_6\text{O}_{12} \times 4\text{H}_2\text{O}$ (782.37): C 18.42, H 2.83, N 21.48; found: C 19.18, H 3.00, N 21.44. DSC (5 $^\circ\text{C min}^{-1}$, onset): 138 $^\circ\text{C}$ (dec.).

Xylitol pentanitrocarbamate (3e): ^1H NMR ($[\text{D}_6]$ acetone): $\delta = 13.9$ (br, 5H, NH), 5.67 (m, 3H, CH), 4.71 (m, 2H, CH_2), 4.49 (m, 2H, CH_2) ppm. $^{13}\text{C}\{^1\text{H}\}$ NMR ($[\text{D}_6]$ acetone): $\delta = 148.1$ (CO), 147.9 (CO), 71.2 (CH), 71.1 ($2\times\text{CH}$), 63.8 (CH_2) ppm. ^{14}N NMR ($[\text{D}_6]$ acetone): $\delta = -46$ (NO_2) ppm. IR (ATR, cm^{-1}): $\nu = 3544$ (w), 3261 (w), 3184 (w), 2984 (w), 1766 (s), 1609 (s), 1441 (m), 1326 (m), 1260 (w), 1147 (s), 982 (m), 961 (m), 856 (w), 849 (w), 807 (w), 735 (s). Raman (1064 nm, 1000 mW, cm^{-1}): $\nu = 2979$ (45), 1778 (41), 1626 (34), 1447 (42), 1327 (100), 1216 (28), 1167 (26), 1099 (28), 1006 (98), 881 (21), 810 (26), 739 (22). MS (FAB $^-$) m/e : 591.2 $[(\text{M}-\text{H})^-]$. Elemental analysis, calcd (%): $\text{C}_{10}\text{H}_{12}\text{N}_{10}\text{O}_{20}\times 2\text{H}_2\text{O}$ (628.29): C 19.12, H 2.57, N 22.29; found: C 19.88, H 2.61, N 22.20. DSC ($5\text{ }^\circ\text{C min}^{-1}$, onset): $142\text{ }^\circ\text{C}$ (dec.).

D-Ribitol pentanitrocarbamate (3f): ^1H NMR ($[\text{D}_6]$ acetone): $\delta = 13.6$ (br, 5H, NH), 5.53 (m, 3H, CH), 4.80 (m, 2H, CH_2), 4.44 (m, 2H, CH_2) ppm. $^{13}\text{C}\{^1\text{H}\}$ NMR ($[\text{D}_6]$ acetone): $\delta = 148.2$ (CO), 147.6 (CO), 147.3 (CO), 71.5 ($2\times\text{CH}$), 71.3 (CH), 63.0 (CH_2) ppm. ^{14}N NMR ($[\text{D}_6]$ acetone): $\delta = -47$ (NO_2) ppm. IR (ATR, cm^{-1}): $\nu = 3542$ (w), 3258 (w), 3184 (w), 2984 (w), 1765 (s), 1609 (s), 1440 (m), 1326 (m), 1284 (w), 1258 (w), 984 (m), 918 (w), 886 (w), 843 (w), 807 (w), 737 (m). Raman (1064 nm, 1000 mW, cm^{-1}): $\nu = 2981$ (42), 1776 (38), 1624 (32), 1450 (42), 1328 (100), 1210 (26), 1159 (25), 1097 (29), 1007 (97), 816 (26), 736 (24). MS (FAB $^-$) m/e : 591.2 $[(\text{M}-\text{H})^-]$. Elemental analysis, calcd (%): $\text{C}_{10}\text{H}_{12}\text{N}_{10}\text{O}_{20}\times 2\text{H}_2\text{O}$ (628.29): C 19.12, H 2.57, N 22.29; found: C 19.12, H 2.57, N 22.24. DSC ($5\text{ }^\circ\text{C min}^{-1}$, onset): $145\text{ }^\circ\text{C}$ (melt.).

5.6 References

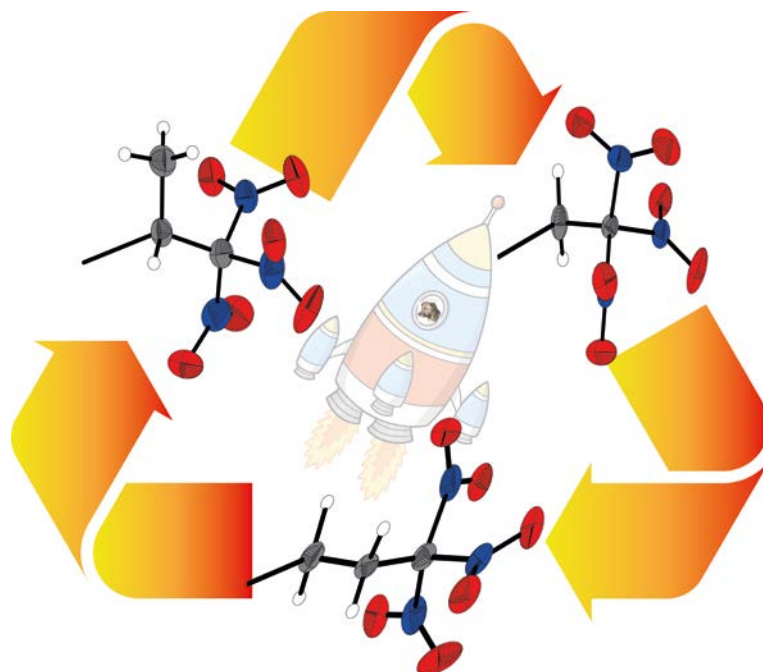
- [1] a) H. Gao, J. M. Shreeve, *Angew. Chem., Int. Ed.* **2015**, *54*, 6335–6338; b) K. O. Christe, W. W. Wilson, G. Bélanger-Chabot, R. Haiges, J. A. Boatz, M. Rahm, G. K. S. Prakash, T. Saal, M. Hopfinger, *Angew. Chem., Int. Ed.* **2015**, *54*, 1316–1320; c) J. Short, R. Kavetsky, D. K. Anand, R. Armstrong, *Energetics Science and Technology in Central Europe*, CALCE EPSC Press, Maryland, **2011**; d) T. M. Klapötke, M. Rusan, J. J. Sabatini, *Angew. Chem., Int. Ed.* **2014**, *53*, 9665–9668.
- [2] a) J. A. Radley, *Industrial Uses of Starch and its Derivatives*, Springer, New York, **1976**; b) J. Köhler, R. Meyer, A. Homburg, *Explosivstoffe*, Wiley-VCH, Weinheim, **2008**.
- [3] J. R. Partington, *A History of Greek Fire and Gunpowder*, The Johns Hopkins University Press, Baltimore, **1999**.
- [4] a) C. Luo, S. Wang, H. Liu, *Angew. Chem., Int. Ed.* **2007**, *46*, 7636–7639; b) H. Kobayashi, Y. Ito, T. Komanoya, Y. Hosaka, P. L. Dhepe, K. Kasai, K. Hara, A. Fukuoka, *Green Chem.* **2011**, *13*, 326–333.
- [5] H. Kobayashi, A. Fukuoka, *Green Chem.* **2013**, *15*, 1740–1763.
- [6] T. L. Lemke, *Review of Organic Functional Groups: Introduction to Medicinal Organic Chemistry*, 5th ed., Lippincott Williams & Wilkins, New York, **2003**.
- [7] a) Q. J. Axthammer, B. Krumm, T. M. Klapötke, *J. Org. Chem.* **2015**, *80*, 6329–6335; b) Q. J. Axthammer, T. M. Klapötke, B. Krumm, R. Moll, S. F. Rest, *Z. Anorg. Allg. Chem.* **2014**, *640*, 76–83; c) Q. J. Axthammer, B. Krumm, T. M. Klapötke, *Eur. J. Org. Chem.* **2015**, *2015*, 723–729.
- [8] D. S. Bohle, Z. Chua, *Inorg. Chem.* **2014**, *53*, 11160–11172.
- [9] a) M. G. Kim, *J. Appl. Polym. Sci.* **2011**, *122*, 2209–2220; b) L. Cotarca, H. Eckert, *Phosgenations — A Handbook*, Wiley-VCH, Weinheim, **2005**.
- [10] A. R. Modarresi-Alam, F. Khamooshi, M. Nasrollahzadeh, H. A. Amirazizi, *Tetrahedron* **2007**, *63*, 8723–8726.
- [11] E. D. McLanahan, M. E. Andersen, J. W. Fisher, *Toxicol. Sci.* **2008**, *102*, 241–253.
- [12] G. Fischer, J. Geith, T. M. Klapötke, B. Krumm, *Z. Naturforsch., B: Chem. Sci.* **2002**, *57*, 19–24.
- [13] a) R. Graf, *Chem. Ber.* **1956**, *89*, 1071–1079; b) P. Kočovský, *Tetrahedron Lett.* **1986**, *27*, 5521–5524.
- [14] a) M. Hirama, T. Oishi, *Trichloroacetyl Isocyanate*, John Wiley & Sons, Ltd, New York, **2001**; b) D. N. Dhar, P. Dhar, *The Chemistry of Chlorosulfonyl Isocyanate*, World Scientific, Singapore, **2002**.
- [15] M. Grembecka, *Eur. Food Res. Technol.* **2015**, *241*, 1–14.
- [16] S. Bienz, L. Bigler, T. Fox, M. Hesse, H. Meier, B. Zeeh, *Spektroskopische Methoden in der Organischen Chemie*, 8th ed., Thieme, Stuttgart, **2014**.

- [17] G. Gattow, W. K. Knoth, *Z. Anorg. Allg. Chem.* **1983**, *499*, 194–204.
- [18] A. Kuksis, *Inositol Phospholipid Metabolism and Phosphatidyl Inositol Kinases*, Elsevier Science, Philadelphia, **2003**.
- [19] V. W. Manner, B. C. Tappan, B. L. Scott, D. N. Preston, G. W. Brown, *Cryst. Growth Des.* **2014**, *14*, 6154–6160.
- [20] T. M. Klapötke, *Chemistry of High-Energy Materials*, 2nd ed., deGruyter, Berlin, **2012**.
- [21] M. Göbel, T. M. Klapötke, *Adv. Funct. Mater.* **2009**, *19*, 347–365.
- [22] a) M. Sućeska, *Propellants, Explos., Pyrotech.* **1991**, *16*, 197–202; b) M. Sućeska, *EXPLO5 V.6.02*, Zagreb, **2013**.
- [23] Oxford Diffraction Ltd., *CrysAlis CCD*, Version 1.171.35. (release 16-05-2011 CrysAlis 171.Net), Abingdon, Oxford, **2011**.
- [24] Oxford Diffraction Ltd., *CrysAlis RED*, Version 1.171.35.11 (release 16-05-2011 CrysAlis 171.NET), Abingdon, Oxford, **2011**.
- [25] A. Altomare, M. C. Burla, M. Camalli, G. L. Cascarano, C. Giacovazzo, A. Guagliardi, A. G. G. Moliterni, G. Polidori, R. Spagna, *J. Appl. Crystallogr.* **1999**, *32*, 115–119.
- [26] a) G. M. Sheldrick, *SHELX-97, Programs for Crystal Structure Determination*, **1997**; b) G. M. Sheldrick, *Acta Crystallogr., Sect. A: Found. Crystallogr.* **2008**, *A64*, 112–122.
- [27] L. Farrugia, *J. Appl. Crystallogr.* **1999**, *32*, 837–838.
- [28] A. Spek, *Acta Crystallogr., Sect. D: Biol. Crystallogr.* **2009**, *65*, 148–155.

6 The 1,1,1-Trinitroprop-2-yl Moiety

As published in *Z. Naturforsch., B: J. Chem. Sci.* **2016**, *in press*.

STUDIES ON THE SYNTHESIS AND PROPERTIES OF 1,1,1-TRINITROPROP-2-YL UREA, CARBAMATE AND NITROCARBAMATE



6.1 Abstract

Potential high energetic dense oxidizers with the 1,1,1-trinitropropan-2-yl moiety are described in this study. The urea, 1,3-bis(1,1,1-trinitropropan-2-yl)urea (**1**), is synthesized by the reaction of urea with acetaldehyde and trinitromethane. The reaction of 1,1,1-trinitropropanol (**2**) with the reagent chlorosulfonyl isocyanate results in the formation of the carbamate 1,1,1-trinitroprop-2-yl carbamate (**3**). The nitration of **3** with anhydrous nitric and sulfuric acid yields the nitrocarbamate **4**. All compounds were fully characterized by multinuclear NMR (^1H , ^{13}C , $^{14/15}\text{N}$) spectroscopy, vibrational spectroscopy, mass spectrometry and elemental analysis (CHN). For analysis of the thermostability differential scanning calorimetry (DSC) was used. Energetic properties, the sensitivities towards impact, friction and electrostatic discharge were tested and compared with the corresponding 2,2,2-trinitroethyl and 3,3,3-trinitropropyl derivatives. In this context, the crystal structures of two compounds with the 1,1,1-trinitroprop-2-yl moiety have been determined by low temperature X-ray diffraction and discussed. The energies of formation were evaluated and several detonation parameters such as the velocity of detonation and the propulsion performance were calculated with the program package EXPLO5.

6.2 Introduction

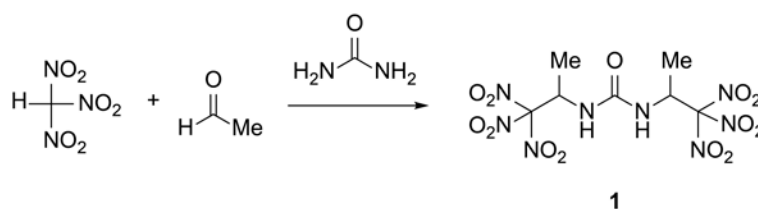
High energy dense oxidizers (HEDOs) are based on CHNO and are a subgroup of energetic compounds which release an excess of oxygen when decomposed.^[1] These class of compounds are mainly used in composite propellants, where they are the main part with around 75%. Further ingredients of such solid rocket propellants are binder and fuel. The released excess of oxygen which is produced by the oxidizer reacts with the carbon backbone and added fuel, which produce hot gases for the propulsion. As a fuel, often aluminum is used which burns very hot, has a low atomic weight and is cheap.^[2] Until now, ammonium perchlorate (AP) is used as oxidizer, due to the high oxygen content, the good stability and the low sensitivity against mechanical stimuli. Unfortunately, the perchlorate anion is toxic to vertebrates, amphibians and other marine organisms.^[3] There is also a proof that the anion perchlorate has negative health effects to humans, especially on the thyroid hormonal balance which is important for the normal growth and development.^[4] Another drawback of AP are the decomposition products like the toxic hydrogen chloride which causes further environmental problems and generates easy visible and detectable expulsion leading to tactical disadvantages.^[5]

The 2,2,2-trinitroethyl moiety is the most commonly used group for the synthesis of new HEDOs and can be obtained by reacting trinitromethane and formaldehyde via a Henry or Mannich reaction.^[6] The trinitropropyl group is less common and two different constitutional isomers are possible. The synthesis, structure and energetic properties of the 3,3,3-trinitropropyl moiety were recently investigated.^[7] The 1,1,1-trinitroprop-2-yl moiety is not much investigated, only patents from the 1960ies with the description of 1,1,1-trinitroprop-2-yl ethers and the urea compound 1,3-bis(1,1,1-trinitropropan-2-yl)urea (**1**) are available.^[8] Although few compounds are reported, nothing is known about their structural and energetic properties and stability.

6.3 Results and Discussion

6.3.1 Synthesis

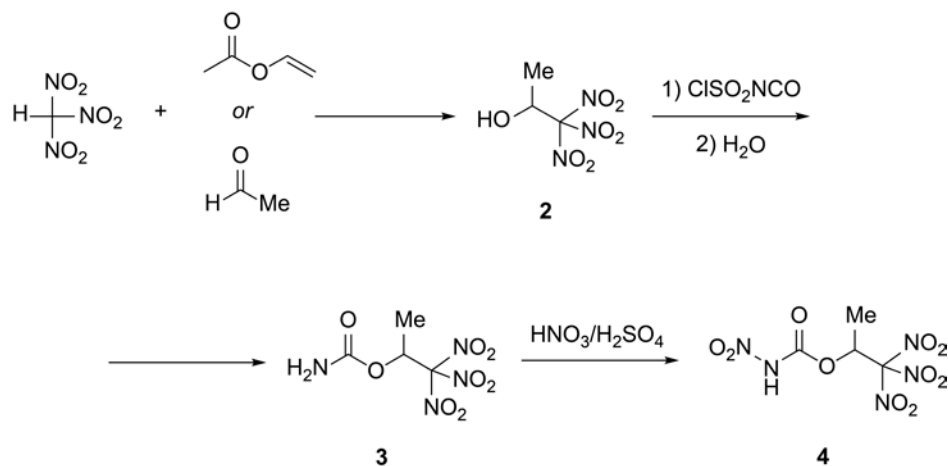
Scheme 6-1 illustrates the synthesis of 1,3-bis(1,1,1-trinitropropan-2-yl)urea (**1**). The starting materials trinitromethane and acetaldehyde were both dissolved in water under stirring, and after few minutes an oil separated very likely the intermediate alcohol 1,1,1-trinitropropan-2-ol (**2**). This carbon-carbon bond forming condensation is referred to a Henry reaction of an aldehyde and polynitroalkane having an acidified proton in α -position to the nitro groups. Urea is added with stirring and within minutes a colorless precipitate of product **1** was formed. This Mannich type condensation is acid catalyzed by the strong acidity of trinitromethane (pK_a 0.15).^[9] Acetaldehyde is a prochiral starting material resulting in a racemic product.



Scheme 6-1: Synthesis of 1,3-bis(1,1,1-trinitropropan-2-yl)urea (**1**).

The above mentioned intermediate alcohol 1,1,1-trinitropropanol (**2**) can be isolated by reacting trinitromethane with either vinyl acetate or acetaldehyde (Scheme 6-2). The vinyl acetate route is literature known and works by the addition of trinitromethane to the unsaturated alkene with subsequent hydrolysis of the ester in water.^[10] The other alternative was performed by the reaction with acetaldehyde and extraction with an organic solvent like chloroform. The alcohol

was obtained in both cases with small impurities, due to the reversible cleavage into trinitromethane and acetaldehyde which has a very high vapor pressure.^[9a, 11]



Scheme 6-2: Synthesis of 1,1,1-trinitropropan-2-yl nitrocarbamate (4) starting from nitroform.

The alcohol **2** can be converted into the corresponding 1,1,1-trinitropropan-2-yl carbamate (**3**) in a one step synthesis by the reaction with chlorosulfonyl isocyanate (CSI). The carbamate was isolated as a colorless pure solid in high yields (78%), in spite of impure starting material. The nitration of the carbamate **3** in an 1:1 mixture of concentrated sulfuric (98%) and nitric acid (100%) leads to the formation of 1,1,1-trinitropropan-2-yl nitrocarbamate (**4**). After quenching with ice-water and extraction with ethyl acetate, the nitrocarbamate **4** was obtained as a colorless oil, as most other 1,1,1-trinitroprop-2-yl compounds.^[8a-c]

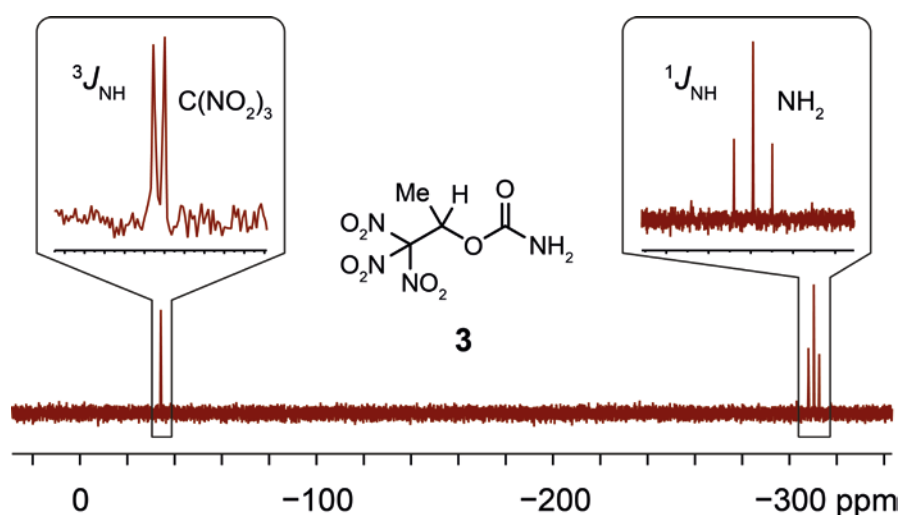
6.3.2 NMR Spectroscopy and Vibrational Spectroscopy

The ^1H , ^{13}C and $^{14/15}\text{N}$ NMR spectra were recorded in CDCl_3 and are summarized in Table 6-1. The urea compound **1** shows three signals in the ^1H NMR. The methyl resonance is located at 4.53 ppm and split into a doublet, due to the 3J coupling with the neighboring hydrogen at the methine unit. The NH group also couples with the CH group which results also in a doublet at 6.62 ppm. In the ^{13}C NMR the carbon resonance of the CH group is found at 50.2 ppm and the CH_3 group at 18.2 ppm. The trinitromethyl group is observed as a typically broadened signal at 129.3 ppm and therefore in the same range than the related compound 1,3-bis(3,3,3-trinitropropan-2-yl)urea (130.8 ppm^[7]).

Table 6-1: Multinuclear NMR resonances (ppm) of 1, 3 and 4 on CDCl₃.

		1	3	4
¹ H	CH ₃	1.53	1.68	1.81
	CH	5.61	6.21	6.32
	NH/NH ₂	6.62	5.10	10.81
¹³ C{ ¹ H}	CH ₃	18.2	16.7	16.6
	CH	50.2	69.3	70.9
	C(NO ₂) ₃	129.3	126.5	125.0
	CO	154.5	153.2	145.2
^{14/15} N	NH ₂ /NH/NHNO ₂	-295	-310.2	-199
	C(NO ₂) ₃	-32	-34.2	-36
	NHNO ₂			-54

The NH resonance of the nitrocarbamate **4** is observed at 10.81 ppm, and compared to the NH₂ of **3** which is located at 5.10 ppm, shifted significantly to lower field, due to the increased acidity of the hydrogen. In the ¹³C{¹H} NMR spectra the resonances of the carbon atoms of the methyl groups were observed at 16.7 (**3**) and 16.6 ppm (**4**), those of the trinitromethyl groups broadened at 126.5 (**3**) and 125.0 ppm (**4**). In the ¹³C NMR spectra, the most obvious characteristic is the resonance of the carbamate carbonyl group, which is shifted strong upfield from the carbamate **3** at 153.2 ppm to 145.2 ppm for the nitrocarbamate **4**, due to increased shielding by the presence of an adjacent nitro group.

Figure 6-1: ¹⁵N NMR spectrum of 1,1,1-trinitropropan-2-yl carbamate (**3**) in CDCl₃.

In the ^{14}N NMR spectra the resonances of the nitro groups of the trinitromethyl moieties are relatively sharp and were found in the range of -32 to -36 ppm. The high solubility of the carbamate **3** qualified for a ^{15}N NMR spectrum and is displayed in Figure 6-1. The resonance of the trinitromethyl group is observed at -34.2 ppm and due to the peculiarity of the structure a doublet is observed by coupling to the methine hydrogen atom with $^3J(^{15}\text{N}, ^1\text{H}) = 1.9$ Hz. The resonance of the carbamate nitrogen is located as expected at -310.2 ppm as a triplet with a coupling constant of $^1J(^{15}\text{N}, ^1\text{H}) = 92.1$ Hz. In the ^{14}N NMR of the nitrocarbamate **4** a very broad resonance for the amide nitrogen atom was detected at -199 ppm and for the additional nitro group at the carbamate moiety at -54 ppm, which are in the typical ranges.^[6a]

Table 6-2: Selected IR and Raman bands of the compounds **1**, **3** and **4**.

	1		3		4	
	IR	Raman	IR	Raman	IR	Raman
νNH	3314 (w)	3011 (9)	3457 (m)	3018 (18)		
			3349 (m)			
νCH	2970 (w)	2957 (59)	2975 (w)	2960 (59)	2975 (w)	2959 (53)
					2886 (w)	2884 (4)
νCO	1648 (s)	1647 (7)	1731 (s)	1733 (12)	1680 (s)	1691 (8)
$\nu_{\text{as}}\text{NO}_2$	1592 (vs)	1616 (23)	1594 (vs)	1618 (32)		1617 (18)
					1587 (vs)	1602 (16)
$\nu_{\text{s}}\text{NO}_2$	1295 (vs)	1298 (33)	1289 (s)	1297 (22)	1291 (vs)	1296 (22)
					1270 (s)	1278 (6)

Frequencies in cm^{-1} ; IR intensities: vs = very strong, s = strong, m = medium, w = weak; Raman intensities in brackets, the strongest were set to 100.

The most characteristic vibration frequencies in the IR and RAMAN spectra are the carbonyl and nitro groups, which are summarized in Table 6-2. Regarding the trinitromethyl group vibrational analysis (RAMAN) of **1**, **3** and **4** showed the characteristic asymmetric $\nu_{\text{as}}(\text{NO}_2)$ stretching vibrations in the narrow range of 1618 to 1616 cm^{-1} and the symmetric stretching vibrations $\nu_{\text{s}}(\text{NO}_2)$ at 1298 to 1296 cm^{-1} . In the nitrocarbamate **4** spectrum an additional nitro vibration was observed with additional bands for the $\nu_{\text{as}}(\text{NO}_2)$ at 1602 cm^{-1} and $\nu_{\text{s}}(\text{NO}_2)$ at 1278 cm^{-1} , which appear at slightly higher wave numbers.^[12] In the urea **1** the $\nu(\text{C}=\text{O})$ is located at

1647 cm^{-1} in the typical range for 1,3-disubstituted urea compounds. The characteristic strong carbonyl stretching vibration of the carbamates **3** are found at 1733 cm^{-1} and that of the nitrocarbamate **4** is shifted to higher wave number at 1691 cm^{-1} .

6.3.3 Single Crystal Structure Analysis

Single crystals suitable for X-ray diffraction measurements were obtained by crystallization at room temperature from ethanol (**1**) and hot water (**3**). A full list of the crystallographic refinement parameters and structure data is shown in the Appendix A.6. To the best of our knowledge, no molecular structure with a 1,1,1-trinitroprop-2-yl moiety is known in the literature.

The urea **1** crystallizes with ethanol in the orthorhombic space group $Pnma$ with four molecules in the unit cell. The asymmetric unit consists of a half molecule which is completed by a mirror plane longitudinal through the carbonyl group C4–O7. The full molecule with atom distances and angles is shown in Figure 6-2. The geometric structure show the same characteristics as the corresponding compounds with the 2,2,2-trinitroethyl and 3,3,3-trinitropropyl moiety.^[6b, 7]

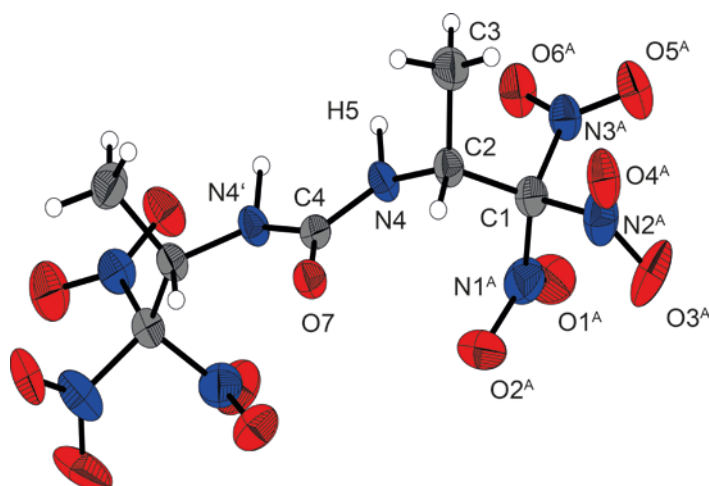


Figure 6-2: X-ray molecular structure of 1,3-bis(1,1,1-trinitropropan-2-yl)urea (1).

Selected atom distances (\AA) and angles (deg): C1–N1A 1.529(5), C1–N3A 1.578(4), C1–C2 1.534(3), C2–C3 1.520(3), C2–N4 1.441(3), C4–N4 1.360(3), C4–O7 1.231(4), N4–C4–N4' 113.7, C2–C1–N1A 113.9(2), C2–C1–N2A 116.3(3), C2–C1–N3A 110.5(2), N2A–C1–N3A 105.0(3), N3A–C1–N1A 104.1(2), N1A–C1–N2A 106.1(3), O7–C4–N4–H5 173(2).

The three nitro groups of the trinitromethyl group are propeller-like arranged around the carbon C1. This geometry results from non-bonded $\text{N}\cdots\text{O}$ intramolecular interactions between the partial positively charged nitrogen and negatively charged oxygen in the nitro groups. These

$N\cdots O$ attractions are displayed in Figure 6-3 and are found with distances in the range of 2.54–2.60 Å, which are much shorter than the sum of the van der Waals radii of nitrogen and oxygen (3.07 Å). They are caused by a slight compression of the trinitromethyl group, which is visible by the $C2-C1-N1A/N2A/N3A$ angles, and values are all larger than the tetrahedral angle.

Furthermore, a disorder of the trinitromethyl group is observed, where two different positions can be identified with a proportion occupation of 65% to 35%, which is displayed as shaded area in Figure 6-3. Another usual feature in such structures is a shortened carbon-carbon bond in α -position to the trinitromethyl group;^[6a, 7] however, in this case such a shortening of the $C1-C2$ distance (1.53 Å) was not at all observed. A reason for this may be some steric force, coming from the additional methyl group in the close position of the big bulky trinitromethyl group.

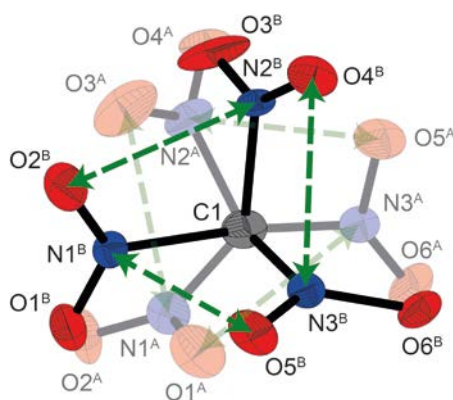


Figure 6-3: Disorder of the trinitromethyl group in the X-ray molecular structure of 1,3-bis(1,1,1-trinitropropan-2-yl)urea (1).

The green lines indicate the nitrogen-oxygen non-bonded intramolecular interactions. Short contact distances: $O3A-N1A$ 2.539(6), $O1A-N3A$ 2.601(8), $O5A-N2A$ 2.545(6), $O5B-N1B$ 2.501(1), $O4B-N3B$ 2.573(8), $O2B-N2B$ 2.545(9).

The carbamate **3** crystallizes in the monoclinic space group $P2_1/c$ with four molecules in the unit cell and one molecule as the asymmetric unit (Figure 6-4) with a density of 1.75 g cm^{-3} . The carbamate moiety, including the methine carbon $C2$ shows a nearly perfect planar adjustment. The conformations of the substituents at $C1$, $C2$ and $C3$ are nearly all staggered. The carbamate group with a short $C-NH_2$ bond (1.32 Å) and shortened $N-H$ bonds (0.81 Å) shows typical values for carbamates. The propeller like conformation of the trinitromethyl group is in this example not perfect, which is also indicated by longer $N\cdots O$ attractions (2.63–2.80 Å). In addition, a strong attractive intermolecular $N\cdots O$ interaction with 2.66 Å is observed between the $O7$ of the carbamate unit and $N3$ of a nitro group of the trinitromethyl functionality.

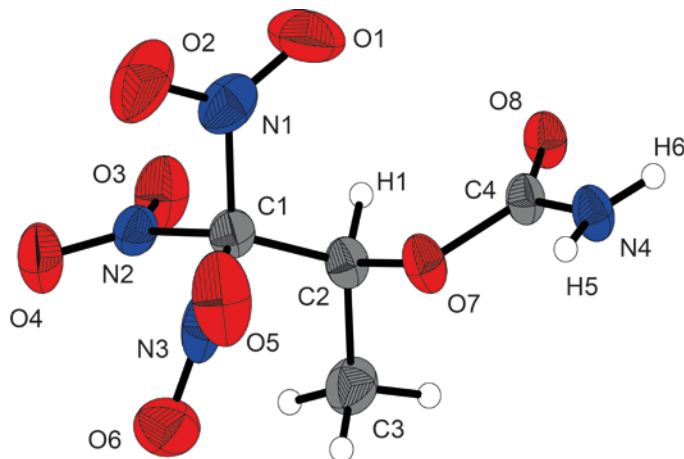
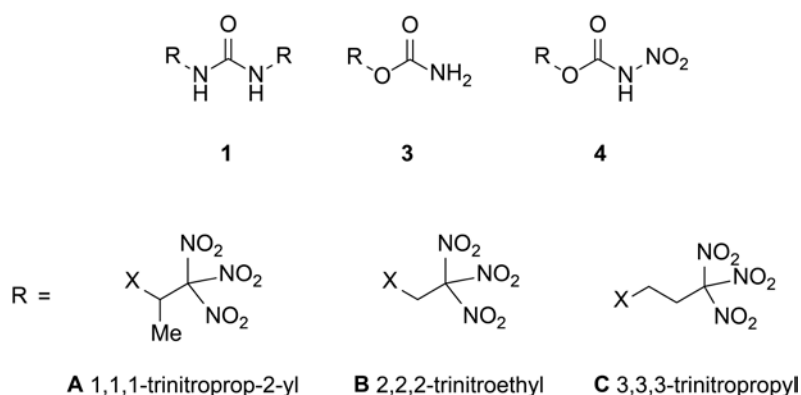


Figure 6-4: X-ray molecular structure of 1,1,1-trinitroprop-2-yl carbamate (3).

Selected bond lengths (Å) and angles (deg): N1–O1 1.188(4), N1–O2 1.207(3), N1–C1 1.535(3), N4–C4 1.320(3), N4–H5 0.81(2), N4–H6 0.81(3), O8–C4 1.216(2), C2–C1–N3 111.3(2), C2–C1–N2 112.6(2), C2–C1–N1 112.8(2), C2–O7–C4 115.9(2), H6–N4–C4–O7 $-180(2)$, H6–N4–C4–O8 1(2), N4–C4–O7–C2 $-176.0(2)$, H1–C2–C3–H3 176(3), O7–C2–C3–H2 169(2), H1–C2–C1–N3 $-174(2)$, O7–C2–C1–N2 $-179.0(2)$, O7–N3 2.749(3), O5–N1 2.625(3), O2–N2 2.796(3), O4–N3 2.664(3).

6.3.4 Thermal Stabilities and Energetic Properties



Scheme 6-3: Overview of molecules containing the 1,1,1-trinitroprop-2-yl, the 2,2,2-trinitroethyl and the 3,3,3-trinitropropyl moieties.

The compounds **1A**, **3A** and **4A** are potential energetic materials and may be used as high energetic dense oxidizers HEDOs, stable to exposure of air and moisture. The physical properties are listed in Table 6-3 and energetic combustion parameters are summarized in Table 6-3. For a better comparison of all energetic properties to the corresponding 2,2,2-trinitroethyl and 3,3,3-trinitropropyl derivatives, those values are also included. The melting points and the thermal stabilities were investigated by differential scanning calorimetry with a heating rate of 5 °C per minute. The highest decomposition point of 154 °C was observed for the carbamate **3A**. The

comparison of the decomposition points of the ureas **1A** with **1B** confirms the tendency of higher thermal stabilities of the latter with 2,2,2-trinitroethyl substituent.

Table 6-3: Physical and sensitivity data of 1A, 3A and 4A and the corresponding 2,2,2-trinitroethyl (B) and 3,3,3-trinitropropyl (C) derivatives.

	1C [7]	3C [7]	4C [7]	1B [11]	3B [6b]	4B [6b]
	C ₇ H ₁₀ N ₈ O ₁₃	C ₄ H ₆ N ₄ O ₈	C ₄ H ₅ N ₅ O ₁₀	C ₅ H ₆ N ₈ O ₁₃	C ₃ H ₄ N ₄ O ₈	C ₃ H ₃ N ₅ O ₁₀
T_m /°C (onset)	-	78	68	185	91	109
T_{dec} /°C (onset)	160	152	134	187	169	153
IS /J	20	>40	30	3	40	10
FS /N	120	>360	360	160	64	96
ESD /J	0.40	0.30	0.20	0.30	0.15	0.10
N /%	27.1	23.5	24.7	29.0	25.0	26.0
O /%	50.2	53.8	56.5	53.9	57.1	59.5
$N+O$ /%	77.3	77.3	81.2	82.9	82.1	85.5
Ω_{CO} /%	+3.9	+6.7	+19.8	+20.7	+21.4	+32.7
Ω_{CO_2} /%	-20.2	-20.2	-2.8	0.00	+0.0	+14.9

	1C [7]	3C [7]	4C [7]
	C ₇ H ₁₀ N ₈ O ₁₃	C ₄ H ₆ N ₄ O ₈	C ₄ H ₅ N ₅ O ₁₀
T_m /°C (onset)	-	78	68
T_{dec} /°C (onset)	160	152	134
IS /J	20	>40	30
FS /N	120	>360	360
ESD /J	0.40	0.30	0.20
N /%	27.1	23.5	24.7
O /%	50.2	53.8	56.5
$N+O$ /%	77.3	77.3	81.2
Ω_{CO} /%	+3.9	+6.7	+19.8
Ω_{CO_2} /%	-20.2	-20.2	-2.8

[a] Onset melting T_m and [b] onset decomposition point T_{dec} from DSC measurement carried out at a heating rate of 5 °C min⁻¹. [c] Impact sensitivity. [d] Friction sensitivity. [e] Sensitivity towards electrostatic discharge. [f] Nitrogen content. [g] Oxygen content. [h] Sum of nitrogen and oxygen content. [i] Oxygen balance assuming the formation of CO and the formation of the formation of [j] CO₂ at the combustion.

The sensitivity towards impact, friction and electrostatic discharge is especially important for the manipulation of energetic materials. The sensitivity towards impact (IS) of a compound is tested by the action of a dropping weight on a sample and at which benchmark a decomposition

or explosion occurs.^[1, 13] The friction sensitivity (FS) is determined by rubbing a small amount with different contact pressures between a porcelain plate and pin.^[14] All three compounds can be classified as insensitive toward friction (≥ 360 N insensitive, 360–80 N sensitive, 80–10 N very sensitive, ≤ 10 N extremely sensitive). The impact sensitivity of **1A** (8 J) and **4A** (15 J) are classified as sensitive, whereas the carbamate **3** is insensitive (≥ 40 J insensitive, 40–35 J less sensitive, 35–4 J sensitive, ≤ 3 J very sensitive). The 1,1,1-trinitroprop-2-yl compounds exhibit for all three examples (**1A**, **3A**, **4A**) a lower sensitivity against impact than the 2,2,2-trinitroethyl derivatives and a moderately higher sensitivity than the 3,3,3-trinitropropyl derivatives.

The urea **1A** shows the highest energy of formation $\Delta_f U^\circ$ with a value of -793 kJ kg⁻¹ which indicates a high energy content in the molecule, demonstrated also the quite high calculated detonation velocity V_{det} of 8469 m s⁻¹ and is in the same range than the well known explosive Nitropenta (PETN) (8403 m s⁻¹).

A very important value for high energetic dense oxidizers is the specific impulse I_{sp} . Oxidizers are the main part in rocket composite propellants and are compounds with an excess of oxygen when burned. This oxygen reacts further with added fuel and the binder to generate hot gaseous products, which can be used for the propulsion of rockets. For a high performing composite propellant a high burning temperature is important, because the specific impulse I_{sp} is proportional to the square root of the temperature.^[1] A second dependence is the molecular weight of the gaseous products at the nozzle of the rocket chamber which is inverse proportional to the square root. This means for a high performance a high burning temperature and a low weight of the gaseous products like CO, CO₂, H₂O, and H₂ is desirable.^[1] High burning temperatures can be achieved from elements with high heats of combustion like aluminum, which is cheap, has a low atomic weight and no hazardous burning products where released.^[2] For the discussion it is important that the payload of the rocket can be doubled if the specific impulse I_{sp} is increased by 20 s.

Table 6-4: Calculated heats of formation and calculated detonation and propulsion parameters using EXPLO5 (V6.02) of 1A, 3A and 4A compared to the corresponding 2,2,2-trinitroethyl (B) and 3,3,3-trinitropropyl (C) derivatives and AP.

	1A	3A	4A	1B [11]	3B [6b]
density RT /g cm ⁻³ [a]	1.82	1.73	1.58	1.86	1.82
$\Delta_f H_m^\circ$ /kJ mol ⁻¹ [b]	-367	-500	-368	-307	-459
$\Delta_f U^\circ$ /kJ kg ⁻¹ [b]	-793	-2005	-1213	-708	-1961
Q_v /kJ kg ⁻¹ [c]	-5390	-4675	-5878	-5970	-5286
T_{ex} /K [d]	3631	3334	4332	4181	3780
V_0 /L kg ⁻¹ [e]	724	744	762	755	761
P_{CJ} /kbar [f]	321	266	228	343	302
V_{det} /m s ⁻¹ [g]	8469	7900	7680	8915	8530
I_{sp} /s [h]	253	236	257	257	246
I_{sp} /s (15% Al) [i]	267	255	262	263	254
I_{sp} /s (15% Al, 14% binder)[j]	249	240	254	256	247
	4B [6b]	1C [7]	3C [7]	4C [7]	AP
density RT /g cm ⁻³ [a]	1.72	1.71	1.73	1.70	1.95
$\Delta_f H_m^\circ$ /kJ mol ⁻¹ [b]	-366	-359	-504	-402	-296
$\Delta_f U^\circ$ /kJ kg ⁻¹ [b]	-1278	-774	-2021	-1331	-2433
Q_v /kJ kg ⁻¹ [c]	-4456	-5385	-4662	-5809	-1422
T_{ex} /K [d]	3618	3692	3328	4175	1735
V_0 /L kg ⁻¹ [e]	750	739	724	755	885
P_{CJ} /kbar [f]	232	294	265	269	158
V_{det} /m s ⁻¹ [g]	7704	8227	7896	8134	6368
I_{sp} /s [h]	232	254	237	256	157
I_{sp} /s (15% Al) [i]	251	267	256	261	235
I_{sp} /s (15% Al, 14% binder)[j]	261	251	240	253	261

[a] Densities at RT measured by gas pycnometer. [b] Heat and energy of formation calculated with by the CBS-4 M method using Gaussian 09.[15] [c] Heat of detonation. [d] Detonation temperature. [e] Volume of gaseous products. [f] Detonation pressure. [g] Detonation velocity. Detonation velocity calculated by using the EXPLO5 (Version 6.02) program package.[16] [h] Specific impulse of the neat compound using the EXPLO5 (Version 6.02) program package at 70.0 bar chamber pressure, isobaric combustion condition (1 bar) and equilibrium expansion.[16] [i] Specific impulse for compositions with aluminum. [j] Specific impulse with aluminum and binder (6% polybutadiene acrylic acid, 6% polybutadiene acrylonitrile and 2% bisphenol A ether).

The specific impulse I_{sp} of the compounds **1A**, **3A** and **4A** were calculated with EXPLO 5 (V6.02)^[16] neat, with aluminum (15%) and with a binder/aluminum system (15% aluminum, 6% polybutadiene acrylic acid, 6% polybutadiene acrylonitrile and 2% bisphenol A ether). Compound **1A** shows an impulse of 253 s neat and with an admixture of 15% aluminum as fuel a great value

of 267 s could be achieved, which is higher than the optimized composite of ammonium perchlorate (AP). The standard mixture consists of 71% AP as oxidizer, 14% of binder and 15% aluminum and produces a specific impulse of 261 s. With this binder system the nitrocarbamate **4A** shows the best performance of 254 s which is quite lower than the AP mixture. Comparing the energetic performance of the 1,1,1-trinitroprop-2-yl group with the 2,2,2-trinitroethyl and 3,3,3-trinitropropyl compounds a clear trend can be observed. The compounds with 1,1,1-trinitroprop-2-yl moiety are less energetic than the 2,2,2-trinitroethyl compounds, due to the lower oxygen balance/content. On the other hand, the branched isomer compounds with the 1,1,1-trinitroprop-2-yl group show in all cases a higher performance than the 3,3,3-trinitropropyl isomers.

6.4 Conclusion

The 1,1,1-trinitroprop-2-yl urea, carbamate and nitrocarbamate compounds **1**, **3** and **4** were prepared and thoroughly characterized, including the molecular structures of **1** and **3** by X-ray diffraction. They exhibit suitable thermal stability and a good to handle sensitivity against mechanic stimuli. For a potential application as high energy dense oxidizer in composite solid rocket propellants, the required energetic performance data were calculated. The most suitable compound, the urea **1** shows a high specific impulse I_{sp} of 267 s within a mixture of 15% aluminum, which is higher than the standard mixture with ammonium perchlorate (AP). Favorably, in contrast by burning ammonium perchlorate AP, no toxic combustion products (such as HCl) are produced. The synthetic effort of the “*iso*” 1,1,1-trinitroprop-2-yl group is compared to the *n*-analogue, the 3,3,3-trinitropropyl, not that complex and leads to similar physical and energetic properties.

6.5 Experimental Section

6.5.1 General Procedures

All chemicals were used as supplied. Raman spectra were recorded in a glass tube with a Bruker MultiRAM FT-Raman spectrometer with Nd:YAG laser excitation up to 1000 mW (at 1064 nm). Infrared spectra were measured with a Perkin–Elmer Spectrum BX-FTIR spectrometer equipped with a Smiths DuraSamplIR II ATR device. All spectra were recorded at ambient (25 °C) temperature. NMR spectra were recorded with a JEOL/Bruker instrument and chemical shifts were determined with respect to external Me₄Si (¹H, 399.8 MHz; ¹³C, 100.5 MHz) and MeNO₂ (¹⁵N, 40.6 MHz; ¹⁴N, 28.9 MHz). Mass spectrometric data were obtained with a JEOL MStation JMS 700 spectrometer (DCI+, DEI+, FAB+, FAB–). Analysis of C/H/N were performed with an Elemental Vario EL Analyzer. Melting and decomposition points were measured with a Perkin-Elmer Pyris6 DSC and an OZM Research DTA 552-Ex with a heating rate of 5 °C min⁻¹ in a temperature range of 15 to 400 °C and checked by a Büchi Melting Point B-540 apparatus (not corrected). The sensitivity data were performed using a BAM drophammer and a BAM friction tester.^[11]

6.5.2 Computational Details

All ab initio calculations were carried out using the program package Gaussian 09 (Rev. A.03)^[15] and visualized by GaussView 5.08^[17]. The initial geometries of the structures were taken from the corresponding, experimentally determined crystal structures. Structure optimizations and frequency analyses were performed with Becke's B3 three parameter hybrid functional using the LYP correlation functional (B3LYP). For C, H, N and O a correlation consistent polarized double- ξ basis set was used (cc-pVDZ). The structures were optimized with symmetry constraints and the energy is corrected with the zero point vibrational energy.^[18] The enthalpies (*H*) and free energies (*G*) were calculated using the complete basis set (CBS) method in order to obtain accurate values. The CBS models use the known asymptotic convergence of pair natural orbital expressions to extrapolate from calculations using a finite basis set to the estimated complete basis set limit. CBS-4 starts with a HF/3-21G(d) geometry optimization, which is the initial guess for the following SCF calculation as a base energy and a final MP2/6-31+G calculation with a CBS extrapolation to correct the energy in second order. The used CBS-4M method additionally implements a MP4(SDQ)/6-31+(d,p) calculation to approximate higher order contributions and

also includes some additional empirical corrections.^[19] The enthalpies of the gas-phase species were estimated according to the atomization energy method.^[20] The liquid (solid) state energies of formation (ΔH_f°) were estimated by subtracting the gas-phase enthalpies with the corresponding enthalpy of vaporization (sublimation) obtained by Trouton's rule.^[21] All calculations affecting the detonation parameters were carried out using the program package EXPLO5 V6.02 (EOS BKWG-S).^[16, 22] The detonation parameters were calculated at the Chapman–Jouguet (CJ) point with the aid of the steady-state detonation model using a modified Becker-Kistiakowski-Wilson equation of state for modeling the system. The CJ point is found from the Hugoniot curve of the system by its first derivative. The specific impulses I_{sp} were also calculated with the program package EXPLO5 V6.02 program, assuming an isobaric combustion of a composition of an oxidizer, aluminum as fuel, 6% polybutadiene acrylic acid, 6% polybutadiene acrylonitrile as binder and 2% bisphenol A as epoxy curing agent.^[16] A chamber pressure of 70.0 bar, an initial temperature of 3300 K and an ambient pressure of 1.0 bar with equilibrium expansion conditions were estimated for the calculations.

6.5.3 X-ray Crystallography

The low-temperature single-crystal X-ray diffraction of were performed on an Oxford XCalibur3 diffractometer equipped with a Spellman generator (voltage 50 kV, current 40 mA) and a KappaCCD detector operating with MoK α radiation ($\lambda = 0.7107 \text{ \AA}$). Data collection was performed using the CRYALIS CCD software.^[23] The data reduction was carried out using the CRYALIS RED software.^[24] The solution of the structure was performed by direct methods (SIR97)^[25] and refined by full-matrix least-squares on F2 (SHELXL)^[26] implemented in the WINGX software package^[27] and finally checked with the PLATON software^[28]. The absorptions were corrected by a SCALE3 ABSPACK multi-scan method.^[29] All non-hydrogen atoms were refined anisotropically. The hydrogen atom positions were located in a difference Fourier map. ORTEP plots are shown with thermal ellipsoids at the 50% probability level. Additional crystallographic data and structure refinement parameters are listed in the Appendix A.6. Crystallographic data for the structures reported in this paper have been deposited at the Cambridge Crystallographic Data Centre (1438955 (**1**), 1438956 (**3**)) and can be obtained free of charge from the Cambridge Crystallographic Data Centre via www.ccdc.cam.ac.uk/data_request/cif.

6.5.4 Synthesis

Safety Announcement: CAUTION! Energetic materials are sensitive toward heat, impact and friction. No hazards occurred during preparation and manipulation; additional proper protective precautions (face shield, leather coat, earthened equipment and shoes, Kevlar gloves, and ear plugs) should be used when undertaking work with these compounds.

1,3-Bis(1,1,1-trinitropropan-2-yl)urea (1): A solution of trinitromethane (0.75 g, 5.0 mmol) in water (5 mL) was added to a stirred aqueous solution of acetaldehyde (0.66 g, 15.0 mmol, 5 mL water) for 10 minutes at room temperature. Another solution of urea (0.12 g, 2.0 mmol, 5 mL water) was added with stirring for one hour. The reaction is cooled in an ice-water bath, the precipitated product was filtered off and washed with ice cold water. The solid was dried to obtain (0.71 g, 6.1 mmol, 85%) colorless pure 1,3-bis(1,1,1-trinitropropan-2-yl)urea (1).

DSC (5 °C min⁻¹, onset): 142 °C (melt.), 144 °C (dec.). IR (ATR, cm⁻¹): ν = 3314 (m), 2970 (w), 1648 (s), 1613 (m), 1592 (vs), 1542 (vs), 1458 (w), 1391 (w), 1295 (s), 1236 (w), 1150 (m), 1030 (w), 934 (w), 852 (m), 798 (vs), 667 (w). Raman (1064 nm, 800 mW, cm⁻¹): ν = 3011 (9), 2957 (50), 2890 (7), 1647 (7), 1616 (23), 1601 (4), 1457 (14), 1371 (16), 1323 (6), 1298 (33), 1136 (22), 1080 (14), 1030 (8), 952 (6), 933 (4), 854 (100), 802 (8), 457 (7), 430 (13), 385 (4), 371 (59), 343 (19), 225 (6). ¹H NMR (CDCl₃): δ = 6.62 (d, NH, ³J_{HH} = 10.2 Hz, 2H), 5.61 (m, CH, 2H), 1.53 (d, CH₃, ³J_{HH} = 6.6 Hz, 6H) ppm. ¹³C{¹H} NMR (CDCl₃): δ = 154.5 (CO), 129.3 (C(NO₂)₃), 50.2 (CH), 18.2 (CH₃) ppm. ¹⁴N HMR (CDCl₃) δ = -32 (C(NO₂)₃), -295 (NH) ppm. Elemental analysis, calcd (%): C₇H₁₀N₈O₁₃ (414.20): C 20.30, H 2.43, N 27.05; found: C 20.48, H 2.53, N 26.75. MS (DEI+) *m/e*: 415.3 (40) [M+H⁺], 264.2 (2) [(M-C(NO₂)₃)⁺]. BAM drophammer: 8 J. Friction tester: >360 N. Electrostatic discharge device 0.20 J (grain size <100 μ m).

1,1,1-Trinitropropan-2-ol (2):*Method A: Synthesis from trinitromethane and vinyl acetate*see Lit. ^[10]*Method B: Synthesis from trinitromethane and acetaldehyde*

A solution of trinitromethane (1.50 g, 10.0 mmol) in water (5 mL) was added to a stirred aqueous solution of acetaldehyde (0.88 g, 20.0 mmol, 10 mL water) at room temperature. The mixture was stirred for 30 minutes causing an oily liquid to separate at the bottom of the flask. The resulting mixture is extracted with chloroform (3×20 mL). The combined organic layers were dried over anhydrous magnesium sulfate and concentrated carefully under reduced pressure. For both methods a slight yellow oil was obtained (1.51 g, 7.7 mmol, 77%) containing small amounts (approx. 2%) of trinitromethane as impurity.

IR (ATR, cm^{-1}): $\nu = 3572$ (w), 3025 (w), 2885 (w), 1711 (w), 1579 (s), 1460 (w), 1389 (w), 1370 (w), 1295 (s), 1127 (m), 1077 (m), 1019 (w), 997 (w), 943 (w), 906 (w), 851 (m), 837 (w), 796 (s), 773 (m), 663 (w). ^1H NMR (CDCl_3): $\delta = 5.18$ (m, 1H, CH), 3.27 (d, 1H, OH, $^3J_{\text{HH}} = 7.2$ Hz), 1.67 (d, 3H, CH_3 , $^3J_{\text{HH}} = 6.8$ Hz) ppm. $^{13}\text{C}\{^1\text{H}\}$ NMR (CDCl_3): $\delta = 128.6$ ($\text{C}(\text{NO}_2)_3$), 70.1 (H), 17.9 (CH_3) ppm. ^{14}N NMR (CDCl_3): $\delta = -38$ ($\text{C}(\text{NO}_2)_3$) ppm.

1,1,1-Trinitropropan-2-yl carbamate (3): Chlorosulfonyl isocyanate (CSI) (1.42 g, 10.0 mmol) was added to **2** (1.51 g, 7.7 mmol) in 20 mL chloroform very slowly at 0 °C. The ice bath was removed, and stirring at room temperature was continued for 1.5 h. The organic solvent was removed under reduced pressure. The residue was again cooled in an ice bath, and ice–water (10 mL) was added. The mixture was stirred for 20 min at room temperature. The reaction was cooled again, the precipitate was filtered off and washed with cold water. The solid was dried to obtain (1.45 g, 6.1 mmol, 79%) colorless pure 1,1,1-trinitropropan-2-yl carbamate (**3**).

DSC (5 °C min^{-1} , onset): 81 °C (mp.), 154 °C (dec.). IR (ATR, cm^{-1}): $\nu = 3457$ (m), 3349 (w), 3298 (w), 2975 (w), 1731 (s), 1594 (s), 1568 (s), 1456 (w), 1390 (m), 1359 (s), 1289 (s), 1158 (m), 1100 (s), 1037 (s), 1021 (s), 954 (m), 861 (m), 853 (s), 805 (s), 794 (s), 769 (s), 685 (w). Raman (1064 nm, 800 mW, cm^{-1}): $\nu = 3018$ (18), 2977 (5), 2960 (59), 1733 (12), 1618 (32), 1583 (4), 1456 (12), 1393 (3), 1363 (35), 1297 (22), 1133 (16), 1041 (2), 1025 (17), 945 (9), 855 (100), 809 (7), 798 (2), 686 (8), 560 (5), 475 (16), 433 (26), 385 (56), 365 (14), 339 (20), 302 (18), 223 (10). ^1H NMR (CDCl_3): $\delta = 6.21$ (q, CH, $^3J_{\text{HH}} = 6.3$ Hz, 1H), 5.10 (s, NH 2, 2H), 1.68 (d, CH_3 , $^3J_{\text{HH}} = 6.3$ Hz, 3H) ppm. $^{13}\text{C}\{^1\text{H}\}$ NMR (CDCl_3): $\delta = 153.2$ (CO), 126.5 ($\text{C}(\text{NO}_2)_3$), 69.3 (CH), 16.7 (CH_3) ppm.

^{15}N HMR (CDCl_3) $\delta = -34.2$ (d, $^3J_{\text{NH}} = 1.9$ Hz, $\text{C}(\text{NO}_2)_3$), -310.2 (t, $^3J_{\text{NH}} = 92.1$ Hz, NH_2) ppm. Elemental analysis, calcd (%): $\text{C}_4\text{H}_6\text{N}_4\text{O}_8$ (238.10): C 20.18, H 2.54, N 23.53; found: C 20.25, H 2.50, N 23.30. MS (DEI+) m/e : 239.1 (16) $[\text{M}+\text{H}^+]$, 223.1 (8) $[(\text{M}-\text{NH}_2)^+]$, 178.1 (5) $[(\text{M}-\text{CHCH}_3\text{C}(\text{NO}_2)_3)^+]$. BAM drophammer: >40 J. Friction tester: >360 N. Electrostatic discharge device 0.15 J (grain size < 100 μm).

1,1,1-Trinitropropan-2-yl nitrocarbamate (4): Fuming nitric acid ($>99.5\%$, 2 mL) was dropped into concentrated sulfuric acid (2 mL) at 0 $^\circ\text{C}$. Into this nitration mixture chilled in an ice-bath, the carbamate **3** (0.48 g, 2.0 mmol) was added in small portions. The mixture was stirred for further 60 min at this temperature, again cooled and poured into ice-water (100 mL). The reaction mixture was extracted with ethyl acetate (3×30 mL). The combined organic phases were washed with 30 mL water and brine ($2-3\times 30$ mL) acid free and dried with magnesium sulfate. The solvent was removed under reduced pressure to obtain a pale heavy liquid (0.51 g, 1.8 mmol, 92%) of 1,1,1-trinitropropan-2-yl nitrocarbamate (**4**).

DSC (5 $^\circ\text{C min}^{-1}$, onset): 133 $^\circ\text{C}$ (dec.). IR (ATR, cm^{-1}): $\nu = 2975$ (w), 2886 (w), 1680 (s), 1587 (s), 1451 (w), 1390 (w), 1323 (w), 1291 (m), 1270 (s), 1126 (w), 1086 (m), 1026 (w), 1086 (m), 1026 (w), 984 (w), 914 (w), 854 (w), 795 (s), 733 (w), 661 (w). Raman (1064 nm, 800 mW, cm^{-1}): $\nu = 3013$ (6), 2959 (53), 2884 (4), 1691 (8), 1617 (18), 1453 (9), 1365 (6), 1326 (11), 1296 (22), 1278 (6), 1133 (7), 1089 (6), 1029 (8), 979 (3), 947 (5), 856 (100), 806 (8), 647 (7), 582 (7), 540 (3). ^1H NMR (CDCl_3): $\delta = 10.81$ (s, 1H, NH), 6.32 (q, 1H, CH, $^3J_{\text{HH}} = 6.6$ Hz), 1.81 (d, 3H, CH_3 , $^3J_{\text{HH}} = 6.6$ Hz) ppm. $^{13}\text{C}\{^1\text{H}\}$ NMR (CDCl_3): $\delta = 145.2$ (O_2NNHCO), 125.0 ($\text{C}(\text{NO}_2)_3$), 70.9 (CCH_3), 16.6 (CH_3) ppm. ^{14}N NMR (CDCl_3): $\delta = -36$ ($\text{C}(\text{NO}_2)_3$), -54 (NHNO_2), -199 (br, NHNO_2) ppm. Elemental analysis, calcd (%): $\text{C}_4\text{H}_5\text{N}_5\text{O}_{10}$ (283.11): C 16.97, H 1.78, N 24.74; found: C 17.16, H 1.88, N 24.29. MS (DEI+) m/e : 284.1 (1) $[\text{M}+\text{H}^+]$, 133.0 (25) $[(\text{M}-\text{C}(\text{NO}_2)_3)^+]$. BAM drophammer: 15 J. Friction tester: >360 N. (liquid).

6.6 References

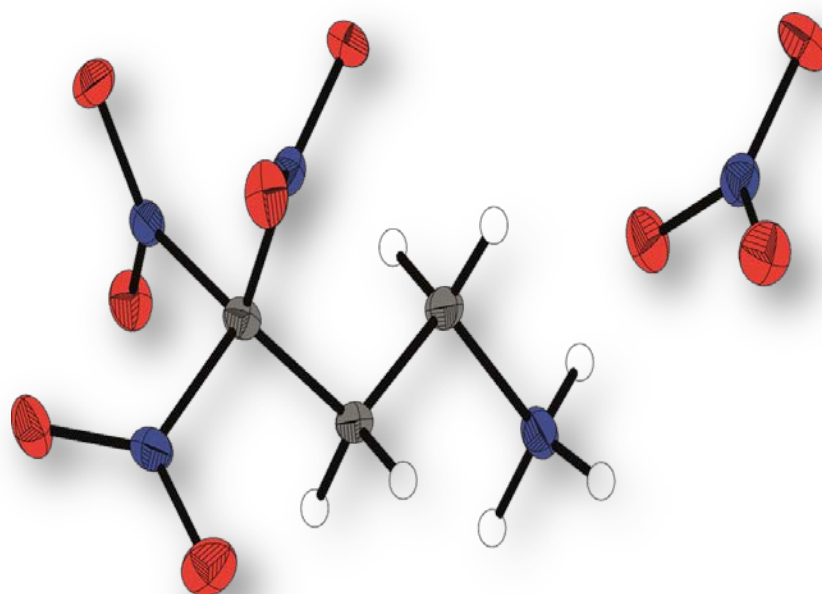
- [1] T. M. Klapötke, *Chemistry of High-Energy Materials*, 2nd ed., deGruyter, Berlin, **2012**.
- [2] J. Akhavan, *The Chemistry of Explosives*, 2nd ed., Royal Soc. of Chemistry, Cambridge, **2004**.
- [3] E. D. McLanahan, J. L. Campbell, D. C. Ferguson, B. Harmon, J. M. Hedge, K. M. Crofton, D. R. Mattie, L. Braverman, D. A. Keys, M. Mumtaz, J. W. Fisher, *Toxicol. Sci.* **2007**, *97*, 308–317.
- [4] a) C. Hogue, *Chem. Eng. News* **2011**, *89*, 6; b) E. D. McLanahan, M. E. Andersen, J. L. Campbell, J. W. Fisher, *Environ. Health Perspect.* **2009**, *117*, 731–738.
- [5] A. M. Mebel, M. C. Lin, K. Morokuma, C. F. Melius, *J. Phys. Chem.* **1995**, *99*, 6842–6848.
- [6] a) Q. J. Axthammer, B. Krumm, T. M. Klapötke, *J. Org. Chem.* **2015**, *80*, 6329–6335; b) Q. J. Axthammer, T. M. Klapötke, B. Krumm, R. Moll, S. F. Rest, *Z. Anorg. Allg. Chem.* **2014**, *640*, 76–83; c) T. M. Klapötke, B. Krumm, S. F. Rest, M. Sućeska, *Z. Anorg. Allg. Chem.* **2014**, *640*, 84–92.
- [7] Q. J. Axthammer, B. Krumm, T. M. Klapötke, R. Scharf, *Chem. – Eur. J.* **2015**, *21*, 16229–16239.
- [8] a) P. O. Tawney **1962**, US 3050565; b) P. O. Tawney, I. J. Schaffner **1962**, US 3027403; c) P. F. Hartman **1963**, US 3084201; d) P. F. Hartman **1962**, US 3028425.
- [9] a) H. Shechter, H. L. Cates, *J. Org. Chem.* **1961**, *26*, 51–53; b) S. S. Novikov, V. I. Slovetkii, S. A. Shevelev, A. A. Fainzil'berg, *Bull. Acad. Sci. USSR, Div. Chem. Sci. (Engl. Transl.)* **1962**, *11*, 552–559.
- [10] Y. A. Volkova, O. A. Ivanova, E. M. Budynina, E. B. Averina, T. S. Kuznetsova, N. S. Zefirov, *Tetrahedron* **2008**, *64*, 3548–3553.
- [11] M. Göbel, T. M. Klapötke, *Adv. Funct. Mater.* **2009**, *19*, 347–365.
- [12] Y. Oyumi, T. B. Brill, A. L. Rheingold, *J. Phys. Chem.* **1985**, *89*, 4824–4828.
- [13] *Commission communication in the framework of the implementation of the Council Directive 93/15/EEC of 5 April 1993 on the harmonisation of the provisions relating to the placing on the market and supervision of explosives for civil uses, Vol. 221, 2006.*
- [14] R. Meyer, J. Köhler, A. Homburg, *Explosives*, Wiley-VCH, Weinheim, **2007**.
- [15] M. J. Frisch, G. W. Trucks, H. B. Schlegel, G. E. Scuseria, M. A. Robb, J. R. Cheeseman, V. B. G. Scalmani, B. Mennucci, G. A. Petersson, H. Nakatsuji, M. Caricato, X. Li, H. P. Hratchian, A. F. Izmaylov, J. Bloino, G. Zheng, J. L. Sonnenberg, M. Hada, M. Ehara, K. Toyota, R. Fukuda, J. Hasegawa, M. Ishida, T. Nakajima, Y. Honda, O. Kitao, H. Nakai, T. Vreven, J. J. A. Montgomery, J. E. Peralta, F. Ogliaro, M. Bearpark, J. J. Heyd, E. Brothers, K. N. Kudin, V. N. Staroverov, R. Kobayashi, J. Normand, K. Raghavachari, A. Rendell, J. C. Burant, S. S. Iyengar, J. Tomasi, M. Cossi, N. Rega, J. M. Millam, M. Klene, J. E. Knox, J. B. Cross, V. Bakken, C. Adamo, J. Jaramillo, R. Gomperts, R. E. Stratmann, O. Yazyev, A. J. Austin, R. Cammi, C. Pomelli, J. W. Ochterski, R. L. Martin, K.

- Morokuma, V. G. Zakrzewski, G. A. Voth, P. Salvador, J. J. Dannenberg, S. Dapprich, A. D. Daniels, Ö. Farkas, J. B. Foresman, J. V. Ortiz, J. Cioslowski, D. J. Fox, *Gaussian 09*, Rev. A.02 ed., Gaussian, Inc., Wallingford CT, **2009**.
- [16] M. Sućeska, *EXPLO5 V.6.02*, Zagreb, **2013**.
- [17] R. D. Dennington, T. A. Keith, J. M. Millam, *GaussView*, Ver. 5.08 ed., Semichem, Inc., Wallingford CT, **2009**.
- [18] J. A. Montgomery, M. J. Frisch, J. W. Ochterski, G. A. Petersson, *J. Chem. Phys.* **2000**, *112*, 6532–6542.
- [19] J. W. Ochterski, G. A. Petersson, J. A. Montgomery, *J. Chem. Phys.* **1996**, *104*, 2598–2619.
- [20] E. F. C. Byrd, B. M. Rice, *J. Phys. Chem.* **2005**, *110*, 1005–1013.
- [21] a) F. Trouton, *Philos. Mag.* **1884**, *18*, 54–57; b) M. S. Westwell, M. S. Searle, D. J. Wales, D. H. Williams, *J. Am. Chem. Soc.* **1995**, *117*, 5013–5015.
- [22] M. Sućeska, *Propellants, Explos., Pyrotech.* **1991**, *16*, 197–202.
- [23] Oxford Diffraction Ltd., *CrysAlis CCD*, Version 1.171.35. (release 16-05-2011 CrysAlis 171.Net), Abingdon, Oxford, **2011**.
- [24] Oxford Diffraction Ltd., *CrysAlis RED*, Version 1.171.35.11 (release 16-05-2011 CrysAlis 171.NET), Abingdon, Oxford, **2011**.
- [25] A. Altomare, M. C. Burla, M. Camalli, G. L. Cascarano, C. Giacovazzo, A. Guagliardi, A. G. G. Moliterni, G. Polidori, R. Spagna, *J. Appl. Crystallogr.* **1999**, *32*, 115–119.
- [26] a) G. M. Sheldrick, *SHELX-97, Programs for Crystal Structure Determination*, **1997**; b) G. M. Sheldrick, *Acta Crystallogr., Sect. A: Found. Crystallogr.* **2008**, *A64*, 112–122.
- [27] L. Farrugia, *J. Appl. Crystallogr.* **1999**, *32*, 837–838.
- [28] A. Spek, *Acta Crystallogr., Sect. D: Biol. Crystallogr.* **2009**, *65*, 148–155.
- [29] Oxford Diffraction Ltd., *SCALE3 ABSPACK - An Oxford Diffraction program 1.04*, Abingdon, Oxford, **2005**.

7 Michael Addition of Nitroform

unpublished results

MICHAEL ADDITION OF NITROFORM AS A SOURCE OF ENERGETIC MATERIALS, SYNTHESIS AND CHARACTERIZATION



7.1 Abstract

The nucleophilic Michael addition of nitroform to unsaturated carbonyl compounds creates a wide variety of energetic products. Several energetic compounds with a trinitromethyl group were synthesized. Owing to their positive oxygen balance, the suitability of these compounds as potential high energetic dense oxidizers (HEDO) in energetic formulations was investigated and discussed. Furthermore a number of important and reactive intermediates for the continuing synthesis of molecules with a high oxygen balance are presented. All compounds were fully characterized, including multinuclear NMR spectroscopy, vibrational analysis (IR, Raman), elemental analysis as well as single crystal X-ray diffraction. Thermal stabilities were studied using differential scanning calorimetry and sensitivity data against friction, impact and electronic discharge were collected. The energies of formation were calculated using Gaussian 09 and energetic properties, like the specific impulse and detonation velocity, were calculated with the EXPLO5 (V6.02) computer code.

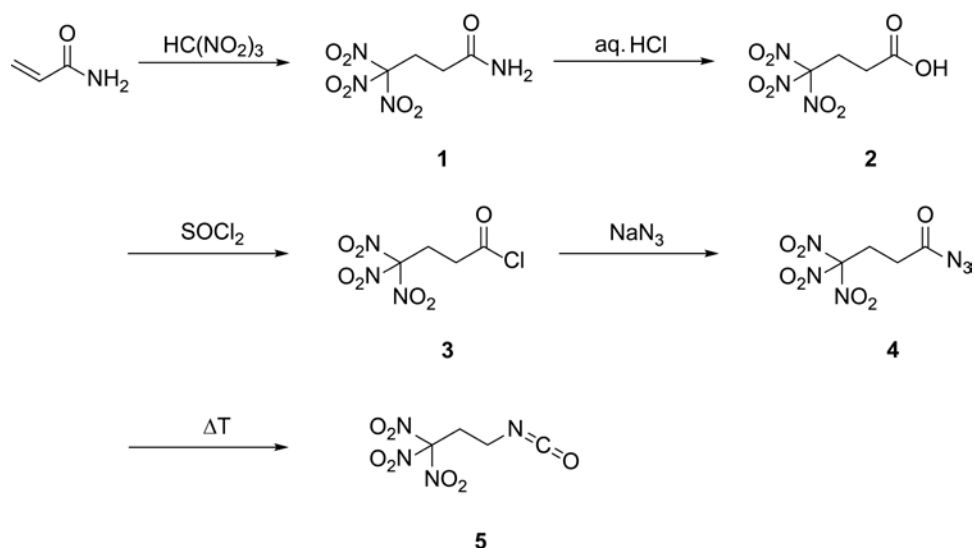
7.2 Introduction

The 1,1,1-trinitromethane unit is an important building block in the chemistry of high energetic explosives, especially in the area of high energy dense oxidizer (HEDO).^[1] This 1,1,1-trinitromethane unit can easily be introduced by a nucleophilic Michael addition on electron deficient α,β -unsaturated starting materials. The so called Michael reaction is one of the most important carbon-carbon bond forming reactions in synthetic organic chemistry. Michael donors are substrates with acidic protons which therefore are capable of forming carbanions, like polynitroaliphatic compounds. This includes anions from trinitromethane (nitroform), fluorodinitromethane, primary nitroalkanes, and secondary nitroalkanes.^[2] The electron deficient alkene in this nucleophilic addition is called the Michael acceptor and includes a wide range of α,β -unsaturated ketones, aldehydes, carboxylic acids, esters, amides and cyanides.^[3]

7.3 Results and Discussion

7.3.1 Synthesis

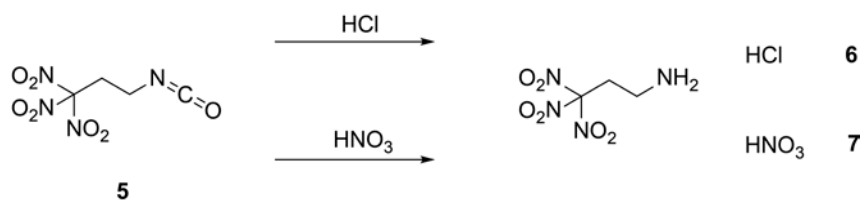
The first step was the synthesis of 4,4,4-trinitrobutanamide (**1**). The latter compound has been reported in literature.^[4] It was synthesized by a Michael reaction of nitroform and acrylamide. The here presented advanced synthesis of **1** was performed by a simple addition of acrylamide to a commercially available aqueous solution of trinitromethane (30%), without the use of further chemicals as mentioned in literature procedures.^[4a, 5] Moreover the reaction time was strongly shortened without the use of heating, and the yield was increased from 63% to 97%. Due to the almost full conversion of acrylamide pure **1** without recrystallization was obtained.



Scheme 7-1: Synthesis of energetic compounds and intermediates starting from nitroform and acrylamide.

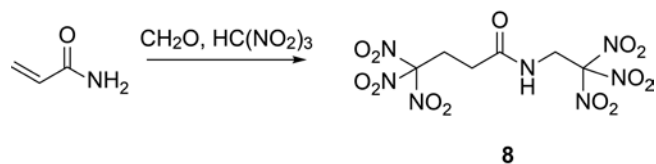
The acid 4,4,4-trinitrobutanoic acid (**2**) was prepared by hydrolysis of the amide **1** in aqueous concentrated hydrochloric acid. The crude material was recrystallized from chloroform to obtain a pure product in 80% yield. The high yields and the straightforward synthesis make **1** and **2** to excellent starting materials for various compounds with the trinitromethyl moiety. The acid **2** was converted to the corresponding acid chloride by refluxing with an excess of thionyl chloride. The reaction time should be longer than 20 hours to ensure complete conversion to the acid chloride and no formation of the acid anhydride.^[6] The 4,4,4-trinitrobutanoyl chloride (**3**) was isolated in 88% yield and could also be used as a starting material for various types of compounds. One of these compounds is the organic azide 4,4,4-trinitrobutanoyl azide (**4**), which was synthesized by the reaction with sodium azide at ambient temperature.^[6] The pure azide **4** could only be obtained,

if the reaction mixture is kept below 30 °C during the whole synthesis and workup procedure. The azide **4** is colorless compound with a melting point of 22 °C and extremely high sensitivity.



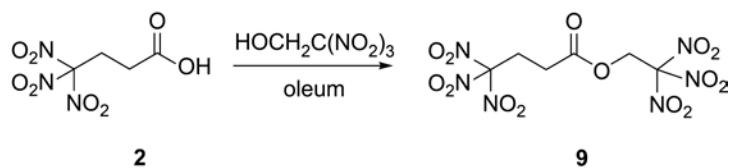
Scheme 7-2: Synthesis of the chloride (**6**) and nitrate (**7**) salt of 3,3,3-trinitropropan-1-amine.

Heating the azide **4** in an organic inert solvent the compound 1,1,1-trinitropropan-3-isocyanate (**5**) was obtained via a Curtius rearrangement. A much safer way for the synthesis of **5** is the subsequent in situ conversion of **4** to the isocyanate **5** without isolation of the very sensitive azide **4** in the pure state. Compound **5** could be used for the synthesis of several energetic carbamates, ureas and amines.^[6-7] The salts of 3,3,3-trinitropropan-1-amine were obtained by controlled hydrolysis of **5**. In the diluted aqueous mineral acids the hydrochloric **6** and the nitrate salt **7** were prepared (Scheme 7-2).^[8]



Scheme 7-3: Synthesis of 4,4,4-trinitro-*N*-(2,2,2-trinitroethyl)-butanamide (**8**).

The nitrate salt 3,3,3-trinitropropan-1-amine nitrate (**7**) is air and moisture stable and has a good positive oxygen balance Ω_{CO} of +15.6%. Another compound, which was synthesized by a Michael reaction is 4,4,4-trinitro-*N*-(2,2,2-trinitroethyl)-butanamide (**8**).^[9] Compound **8** was prepared by a simple one pot reaction which includes a Michael reaction and a Mannich condensation of one mole acrylamide and formaldehyde and two moles of nitroform.



Scheme 7-4: Synthesis of 2,2,2-trinitroethyl-4,4,4-trinitrobutanoate (**9**).

An oxygen rich molecule was also prepared by the esterification of the acid **2** with the also oxygen rich alcohol 2,2,2-trinitroethanol. The reaction was performed in oleum as strong dehydrating agent.^[10] After recrystallization from water/methanol the ester 2,2,2-trinitroethyl-4,4,4-trinitrobutanoate (**9**) was obtained as a pure colorless solid.

7.3.2 NMR Spectroscopy

All compounds were thoroughly characterized by ¹H, ¹³C and ¹⁴N NMR spectroscopy. In the ¹H NMR spectra the two neighboring CH₂ groups are within the range of 3.90 to 2.52 ppm. The methylene unit next to the trinitromethyl moiety is often shifted to higher field compared to the CH₂ groups next to nitrogen or oxygen. The vicinal coupling constants of the hydrogen atoms in the ethylene group are not equal due to the rotation around the C–C bond, which is causing a AA'XX' spin systems.^[11] The CH₂ moiety of the trinitroethyl group is at lower field at 4.96 ppm (**8**) and 5.20 ppm (**9**) compared to the trinitropropyl group. In the ¹³C NMR spectra the carbon resonances of the two CH₂ groups of the trinitropropyl part are very variable and are found in the range of 40.5 to 27.6 ppm. The carbon resonance of the trinitromethyl moiety is observed as a broadened signal; in the case of trinitropropyl always located at around 128 ppm. By comparing this with that of the trinitroethyl unit in **8** and **9**, a small upfield shift to approximately 126 ppm is obvious. In the ¹⁴N NMR spectra the resonances for the nitro groups of the trinitromethyl moieties are all quite sharp and found in the range of –28 to –31 ppm.

7.3.3 Vibrational Spectroscopy

All compounds were also characterized by their molecular vibration frequencies by IR and Raman spectroscopy. The most characteristic frequencies in the compounds are the carbonyl and nitro groups. For the trinitromethyl units both the asymmetric $\nu_{as}(\text{NO}_2)$ in the range of 1604–1582 cm⁻¹ and the symmetric stretching vibrations $\nu_s(\text{NO}_2)$ at 1303–1288 cm⁻¹ are observed. The characteristic $\nu(\text{C}=\text{O})$ stretching vibration is located in a large range from 1785 to 1676 cm⁻¹. It is observed that the carbonyl stretching bands are shifted to higher wave numbers in molecules when they are connected to electron-withdrawing moieties. The maxima is the acid chloride **3** where the $\nu(\text{C}=\text{O})$ is located at 1785 cm⁻¹, while the two amides **1** and **8** are observed at 1695 and 1676 cm⁻¹.

7.3.4 Single Crystal Structure Analysis

Single crystals suitable for X-ray diffraction measurements were obtained by crystallization at ambient temperature from water (**1**, **2**, **6**, **7**), from neat material (**4**) or from chloroform (**9**). A full list of the crystallographic refinement parameters and structure data are found in the Appendix A.7.

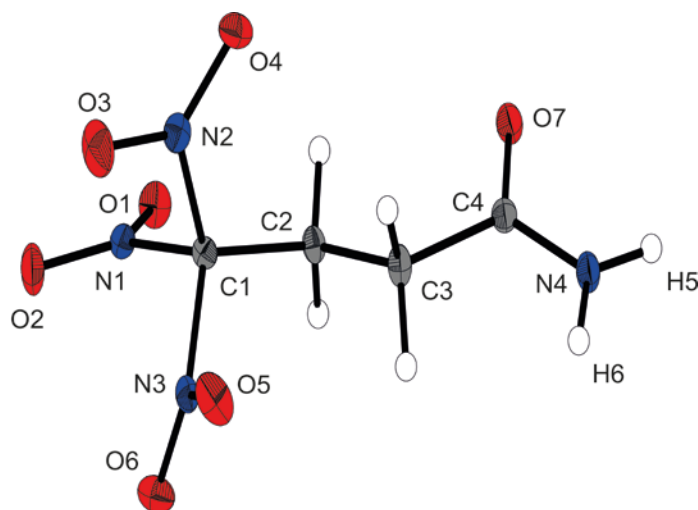


Figure 7-1: X-ray molecular structure of 4,4,4-trinitrobutanamide (1).

Selected atom distances (Å) and angles (deg): C1–C2 1.502(2), C1–N1 1.540(2), C1–N2 1.538(2), C1–N3 1.521(1), C2–C3 1.524(2), C3–C4 1.522(2), C4–N4 1.332(2), C4–O7 1.237(1), N1–O1 1.211(1), N4–H5 0.89(2), N4–H6 0.87(1), C2–C1–N2 114.15(9), C2–C1–N1 112.09(9), C2–C1–N3 110.49(9), H6–N4–C4–C3 $-178(1)$, H5–N4–C4–O7 $-177(1)$, N4–C4–C3–C2 $-157.3(1)$, C3–C2–C1–N1 $-175.87(9)$.

The amide **1** crystallizes in the triclinic space group $P\bar{1}$ with one molecule as asymmetric unit. The density is 1.835 g cm^{-3} and the molecular structure is shown in Figure 7-1. The geometry of the structure has some very typical characteristics of trinitromethyl compounds.^[7b, 12] The C–N bond lengths in the trinitromethyl moiety are in the range of 1.54 Å , which is significantly longer than a regular C–N bond (1.47 Å) and results from steric repulsion of the proportionally large nitro groups.^[1b] As expected, the amide unit is nearly planar and shows typical bond geometry, like a short C–N bond.

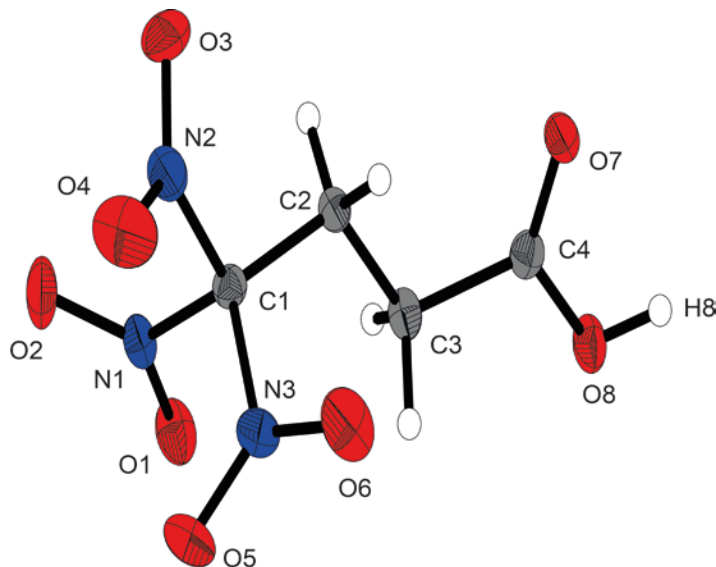


Figure 7-2: X-ray molecular structure of 4,4,4-trinitrobutanoic acid (2).

Selected atom distances (Å) and angles (deg.): C1–N1 1.523(2), C2–C3 1.528(2), C3–C4 1.509(2), C3–H3 0.99(2), C4–O7 1.218(2), C4–O8 1.311(2), N1–O1 1.216(1), O8–H5 0.86(2), C2–C1–N1 115.2(1), H5–O8–C4–C3 $-175(1)$, O8–C4–C3–C2 179.0(1), C4–C3–C2–C1 $-158.4(1)$, C3–C2–C1–N2 178.3(1), N2–O2 2.557(2), O5–N1 2.571(1), N3–O4 2.550(2).

The acid **2** crystallizes in the monoclinic space group $P2_1/n$ with a quite low density of 1.720 g cm^{-3} and is shown in Figure 7-2. Here, another characteristic structure feature, the propeller like arrangement of the trinitromethyl group could be observed. The three nitro groups are organized around the carbon in a propeller-like geometry to optimize the non-bonded $\text{N}\cdots\text{O}$ intramolecular attractions ($\text{N2}\cdots\text{O2}$, $\text{O5}\cdots\text{N1}$, $\text{N3}\cdots\text{O4}$). This results in an intramolecular interaction between the partial positive charged nitrogen and the negative charged oxygen in the nitro group. These $\text{N}\cdots\text{O}$ attractions are found with distances in the range of 2.55 \AA , which are much shorter than the sum of the van der Waals radii of nitrogen and oxygen (3.07 \AA).^[1b, 13]

The carbonyl azide **4** crystallizes in the triclinic space group $P-1$ with one molecule as an asymmetric unit and shows the propeller like geometry of the trinitromethyl group. The molecular structure is shown in Figure 7-3. The azide, the carbonyl and the carbon backbone inclusively, shows a nearly planar arrangement which is shown by the torsion angle of N5–N4–C4–O7 $1.2(2)$. The azide group is bent, and the N–N–N angle exhibits a typical value of 174.2° . The N4–N5 and N5–N6 bond lengths ($1.273(3)$ and $1.121(3) \text{ \AA}$, respectively) are comparable with those in other carbonyl azides.

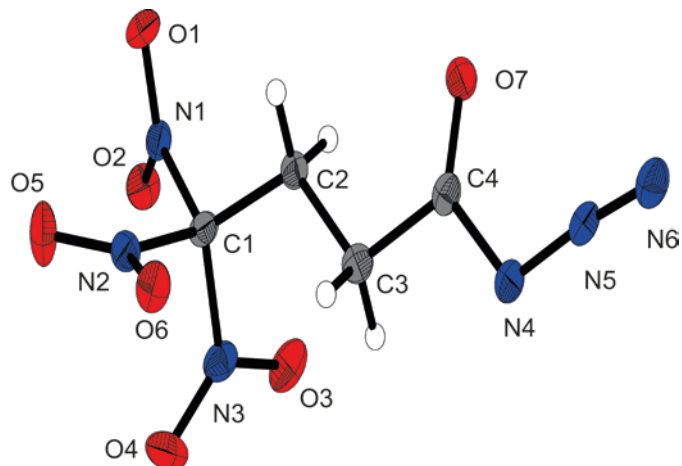


Figure 7-3: X-ray molecular structure of 4,4,4-trinitrobutanoyl azide (4).

Selected atom distances (Å) and angles (deg.): C1–C2 1.512(2), C1–N1 1.532(2), C2–C3 1.528(3), C3–C4 1.503(2), C4–N4 1.409(2), C4–O7 1.205(2), N4–N5 1.273(2), N5–N6 1.112(2), C2–C1–N3 114.4(1), C4–N4–N5 111.5(1), N4–N5–N6 174.2(2), N6–N5–N4–C4 –176(1), N5–N4–C4–O7 1.2(2), N4–C4–C3–C2 –175.0(1), C4–C3–C2–C1 178.0(1), O2–N2 2.573(2), N1–O5 2.577(2), O4–N3 2.541(1).

The salt **6** crystallizes as a monohydrate in the triclinic space group $P\bar{1}$ and a density of 1.733 g cm^{-3} . The asymmetric unit is shown in Figure 7-4. The conformations of the substituents at C1, C2, C3 and N4 are all almost perfectly staggered. The extended structure involves secondary interactions in terms of classical intermolecular N–H \cdots O hydrogen bonds and unusual so-called non-classical hydrogen bonds of the type C–H \cdots O. The majority are classified as quite strong.^[14]

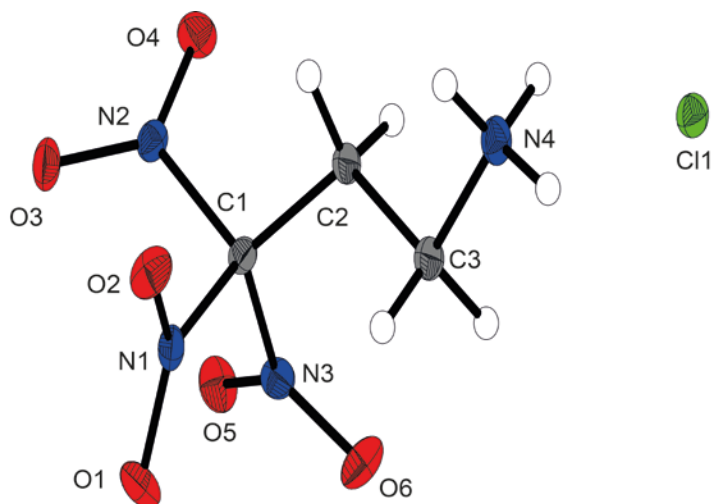


Figure 7-4: X-ray molecular structure of 3,3,3-trinitropropan-1-amine hydrochloride (6).

Selected atom distances (Å) and angles (deg.): C1–C2 1.507(2), C1–N1 1.522(2), C2–C3 1.533(2), C3–N4 1.491(2), N1–O1 1.217(1), N4–H6 0.89(2), N4–H7 0.88(2), N4–H8 0.88(2), C2–C1–N3 114.5(1), C3–N4–H7 111(1), C3–N4–H8 107(1), C3–N4–H6 109(1), H7–N4–C3–C2 –178(1), N4–C3–C2–C1 –160.1(1), O5–N2 2.582(2), O1–N3 2.555(2), N1–O3 2.545(2).

The nitrate salt **7** crystallizes in the orthorhombic space group $P2_12_12_1$ with a density of 1.804 g cm^{-3} . The asymmetric unit consists of one anion and cation and is illustrated in Figure 7-5. The protonated form of the 3,3,3-trinitropropan-1-amine shows the same structure characteristics as the hydrochloric salt **6**.

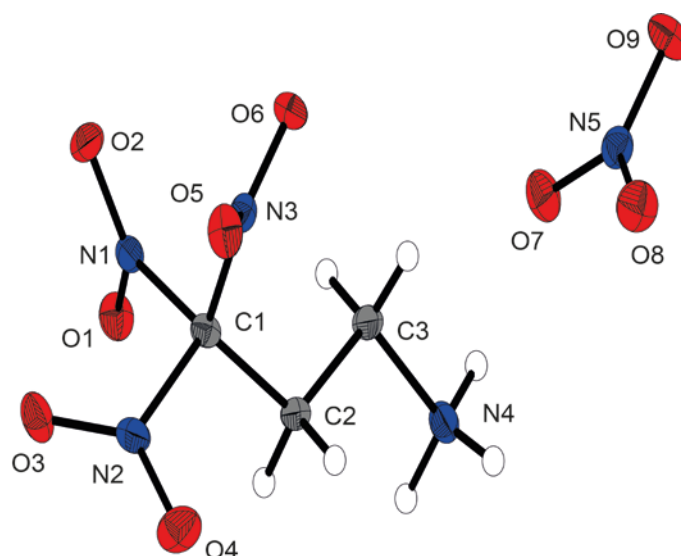


Figure 7-5: X-ray molecular structure of 3,3,3-trinitropropan-1-amine nitrate (7).

Selected atom distances (Å) and angles (deg.): C1–C2 1.512(2), C1–N1 1.529(2), C2–C3 1.526(2), C3–N4 1.492(2), N1–O1 1.223(2), N5–O7 1.269(2), N5–O8 1.233(2), N5–O9 1.266(2), N4–C3–C2–C1 $-173.7(1)$, C3–C2–C1–N2 $175.8(1)$, H6–N4–C3–C2 $170(1)$, O8–N5–O7–O9 $179.7(3)$, O5–N2 2.581(2), O2–N3 2.587(2), N1–O3 2.530(2).

The ester **9** crystallizes in the monoclinic space group $P2_1/n$ with four formula units per unit cell. The asymmetric unit consists of one molecule and is displayed in Figure 7-6. The average of the N–O and C–NO₂ bond lengths of the trinitromethyl units are all in the same range of 1.21 Å in N–O and 1.52 Å in C–NO₂ whereas no distinction between the ethyl and propyl moiety is visible. Also both trinitromethyl groups show independently the propeller-like orientation of the nitro groups. Also the carbon-carbon bonds are virtually identical within a range of 1.50 to 1.52 Å . The crystal density is 1.869 g cm^{-3} , which is the highest density of all here presented compounds. This is striking because of the impossibility of forming classical hydrogen bonds. However, non-classical hydrogen bonds of the type C–H \cdots O are found, whereat the majority is classified as quite strong.^[14]

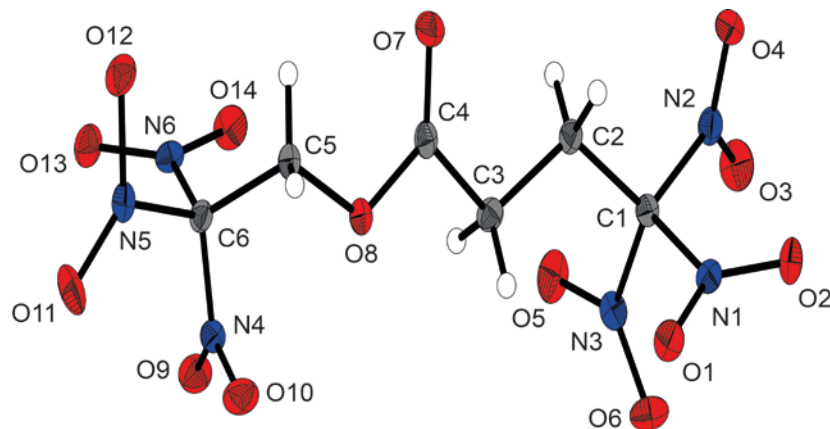


Figure 7-6: X-ray molecular structure of 2,2,2-trinitroethyl-4,4,4-trinitrobutanoate (9).

Selected atom distances (Å) and angles (deg.): C1–C2 1.515(2), C1–N1 1.528(2), C2–C3 1.514(2), C3–C4 1.497(2), C4–O7 1.200(2), C4–O8 1.363(2), C5–C6 1.520(2), C5–O8 1.424(2), C6–N4 1.525(2), N1–O1 1.222(1), N4–O9 1.213(2), N2–C1–C2–C3 161.5(1), C1–C2–C3–C4 169.4(1), C3–C4–O8–C5 –175.6(1), C4–O8–C5–C6 131.7(1), O8–C5–C6–N5 160.2(1), N3–O3 2.558(2), O6–N1 2.567(2), N2–O2 2.534(1), N4–O11 2.608(2), N5–O13 2.583(2), O9–N6 2.557(1).

7.3.5 Thermal Stabilities and Energetic Properties

Compounds **1**, **2**, **6**, **7**, **8** and **9** were stable when exposed to air and moisture. The azide **4** has to be handled very carefully, owing to its high sensitivity towards heat. Reactions of the isocyanate **5** must be carried out with exclusion of moisture. Furthermore it should be stored frozen and is not longtime stable, due to rapid polymerization. The thermal stabilities of all compounds were investigated by performing various DSC measurements with a heating rate of 5 °C min⁻¹. The temperatures at which melting and decomposition occurred are shown in Table 7-1 with other physical properties. A remarkably high decomposition point of 178 °C was observed for compound **6**, likely owing to its stability to form strong hydrogen bonds through the salt structure. Moreover, compounds **8** and **9** (both 155 °C) showed satisfying decomposition points for applications as high-energy dense oxidizers based on CHNO compounds. The sensitivities of compounds **2–10** towards impact, friction, and electrostatic discharge were experimentally determined; the results are displayed in Table 7-1. All compounds, with the exception of the azide **4** showed moderate impact and friction sensitivities (≥ 360 N insensitive, 360–80 N sensitive, 80–10 N very sensitive, ≤ 10 N extremely sensitive), and some are sensitive to impact (≥ 40 J insensitive, 40–35 J less sensitive, 35–4 J sensitive, ≤ 3 J very sensitive).^[1a, 15] The amide **1** shows a quite high sensitivity towards impact with a value of 6 J and is in the range of the well-known explosive Hexogen (RDX).

Table 7-1: Physical properties of the compounds 1, 2, 4, 6, 7, 8 and 9 in comparison to ammonium perchlorate (AP).

	1	2	4	6
formula	C ₄ H ₆ N ₄ O ₇	C ₄ H ₅ N ₃ O ₈	C ₄ H ₄ N ₆ O ₇	C ₃ H ₇ N ₄ O ₆ Cl
$\rho / \text{g cm}^{-3}$ (RT) [a]	1.78	1.67	1.71	1.76
$T_m / ^\circ\text{C}$ (onset) [b]	93	55	22	161
$T_{\text{dec}} / ^\circ\text{C}$ (onset) [c]	120	176	85	178
IS / J [d]	6	40	2	20
FS / N [e]	360	324	144	>360
ESD / J [f]	0.5	0.3	0.1	0.4
$N / \%$ [g]	25.2	18.8	33.9	24.3
$O / \%$ [h]	50.4	57.4	45.1	41.6
$N+O / \%$ [i]	75.6	76.2	79.0	65.9
$\Omega_{\text{CO}} / \%$ [j]	0.0	+10.1	+6.5	0.0
$\Omega_{\text{CO}_2} / \%$ [j]	-28.1	-17.9	-19.4	-2.4
$\Delta H_f^\circ / \text{kJ mol}^{-1}$ [k]	-326	-506	54	-96
$\Delta U_f^\circ / \text{kJ kg}^{-1}$ [l]	-1374	-2178	301	-318
	7	8	9	AP
formula	C ₃ H ₇ N ₅ O ₉	C ₆ H ₆ N ₆ O ₁₄	C ₆ H ₇ N ₇ O ₁₃	NH ₄ ClO ₄
$\rho / \text{g cm}^{-3}$ (RT) [a]	1.77	1.83	1.84	1.95
$T_m / ^\circ\text{C}$ (onset) [b]	135	92	150	-
$T_{\text{dec}} / ^\circ\text{C}$ (onset) [c]	138	155	155	240
IS / J [d]	6	30	10	15
FS / N [e]	120	240	240	>360
ESD / J [f]	0.2	0.1	0.2	>1.5
$N / \%$ [g]	27.2	21.8	25.5	11.9
$O / \%$ [h]	56.0	58.0	54.0	54.5
$N+O / \%$ [i]	83.2	79.8	79.5	66.4
$\Omega_{\text{CO}} / \%$ [j]	+15.6	+20.7	+14.5	+34.6
$\Omega_{\text{CO}_2} / \%$ [j]	-3.1	-4.1	-10.4	+34.6
$\Delta H_f^\circ / \text{kJ mol}^{-1}$ [k]	-169	-466	-330	-296
$\Delta U_f^\circ / \text{kJ kg}^{-1}$ [l]	-554	-1124	-770	-2433

[a] Densities at RT measured by gas pycnometer. [b] Onset melting T_m and [c] onset decomposition point T_{dec} from DSC measurement carried out at a heating rate of 5°C min^{-1} . [d] Impact sensitivity. [e] Friction sensitivity. [f] Sensitivity toward electrostatic discharge. [g] Nitrogen content. [h] Oxygen content. [i] Sum of nitrogen and oxygen content. [j] Oxygen balance assuming the formation of CO and the formation of [j] CO₂ at the combustion. [k] Enthalpy and [l] energy of formation calculated by the CBS-4M method using Gaussian 09.

Table 7-2: Calculated detonation and combustion parameters (using EXPLO5 V6.02) in comparison to ammonium perchlorate (AP).

	1	2	4	6
Q_v /kJ kg ⁻¹ [a]	-4956	-4786	-5607	-5281
T_{ex} /K [b]	3383	3505	4071	3793
V_0 /L kg ⁻¹ [c]	733	731	759	744
P_{CJ} /kbar [d]	292	246	291	282
V_{det} /m s ⁻¹ [e]	8187	7624	8259	8019
I_{sp} /s [f]	238	241	261	255
I_{sp} /s (5% Al) [g]	248	248	266	261
I_{sp} /s (10% Al) [g]	256	253	269	267
I_{sp} /s (15% Al) [g]	261	256	270	269
I_{sp} /s (20% Al) [g]	262	258	265	267
I_{sp} /s (25% Al) [g]	251	256	252	265
I_{sp} /s (5% Al, 14% binder) [h]	216	215	237	230
I_{sp} /s (10% Al, 14% binder) [h]	232	229	248	243
I_{sp} /s (15% Al, 14% binder) [h]	244	241	247	247
	7	8	9	AP
Q_v /kJ kg ⁻¹ [a]	-6697	-6121	-5820	-1422
T_{ex} /K [b]	4319	4277	4009	1735
V_0 /L kg ⁻¹ [c]	821	719	718	885
P_{CJ} /kbar [d]	335	324	335	158
V_{det} /m s ⁻¹ [e]	8913	8616	8628	6368
I_{sp} /s [f]	274	258	262	157
I_{sp} /s (5% Al) [g]	276	261	264	198
I_{sp} /s (10% Al) [g]	277	262	266	224
I_{sp} /s (15% Al) [g]	278	263	267	235
I_{sp} /s (20% Al) [g]	276	263	267	244
I_{sp} /s (25% Al) [g]	275	262	264	247
I_{sp} /s (5% Al, 14% binder) [h]	258	242	239	250
I_{sp} /s (10% Al, 14% binder) [h]	264	251	248	257
I_{sp} /s (15% Al, 14% binder) [h]	270	255	253	261

[a] Heat of detonation. [b] Detonation temperature. [c] Volume of gaseous products. [d] Detonation pressure. [e] Detonation velocity calculated by using the EXPLO5 (Version 6.02) program package.^[16] [f] Specific impulse of the neat compound using the EXPLO5 (Version 6.02) program package at 70.0 bar chamber pressure and an initial temperature of 3300 K, an ambient pressure of 1.0 bar with equilibrium expansion conditions.^[16] [g] Specific impulse for compositions with different amount of aluminum. [h] Specific impulse for compositions with different amounts of oxidizer/compound and aluminum, and 14% binder (6% polybutadiene acrylic acid, 6% polybutadiene acrylonitrile and 2% bisphenol A ether).

Predictions of the detonation and combustion parameters by using the EXPLO5 V6.02^[16-17] code have been performed based on the heats of formations that were obtained from ab initio calculations. The energetic parameters were calculated with the room temperature densities, which were measured experimentally by a gas pycnometer. The resulting heats of detonation Q_v , detonation temperatures T_{ex} , detonation pressures p , and detonation velocities V_{det} for compounds **1**, **2**, **4**, and **6–9** are shown in Table 7-2, as well as the combustion parameters for the use as oxidizers in different propellant mixtures. The nitrate salt **7** has the highest detonation parameters. The important value of the detonation velocity V_{det} is 8913 m s⁻¹ which is comparable to the high energetic military explosive Hexogen (8838 m s⁻¹).

The specific impulses I_{sp} of compounds **1**, **2**, **4**, and **6–9** were calculated for compositions with different amounts of aluminum as fuel, and additional with binder. These impulses were compared with the calculated impulse of ammonium perchlorate (AP) in an analogous composition. The chosen mixture with AP as an oxidizer provided a specific impulse of 261 s. All compounds show good properties, especially at the calculation without the binder system. The value of the specific impulse of the nitrate salt **7** exceeds all others. The specific impulse of the neat compound is calculated to 274 s, with an admixture of 15% aluminum as fuel 278 s could be achieved. In the composite of 14% binder and 15% aluminum a specific impulse of 270 s is possible which is already higher than the standard optimized mixture of AP (261 s). A further advantage of the compound is the burning residues, which are harmless compared to the hydrochloric acid which is formed in AP propulsion systems.

7.4 Conclusion

Based on the Michael addition of nitroform several energetic polynitro compounds with a positive oxygen balance were synthesized. All of the compounds were characterized by using multinuclear NMR spectroscopy, vibrational spectroscopy, elemental analysis, and mass spectrometry; in addition, most compounds were also characterized by single-crystal X-ray crystallography. The thermal stabilities of these compounds were investigated by DSC measurements. The sensitivities of these compounds were determined and their energetic parameters were estimated by theoretical calculations. With respect to application as high-energy dense oxidizers in composite solid rocket propellants, several energetic performance data were calculated. The best compound, with excellent detonation parameters, is the nitrate salt **7**, which has a very high detonation velocity (8838 m s⁻¹), significantly above those of TNT, RDX, and PETN. Additionally, **7** seem to serve as a good oxidizer candidate for composite rocket propellants. The specific impulse I_{sp}

reaches 270 s within a mixture of 15% aluminum as fuel and 14% binder, which is a result of the high energy in the trinitromethyl group compared with the nitric acid salt. However, the synthesis of 3,3,3-trinitropropylamine materials need five steps, albeit only common chemicals are needed.

7.5 Experimental Section

7.5.1 General Procedures

All chemicals were used as supplied. Raman spectra were recorded in a glass tube with a Bruker MultiRAM FT-Raman spectrometer with Nd:YAG laser excitation up to 1000 mW (at 1064 nm) in the range between 400 and 4000 cm^{-1} . Infrared spectra were measured with a Perkin–Elmer Spectrum BX-FTIR spectrometer equipped with a Smiths DuraSamplIR II ATR device. All spectra were recorded at ambient (20 °C) temperature. NMR spectra were recorded with a JEOL Eclipse 400 instrument and chemical shifts were determined with respect to external Me_4Si (^1H , 399.8 MHz; ^{13}C , 100.5 MHz) and MeNO_2 (^{15}N , 40.6 MHz; ^{14}N , 28.9 MHz). Mass spectrometric data were obtained with a JEOL MStation JMS 700 spectrometer (DCI+, DEI+). Analysis of C/H/N were performed with an Elemental Vario EL Analyzer. Melting and decomposition points were measured with a Perkin-Elmer Pyris6 DSC and an OZM Research DTA 552-Ex with a heating rate of 5 °C min^{-1} in a temperature range of 15 to 400 °C and checked by a Büchi Melting Point B-540 apparatus (not corrected).

7.5.2 Computational Details

All ab initio calculations were carried out using the program package Gaussian 09 (Rev. A.03)^[18] and visualized by GaussView 5.08^[19]. The initial geometries of the structures were taken from the corresponding, experimentally determined crystal structures. Structure optimizations and frequency analyses were performed with Becke's B3 three parameter hybrid functional using the LYP correlation functional (B3LYP). For C, H, N and O a correlation consistent polarized double- ξ basis set was used (cc-pVDZ). The structures were optimized with symmetry constraints and the energy is corrected with the zero point vibrational energy^[20]. The enthalpies (H) and free energies (G) were calculated using the complete basis set (CBS) method in order to obtain accurate values. The CBS models use the known asymptotic convergence of pair natural orbital expressions to extrapolate from calculations using a finite basis set to the estimated complete basis set limit. CBS-4 starts with a HF/3-21G(d) geometry optimization, which is the initial guess for

the following SCF calculation as a base energy and a final MP2/6-31+G calculation with a CBS extrapolation to correct the energy in second order. The used CBS-4M method additionally implements a MP4(SDQ)/6-31+(d,p) calculation to approximate higher order contributions and also includes some additional empirical corrections^[21]. The enthalpies of the gas-phase species were estimated according to the atomization energy method^[22]. The liquid (solid) state energies of formation (ΔH_f°) were estimated by subtracting the gas-phase enthalpies with the corresponding enthalpy of vaporization (sublimation) obtained by Trouton's rule^[23]. All calculations affecting the detonation parameters were carried out using the program package EXPLO5 V6.02 (EOS BKWG-S)^[16-17]. The detonation parameters were calculated at the Chapman–Jouguet (CJ) point with the aid of the steady-state detonation model using a modified Becker-Kistiakowski-Wilson equation of state for modeling the system. The CJ point is found from the Hugoniot curve of the system by its first derivative. The specific impulses I_{sp} were also calculated with the program package EXPLO5 V6.02 program, assuming an isobaric combustion of a composition of an oxidizer, aluminum as fuel, 6% polybutadiene acrylic acid, 6% polybutadiene acrylonitrile as binder and 2% bisphenol A as epoxy curing agent^[16]. A chamber pressure of 70.0 bar, an initial temperature of 3300 K and an ambient pressure of 1.0 bar with equilibrium expansion conditions were estimated for the calculations.

7.5.3 X-ray Crystallography

The low-temperature single-crystal X-ray diffraction of were performed on an Oxford XCalibur3 diffractometer equipped with a Spellman generator (voltage 50 kV, current 40 mA) and a KappaCCD detector operating with MoK α radiation ($\lambda = 0.7107 \text{ \AA}$). Data collection was performed using the CRYVALIS CCD software.^[24] The data reduction was carried out using the CRYVALIS RED software.^[25] The solution of the structure was performed by direct methods (SIR97)^[26] and refined by full-matrix least-squares on F2 (SHELXL)^[27] implemented in the WINGX software package^[28] and finally checked with the PLATON software^[29]. All non-hydrogen atoms were refined anisotropically. The hydrogen atom positions were located in a difference Fourier map. ORTEP plots are shown with thermal ellipsoids at the 50% probability level. Additional crystallographic data and structure refinement parameters are listed in the Appendix A.7.

7.5.4 Synthesis

Safety Announcement: CAUTION! Energetic materials are sensitive toward heat, impact and friction. No hazards occurred during preparation and manipulation; additional proper protective precautions (face shield, leather coat, earthened equipment and shoes, Kevlar gloves, and ear plugs) should be used when undertaking work with these compounds.

4,4,4-Trinitrobutanamide (1): An aqueous solution of nitroform (30%, 22.6 g, 45 mmol) was cooled in an ice-bath and acrylamide (3.2 g, 45 mmol) was added. The mixture was stirred 10 minutes at this temperature and 5 h at ambient temperature. The formed precipitate was filtered off and washed several times with cold ethanol and diethyl ether, to obtain a colorless product. It was dried on air to obtain 9.7 g (43.7 mmol, 97%) of pure product.

DSC (5 °C min⁻¹): 93 °C (mp.), 120 °C (dec.). IR (ATR): $\nu = 3477$ (m), 3369 (w), 3309 (w), 3192 (w), 3010 (w), 2948 (w), 1695 (s), 1596 (s), 1568 (vs), 1418 (m), 1364 (w), 1344 (w), 1288 (s), 1217 (w), 1155 (w), 1117 (w), 878 (w), 856 (m), 816 (s), 798 (vs), 745 (w), 667 (w) cm⁻¹. Raman (500 mW): $\nu = 3009$ (41), 2969 (24), 2938 (78), 1679 (17), 1615 (29), 1599 (43), 1575 (11), 1433 (16), 1417 (43), 1367 (43), 1348 (26), 1307 (31), 1125 (24), 1066 (13), 1055 (14), 967 (13), 904 (12), 881 (43), 858 (60), 811 (20), 546 (18), 441 (71), 390 (100), 364 (73), 312 (69), 274 (17), 208 (66) cm⁻¹. ¹H NMR ([D₆]DMSO) $\delta = 7.48$ (s, 1H, NH₂), 7.09 (s, 1H, NH₂), 3.59 (m, 2H, CH₂C(NO₂)₃), 2.52 (m, 2H, OCCH₂) ppm. ¹³C NMR ([D₆]DMSO) $\delta = 170.7$ (CO), 131.7 (C(NO₂)₃), 29.1 (CH₂), 29.0 (CH₂) ppm. ¹⁴N NMR ([D₆]DMSO) $\delta = -28$ (C(NO₂)₃) ppm. MS (DEI+) *m/e*: 223.2 [(M+H)⁺]. EA (C₄H₆N₄O₇, 222.11): calc.: C 21.63, H 2.72, N 25.22 %; found: C 21.65, H 2.65, N 25.05 %. BAM drophammer: 6 J. friction tester: 360 N. ESD: >0.5 J (grain size 250–500 μm).

4,4,4-Trinitrobutanoic acid (2): 4,4,4-trinitrobutanamide (1) (2.0 g, 9.0 mmol) was added to a mixture of water (2 mL) and concentrated hydrochloric acid (37%, 5 mL) and refluxed for 4 hours. The oily layer which formed solidified after standing overnight at 4 °C. The solid was filtered off and recrystallized from chloroform. It was dried in the desiccator to obtain 1.4 g (6.3 mmol, 70%) of pure colorless product.

DSC (5 °C min⁻¹): 55 °C (mp.), 167 °C (dec.). IR: (ATR): $\nu = 3006$ (w), 2958 (w), 2880 (w), 2730 (w), 2651 (w), 2527 (w), 1709 (s), 1587 (vs), 1440 (m), 1425 (m), 1312 (s), 1297 (s), 1237 (s), 1153 (m), 1070 (m), 928 (m), 906 (m), 816 (s), 798 (vs), 665 (m). cm⁻¹. Raman (500 mW): $\nu = 3006$ (8), 2987 (11), 2956 (89), 1652 (10), 1605 (33), 1454 (9), 1418 (46), 1380 (25), 1359 (22), 1312 (31), 1226 (8), 1154 (13), 1071 (21), 982 (21), 908 (42), 857 (101), 802 (8), 655 (11), 628 (9), 546 (7), 484

(11), 412 (56), 402 (58), 377 (91), 313 (35), 275 (9) cm^{-1} . ^1H NMR ([D6]acetone) $\delta = 3.71$ (m, 2H, $\text{CH}_2\text{C}(\text{NO}_2)_3$), 2.89 (m, 2H, OCCH_2) ppm. ^{13}C NMR ([D6]acetone) $\delta = 170.4$ (CO), 126.3 ($\text{C}(\text{NO}_2)_3$), 29.2 (CH_2), 27.6 (CH_2) ppm. ^{14}N NMR ([D6]acetone) $\delta = -29$ ($\text{C}(\text{NO}_2)_3$) ppm. MS (DCI+) m/e : 224.1 [(M+H) $^+$]. EA ($\text{C}_4\text{H}_5\text{N}_3\text{O}_8$, 223.10): calc.: C 21.53, H 2.26, N 18.83 %; found: C 21.39, H 2.24, N 18.70 %. BAM drophammer: 40 J. friction tester: 324 N. ESD: >0.5 J (grain size 250–500 μm).

4,4,4-Trinitrobutanoyl chloride (3): A mixture of 4,4,4-trinitrobutanoic acid (**2**) (6.7 g, 30 mmol) and thionyl chloride (16.7 mL, 200 mol) was stirred at room temperature for one hour. After this the reaction mixture was refluxed for 24 hours under exclusion of moisture. The excess of thionyl chloride is removed and the remaining oil was distilled yielding 6.4 g of colorless pure product (88%, 27 mmol).

IR: (ATR): $\nu = 2997$ (w), 2957 (w), 2892 (w), 1785 (s), 1585 (vs), 1425 (m), 1411 (w), 1356 (w), 1294 (s), 1216 (w), 1153 (w), 1062 (w), 996 (m), 943 (s), 857 (m), 799 (s), 780 (s), 693 (m) cm^{-1} . Raman (400 mW): $\nu = 2950$ (51), 1792 (16), 1608 (25), 1414 (24), 1381 (22), 1358 (35), 1304 (30), 1224 (11), 1155 (15), 1065 (26), 998 (13), 948 (15), 905 (17), 858 (102), 784 (21), 694 (19), 635 (17), 532 (20), 456 (58), 396 (44), 374 (65), 275 (50), 233 (31) cm^{-1} . ^1H NMR (CDCl_3) $\delta = 3.38$ (m, 4H, OCCH_2 , $\text{CH}_2\text{C}(\text{NO}_2)_3$) ppm. ^{13}C NMR (CDCl_3) $\delta = 171.1$ (CO), 127.9 ($\text{C}(\text{NO}_2)_3$), 40.5 (OCCH_2), 29.4 ($\text{CH}_2(\text{NO}_2)_3$) ppm. ^{14}N NMR (CDCl_3) $\delta = -31$ ($\text{C}(\text{NO}_2)_3$) ppm. MS (DEI+) m/e : 206.1 [(M-Cl) $^+$]. EA ($\text{C}_4\text{H}_4\text{N}_3\text{O}_7\text{Cl}$, 241.54): calc.: C 19.89, H 1.67, N 17.40 %; found: C 19.75, H 1.68, N, 17.80 %.

4,4,4-Trinitrobutanoyl azide (4): A solution of sodium azide (0.31 g, 4.8 mmol) in water (2 mL) was cooled to 4 $^\circ\text{C}$. The solution was stirred and a pre-cooled solution of 4,4,4-trinitrobutanoyl chloride (**3**) (0.59 g, 2.4 mmol) in acetone (1 mL) was added slowly. After the addition the solution was allowed to warm to room temperature and was stirred at this temperature for two hours. The reaction mixture was extracted with chloroform (3x20 mL). The combined organic phases were washed with ice-water (1x20 mL), sodium bisulfate solution (5%, 1x20 mL), again with ice-water (2x20 mL) and at the end with a saturated solution of sodium chloride (1x20 mL). The extracts were dried over magnesium sulfate and the organic solvent was removed at a temperature below 20 $^\circ\text{C}$. The remaining oil solidified in the refrigerator over-night and 0.40 g of colorless pure product (66%, 1.6 mmol) was obtained.

DSC (5 $^\circ\text{C min}^{-1}$): 22 $^\circ\text{C}$ (mp.), 85 $^\circ\text{C}$ (dec.). IR: (ATR): $\nu = 3000$ (w), 2956 (w), 2893 (w), 2148 (s), 1711 (s), 1585 (vs), 1427 (m), 1359 (m), 1296 (s), 1153 (vs), 1098 (s), 1047 (s), 967 (w), 908 (w),

855 (s), 800 (vs), 704 (m) cm^{-1} . Raman (500 mW): $\nu = 2947$ (71), 2156 (26), 2147 (26), 1716 (22), 1608 (26), 1419 (26), 1360 (36), 1305 (30), 1151 (9), 1101 (16), 1050 (14), 968 (12), 910 (31), 857 (101), 788 (10), 669 (26), 543 (9), 502 (29), 373 (69), 279 (39), 262 (36) cm^{-1} . ^1H NMR (CDCl_3) $\delta = 3.38$ (m, 2H, $\text{CH}_2\text{C}(\text{NO}_2)_3$), 2.78 (m, 2H, OCCH_2) ppm. ^{13}C NMR (CDCl_3) $\delta = 176.2$ (CO), 128.6 ($\text{C}(\text{NO}_2)_3$), 30.6 (CH_2), 29.3 (CH_2) ppm. ^{14}N NMR (CDCl_3) $\delta = -30$ ($\text{C}(\text{NO}_2)_3$), -136 (N_β), -147 (N_γ) ppm. EA ($\text{C}_4\text{H}_4\text{N}_6\text{O}_7$, 248.11): calc.: C 19.36, H 1.62, N 33.87 %; found: C 19.89, H 1.65, N 33.54 %. BAM drophammer: 2 J. friction tester: 144 N, ESD 0.3 J (grain size 250–500 μm).

1,1,1-Trinitropropan-3-isocyanate (5): A solution of sodium azide (0.31 g, 4.8 mmol) in water (2 mL) was cooled to 4 °C. The solution was stirred and a pre-cooled solution of 4,4,4-trinitrobutanoyl chloride (**3**) (0.59 g, 2.4 mmol) in acetone (1 mL) was added slowly. After the addition the solution was allowed to warm to room temperature and was stirred at this temperature for two hours. The reaction mixture was extracted with chloroform (3x20 mL). The combined organic phases were washed with ice-water (1x20 mL), sodium bisulfate solution (5%, 1x20 mL), again with ice-water (2x20 mL) and at the end with a saturated solution of sodium chloride (1x20 mL). The extracts were dried over magnesium sulfate and were slowly heated up to 55 °C and kept at this temperature until no more nitrogen evolved (2 h). The organic solvent was removed to get 0.36 g of colorless liquid product (68%, 1.7 mmol).

Raman (500 mW): $\nu = 2953$ (70), 2156 (13), 2147 (13), 1718 (11), 1610 (24), 1451 (18), 1421 (22), 1363 (37), 1304 (30), 1100 (10), 1051 (13), 914 (20), 887 (12), 856 (100), 811 (10), 535 (10), 502 (16), 460 (10), 375 (68), 305 (17), 279 (22), 254 (20) cm^{-1} . ^1H NMR (CDCl_3) $\delta = 3.90$ (m, 2H, CH_2), 3.32 (m, 2H, CH_2) ppm. ^{13}C NMR (CDCl_3) $\delta = 127.4$ ($\text{C}(\text{NO}_2)_3$), 123.6 (NCO), 37.4 (CH_2), 35.0 (CH_2) ppm. ^{14}N NMR (CDCl_3) $\delta = -31$ ($\text{C}(\text{NO}_2)_3$), -360 (NCO) ppm. EA ($\text{C}_4\text{H}_4\text{N}_4\text{O}_7$, 220.10): calc.: C 21.83, H 1.83, N 25.46 %; found: C 21.31, H 1.80, N 26.07 %.

3,3,3-Trinitropropan-1-amine hydrochloride (6): 1,1,1-Trinitropropan-3-isocyanate (**5**) (1.10 g, 5.0 mmol) was heated under reflux with hydrochloric acid (6M, 10 mL) for five hours. The solution was concentrated to dryness to get a white powder. This was recrystallized from methanol, to obtain 1.04 g (90%, 4.5 mmol) of colorless white pure product.

DSC (5 °C min^{-1}): 161 °C (mp.), 178 °C (dec.). IR: (ATR): $\nu = 3132$ (m), 3101 (m), 3035 (m), 2977 (m), 2890 (m), 2833 (m), 2783 (w), 2705 (w), 2655 (w), 2567 (w), 2500 (w), 1597 (s), 1499 (w), 1478 (w), 1458 (m), 1425 (w), 1303 (m), 999 (w), 973 (w), 954 (w), 895 (w), 790 (w) cm^{-1} . RAMAN (300 mW): $\nu = 3038$ (9), 2993 (18), 2965 (34), 2937 (37), 2850 (6), 2806 (8), 1606 (45),

1471 (10), 1434 (12), 1370 (52), 1346 (17), 1312 (26), 1301 (23), 1162 (12), 1147 (14), 1022 (11), 989 (15), 924 (12), 911 (17), 858 (100), 802 (8), 739 (6), 656 (6), 643 (6), 557 (9), 408 (66), 383 (64), 343 (47), 289 (20), 221 (7) cm^{-1} . ^1H NMR (CD_3CN) δ = 7.92 (br, 3H, NH_3), 3.69 (m, 2H, CH_2), 3.42 (m, 2H, CH_2) ppm. ^{13}C NMR (CD_3CN) δ = 125.7 ($\text{C}(\text{NO}_2)_3$), 34.6 (CH_2), 30.8 (CH_2) ppm. ^{14}N NMR (CD_3CN) δ = -31 ($\text{C}(\text{NO}_2)_3$), -349 (NH_3) ppm. EA ($\text{C}_3\text{H}_9\text{N}_4\text{O}_7$, 230.56): calc.: C 15.63, H 3.06, N 24.30 %; found: C 16.09, H 3.06, N 24.30 %. BAM drophammer: 20 J. friction tester: 360 N, ESD >0.5 J (grain size 100–250 μm).

3,3,3-Trinitropropan-1-amine nitrate (7): 1,1,1-Trinitropropan-3-isocyanate (**5**) (1.10 g, 5.0 mmol) was heated under reflux with nitric acid (6M, 10 mL) for five hours. The solution was concentrated to dryness to give a yellow powder. This was recrystallized from ethyl acetate to obtain 1.15 g (89%, 4.5 mmol) of colorless white pure product.

DSC (5 $^\circ\text{C min}^{-1}$): 135 $^\circ\text{C}$ (mp.), 138 $^\circ\text{C}$ (dec.). IR: (ATR): ν = 3120 (m), 3070 (m), 3032 (m), 2977 (m), 2889 (m), 2840 (m), 2763 (w), 2716 (w), 2666 (w), 2588 (w), 2503 (w), 1604 (s), 1506 (w), 1479 (w), 1460 (m), 1425 (w), 1303 (m), 1040 (w), 996 (w), 972 (w), 934 (w), 875 (w), 850 (w), 806 (m), 799 (w), 766 (w), 735 (w), 680 (w) cm^{-1} . ^1H NMR (CD_3CN) δ = 8.61 (br, 3H, NH_3), 3.75 (m, 2H, CH_2), 3.14 (m, 2H, CH_2) ppm. ^{13}C NMR (CD_3CN , 25 $^\circ\text{C}$, ppm) δ = 129.0 ($\text{C}(\text{NO}_2)_3$), 34.0 (CH_2), 30.9 (CH_2) ppm. ^{14}N NMR (CD_3CN , 25 $^\circ\text{C}$, ppm) δ = -4 (NO_3^-), -30 ($\text{C}(\text{NO}_2)_3$), -357 (NH_3) ppm. EA ($\text{C}_3\text{H}_7\text{N}_5\text{O}_9$, 257.12): calc.: C 14.01, H 2.74, N 27.24 %; found: C 13.89, H 2.76, N 27.01 %. BAM drophammer: 6 J. friction tester: 120 N, ESD 0.3 J (grain size 250–500 μm).

4,4,4-Trinitro-*N*-(2,2,2-trinitroethyl)-butanamide (8): To a saturated solution of barium hydroxide in water (10 mL) was added acrylamide (1.30 g, 18.2 mmol) and aqueous formaldehyde (37%, 1.50 g, 18.2 mmol) and stirred for 20 minutes. The solution was treated with solid carbon dioxide (5 g) and the precipitated barium carbonate was filtered off. To the filtrate was added aqueous nitroform solution (30%, 18.3 g, 36.4 mmol), stirred for 20 minutes and refluxed for further 30 minutes. The reaction mixture was cooled in an ice-water bath and the formed precipitate was filtered off. The yellow powder was recrystallized two times from a mixture of methanol/water, to yield 3.93 g (10.2 mmol, 56%) of colorless pure product.

DSC (5 $^\circ\text{C min}^{-1}$): 150 $^\circ\text{C}$ (mp.), 155 $^\circ\text{C}$ (dec.). IR: (ATR): ν = 3304 (w), 3071 (w), 3011 (w), 2960 (w), 2892 (w), 1676 (m), 1589 (vs), 1543 (s), 1418 (w), 1363 (w), 1299 (s), 1236 (w), 1217 (w), 1155 (w), 1115 (w), 1092 (w), 1050 (w), 935 (w), 854 (m), 803 (s). Raman (400 mW): ν = 3006 (19), 2957 (39), 1677 (18), 1605 (29), 1421 (24), 1365 (28), 1337 (20), 1305 (36), 1117 (14), 1058 (13), 936

(15), 913 (13), 857 (102), 545 (18), 412 (46), 394 (47), 377 (68), 278 (29) cm^{-1} . ^1H NMR (CD_3CN) $\delta = 7.21$ (s, 1H, NH), 4.96 (d, 2H, $^3J = 6.8$ Hz, CH_2NH), 3.47 (m, 2H, $\text{CH}_2\text{C}(\text{NO}_2)_3$), 2.70 (m, 2H, OCCH_2) ppm. ^{13}C NMR (CD_3CN) $\delta = 169.9$ (CO), 131.4 ($\text{C}(\text{NO}_2)_3$), 127.5 ($\text{NHCH}_2\text{C}(\text{NO}_2)_3$), 42.2 (NHCH_2), 28.8 (CH_2), 28.6 (CH_2) ppm. ^{14}N NMR (CD_3CN) $\delta = -29$ ($\text{C}(\text{NO}_2)_3$), -32 ($\text{NHCH}_2\text{C}(\text{NO}_2)_3$) ppm. MS (DCI+) m/e : 386.2 [(M+H) $^+$]. EA ($\text{C}_6\text{H}_7\text{N}_7\text{O}_{13}$, 385.16): calc.: C 18.71, H 1.83, N 25.46 %; found: C 18.83, H 1.81, N 25.49 %. BAM drophammer: 10 J. friction tester: 240 N. ESD 0.2 J (grain size 100 μm).

2,2,2-Trinitroethyl 4,4,4-trinitrobutanoate (9): To a mixture of fuming sulfuric acid (30% SO_3 , 4 mL) and concentrated sulfuric acid (8 mL) was added 4,4,4-trinitrobutanoic acid (**2**) (1.7 g, 7.8 mmol) in small portions with cooling to 4°C and stirred till complete solution. 2,2,2-Trinitroethanol (1.53 g, 7.8 mmol) was dissolved in water (0.5 mL) and is added very carefully to the reaction mixture at 4 °C and stirred for further 12 hours at room temperature. The reaction is quenched with ice-water (5 mL) and the colorless precipitate is filtered off. The product was washed three times with water (20 mL) and dried to obtain 1.20 g (3.1 mmol, 40%) of pure product.

DSC (5 °C min^{-1}): 92 °C (mp.), 155 °C (dec.). IR: (ATR): $\nu = 3007$ (w), 2964 (w), 2895 (w), 1761 (s), 1582 (vs), 1441 (w), 1430 (m), 1419 (w), 1400 (w), 1379 (w), 1363 (w), 1299 (s), 1222 (w), 1169 (s), 1100 (w), 1086 (m), 1037 (w), 1015 (w), 913 (w), 873 (w), 855 (m), 799 (vs), 780 (m), 759 (w), 744 (w), 730 (w), 689 (w), 655 (w) cm^{-1} . Raman (500 mW): $\nu = 3009$ (12), 2987 (21), 2953 (49), 1762 (18), 1609 (36), 1442 (10), 1419 (27), 1401 (129, 1364 (38), 1302 (36), 1263 (10), 1154 (9), 1086 (18), 1038 (10), 1015 (13), 972 (8), 915 (21), 873 (13), 857 (105), 798 (11), 781 (9), 744 (6), 647 (11), 539 (17), 487 (11), 404 (70), 373 (95), 341 (13), 326 (12), 269 (28), 232 (21) cm^{-1} . ^1H NMR (CDCl_3) $\delta = 5.44$ (s, 2H, OCH_2), 3.43 (m, 2H, $\text{CH}_2\text{C}(\text{NO}_2)_3$), 2.90 (m, 2H, OCCH_2) ppm. ^{13}C NMR (CDCl_3) $\delta = 167.4$ (CO), 128.2 ($\text{C}(\text{NO}_2)_3$), 122.5 ($\text{OCH}_2\text{C}(\text{NO}_2)_3$), 61.3 (OCCH_2), 29.3 (CH_2), 28.0 (CH_2) ppm. ^{14}N NMR (CDCl_3) $\delta = -31$ ($\text{C}(\text{NO}_2)_3$), -35 ($\text{C}(\text{NO}_2)_3$) ppm. MS (DCI+) m/e : 387.1 [(M+H) $^+$]. EA ($\text{C}_6\text{H}_6\text{N}_6\text{O}_{14}$, 386.14): calc.: C 18.66, H 1.57, N 21.76 %; found: C 18.92, H 1.59, N 21.46 %. BAM drophammer: 30 J. friction tester: 240 N. ESD 0.1 J (grain size 100 μm).

7.6 References

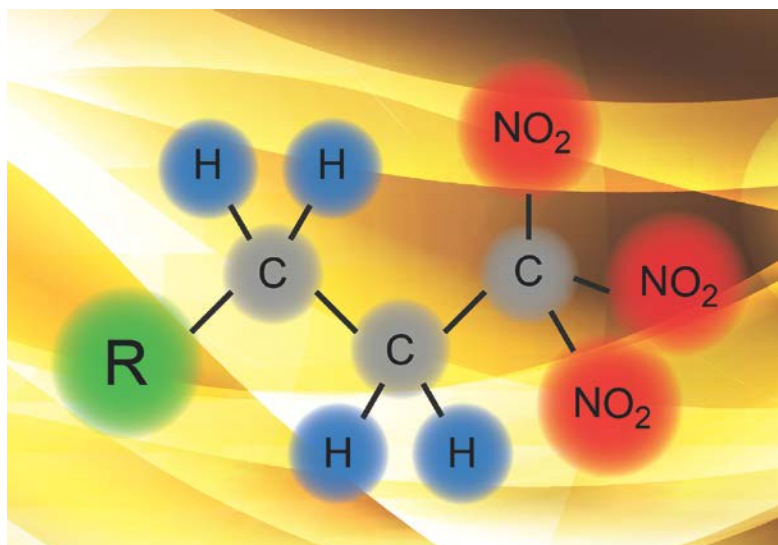
- [1] a) T. M. Klapötke, *Chemistry of High-Energy Materials*, 2nd ed., deGruyter, Berlin, **2012**; b) Q. J. Axthammer, T. M. Klapötke, B. Krumm, R. Moll, S. F. Rest, *Z. Anorg. Allg. Chem.* **2014**, *640*, 76–83; c) Q. J. Axthammer, B. Krumm, T. M. Klapötke, *J. Org. Chem.* **2015**, *80*, 6329–6335.
- [2] a) M. Göbel, T. M. Klapötke, P. Mayer, *Z. Anorg. Allg. Chem.* **2006**, *632*, 1043–1050; b) M. Göbel, T. M. Klapötke, *Adv. Funct. Mater.* **2009**, *19*, 347–365; c) M. Göbel, T. M. Klapötke, *Z. Anorg. Allg. Chem.* **2007**, *633*, 1006–1017.
- [3] J. P. Agrawal, *High Energy Materials*, Wiley-VCH, Weinheim, **2010**.
- [4] a) M. J. Kamlet, J. C. Dacons, J. C. Hoffsommer, *J. Org. Chem.* **1961**, *26*, 4881–4886; b) I. J. Schaffner **1962**, US 3051743.
- [5] D. J. Glover, J. C. Dacons, D. V. Sickman, M. E. Hill, M. J. Kamlet **1964**, US 3125606.
- [6] M. H. Gold, M. B. Frankel, G. B. Linden, K. Klager, *J. Org. Chem.* **1962**, *27*, 334–336.
- [7] a) M. B. Frankel, *Tetrahedron* **1963**, *19*, 213–217; b) Q. J. Axthammer, B. Krumm, T. M. Klapötke, R. Scharf, *Chem. – Eur. J.* **2015**, *21*, 16229–16239.
- [8] a) M. B. Frankel **1961**, US 3000945; b) M. B. Frankel **1961**, US 2978509.
- [9] a) H. Feuer, U. E. Lynch-Hart, *J. Org. Chem.* **1961**, *26*, 391–394; b) H. Feuer, U. E. Lynch-Hart, *J. Org. Chem.* **1961**, *26*, 587–589; c) I. J. Schaffner **1962**, US 3038009.
- [10] a) R. H. Saunders **1961**, US 2996537; b) M. E. Hill **1966**, US 3230247.
- [11] S. Bienz, L. Bigler, T. Fox, M. Hesse, H. Meier, B. Zeeh, *Spektroskopische Methoden in der Organischen Chemie*, 8th ed., Thieme, Stuttgart, **2014**.
- [12] a) Q. J. Axthammer, B. Krumm, T. M. Klapötke, *J. Org. Chem.* **2015**, *80*, 6329–6335; b) Q. J. Axthammer, T. M. Klapötke, B. Krumm, R. Moll, S. F. Rest, *Z. Anorg. Allg. Chem.* **2014**, *640*, 76–83.
- [13] T. M. Klapötke, B. Krumm, R. Moll, S. F. Rest, Y. V. Vishnevskiy, C. Reuter, H.-G. Stammer, N. W. Mitzel, *Chem. – Eur. J.* **2014**, *20*, 12962–12973.
- [14] T. Steiner, *Angew. Chem., Int. Ed.* **2002**, *41*, 48–76.
- [15] *Commission communication in the framework of the implementation of the Council Directive 93/15/EEC of 5 April 1993 on the harmonisation of the provisions relating to the placing on the market and supervision of explosives for civil uses, Vol. 221*, **2006**.
- [16] M. Sućeska, *EXPLO5 V.6.02*, Zagreb, **2013**.
- [17] M. Sućeska, *Propellants, Explos., Pyrotech.* **1991**, *16*, 197–202.
- [18] M. J. Frisch, G. W. Trucks, H. B. Schlegel, G. E. Scuseria, M. A. Robb, J. R. Cheeseman, V. B. G. Scalmani, B. Mennucci, G. A. Petersson, H. Nakatsuji, M. Caricato, X. Li, H. P. Hratchian, A. F. Izmaylov, J. Bloino, G. Zheng, J. L. Sonnenberg, M. Hada, M. Ehara, K. Toyota, R. Fukuda, J. Hasegawa, M. Ishida, T. Nakajima, Y. Honda, O. Kitao, H. Nakai,

- T. Vreven, J. J. A. Montgomery, J. E. Peralta, F. Ogliaro, M. Bearpark, J. J. Heyd, E. Brothers, K. N. Kudin, V. N. Staroverov, R. Kobayashi, J. Normand, K. Raghavachari, A. Rendell, J. C. Burant, S. S. Iyengar, J. Tomasi, M. Cossi, N. Rega, J. M. Millam, M. Klene, J. E. Knox, J. B. Cross, V. Bakken, C. Adamo, J. Jaramillo, R. Gomperts, R. E. Stratmann, O. Yazyev, A. J. Austin, R. Cammi, C. Pomelli, J. W. Ochterski, R. L. Martin, K. Morokuma, V. G. Zakrzewski, G. A. Voth, P. Salvador, J. J. Dannenberg, S. Dapprich, A. D. Daniels, Ö. Farkas, J. B. Foresman, J. V. Ortiz, J. Cioslowski, D. J. Fox, *Gaussian 09*, Rev. A.02 ed., Gaussian, Inc., Wallingford CT, **2009**.
- [19] R. D. Dennington, T. A. Keith, J. M. Millam, *GaussView*, Ver. 5.08 ed., Semichem, Inc., Wallingford CT, **2009**.
- [20] J. A. Montgomery, M. J. Frisch, J. W. Ochterski, G. A. Petersson, *J. Chem. Phys.* **2000**, *112*, 6532–6542.
- [21] J. W. Ochterski, G. A. Petersson, J. A. Montgomery, *J. Chem. Phys.* **1996**, *104*, 2598–2619.
- [22] E. F. C. Byrd, B. M. Rice, *J. Phys. Chem.* **2005**, *110*, 1005–1013.
- [23] a) F. Trouton, *Philos. Mag.* **1884**, *18*, 54–57; b) M. S. Westwell, M. S. Searle, D. J. Wales, D. H. Williams, *J. Am. Chem. Soc.* **1995**, *117*, 5013–5015.
- [24] Oxford Diffraction Ltd., *CrysAlis CCD*, Version 1.171.35. (release 16-05-2011 CrysAlis 171.Net), Abingdon, Oxford, **2011**.
- [25] Oxford Diffraction Ltd., *CrysAlis RED*, Version 1.171.35.11 (release 16-05-2011 CrysAlis 171.NET), Abingdon, Oxford, **2011**.
- [26] A. Altomare, M. C. Burla, M. Camalli, G. L. Cascarano, C. Giacovazzo, A. Guagliardi, A. G. G. Moliterni, G. Polidori, R. Spagna, *J. Appl. Crystallogr.* **1999**, *32*, 115–119.
- [27] a) G. M. Sheldrick, *SHELX-97, Programs for Crystal Structure Determination*, **1997**; b) G. M. Sheldrick, *Acta Crystallogr., Sect. A: Found. Crystallogr.* **2008**, *A64*, 112–122.
- [28] L. Farrugia, *J. Appl. Crystallogr.* **1999**, *32*, 837–838.
- [29] A. Spek, *Acta Crystallogr., Sect. D: Biol. Crystallogr.* **2009**, *65*, 148–155.

8 The 3,3,3-Trinitropropyl Unit

As published in *Chem — Eur. J.* **2015**, *640*, 76–83.

A STUDY OF THE 3,3,3-TRINITROPROPYL UNIT AS POTENTIAL ENERGETIC BUILDING BLOCK



8.1 Abstract

Compared to the well established 2,2,2-trinitroethyl group in the topic of energetic material chemistry, the 3,3,3-trinitropropyl is a less common unit. Also, little is known regarding of the chemical and energetic properties. Investigations on the syntheses of several compounds containing the 3,3,3-trinitropropyl group were performed and compared to the one methylene shorter, 2,2,2-trinitroethyl group. All materials were thoroughly characterized, including single crystal X-ray diffraction studies. The thermal stabilities were examined using differential thermal analysis (DSC) and the sensitivities towards impact, friction and electrostatic discharge were tested using a drop hammer, a friction tester as well as an electrical discharge device. The energies of formation were calculated and several detonation parameters such as the velocity of detonation and the propulsion performance were estimated with the program package EXPLO5.

8.2 Introduction

The 2,2,2-trinitroethyl group is a central building block in the synthesis of energetic materials, especially in the subgroup of *high energetic dense oxidizers* (HEDO). This unit can readily be obtained by reacting trinitromethane and formaldehyde via a Henry reaction or by a Mannich condensation of an amine, formaldehyde and trinitromethane.^[1] Reams of compounds with this moiety have been synthesized and characterized in the recent years.^[2] Unfortunately, the trinitroethyl moiety is unstable towards bases and nucleophiles and decompose into their starting materials.^[3] In contrast to this, the 3,3,3-trinitropropyl moiety shows a higher chemical stability since such reverse Henry or Mannich reactions are not possible.^[4] A disadvantage of the 3,3,3-trinitropropyl group is its complex synthesis and the lower oxygen content.^[5] Although some compounds with a 3,3,3-trinitropropyl moiety are reported, nothing is known about the energetic properties, the molecular structure and the stability of such materials.

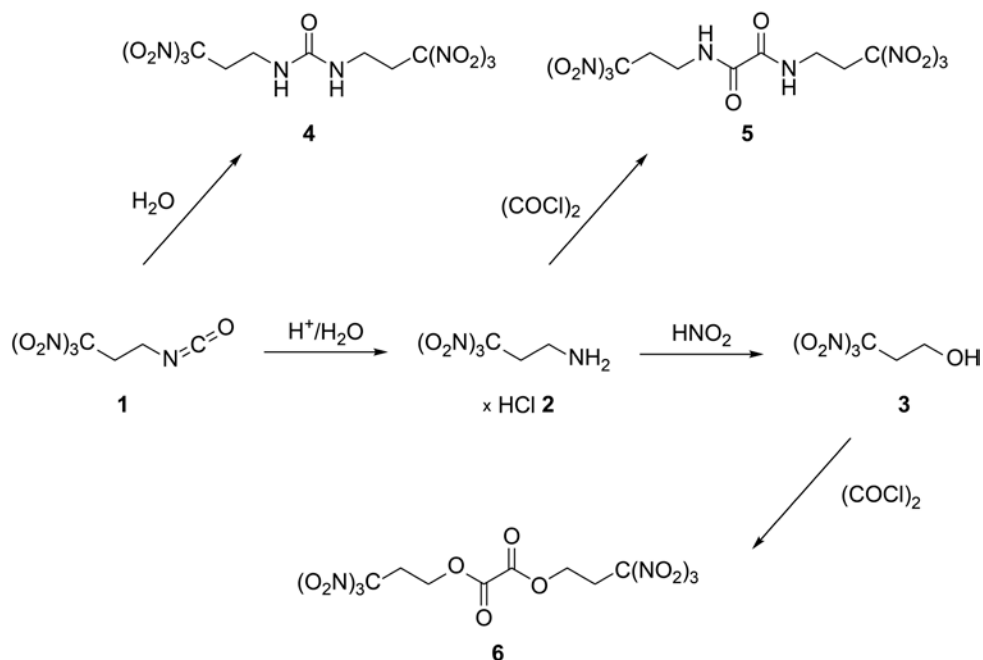
High energy dense oxidizers (HEDO's) are energetic compounds which are based on CHNO and release the excess of included oxygen when it burned or decompose.^[1b] These oxidizers are, besides further components such as binder and fuel, the main part (>70%) in solid rocket propellants.^[6] The released oxygen reacts with the fuel such as carbon-backbones or aluminum and produces plenty of hot gases which are used for the impulsion of rockets.^[7] Until now ammonium perchlorate (AP) is due to its high oxygen content and the low price the most commonly used oxidizer in composite propellants. Unfortunately, the combustion of AP releases

large amounts of toxic gases such as hydrogen chloride causing environmental problems.^[8] In addition the application of AP causes pollution of the groundwater in large areas throughout the world.^[9] There is also a proof that the perchlorate anion has negative health effects especially on the hormonal balance of humans and amphibians.^[10] For these reasons new halogen-free propellants with high performance and good stability are desirable.

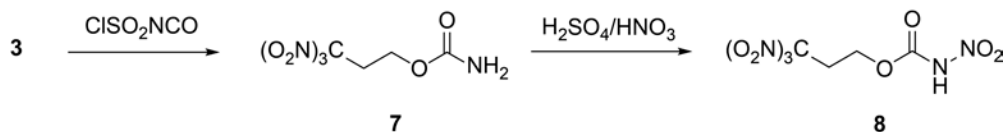
8.3 Results and Discussion

8.3.1 Synthesis

The central precursor for this work (Scheme 8-1) is the reactive isocyanate 1,1,1-trinitropropan-3-isocyanate (**1**), which is available in a multi-step synthesis, starting from a Michael addition of trinitromethane with acrylamide.^[11] The salt 3,3,3-trinitropropan-1-amine hydrochloride (**2**) was obtained by controlled hydrolysis of **1** in hydrochloric acid. The amine was further converted into the corresponding alcohol 3,3,3-trinitropropanol (**3**) by a Sandmeyer reaction.^[12] In this reaction a diazonium salt is formed by in situ generated nitrous acid, which is subsequently displaced by a nucleophilic substitution with water. The urea derivative **4** is obtained by the reaction of two molecules of **1** by partial hydrolysis.^[5b]

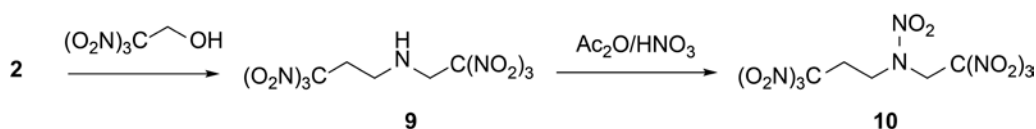


Scheme 8-1: Synthetic overview of 3,3,3-trinitropropyl based compounds Part I.



Scheme 8-2: Synthetic overview of 3,3,3-trinitropropyl based compounds Part II.

For the synthesis of bis(3,3,3-trinitropropyl) oxamide (**5**) the free amine of the hydrochloride salt **2** was extracted in an organic solvent where it is reacted with oxalyl chloride (Figure 8-1).^[13] The oxalate derivative bis(3,3,3-trinitropropyl) oxalate (**6**) was synthesized by the reaction of oxalyl chloride and the alcohol **3**. The conversion of the alcohol into 3,3,3-trinitropropyl carbamate (**7**) was first mentioned in the 1990s and was realized by a two step synthesis. First, phosgene was reacted with **3** to form the chloroformate, which was further converted with aqueous ammonia to obtain the carbamate **7**.^[14] Now, a one step synthesis was achieved by using the reagent chlorosulfonyl isocyanate (CSI). The advantages of CSI are much shorter reaction times, easier handling of the starting materials and trouble-free work up (Figure 8-2).^[15] The carbamate **7** was obtained as a colorless pure product in high yield compared to the old route.^[14] The nitration of **7** resulted in the 3,3,3-trinitropropyl nitrocarbamate (**8**), performed in a mixture of concentrated sulfuric and nitric acid.^[15c, 16] After quenching in water, extracting and recrystallization from tetrachloromethane colorless crystals of pure nitrocarbamate **8** were obtained.



Scheme 8-3: Synthetic overview of 3,3,3-trinitropropyl based compounds Part III.

Mannich condensations between an organic nitro compound, an aldehyde and an amine are very popular and useful reactions.^[17] The condensation of the amine **2** with formaldehyde and trinitromethane produced the secondary amine 3,3,3-trinitropropyl-*N*-(2,2,2-trinitroethyl)propan-1-amine (**9**) as a solid with a limited stability (Figure 8-3).^[5a] Upon nitration of **9** in a mixture of acetic anhydride and anhydrous nitric acid, the highly energetic nitramine, *N*-(2,2,2-trinitroethyl)-*N*-(3,3,3-trinitropropyl) nitramine (**10**) was obtained.^[5a] The nitramine **10** is air and moisture stable, has an oxygen and nitrogen content of 84% and a very high oxygen balance Ω_{CO} of +23.9%.

8.3.2 NMR Spectroscopy

The ^1H , ^{13}C and ^{14}N NMR were recorded in CDCl_3 (**1**, **3**, **4**, **9**), CD_3CN (**2**, **9**) and $[\text{D}_6]\text{acetone}$ (**5**–**8**). In the ^1H NMR spectra the two CH_2 groups are within the range of 4.84 to 3.14 ppm. The methylene unit next to the trinitromethyl moiety is shifted to higher field compared to the CH_2 groups next to nitrogen or oxygen. The vicinal coupling constants of the hydrogen atoms in the ethylene group are not equal due to the rotation around the C–C bond, causing a AA'XX' spin systems.^[18]

In the ^{13}C NMR spectra the carbon resonances of the two CH_2 groups are found in the range of 58.0 to 33.2 ppm. As expected, the same effect as in the proton NMR spectra is also observed in the ^{13}C NMR. The carbon resonances next to the trinitromethyl unit are always upfield shifted compared to those connected to the electron withdrawing elements nitrogen and oxygen. The carbon resonance of the trinitromethyl moiety is observed as a broadened signal; in the case of 3,3,3-trinitropropyl always located at around 130 ppm. By comparing this with that of the 2,2,2-trinitroethyl unit in **9** and **10**, a significant upfield shift to approximately 125 ppm is obvious.

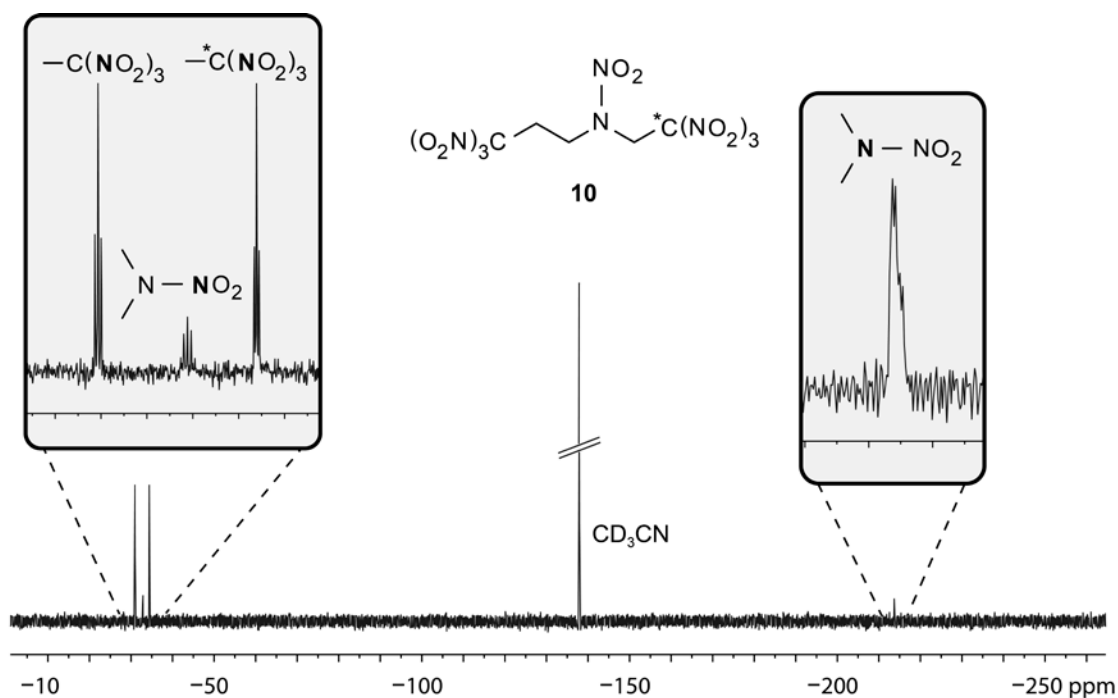


Figure 8-1: ^{15}N NMR spectrum of *N*-(2,2,2-trinitroethyl)-*N*-(3,3,3-trinitropropyl) nitramine (**10**) in CD_3CN .

In the ^{14}N NMR spectra the resonances for the nitro groups of the trinitromethyl moieties are all quite sharp and found in the range of -29 to -32 ppm. For the nitramine **10** a ^{15}N NMR spectrum is recorded and shown in Figure 8-1, with full assignment of all nitrogen atoms. The

nitrogen resonances of the trinitromethyl moieties were observed at -31.0 ppm for the 3,3,3-trinitropropyl unit and at -34.5 ppm for the 2,2,2-trinitroethyl unit, respectively. For both resonances a triplet caused by coupling with the two neighboring methylene hydrogen atoms, with a coupling constant of ${}^3J({}^{15}\text{N}, {}^1\text{H}) = 2.8$ Hz and ${}^3J({}^{15}\text{N}, {}^1\text{H}) = 1.9$ Hz. The two nitrogen resonances of the nitramine moiety are located as multiplets as expected. The nitro group is located between the two triplets of the trinitromethyl groups at -32.9 ppm and that of the amine upfield at -213.7 ppm.

8.3.3 Vibrational Spectroscopy

All compounds were also characterized by their molecular vibration frequencies by IR and RAMAN spectroscopy. The most characteristic frequencies in the compounds are the carbonyl and nitro groups which are summarized in Table 8-1.

Table 8-1: Selected IR and Raman bands for 1–10.

	1		2		3		4	
	IR	Raman	IR	Raman	IR	Raman	IR	Raman
ν CO	-	-	-	-	-	-	1642 (m)	1644 (12)
ν_{as} NO ₂	1586 (s)	1610 (24)	1597 (s)	1606 (45)	1581 (s)	1608 (19)	1587 (m)	1593 (28)
ν_{s} NO ₂	1298 (m)	1304 (30)	1303 (m)	1312 (26)	1296 (s)	1306 (25)	1298 (m)	1309 (33)
	5		6		7		8	
	IR	Raman	IR	Raman	IR	Raman	IR	Raman
ν CO	1659 (m)	1694 (41)	1764 (m)	1769 (51)	1704 (m)	1699 (15)	1758 (m)	1760 (41)
ν_{as} NO ₂	1583 (s)	1607 (22)	1600 (s)	1615 (25)	1583 (s)	1617 (36)	1590 (s)	1617 (32)
ν_{s} NO ₂	1297 (m)	1299 (40)	1296 (m)	1292 (29)	1298 (m)	1299 (25)	1291 (m)	1307 (30) 1290 (31)
	9		10					
	IR	Raman	IR	Raman				
ν CO	-	-	-	-				
ν_{as} NO ₂	1581 (s)	1604 (21)	1599 (s) 1555 (s)	1613 (35)				
ν_{s} NO ₂	1302 (s)	1309 (27)	1285 (s) 1268 (s)	1294 (23) 1270 (25)				

Frequencies in cm^{-1} ; IR intensities: vs = very strong, s = strong, m = medium, w = weak; Raman intensities in brackets.

For the trinitromethyl units both the asymmetric $\nu_{\text{as}}(\text{NO}_2)$ in the range of 1600–1581 cm^{-1} and the symmetric stretching vibrations $\nu_{\text{s}}(\text{NO}_2)$ at 1285–1307 cm^{-1} are observed. For **8** and **10** additional NNO_2 groups are included and also additional $\nu_{\text{as}}(\text{NO}_2)$ and $\nu_{\text{s}}(\text{NO}_2)$ vibrations appear at slightly higher wave number.^[19] Furthermore, it is observed that the $\nu_{\text{as}}(\text{NO}_2)$ are shifted to higher wave numbers in molecules when they are connected to electron-withdrawing moieties such as the carboxylate moiety in **6** (1600 cm^{-1}) compared to the carbamate moiety in **7** (1583 cm^{-1}). The same effect influences the C=O stretching vibrations $\nu(\text{C}=\text{O})$. An example is the urea derivative **4** where the $\nu(\text{C}=\text{O})$ is located at 1642 cm^{-1} , while in the carbamate **7** (1704 cm^{-1}) and in the nitrocarbamate **8** (1758 cm^{-1}) a significant shift to higher energies are observed.

8.3.4 Single Crystal Structure Analysis

Single crystals suitable for X-ray diffraction studies were obtained by crystallization at room temperature from dichloromethane (**6**, **8**, **10**), chloroform (**9**) and acetonitrile (**5**, **7**). A full list of the crystallographic refinement parameters and structure data for compounds **4–10** is shown in the Appendix A.8. Until now no molecular structure with a 3,3,3-trinitropropyl moiety is known in the literature.

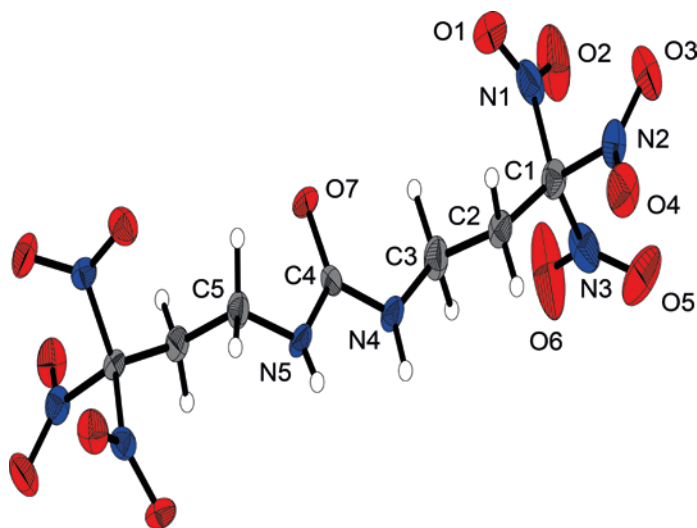


Figure 8-2: X-ray molecular structure of bis(3,3,3-trinitropropyl) urea (4).

Selected atom distances (Å) and angles (deg): C1–C2 1.49 5(7), C1–N1 1.519(6), C1–N2 1.539(6), C1–N3 1.526(6), C2–C3 1.535(7), C3–N4 1.447(7), C4–N4 1.352(7), C4–N5 1.343(7), C4–O7 1.233(5), C5–N5–C4 123.0(5), O7–C4–N4 121.9(5), C4–N4–H5 120(4), H5–N4–C3 118(4), C3–N4–C4–O7 $-6.5(8)$, H5–N4–C4–O7 $-175(5)$, O7–C4–N5–C5 3.3(8).

The urea compound **4** crystallizes in the orthorhombic space group $Pccn$ in a large unit cell containing twelve molecules. The asymmetric unit consists of one and a half molecules. The full molecule is shown in Figure 8-2. The C–N bond lengths in the trinitromethyl moiety are in the range of 1.53 Å, which is significantly longer than a regular C–N bond with 1.47 Å and results from steric repulsion of the proportionally large nitro groups around one carbon atom.^[16] The three nitro groups are organized around the carbon in a propeller-like geometry to optimize the non-bonded N···O intramolecular attractions. This results in an intramolecular interaction between the partial positive charged nitrogen and the negative charged oxygen in the nitro groups.

[16]

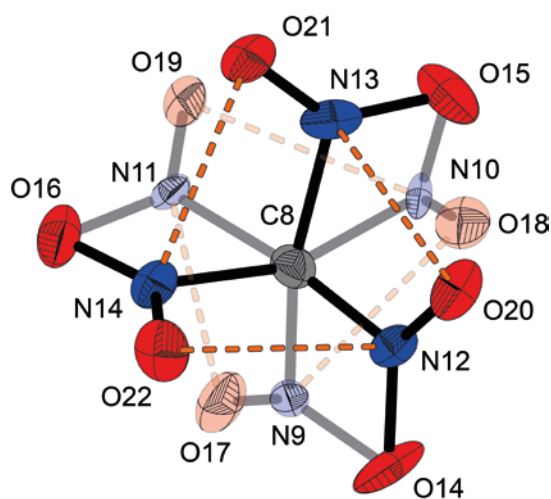


Figure 8-3: Disorder of the C(NO₂)₃ in the molecular structure of bis(3,3,3-trinitropropyl) urea (4**). The orange dotted lines indicate the nitrogen oxygen non-bonded intramolecular interactions.**

These N···O attractions can be found with distances in the range of 2.41 to 2.63 Å, which are much shorter than the sum of the van der Waals radii of nitrogen and oxygen (3.07 Å).^[16, 20] This steric arrangement of the nitro groups was also observed in the half molecule of the asymmetric unit, which is completed by a proper two fold rotation axis. Furthermore a disorder of the trinitromethyl group is observed. Two different positions can be identified with a nearly equivalent proportion. In the disorder the nitro groups always share an oxygen which is fully occupied whereas the other oxygen and the nitrogen are independent (Figure 8-3). Another result of the trinitromethyl group with its quite strong electron-withdrawing effect of the nitro groups is the reduced bond length of the neighboring carbon-carbon bond (C1–C2 1.485 Å).^[21] As expected the urea unit is nearly planar and shows typical bond geometry.

The oxamide **5** (Figure 8-4) and the oxalate **6** (Figure 8-5) both crystallize in the monoclinic space group $P2_1/c$ and show the propeller-like steric geometry of the trinitromethyl group. In **5** the asymmetric unit consists of two half independent molecules that are almost equal.

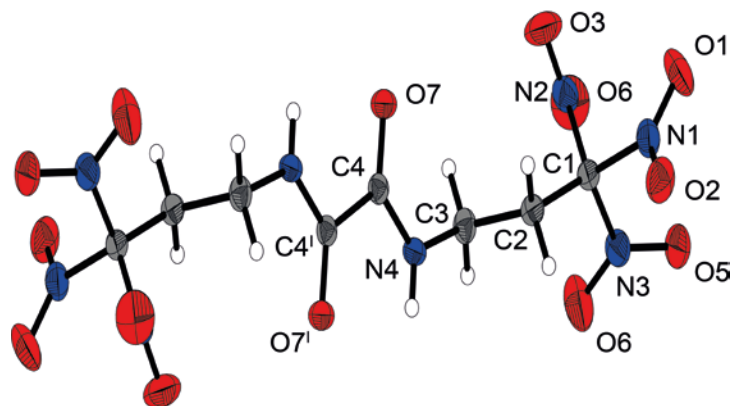


Figure 8-4: X-ray molecular structure of bis(3,3,3-trinitropropyl) oxamide (5).

Selected atom distances (Å) and angles (deg): C2–C1 1.506(2), C3–C2 1.531(3), C4–C4' 1.538(2), N4–C3 1.449(2), N4–C4 1.320(2), C3–N4–C4 121.8(2), H5–N4–C4 120(1), O7–C4–N4 125.0(2), O7–C4–C4 121.6(1), N4–C4–C4 113.4(1), C3–N4–C4–C4 178.3(1), N4–C4–C4–N4 $-180.0(2)$, H5–N4–C4–O7 172(2).

An inversion center in the center of the carbon-carbon bond of the oxamide moiety completes the molecule. The length of this bond (1.54 Å) is quite long for a sp^2 carbon bond, but is common for an oxamide structure.^[22] The same was observed in the structure of oxalate **6** (Figure 8-5). The unique unit is here only one half of the molecule. The 3,3,3-trinitropropyl arm is nipped off to the oxygen O2 of the oxalate unit. This causes an additional $N\cdots O$ intramolecular attraction between the partial positive charged nitrogen N3 and O2 and is confirmed by the short distance (2.80 Å).

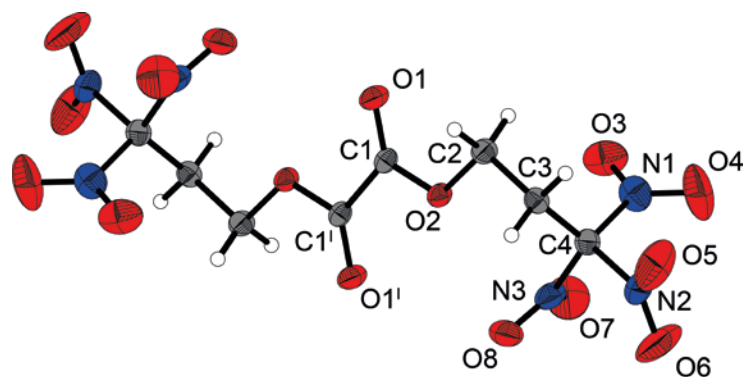


Figure 8-5: X-ray molecular structure of bis(3,3,3-trinitropropyl) oxalate (6).

Selected atom distances (Å) and angles (deg): C1–O1 1.198(2), C1–O2 1.325(2), C1–C1' 1.540(2), C2–C3 1.513(2), C2–O2 1.454(2), C3–C4 1.504(2), N2–O4 2.535(2), N1–O7 2.632(2), N3–O6 2.554(2), N3–O2 2.800(2), O1–C1–O2 126.2(1), C3–C2–O2 107.6(1), O1–C1–O2–C2 4.0(2), C1–O2–C2–C3 173.3(1).

The carbamate **7** crystallizes in the orthorhombic space group *Pbca* with eight molecules in the unit cell and one molecule as the asymmetric unit (Figure 8-6). The carbamate moiety inclusively the carbon C2 shows a nearly planar arrangement. The bond lengths of the C1–N1 (1.33 Å) and the two N1–H bonds (0.85 and 0.86 Å) in the carbamate part are shortened which is typical for such moieties.^[16] The conformation of the substituent at C2, C3 and C4 are all almost perfect staggered. The extended structure involves secondary interactions in terms of classical intermolecular N–H···O hydrogen bonding and unusual hydrogen bonding with carbon as donor (C–H···O) (further information see Appendix A.8). The carbamate unit forms with another unit a nearly perfect planar eight-membered ring (see Figure 8-6).

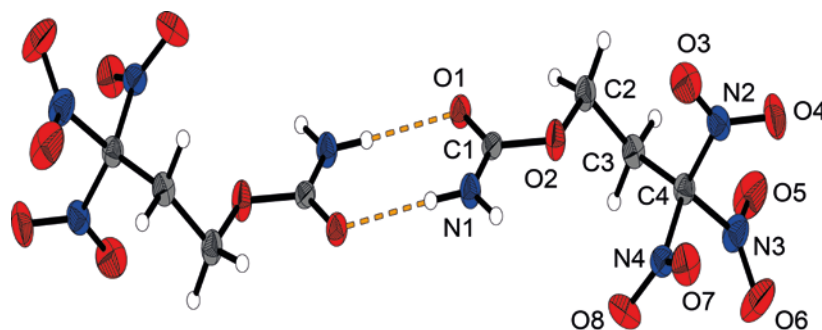


Figure 8-6: X-ray molecular structure of two molecules of 3,3,3-trinitropropyl carbamate (7).

Selected atom distances (Å) and angles (deg): C1–N1 1.325(2), C1–O1 1.224(1), C1–O2 1.355(1), C2–C3 1.515(2), C2–O2 1.440(2), C3–C4 1.510(2), N1–H1 0.86(1), N1–H2 0.85(2), O2–N4 2.946(1), N4–O6 2.526(1), O7–N2 2.565(1), O3–N3 2.541(2), N1–C1–O1 125.9(1), N1–C1–O2 111.3(1), O1–C1–O2 122.7(1), C3–C2–O2 109.6(1), C2–C3–C4 117.4(1), H2–N1–C1–O1 –175(1), N1–C1–O2–C2 –179.1(1).

The crystal growing, data collection, solution and refinement of the 3,3,3-trinitropropyl nitrocarbamate (**8**) was difficult, as illustrated by the quite high refinement values. The data collection also had to be performed at ambient temperature due to a phase transition at lower temperature. This is particularly interesting since the related compound 2,2,2-trinitroethyl nitrocarbamate shows the same behavior.^[16]

Compound **8** crystallizes in the orthorhombic space group *Pccn* with one molecule as asymmetric unit (Figure 8-7). The nitrocarbamate moiety is in a perfect plane including the carbon atom C2. The N1–N2 bond length of the nitramine is 1.37 Å which indicates a significant double bond character, which is achieved by delocalization of the nitrogen lone pair on N2. The carbonyl group (C1–O3) shows compared to the carbamate structure of **7** a slight shortening as a result of the electron withdrawing nitro group.

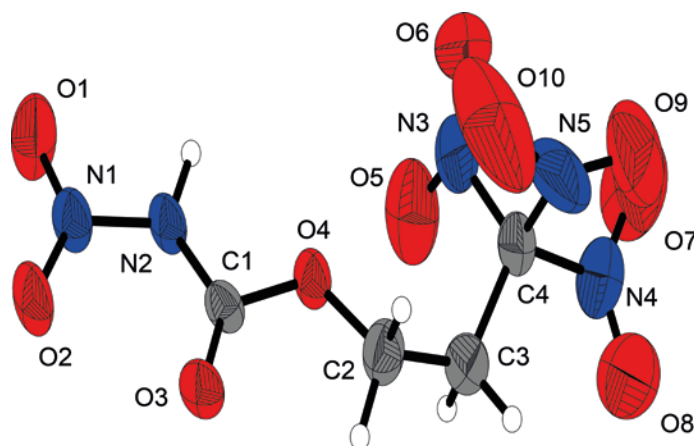


Figure 8-7: X-ray molecular structure of 3,3,3-trinitropropyl nitrocarbamate (8).

Selected atom distances (Å) and angles (deg): O4–C1 1.329(5), O4–C2 1.430(6), O3–C1 1.182(4), C1–N2 1.367(5), N2–N1 1.367(6), C2–C3 1.491(8), C3–C4 1.501(8), C2–O4–C1 115.8(3), N2–C1–O4 107.0(4), N1–N2–C1 124.0(4), O1–N1–N2–C1 176.4(4), O2–N1–N2–H1 –176(3), H1–N2–C1–O3 172(3), N2–C1–O4–C2 177.3(3).

The Mannich condensation product **9** crystallizes in the monoclinic space group $P2_1/c$ with two formula units per unit cell. The asymmetric unit consists of one and a half molecules which is only possible through a disorder in the half molecule (Figure 8-9). The interesting disorder shows a statistically occupation of nitrogen and oxygen (1:1) at the same position (see Figure 8-8). This disorder occurs as a result of an inversion center which is located on the b axes of the cell.^[2c] The average of the N–O and C–NO₂ bond lengths of the trinitromethyl units in the ethyl and propyl moiety are all in the same range of 1.21 Å in N–O and 1.52 Å in C–NO₂. Also both trinitromethyl groups show independently the propeller-like orientation of the nitro groups. Also the carbon-carbon bonds are virtually identical within a range of 1.50 to 1.52 Å. The geometry around the nitrogen of the secondary amine is nearly tetrahedral with angles of 108.7, 111.6 and 111.6 °.

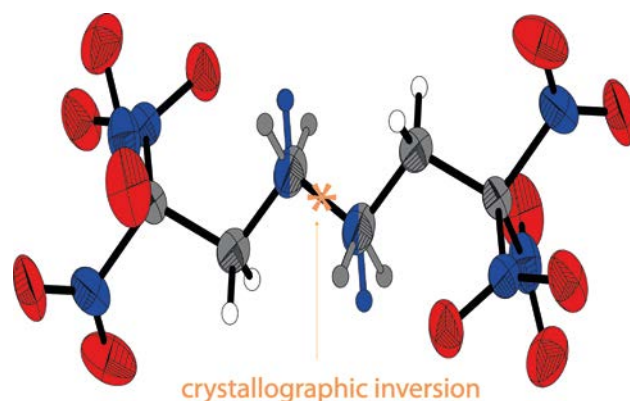


Figure 8-8: X-ray molecular structure of 3,3,3-trinitro-*N*-(2,2,2-trinitroethyl) propan-1-amine (9) showing a C/N disorder.

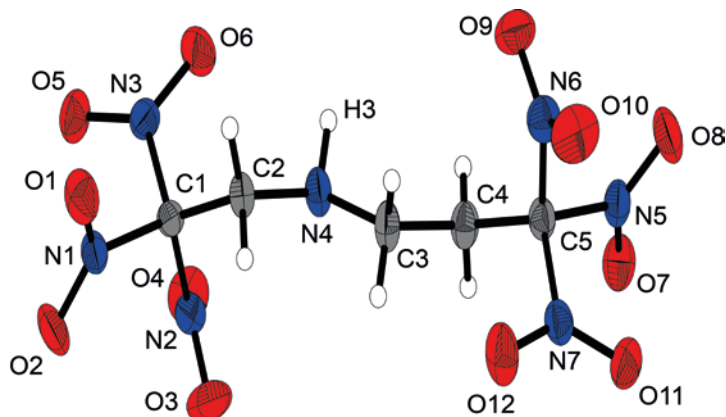


Figure 8-9: X-ray molecular structure of 3,3,3-trinitro-*N*-(2,2,2-trinitroethyl) propan-1-amine (9).

Selected bond lengths (Å) and angles (deg): N4–C2 1.467(3), N4–C3 1.451(3), N4–H3 0.92(2), C1–C2 1.513(3), C3–C4 1.515(3), C4–C5 1.503(3), C2–C1–N1 112.0(2), C2–C1–N2 110.5(2), C2–C1–N3 114.5(2), C4–C5–N5 111.7(2), C4–C5–N6 113.3(2), C4–C5–N7 114.5(2), C3–N4–H3 109(2), H3–N4–C2 111(2), C3–N4–C2 111.6(2).

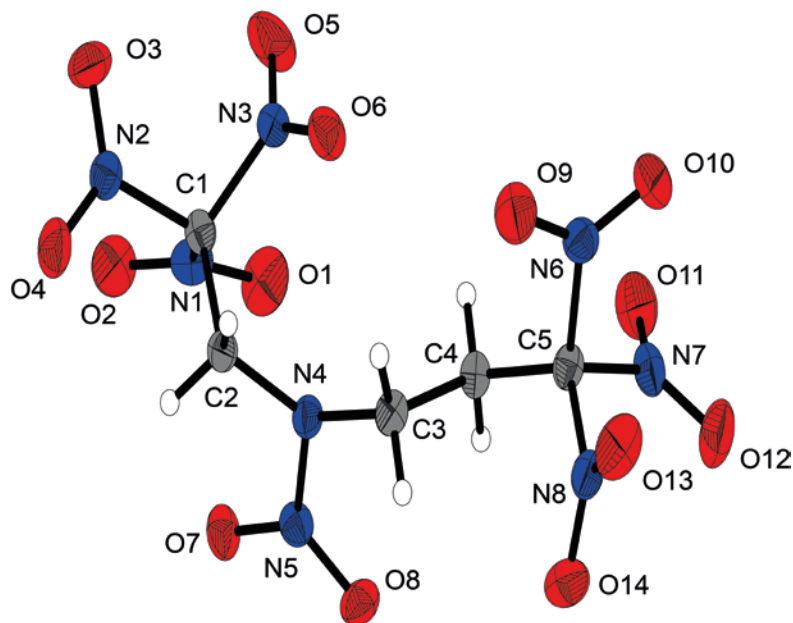


Figure 8-10: X-ray molecular structure of *N*-(2,2,2-trinitroethyl)-*N*-(3,3,3-trinitropropyl) nitramine (10).

Selected bond lengths (Å) and angles (deg): O8–N5 1.219(3), O7–N5 1.234(2), N5–N4 1.370(3), N4–C2 1.447(3), N4–C3 1.469(3), C1–C2 1.527(3), C3–C4 1.540(3), C5–C4 1.509(3), C2–N4–N5 115.6(2), N5–N4–C3 116.5(2), C2–N4–C3 122.0(2), C2–N4–N5–O8 $-159.3(2)$, O7–N5–N4–C3 $175.8(2)$, C5–C4–C3–N4 $-179.6(2)$, N2–C1–C2–N4 $176.8(2)$.

The nitramine **10** crystallizes in the monoclinic space group Pc with glide planes as the only symmetry operation. In the unit cell are two identical formula units (Figure 8-10). The geometric environment of the nitramine shows more a planar structure around the nitrogen atom N4 which is demonstrated by the quite high angle values of 115.6, 116.5 and 122.0 Å. This is achieved by the delocalization of the electron lone pair of the nitrogen atom N4 and is affected by the strong

electron withdrawing effect of the nitro group. Otherwise, the distances, angles and the propeller-like structure are very identical to **9**. Very striking for this structure is the high density of 1.902 g cm^{-3} at 173 K. This is even more remarkable because of the impossibility of forming classical hydrogen bonds. However, for each hydrogen atom a so-called non-classical hydrogen bond of the type $\text{C-H}\cdots\text{O}$ is found, whereat the majority is classified as quite strong.^[23]

8.3.5 Thermal and Energetic Properties

Compounds **4–10** are possible energetic materials and therefore potential high energetic dense oxidizers (HEDO). All molecules are stable when exposed to air and or moisture. Table 8-2 summarizes the physical and thermal properties. Melting points and thermal stabilities were investigated by differential scanning calorimetry (DSC) with a heating rate of $5 \text{ }^\circ\text{C}$ per minute.

Quite high and satisfying melting and decomposition points were observed. For example the oxamide **5** shows the highest decomposition point at $181 \text{ }^\circ\text{C}$. A clear trend that the 3,3,3-trinitropropyl shows higher thermal stability than the 2,2,2-trinitroethyl group, as expected, could be not confirmed. However, in the case of the nitramine **10** the exchange of one ethyl into a propyl group leads to a tremendous difference. **10** shows a $57 \text{ }^\circ\text{C}$ higher decomposition point than the corresponding ethyl derivative bis(2,2,2-trinitroethyl) nitramide.^[24] For a direct comparison with all corresponding 2,2,2-trinitroethyl derivatives see Appendix A.8.

For the manipulation of energetic materials the sensitivity toward impact, friction and electrostatic discharge is especially important. The sensitiveness towards impact (IS) of a compound is tested by the action of a dropping weight on a sample. The friction sensitivity (FS) is determined by rubbing a small amount between a porcelain plate and a pin with different contact pressures.^[25] Some compounds can be classified as sensitive toward friction ($\geq 360 \text{ N}$ insensitive, $360\text{--}80 \text{ N}$ sensitive, $80\text{--}10 \text{ N}$ very sensitive, $\leq 10 \text{ N}$ extremely sensitive), and some are sensitive to impact ($\geq 40 \text{ J}$ insensitive, $40\text{--}35 \text{ J}$ less sensitive, $35\text{--}4 \text{ J}$ sensitive, $\leq 3 \text{ J}$ very sensitive).^[1b, 26] The compounds **9** and **10** take a special position due to their high sensitiveness to impact and are in the range of the well known explosive Hexogen (RDX). The relative ESD sensitivity of an explosive is tested with an apparatus, whereby variable capacitive resistances and loading voltages generates different spark energies. The electric discharge were determined which is needed to initiate a decomposition or an explosion. The lowest value for an initialization was found for the nitramine **10** with an energy of 0.15 J , which is in the range of secondary explosives like PETN and RDX.^[25]

Table 8-2: Physical and chemical properties of 3–10.

	3	4	5	6	7	8
formula	C ₃ H ₅ N ₃ O ₇	C ₇ H ₁₀ N ₈ O ₁₃	C ₈ H ₁₀ N ₈ O ₁₄	C ₈ H ₈ N ₆ O ₁₆	C ₄ H ₆ N ₄ O ₈	C ₄ H ₅ N ₅ O ₁₀
T_m /°C (onset) ^[a]	(liquid)	-	-	121	78	68
T_{dec} /°C (onset) ^[b]	141	160	181	170	152	134
IS /J ^[c]	> 40	20	10	> 40	> 40	> 30
FS /N ^[d]	> 360	120	160	> 360	> 360	360
ESD /J ^[e]	(liquid)	0.40	0.50	0.40	0.30	0.20
N /% ^[f]	21.5	27.1	25.3	18.9	23.5	24.7
O /% ^[g]	57.4	50.2	50.7	57.6	53.8	56.5
$N+O$ /% ^[h]	78.9	77.3	76.0	76.5	77.3	81.2
Ω_{CO} /% ^[i]	+12.3	+3.9	+3.6	+14.4	+6.7	+19.8
Ω_{CO_2} /% ^[j]	-12.3	-20.2	-20.3	-14.4	-20.2	-2.8
	9	10	AP	TNT	RDX	
formula	C ₅ H ₇ N ₇ O ₁₂	C ₅ H ₆ N ₈ O ₁₄	NH ₄ ClO ₄	C ₇ H ₅ N ₃ O ₆	C ₃ H ₆ N ₆ O ₆	
T_m /°C (onset) ^[a]	65	141	-	81	204	
T_{dec} /°C (onset) ^[b]	96	153	240	248	228	
IS /J ^[c]	7	7	20	15	7	
FS /N ^[d]	120	160	360	360	120	
ESD /J ^[e]	0.20	0.15	0.50	0.45	0.20	
N /% ^[f]	27.5	27.9	11.9	18.5	37.8	
O /% ^[g]	53.8	55.7	54.5	42.3	43.2	
$N+O$ /% ^[h]	81.3	83.6	66.4	60.8	81.0	
Ω_{CO} /% ^[i]	+15.7	+23.9	+34.0	-24.7	0.0	
Ω_{CO_2} /% ^[j]	-6.7	+4.0	+34.0	-74.0	-21.6	

[a] Onset melting T_m and [b] onset decomposition point T_{dec} from DSC measurement carried out at a heating rate of 5 °C min⁻¹. [c] Impact sensitivity. [d] Friction sensitivity. [e] Sensitivity towards electrostatic discharge. [f] Nitrogen content. [g] Oxygen content. [h] Sum of nitrogen and oxygen content. [i] Oxygen balance assuming the formation of CO and the formation of the formation of [j] CO₂ at the combustion.

The main performance criteria of energetic materials are the heat of explosion Q_v , the detonation velocity V_{det} and the detonation pressure P_{CJ} . All these detonation and combustion parameters are summarized in Table 8-3 (For further values see Appendix A.8). The performance data were calculated by the computer code EXPLO5 (V.6.02)^[27] and based on the calculated energy of formation using CBS-4 M *ab initio* calculation. The nitramine **10** has the highest energy of formation $\Delta_f U^\circ$ with a value of -79.7 kJ kg⁻¹ which indicates a high energy content in the molecule. This and the high density is reflected by the very high detonation velocity V_{det} of

9119 m s⁻¹ compared to RDX with 8838 m s⁻¹. The other compounds show also quite high detonation velocities V_{det} in the range of 7732 to 8713 m s⁻¹ and they are in the range of well known explosives like PETN (8403 m s⁻¹) and TNT (7241 m s⁻¹).

Another very important value especially for high energetic dense oxidizers is the specific impulse I_{sp} . Oxidizers are the main part in composite propellants and are compounds that release the excess of included oxygen when burned. This oxygen is used for the oxidation of further added fuel to generate a lot of heat and gases for the propulsion. As a effective fuel aluminum is used which has a very high heat of combustion and thereby produces a very hot burning temperature.^[8] Another advantage of aluminum is its low price, the low atomic weight and its nonhazardous combustion product (Al₂O₃). The so generated high burning temperature is important, because the specific impulse I_{sp} is proportional to the square root of the temperature.^[1b] A further important factor is the molecular weight of the gaseous products at the nozzle exit of the rocket chamber which is inverse proportional to the square root.^[1b] This means for high performance a high burning temperature and a low weight of the gaseous products like CO, CO₂, H₂O, and H₂ is required. For the discussion it is important that the payload of the rocket can be doubled if the specific impulse is increased by 20 s. The specific impulses I_{sp} of the compounds **3–10** were calculated neat, with aluminum (15%) and with a binder/aluminum system (16% aluminum, 6% polybutadiene acrylic acid, 6% polybutadiene acrylonitrile and 2% bisphenol A ether). These impulses were compared with the calculated impulse of ammonium perchlorate (AP) in an analogous composition. The specific impulses I_{sp} for the neat compounds show altogether much higher values than AP, which is predictable since the compounds have their own fuel in kind of the carbon-backbone. The neat compounds **9** and **10** shows an impulse of 272 s and 264 s which are already higher than the optimized composite of AP with a value of 261 s. A further advantage of the neat compounds are the burning residues which are not harmful and are just gaseous products which make the RADAR detection of such propulsion system is quite complicated.^[1a] The addition of aluminum (15%) as fuel increases the values for all compounds, whereas the carbamate **7** with 256 s is the lowest and the amine **9** with 274 s is the highest specific impulse. The optimized standard mixture for AP is composed of 71% oxidizer, 15% aluminum and 14% binder. In such a system all impulses decrease which is caused by the rise of the carbon content. Only the nitramine **10** can outperform AP with a value of 267 s in such a binder mixture. Therefore, smaller amounts of binder are better suitable for this type of CHNO oxidizers. For example with only the half of binder the value of the specific impulse of **10** could be enhanced to 275 s.

Table 8-3: Calculated heat of formation, predicted detonation and combustion parameters (using the EXPLO5 V6.02 code) for 4–10.

	4	5	6	7	8	9	10
density RT /g cm ⁻³ [a]	1.75	1.71	1.67	1.73	1.70	1.78	1.89
$\Delta_f H^\circ$ /kJ mol ⁻¹ [b]	-359.1	-522.3	-789.4	-503.5	-401.7	-86.4	-66.8
$\Delta_f U^\circ$ /kJ kg ⁻¹ [c]	-774.1	-1091.5	-1693.5	-2021.0	-1331.3	-151.7	-79.7
Q_v /kJ kg ⁻¹ [d]	-5385	-5095	-5126	-4662	-5809	-6565	-6377
T_{ex} /K [e]	3692	3605	3808	3328	4175	4445	4420
V_0 /L kg ⁻¹ [f]	739	732	724	724	755	738	756
P_{CJ} /kbar [g]	294	268	256	265	269	330	367
V_{det} /m s ⁻¹ [h]	8227	7937	7732	7896	8134	8713	9119
I_{sp} /s [i]	254	245	250	237	256	272	264
I_{sp} /s (15% Al) [j]	267	263	259	256	261	274	269
I_{sp} /s (15% Al, 14% binder) ^[k]	251	245	246	240	253	261	267

[a] RT densities are recalculated from X-ray densities. [b] Enthalpy and [c] energy of formation calculated by the CBS-4 M method using Gaussian 09. [d] Heat of explosion. [e] Explosion temperature. [f] Volume of gaseous products. [g] Detonation pressure and [h] detonation velocity calculated by using the EXPLO5 (Version 6.02) program package.^[27] [i] Specific impulse of the neat compound using the EXPLO5 (Version 6.02) program package at 70.0 bar chamber pressure.^[27] [j] Specific impulse for compositions with 85% oxidizer/compound and 15% aluminum. [k] Specific impulse for compositions with 71% oxidizer/compound, 15% aluminum and 14% binder (6% polybutadiene acrylic acid, 6% polybutadiene acrylonitrile and 2% bisphenol A ether).

8.4 Conclusion

Several compounds with energetic properties based on the 3,3,3-trinitropropyl group were synthesized and thoroughly characterized including X-ray diffraction. The thermal stabilities by different scanning calorimetry (DSC) were measured. In general, the expected higher decomposition points compared to the 2,2,2-trinitroethyl group could not be confirmed, however, some higher stabilities were detected. As well, this is confirmed by the lower sensitivities of the here discussed 3,3,3-trinitropropyl compounds.

With respect to an application as high energy dense oxidizer in composite solid rocket propellants, several energetic performance data were calculated. The best compound with excellent detonation parameters is the nitramine **10**, with a very high detonation velocity of 9119 m s⁻¹ and in addition a strong detonation pressure, both values are significantly above those of TNT, RDX and PETN. Apart from this, **10** seems to serve as a good oxidizer candidate for composite rocket propellants. The specific impulse I_{sp} reaches 269 s within a mixture of 15%

aluminum as fuel, which is an effect of the quite high energy of formation and the positive oxygen balance of Ω_{CO} of +23.9. However, the synthesis of such 3,3,3-trinitropropyl containing materials is more elaborate compared to compounds containing 2,2,2-trinitroethyl groups.

8.5 Experimental Section

8.5.1 General Procedures

All chemicals were used as supplied. Raman spectra were recorded in a glass tube with a Bruker MultiRAM FT-Raman spectrometer with Nd:YAG laser excitation up to 1000 mW at 1064 nm in the range between 400 and 4000 cm^{-1} . Infrared spectra were measured with a Perkin-Elmer Spectrum BX-FTIR spectrometer equipped with a Smiths DuraSamplIR II ATR device. All spectra were recorded at ambient temperature. NMR spectra were recorded with a JEOL Eclipse 400 instrument and chemical shifts were determined with respect to external standards Me_4Si (^1H , 399.8 MHz; ^{13}C , 100.5 MHz) and MeNO_2 (^{15}N , 40.6 MHz; ^{14}N , 28.8 MHz). Mass spectrometric data were obtained with a JEOL MStation JMS 700 spectrometer (DCI+, DEI+). Analysis of C/H/N were performed with an Elemental VarioEL Analyzer. Melting and decomposition points were measured with a Perkin-Elmer Pyris6 DSC and an OZM Research DTA 552-Ex with a heating rate of 5 $^\circ\text{C min}^{-1}$ in a temperature range of 15 to 400 $^\circ\text{C}$ and checked by a Büchi Melting Point B-540 apparatus (not corrected). The sensitivity data were performed using a BAM drophammer and a BAM friction tester.^[26, 28]

8.5.2 X-ray Crystallography

Crystals suitable for X-ray crystallography were selected by means of a polarization microscope, mounted on the tip of a glass fiber. The measurements were investigated with an Oxford XCalibur3 (4, 5, 6, 7, 9, and 10) or a Bruker-Nonius KappaCCD diffractometer (8). The diffractometers are equipped with a generator (voltage 50 kV, current 40 mA) and a KappaCCD detector operating with $\text{MoK}\alpha$ radiation ($\lambda = 0.7107 \text{ \AA}$). The solution of the structure was performed by direct methods (SIR97)^[29] and refined by full-matrix least-squares on F^2 (SHELXL)^[30] implemented in the WINGX software package^[31] and finally checked with the PLATON software^[32]. All non-hydrogen atoms were refined anisotropically. The hydrogen atom positions were located in a difference Fourier map. ORTEP plots are shown with thermal ellipsoids at the 50% probability level. Crystallographic data (excluding structure factors) for the

structures reported in this paper have been deposited at the Cambridge Crystallographic Data Centre (1062382 (4), 1062383 (5), 1062384 (6), 1062385 (7), 1062386 (8), 1062387 (9), 1062388 (10)).

1.5.3 Computational Details

All ab initio calculations were carried out using the program package Gaussian 09 (Rev. A.02)^[33] and visualized by GaussView 5.08.^[34] Structure optimizations and frequency analyses were performed with Becke's B3 three parameter hybrid functional using the LYP correlation functional (B3LYP). For C, H, N and O a correlation consistent polarized double-zeta basis set cc-pVDZ was used. The structures were optimized with symmetry constraints and the energy is corrected with the zero point vibrational energy.^[35] The enthalpies (H) and free energies (G) were calculated using the complete basis set (CBS) method in order to obtain accurate values. The CBS models used the known asymptotic convergence of pair natural orbital expressions to extrapolate from calculations using a finite basis set to the estimated complete basis set limit. CBS-4 M starts with a HF/3-21G(d) geometry optimization, which is the initial guess for the following SCF calculation as a base energy and a final MP2/6-31+G calculation with a CBS extrapolation to correct the energy in second order. The used CBS-4 M method additionally implements a MP4(SDQ)/6-31+(d,p) calculation to approximate higher order contributions and also includes some additional empirical corrections.^[36] The enthalpies of the gas-phase species were estimated according to the atomization energy method.^[37]

All calculations affecting the detonation parameters were carried out using the program package EXPLO5 V6.02.^[27, 38] The detonation parameters were calculated at the Chapman-Jouguet point with the aid of the steady-state detonation model using a modified Becker-Kistiakowski-Wilson equation of state for modeling the system. The CJ point is found from the Hugoniot curve of the system by its first derivative. The specific impulses I_{sp} were also calculated with the EXPLO5 V6.02 program, assuming an isobaric combustion of a composition of 70% oxidizer, 16% aluminum as fuel, 6% polybutadiene acrylic acid, 6% polybutadiene acrylonitrile as binder and 2% bisphenol A ether as epoxy curing agent. A chamber pressure of 70.0 bar and an ambient pressure of 1.0 bar with equilibrium expansion conditions were assumed for the calculations.

8.5.4 Synthesis

CAUTION! All prepared compounds are energetic materials with sensitivity toward heat, impact and friction. No hazards occurred during preparation and manipulation, additional proper protective precautions (face shield, leather coat, earthened equipment and shoes, Kevlar® gloves and ear plugs) should be used when undertaking work with these compounds.

1,1,1-Trinitropropan-3-isocyanate (1). Prepared according to reference.^[4, 11] ¹H NMR (CDCl₃): δ = 3.90 (m, 2H, CH₂), 3.32 (m, 2H, CH₂) ppm; ¹³C NMR (CDCl₃): δ = 127.4 (C(NO₂)₃), 123.6 (NCO), 37.4 (CH₂), 35.0 (CH₂) ppm; ¹⁴N NMR (CDCl₃): δ = -31 (C(NO₂)₃), -360 (NCO) ppm; elemental analysis calcd (%) C₄H₄N₄O₇ (220.10): C 21.83, H 1.83, N 25.46; found: C 21.31, H 1.80, N 26.07; IR (ATR): ν = 3380 (w), 2956 (w), 2897 (w), 2269 (m, ν (NCO)), 2155 (w), 1721 (m), 1584 (s, ν_{as} (NO₂)), 1423 (m), 1364 (m), 1297 (s, ν_s (NO₂)), 1227 (m), 1195 (m), 1148 (m), 1092 (w), 1065 (w), 980 (w), 897 (w), 854 (m), 811 (m), 798 (s), 754 (m), 667 (w) cm⁻¹; Raman (1000 mW): ν = 2953 (70), 2156 (13), 2147 (13), 1718 (11), 1610 (24, ν_{as} (NO₂)), 1451 (18), 1421 (22), 1363 (37), 1304 (30, ν_s (NO₂)), 1100 (10), 1051 (13), 914 (20), 887 (12), 856 (100), 811 (10), 535 (10), 502 (16), 460 (10), 375 (68), 305 (17), 279 (22), 254 (20) cm⁻¹.

3,3,3-Trinitropropan-1-amine hydrochloride (2). Prepared according to reference.^[5b, 11] ¹H NMR (CD₃CN): δ = 7.92 (br, NH₃), 3.69 (m, 2H, CH₂), 3.42 (m, 2H, CH₂) ppm; ¹³C NMR (CD₃CN): δ = 125.7 (C(NO₂)₃), 34.6 (CH₂), 30.8 (CH₂) ppm; ¹⁴N NMR (CD₃CN): δ = -31 (C(NO₂)₃), -349 (NH₃) ppm; elemental analysis calcd (%) C₃H₉N₄O₇ (230.56): C 15.63, H 3.06, N 24.30; found: C 15.94, H 3.06, N 24.30; IR (ATR): ν = 3132 (m), 3101 (m), 3035 (m), 2977 (m), 2890 (m), 2833 (m), 2783 (w), 2705 (w), 2655 (w), 2567 (w), 2500 (w), 1597 (s, ν_{as} (NO₂)), 1499 (w), 1478 (w), 1458 (m), 1425 (w), 1303 (m, ν_s (NO₂)), 999 (w), 973 (w), 954 (w), 895 (w), 790 (w) cm⁻¹; Raman (300 mW): ν = 3038 (9), 2993 (18), 2965 (34), 2937 (37), 2850 (6), 2806 (8), 1606 (45, ν_{as} (NO₂)), 1471 (10), 1434 (12), 1370 (52), 1346 (17), 1312 (26, ν_s (NO₂)), 1301 (23, ν_s (NO₂)), 1162 (12), 1147 (14), 1022 (11), 989 (15), 924 (12), 911 (17), 858 (100), 802 (8), 739 (6), 656 (6), 643 (6), 557 (9), 408 (66), 383 (64), 343 (47), 289 (20), 221 (7) cm⁻¹; IS: 20 J (grain size 100–250 μ m); FS: 360 N (grain size 100–250 μ m); ESD: >0.5 J (grain size 100–250 μ m); ESD >0.4 J (grain size 100–250 μ m); DSC (5 °C min⁻¹, onset): 161 °C (m.p.), 178 °C (dec.).

3,3,3-Trinitropropanol (3). 3,3,3-Trinitropropan-1-amine hydrochloride (2) (1.0 g, 4.3 mmol) was dissolved in water (10 mL) and solution of NaNO₂ (0.60 g, 8.7 mmol) in water (10 mL) was slowly added at 0 °C. The yellow solution was stirred at 0 °C for 1 h and at 60 °C for 1.5 h. The reaction mixture was extracted three times with dichloromethane (3 x 25 mL), washed with brine

(25 mL) and dried over MgSO_4 . After removing the solvent *in vacuo* 3,3,3-trinitropropanol (**3**) was obtained as a slight yellow oil (0.65 g, 78%). ^1H NMR (CDCl_3): $\delta = 4.12$ (m, 2H, CH_2), 3.33 (m, 2H, CH_2), 1.99 (s, 1H, OH) ppm; ^{13}C NMR (CDCl_3): $\delta = 128.1$ ($\text{C}(\text{NO}_2)_3$), 56.5 (CH_2OH), 36.6 (CH_2) ppm; ^{14}N NMR (CDCl_3): $\delta = -30$ (NO_2) ppm; EA: $\text{C}_3\text{H}_5\text{N}_3\text{O}_7$ (195.09): calc. C 18.47, H 2.58, N 21.54 %; found C 18.92, H 2.59, N 21.49%; IR (ATR): $\nu = 3599$ (w), 3385 (br, w, $\nu(\text{OH})$), 2947 (w), 2904 (w), 1581 (s, $\nu_{\text{as}}(\text{NO}_2)$), 1473 (w), 1420 (w), 1368 (m), 1296 (s, $\nu_{\text{s}}(\text{NO}_2)$), 1223 (w), 1140 (w), 1071 (m), 1035 (m), 984 (w), 924 (w), 854 (m), 842 (m), 811 (m), 798 (s), 771 (m) cm^{-1} ; Raman (300 mW): $\nu = 2992$ (60), 2984 (60), 2949 (100), 2913 (41), 1608 (19, $\nu_{\text{as}}(\text{NO}_2)$), 1478 (7), 1458 (9), 1425 (15), 1368 (35), 1350 (23), 1306 (25, $\nu_{\text{s}}(\text{NO}_2)$), 1082 (8), 926 (7), 857 (57), 472 (6), 375 (23), 336 (6) cm^{-1} ; IS: > 40 J; FS: >360 N; DSC (5 $^\circ\text{C min}^{-1}$, onset): 141 $^\circ\text{C}$ (boil. with dec.).

Bis(3,3,3-trinitropropyl) urea (4). 3,3,3-Trinitropropyl-1-isocyanate (**1**) (2.20 g, 10 mmol) was dissolved in a mixture of acetone/water (3:1; 12 mL) and refluxed for 3 h. After evaporating of the solvent *in vacuo* a yellow solid was obtained which was recrystallized from chloroform. Bis(3,3,3-trinitropropyl) urea (**4**) was obtained as a pure colorless solid (1.82 g, 88%). ^1H NMR (CDCl_3): $\delta = 4.58$ (br, 2H, NH), 3.64 (m, 4H, CH_2), 3.35 (m, 4H, CH_2) ppm; ^{13}C NMR ($(\text{CD}_3)_2\text{CO}$): $\delta = 158.5$ (CO), 130.8 ($\text{C}(\text{NO}_2)_3$), 35.9 (CH_2), 35.0 (CH_2) ppm; ^{14}N NMR (CDCl_3): $\delta = -30$ (NO_2) ppm; elemental analysis calcd (%) $\text{C}_7\text{H}_{10}\text{N}_8\text{O}_{13}$ (414.20): C 20.30, H 2.43, N 27.05; found: C 20.32, H 2.36, N 26.80; IR (ATR): $\nu = 3345$ (w), 2945 (w), 2881 (w), 1642 (m, $\nu(\text{CO})$), 1587 (s, $\nu_{\text{as}}(\text{NO}_2)$), 1566 (s), 1460 (w), 1442 (w), 1425 (w), 1392 (w), 1365 (w), 1298 (m, $\nu_{\text{s}}(\text{NO}_2)$), 1262 (m), 1246 (m), 1144 (m), 1101 (w), 1037 (w), 943 (w), 892 (w), 856 (m), 826 (w), 796 (s), 770 (w) cm^{-1} ; Raman (1000 mW): $\nu = 2979$ (35), 2944 (53), 1644 (12, $\nu(\text{CO})$), 1593 (28, $\nu_{\text{as}}(\text{NO}_2)$), 1443 (19), 1427 (24), 1388 (25), 1367 (50), 1309 (33, $\nu_{\text{s}}(\text{NO}_2)$), 1147 (16), 1119 (15), 1045 (30), 977 (10), 924 (14), 896 (14), 859 (100), 800 (10), 769 (9), 635 (14), 597 (11), 518 (19), 406 (53), 376 (51), 278 (34) cm^{-1} ; IS: 20 J (grain size 100–250 μm); FS: 120 N (grain size 100–250 μm); ESD: >0.4 J (grain size 100–250 μm); DSC (5 $^\circ\text{C min}^{-1}$, onset): 160 $^\circ\text{C}$ (dec.).

Bis(3,3,3-trinitropropyl) oxamide (5).^[13] 3,3,3-Trinitropropan-1-amine hydrochloride (**2**) (1.00 g, 4.3 mmol) was dissolved in water (15 mL). The solution was overlaid with diethyl ether (30 mL) and cooled to 0 $^\circ\text{C}$. Sodium hydrogen carbonate (0.40 g, 4.8 mmol) was added in small portions and the mixture was further stirred for 30 min. at 0 $^\circ\text{C}$. The organic layer was separated and the aqueous solution was extracted with diethyl ether (2 x 25 mL). The combined organic phase was dried over MgSO_4 and cooled to 0 $^\circ\text{C}$. Oxalyl chloride (0.20 g, 1.7 mmol) was slowly added to the organic phase. After 20 min the precipitated solid was filtered off, washed with cooled diethyl ether and dried. Bis(3,3,3-trinitropropyl) oxamide (**5**) was obtained as a pure

colorless solid (0.61, 75%). ^1H NMR ($(\text{CD}_3)_2\text{CO}$): $\delta = 8.56$ (br, 2H, NH), 3.83 (m, 4H, CH_2), 3.69 (m, 4H, CH_2) ppm; ^{13}C NMR ($(\text{CD}_3)_2\text{CO}$): $\delta = 160.8$ ($\text{C}(\text{O})\text{O}$), 130.4 ($\text{C}(\text{NO}_2)_3$), 35.0 (CH_2), 33.8 (CH_2) ppm; ^{14}N NMR ($(\text{CD}_3)_2\text{CO}$): $\delta = -29$ (NO_2) ppm; elemental analysis calcd (%) $\text{C}_8\text{H}_{10}\text{N}_8\text{O}_{14}$ (442.21): C 21.73, H 2.28, N 25.34; found: C 21.63, H 2.29, N 25.26; IR (ATR): $\nu = 3273$ (w), 3066 (w), 2949 (w), 2892 (w), 1687 (w), 1659 (m, $\nu(\text{CO})$), 1621 (m), 1583 (s, $\nu_{\text{as}}(\text{NO}_2)$), 1521 (s), 1444 (w), 1423 (w), 1376 (w), 1325 (w), 1297 (m, $\nu_{\text{s}}(\text{NO}_2)$), 1258 (m), 1227 (m), 1147 (w), 1112 (w), 1053 (w), 1029 (w), 939 (w), 857 (w), 825 (m), 798 (m), 781 (m), 751 (w), 725 (w) cm^{-1} ; Raman (300 mW): $\nu = 3298$ (7), 3282 (8), 3025 (10), 2985 (24), 2950 (67), 1694 (41, $\nu(\text{CO})$), 1607 (22, $\nu_{\text{as}}(\text{NO}_2)$), 1561 (18), 1447 (18), 1430 (19), 1367 (39), 1336 (22), 1299 (40, $\nu_{\text{s}}(\text{NO}_2)$), 1244 (17), 1117 (10), 1050 (22), 947 (16), 885 (18), 859 (100), 801 (12), 750 (7), 648 (8), 584 (12), 515 (9), 452 (11), 422 (28), 397 (37), 382 (54), 309 (9), 275 (35), 229 (14) cm^{-1} ; IS: 10 J (grain size 100–250 μm); FS: 160 N (grain size 100–250 μm); ESD: >0.5 J (grain size 100–250 μm); DSC (5 $^\circ\text{C min}^{-1}$, onset): 181 $^\circ\text{C}$ (dec.).

Bis(3,3,3-trinitropropyl) oxalate (6): 3,3,3-Trinitropropanol (**3**) (0.50 g, 2.6 mmol) was added slowly at 0 $^\circ\text{C}$ to a solution of oxalyl chloride (0.16 g, 1.3 mmol) in THF (10 mL). The reaction mixture was stirred for 1 h at 25 $^\circ\text{C}$ and refluxed for further 16 h. The reaction mixture was cooled and the solvent was removed *in vacuo*. The crude solid product was recrystallization from acetone yielding pure bis(3,3,3-trinitropropyl) oxalate (**6**) (0.50 g, 87%) as a colorless solid. ^1H NMR ($(\text{CD}_3)_2\text{CO}$): $\delta = 4.83$ (m, 2H, CH_2), 4.02 (m, 2H, CH_2) ppm; ^{13}C NMR ($(\text{CD}_3)_2\text{CO}$): $\delta = 156.3$ ($\text{C}(\text{O})\text{O}$), 129.8 ($\text{C}(\text{NO}_2)_3$), 60.6 (CH_2O), 33.2 (CH_2) ppm; ^{14}N NMR ($(\text{CD}_3)_2\text{CO}$): $\delta = -30$ (NO_2) ppm; elemental analysis calcd (%) $\text{C}_8\text{H}_8\text{N}_6\text{O}_{16}$ (444.18): C 21.63, H 1.82, N 18.92; found: C 22.01, H 1.91, N 18.62; IR (ATR): $\nu = 2998$ (w), 2960 (w), 1764 (m, $\nu(\text{CO})$), 1753 (m), 1600 (s, $\nu_{\text{as}}(\text{NO}_2)$), 1580 (s), 1463 (w), 1412 (w), 1387 (w), 1373 (w), 1296 (m, $\nu_{\text{s}}(\text{NO}_2)$), 1261 (w), 1244 (w), 1193 (s), 1143 (w), 1105 (w), 1043 (m), 922 (w), 854 (w), 832 (w), 801 (m), 792 (m), 765 (m), 660 (w) cm^{-1} ; Raman (300 mW): $\nu = 3029$ (16), 2998 (46), 2982 (58), 2959 (77), 2905 (11), 1769 (51, $\nu(\text{CO})$), 1615 (25, $\nu_{\text{as}}(\text{NO}_2)$), 1597 (22), 1462 (17), 1415 (21), 1377 (32), 1352 (15), 1292 (29, $\nu_{\text{s}}(\text{NO}_2)$), 1246 (14), 1107 (12), 1053 (23), 938 (22), 923 (24), 855 (100), 821 (10), 801 (8), 767 (7), 632 (8), 510 (11), 466 (15), 416 (41), 391 (64), 368 (58), 323 (8), 258 (18), 230 (15) cm^{-1} ; IS: > 40 J (grain size <100 μm); FS: >360 N (grain size <100 μm); ESD: >0.4 J (grain size <100 μm); DSC (5 $^\circ\text{C min}^{-1}$, onset): 121 $^\circ\text{C}$ (melt.), 170 $^\circ\text{C}$ (dec.).

3,3,3-Trinitropropyl carbamate (7): 3,3,3-Trinitropropanol (**3**) (1.20 g, 6.1 mmol) was dissolved in dry acetonitrile (20 mL) and cooled to 0 $^\circ\text{C}$. Chlorosulfonyl isocyanate (CSI, 0.95 g, 6.7 mmol) was added slowly. The ice bath was removed and stirring at room temperature was continued for

1 h. The reaction mixture was again cooled with an ice bath and water (10 mL) was added with caution. The reaction mixture was stirred further 10 min at room temperature to complete hydrolysis. The organic solvent was removed *in vacuo* and the formed precipitate was filtered. The light yellow precipitate was recrystallized from a mixture of ethanol and water (7:1) and colorless 3,3,3-trinitropropyl carbamate (**7**) was obtained (1.06 g, 82%). ^1H NMR ($(\text{CD}_3)_2\text{CO}$): δ = 6.07 (br, NH_2), 4.51 (m, 2H, CH_2O), 3.78 (m, 2H, CH_2) ppm; ^{13}C NMR ($(\text{CD}_3)_2\text{CO}$): δ = 156.5 (CO), 130.1 ($\text{C}(\text{NO}_2)_3$), 58.0 (CH_2O), 34.3 (CH_2) ppm; ^{14}N NMR ($(\text{CD}_3)_2\text{CO}$): δ = -29 (NO_2), -311 (NH_2) ppm; elemental analysis calcd (%): $\text{C}_4\text{H}_6\text{N}_4\text{O}_8$ (238.11): C 20.18, H 2.54, N 23.53; found: C 20.10, H 2.63, N 23.22; IR (ATR): ν = 3393 (w), 3334 (w), 3275 (w), 3197 (w), 2985 (w), 1751 (w), 1704 (m, $\nu(\text{CO})$), 1608 (m), 1583 (s, $\nu_{\text{as}}(\text{NO}_2)$), 1469 (w), 1410 (m), 1371 (w), 1353 (m), 1332 (m), 1298 (m, $\nu_{\text{s}}(\text{NO}_2)$), 1132 (m), 1103 (m), 1081 (s), 976 (m), 934 (w), 893 (w), 854 (w), 819 (m), 800 (m), 780 (m), 758 (w), 673 (w) cm^{-1} ; Raman (500 mW): ν = 3264 (5), 3196 (6), 3021 (15), 2993 (39), 2949 (60), 1699 (15, $\nu(\text{CO})$), 1617 (36, $\nu_{\text{as}}(\text{NO}_2)$), 1589 (24), 1471 (13), 1414 (20), 1373 (47), 1339 (19), 1299 (25, $\nu_{\text{s}}(\text{NO}_2)$), 1282 (24), 1141 (20), 1104 (11), 1018 (11), 978 (23), 936 (25), 895 (24), 855 (100), 820 (12), 802 (11), 758 (11), 670 (10), 654 (10), 633 (12), 542 (19), 508 (21), 475 (23), 416 (55), 396 (68), 373 (83), 291 (17) cm^{-1} ; IS: > 40 J (grain size 500–1000 μm); FS: >360 N (grain size 500–1000 μm); ESD: >0.3 J (grain size 500–1000 μm); DSC (5 $^\circ\text{C}$ min^{-1} , onset): 78 $^\circ\text{C}$ (melt.)(82 $^\circ\text{C}$ Lit.)^[14], 152 $^\circ\text{C}$ (dec.).

3,3,3-Trinitropropyl nitrocarbamate (8). Nitric acid (100%, 2 mL) was dropped into concentrated sulfuric acid (2 mL) at 0 $^\circ\text{C}$. Into this nitration mixture chilled in an ice bath, **7** (0.48 g, 2.0 mmol) was added in small portions. The suspension was stirred for 10 min. at 0 $^\circ\text{C}$ and one hour at ambient temperature. The nitration mixture was poured onto ice-water (200 mL), extracted with ethyl acetate (3 x 50 mL) and the combined organic phases were dried over magnesium sulfate. The solvent was removed under reduced pressure and the crude solid product was recrystallized from carbon tetrachloride to obtain 0.37 g (65%) colorless 3,3,3-trinitropropyl nitrocarbamate (**8**). ^1H NMR ($(\text{CD}_3)_2\text{CO}$): δ = 13.6 (br, NH), 4.80 (m, 2H, CH_2O), 3.98 (m, 2H, CH_2) ppm; ^{13}C NMR ($(\text{CD}_3)_2\text{CO}$): δ = 148.7 (CO), 129.9 (br, $\text{C}(\text{NO}_2)_3$), 60.3 (CH_2O), 33.6 (CH_2) ppm; ^{14}N NMR ($(\text{CD}_3)_2\text{CO}$): δ = -29 (NO_2), -46 (NO_2) ppm; elemental analysis calcd (%): $\text{C}_4\text{H}_5\text{N}_5\text{O}_{10}$ (283.11): C 16.97, H 1.78, N 24.74; found: C 16.89, H 1.87, N 24.33; IR (ATR): ν = 3134 (w), 3037 (w), 2895 (w), 1758 (m, $\nu(\text{CO})$), 1590 (s, $\nu_{\text{as}}(\text{NO}_2)$), 1458 (m), 1410 (w), 1390 (w), 1367 (w), 1334 (m), 1291 (m, $\nu_{\text{s}}(\text{NO}_2)$), 1255 (m), 1175 (s), 1099 (m), 1046 (m), 1001 (m), 921 (m), 851 (m), 798 (s), 749 (m), 736 (m) cm^{-1} ; Raman (500 mW): ν = 3149 (6), 2994 (35), 2958 (55), 1760 (41, $\nu(\text{CO})$), 1617 (32, $\nu_{\text{as}}(\text{NO}_2)$), 1455 (24), 1413 (24), 1370 (43), 1330 (49), 1307 (30, $\nu_{\text{s}}(\text{NO}_2)$), 1290 (31, $\nu_{\text{s}}(\text{NO}_2)$), 1255 (11), 1182 (12), 1152 (6), 1103 (13), 1049 (35), 996 (50), 935

(25), 855 (100), 802 (10), 765 (8), 738 (11), 659 (8), 633 (8), 529 (17), 484 (20), 459 (30), 425 (33), 383 (62), 307 (17), 250 (23), 206 (32) cm^{-1} ; IS: 30 J (grain size $<100 \mu\text{m}$); FS: 288 N (grain size $<100 \mu\text{m}$); ESD: $>0.2 \text{ J}$ (grain size $<100 \mu\text{m}$); DSC ($5 \text{ }^\circ\text{C min}^{-1}$, onset): $68 \text{ }^\circ\text{C}$ (melt.), $134 \text{ }^\circ\text{C}$ (dec.).

3,3,3-Trinitro-*N*-(2,2,2-trinitroethyl)propan-1-amine (9).^[4-5] 2,2,2-trinitroethanol (0.41 g, 2.2 mmol) was dissolved in water (20 mL) and added to a solution of **2** (0.50 g, 2.2 mmol) in water (5 mL). Another solution of sodium hydroxide (1 mL, 2m) was added and the reaction mixture was stirred at $25 \text{ }^\circ\text{C}$ for 1 h. The precipitated solid was filtered off, washed with small portions of cold water, dried and stored in the desiccator. 3,3,3-Trinitro-*N*-(2,2,2-trinitroethyl)propan-1-amine (**9**) was obtained as a yellow solid (0.49 g, 63%). $^1\text{H NMR}$ (CDCl_3): $\delta = 4.15$ (m, 2H, CH_2), 3.24 (m, 2H, CH_2), 3.15 (m, 2H, CH_2), 2.16 (m, 1H, NH) ppm; $^{13}\text{C NMR}$ (CDCl_3): $\delta = 128.0$ ($\text{C}(\text{NO}_2)_3$), 126.9 ($\text{C}(\text{NO}_2)_3$), 52.6, 44.5, 34.9 ppm; $^{14}\text{N NMR}$ (CDCl_3): $\delta = -31$ (NO_2), -32 (NO_2) ppm; elemental analysis calcd (%): $\text{C}_5\text{H}_7\text{N}_7\text{O}_{12}$ (357.15): C 16.82, H 1.98, N 27.45; found: C 16.68, H 2.12, N 27.08; IR (ATR): $\nu = 3366$ (w), 2945 (w), 2880 (w), 1581 (s, $\nu_{\text{as}}(\text{NO}_2)$), 1479 (w), 1416 (w), 1367 (w), 1302 (s, $\nu_{\text{s}}(\text{NO}_2)$), 1236 (w), 1185 (w), 1132 (m), 1039 (w), 901 (w), 878 (w), 856 (w), 829 (w), 800 (s), 766 (m), 655 (w) cm^{-1} ; Raman (700 mW): $\nu = 2983$ (17), 2952 (31), 2881 (12), 1604 (21, $\nu_{\text{as}}(\text{NO}_2)$), 1474 (11), 1420 (9), 1373 (29), 1348 (16), 1309 (27, $\nu_{\text{s}}(\text{NO}_2)$), 1151 (10), 1001 (6), 933 (6), 859 (87), 800 (5), 646 (10), 543 (13), 405 (47), 376 (62), 313 (9), 273 (5), 244 (7) cm^{-1} ; IS: 7 J (grain size 100–250 μm); FS: 120 N (grain size 100–250 μm); ESD: $>0.4 \text{ J}$ (grain size 100–250 μm); DSC ($5 \text{ }^\circ\text{C min}^{-1}$, onset): $44 \text{ }^\circ\text{C}$ (phase trans.), $65 \text{ }^\circ\text{C}$ (melt.), $96 \text{ }^\circ\text{C}$ (dec.).

***N*-(2,2,2-Trinitroethyl)-*N*-(3,3,3-trinitropropyl) nitramine (10).** The synthesis is according to the literature procedure^[4] with minor changes. Acetic anhydride (1.4 mL, 14.8 mmol) was added to 100% nitric acid (1.4 mL, 33.6 mmol) at $0 \text{ }^\circ\text{C}$. The amine **9** (240 mg, 0.7 mmol) was added and the mixture was allowed to warm to $30 \text{ }^\circ\text{C}$ until **9** was completely dissolved (1.5 h). After 15 h at $25 \text{ }^\circ\text{C}$ the reaction mixture was poured onto ice water (25 mL). The precipitated solid was filtered, washed with water and dried. *N*-(2,2,2-Trinitroethyl)-*N*-(3,3,3-trinitropropyl) nitramine (**10**) was obtained as a colorless solid (204 mg, 75%). NMR (CD_3CN): $\delta = 5.59$ (s, 2H, CH_2), 4.27 (m, 2H, CH_2), 3.65 (m, 2H, CH_2) ppm; $^{13}\text{C NMR}$ (CD_3CN): $\delta = 129.4$ ($\text{C}(\text{NO}_2)_3$), 124.2 ($\text{C}(\text{NO}_2)_3$), 55.2, 49.5, 31.6 ppm; $^{15}\text{N NMR}$ (CD_3CN): $\delta = -31.0$ (t, $^3J = 2.8 \text{ Hz}$, $\text{C}(\text{NO}_2)_3$), -32.9 (m, NNO_2), -34.5 (t, $^3J = 1.9 \text{ Hz}$, $\text{C}(\text{NO}_2)_3$), -213.7 (m, NNO_2) ppm; elemental analysis calcd (%): $\text{C}_5\text{H}_6\text{N}_8\text{O}_{14}$ (402.15): C 14.93, H 1.50, N 27.86; found: C 15.02, H 1.55, N 27.58%; IR (ATR): $\nu = 3020$ (w), 1599 (s, $\nu_{\text{as}}(\text{NO}_2)$), 1555 (s, $\nu_{\text{as}}(\text{NO}_2)$), 1454 (w), 1412 (w), 1395 (w), 1342 (w), 1285 (s, $\nu_{\text{s}}(\text{NO}_2)$), 1268 (s, $\nu_{\text{s}}(\text{NO}_2)$), 1208 (w), 1138 (w), 1062 (w), 1007 (w), 876 (w), 858 (m), 799 (s), 780 (m), 763

(m), 662 (w) cm^{-1} ; Raman (300 mW): $\nu = 3046$ (11), 3020 (15), 3000 (19), 2977 (36), 2958 (41), 1613 (35, $\nu_{\text{as}}(\text{NO}_2)$), 1456 (9), 1429 (7), 1413 (10), 1396 (15), 1386 (18), 1367 (20), 1345 (40), 1294 (23, $\nu_{\text{s}}(\text{NO}_2)$), 1270 (25, $\nu_{\text{s}}(\text{NO}_2)$), 1063 (9), 1049 (12), 989 (7), 919 (12), 877 (26), 858 (100), 640 (10), 599 (7), 549 (9), 452 (8), 428 (16), 408 (41), 391 (37), 375 (34), 364 (40), 294 (25), 235 (11) cm^{-1} ; IS: 7 J (grain size 100–250 μm); FS: 160 N (grain size 100–250 μm); ESD: >0.4 J (grain size 100–250 μm); DSC (5 $^{\circ}\text{C min}^{-1}$, onset): 141 $^{\circ}\text{C}$ (melt.), 153 $^{\circ}\text{C}$ (dec.).

8.6 References

- [1] a) Q. Zhang, J. Zhang, D. A. Parrish, J. M. Shreeve, *Chem. – Eur. J.* **2013**, *19*, 11000–11006; b) T. M. Klapötke, *Chemistry of High-Energy Materials*, 2nd ed., deGruyter, Berlin, **2012**.
- [2] a) Q. J. Axthammer, T. M. Klapötke, B. Krumm, R. Moll, S. F. Rest, *Z. Anorg. Allg. Chem.* **2014**, *640*, 76–83; b) A. S. Ermakov, P. V. Bulatov, D. B. Vinogradov, V. A. Tartakovskii, *Russ. J. Org. Chem.* **2004**, *40*, 1062–1063; c) T. M. Klapötke, B. Krumm, R. Moll, S. F. Rest, W. Schnick, M. Seibald, *J. Fluorine Chem.* **2013**, *156*, 253–261.
- [3] a) H. Feuer, T. Kucera, *J. Org. Chem.* **1960**, *25*, 2069–2070; b) W. H. Gilligan, S. L. Stafford, *Synthesis* **1979**, 600–602.
- [4] M. B. Frankel, *Tetrahedron* **1963**, *19*, 213–217.
- [5] a) M. B. Frankel, K. Klager, *J. Chem. Eng. Data* **1962**, *7*, 412–413; b) M. H. Gold, M. B. Frankel, G. B. Linden, K. Klager, *J. Org. Chem.* **1962**, *27*, 334–336.
- [6] a) M. Göbel, T. M. Klapötke, *Z. Anorg. Allg. Chem.* **2007**, *633*, 1006–1017; b) NASA, Space Shuttle News Reference, **1981**, p. 306; c) NASA, http://www.nasa.gov/pdf/203212main_sts122_presskit2.pdf (10/2015), p. 118.
- [7] J. Akhavan, *The Chemistry of Explosives*, 2nd ed., Royal Soc. of Chemistry, Cambridge, **2004**.
- [8] A. M. Mebel, M. C. Lin, K. Morokuma, C. F. Melius, *J. Phys. Chem.* **1995**, *99*, 6842–6848.
- [9] C. Hogue, *Chem. Eng. News* **2011**, *89*, 6.
- [10] a) J. Dumont, The Effects of Ammonium Perchlorate on Reproduction and Development of Amphibians, <http://www.dtic.mil/cgi-bin/GetTRDoc?Location=U2&doc=GetTRDoc.pdf&AD=ADA495519> (12/2015), **2008**; b) E. D. McLanahan, M. E. Andersen, J. L. Campbell, J. W. Fisher, *Environ. Health Perspect.* **2009**, *117*, 731–738.
- [11] Q. J. Axthammer, C. Evangelisti, T. M. Klapötke, R. Meyer, *New Trends Res. Energ. Mater., Proc. Semin., 17th* **2014**, *2*, pp. 549–562.
- [12] W. M. Koppes, M. E. Sitzmann, H. G. Adolph, *J. Chem. Eng. Data* **1986**, *31*, 119–123.
- [13] M. B. Frankel **1961**, US 3000945.
- [14] M. E. Sitzmann, R. D. Gilardi, *J. Fluorine Chem.* **1993**, *63*, 203–215.
- [15] a) R. Graf, *Angew. Chem., Int. Ed.* **1968**, *7*, 172–182; b) J. K. Rasmussen, A. Hassner, *Chem. Rev. (Washington, DC, U. S.)* **1976**, *76*, 389–408; c) Q. J. Axthammer, B. Krumm, T. M. Klapötke, *Eur. J. Org. Chem.* **2015**, *2015*, 723–729.
- [16] Q. J. Axthammer, T. M. Klapötke, B. Krumm, R. Moll, S. F. Rest, *Z. Anorg. Allg. Chem.* **2014**, *640*, 76–83.
- [17] a) S. V. Lieberman, E. C. Wagner, *J. Org. Chem.* **1949**, *14*, 1001–1012; b) H. Feuer, G. B. Bachman, C. R. Koller, W. A. Swarts, *Tetrahedron* **1963**, *19*, 165–176.
- [18] S. Bienz, L. Bigler, T. Fox, M. Hesse, H. Meier, B. Zeeh, *Spektroskopische Methoden in der Organischen Chemie*, 8th ed., Thieme, Stuttgart, **2014**.
- [19] Y. Oyumi, T. B. Brill, A. L. Rheingold, *J. Phys. Chem.* **1985**, *89*, 4824–4828.

- [20] T. M. Klapötke, B. Krumm, R. Moll, S. F. Rest, Y. V. Vishnevskiy, C. Reuter, H.-G. Stammer, N. W. Mitzel, *Chem. – Eur. J.* **2014**, *20*, 12962–12973.
- [21] a) T. M. Klapötke, B. Krumm, S. F. Rest, M. Sućeska, *Z. Anorg. Allg. Chem.* **2014**, *640*, 84–92; b) A. Baumann, A. Erbacher, C. Evangelisti, T. M. Klapötke, B. Krumm, S. F. Rest, M. Reynders, V. Sproll, *Chem. – Eur. J.* **2013**, *19*, 15627–15638.
- [22] C. Romers, *Acta Crystallogr.* **1953**, *6*, 429.
- [23] T. Steiner, *Angew. Chem., Int. Ed.* **2002**, *41*, 48–76.
- [24] D. A. Nesterenko, V. A. Garanin, A. I. Kazakov, A. G. Korepin, L. B. Romanova, *Russ. J. Phys. Chem. B* **2014**, *8*, 701–711.
- [25] R. Meyer, J. Köhler, A. Homburg, *Explosives*, Wiley-VCH, Weinheim, **2007**.
- [26] *Commission communication in the framework of the implementation of the Council Directive 93/15/EEC of 5 April 1993 on the harmonisation of the provisions relating to the placing on the market and supervision of explosives for civil uses, Vol. 221*, **2006**.
- [27] M. Sućeska, *EXPLO5 V.6.02*, Zagreb, **2013**.
- [28] M. Göbel, T. M. Klapötke, *Adv. Funct. Mater.* **2009**, *19*, 347–365.
- [29] A. Altomare, M. C. Burla, M. Camalli, G. L. Cascarano, C. Giacovazzo, A. Guagliardi, A. G. G. Moliterni, G. Polidori, R. Spagna, *J. Appl. Crystallogr.* **1999**, *32*, 115–119.
- [30] a) G. M. Sheldrick, *SHELX-97, Programs for Crystal Structure Determination*, **1997**; b) G. M. Sheldrick, *Acta Crystallogr., Sect. A: Found. Crystallogr.* **2008**, *A64*, 112–122.
- [31] L. Farrugia, *J. Appl. Crystallogr.* **1999**, *32*, 837–838.
- [32] A. Spek, *Acta Crystallogr., Sect. D: Biol. Crystallogr.* **2009**, *65*, 148–155.
- [33] M. J. Frisch, G. W. Trucks, H. B. Schlegel, G. E. Scuseria, M. A. Robb, J. R. Cheeseman, V. B. G. Scalmani, B. Mennucci, G. A. Petersson, H. Nakatsuji, M. Caricato, X. Li, H. P. Hratchian, A. F. Izmaylov, J. Bloino, G. Zheng, J. L. Sonnenberg, M. Hada, M. Ehara, K. Toyota, R. Fukuda, J. Hasegawa, M. Ishida, T. Nakajima, Y. Honda, O. Kitao, H. Nakai, T. Vreven, J. J. A. Montgomery, J. E. Peralta, F. Ogliaro, M. Bearpark, J. J. Heyd, E. Brothers, K. N. Kudin, V. N. Staroverov, R. Kobayashi, J. Normand, K. Raghavachari, A. Rendell, J. C. Burant, S. S. Iyengar, J. Tomasi, M. Cossi, N. Rega, J. M. Millam, M. Klene, J. E. Knox, J. B. Cross, V. Bakken, C. Adamo, J. Jaramillo, R. Gomperts, R. E. Stratmann, O. Yazyev, A. J. Austin, R. Cammi, C. Pomelli, J. W. Ochterski, R. L. Martin, K. Morokuma, V. G. Zakrzewski, G. A. Voth, P. Salvador, J. J. Dannenberg, S. Dapprich, A. D. Daniels, Ö. Farkas, J. B. Foresman, J. V. Ortiz, J. Cioslowski, D. J. Fox, *Gaussian 09*, Rev. A.02 ed., Gaussian, Inc., Wallingford CT, **2009**.
- [34] R. D. Dennington, T. A. Keith, J. M. Millam, *GaussView*, Ver. 5.08 ed., Semichem, Inc., Wallingford CT, **2009**.
- [35] J. A. Montgomery, M. J. Frisch, J. W. Ochterski, G. A. Petersson, *J. Chem. Phys.* **2000**, *112*, 6532–6542.
- [36] J. W. Ochterski, G. A. Petersson, J. A. Montgomery, *J. Chem. Phys.* **1996**, *104*, 2598–2619.
- [37] E. F. C. Byrd, B. M. Rice, *J. Phys. Chem.* **2005**, *110*, 1005–1013.
- [38] M. Sućeska, *Propellants, Explos., Pyrotech.* **1991**, *16*, 197–202.

9 New FOX-7 Derivatives

unpublished results

NEW CHEMISTRY WITH 1,1-DIAMINO-2,2-DINITROETHENE (FOX-7)

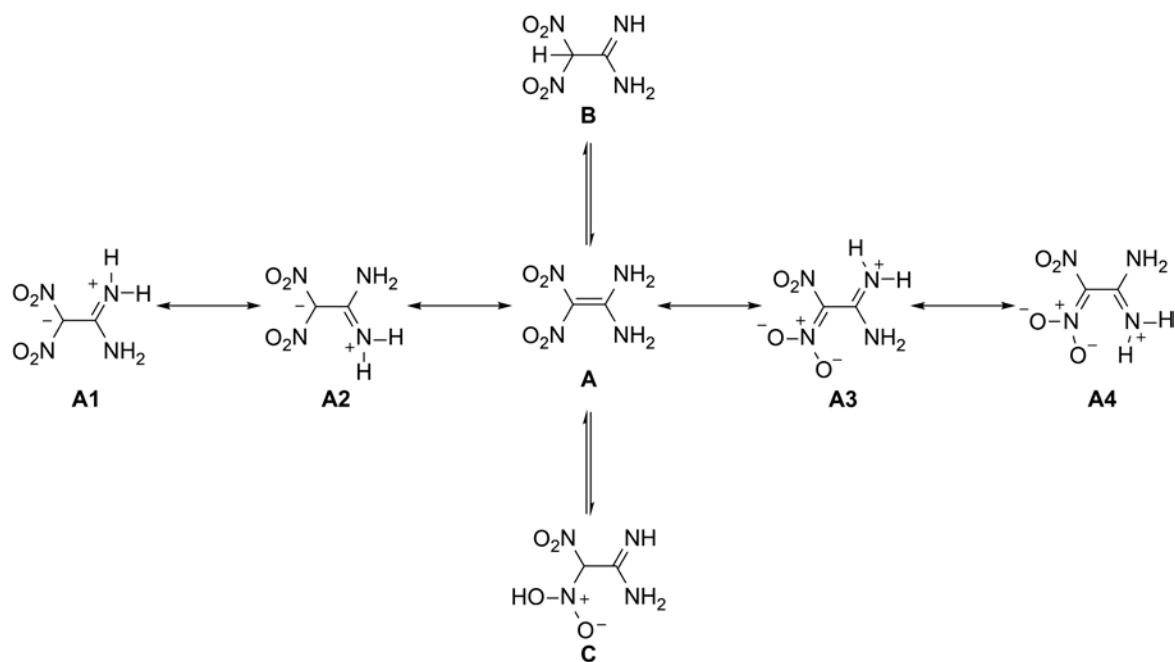


9.1 Abstract

1,1-Diamino-2,2-dinitroethene (FOX-7) is a relatively new high energetic material, with good explosive performance and a low sensitivity against mechanical stimuli and thermal stress. Therefore, FOX-7 is very stable and thus a less reactive starting material. On the other hand chlorosulfonyl isocyanate ClSO₂NCO (CSI), is a very reactive reagent and is the analog form of a highly activated isocyanic acid HNCO. New derivatives of FOX-7 and its hydrazine analog, 1-amino-1-hydrazino-2,2-dinitroethene (HFOX), along with their synthesis and the full characterization are described. Furthermore, the structures of all compounds were investigated and discussed by single-crystal X-ray diffraction. The compounds demonstrate good thermal stabilities, very high densities and excellent sensitivity values. The heats of formations have been calculated using Gaussian 09 (Revision A02) and together with the room temperature densities the energetic parameters were estimated using the EXPLO5 V.6.02 computer code. The compounds are potential candidates as insensitive high-energy-density materials (HEDM) and starting materials for reams of new ones.

9.2 Introduction

1,1-Diamino-1,1-dinitroethene (FOX-7) was first mentioned in 1998 and is therefore a relatively new highly energetic dense molecule.^[1] FOX-7 has captured an important role in the research of energetic materials, due to its thermal stability and its insensitivity to impact and friction, while the performance exhibits the currently used common secondary explosives RDX (Hexogen, Cyclotrimethyltrinitramin) and PETN (Pentaerythritol tetranitrate).^[2] The structural features of FOX-7 are the alternating amino and nitro groups in the solid state structure. This special arrangement and the associated high grade of hydrogen bonds causes an extremely insensitive energetic material.^[3] The location of two electron-donating, NH₂ groups on one carbon, and two electron-withdrawing NO₂ groups on the other carbon make FOX-7 a good example of a push-pull alkene with strong polarization of the double bond.^[4] The molecule can be seen as a resonance hybrid between the mesomeric structures **A**, **A1**, **A2**, **A3**, and **A4** and the tautomers **B** and **C** (Scheme 9-1). The main consequences of this polarization are (1) the carbon bearing the amino groups are relatively electron deficient and susceptible to attack by nucleophiles, (2) the hydrogen atoms are more acidic than those of simple amines, and (3) the amine nitrogen atoms are poor nucleophiles.^[4]



Scheme 9-1: Resonance hybrid structures of FOX-7.

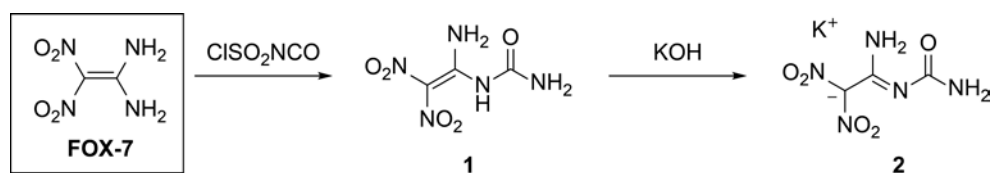
All of these aspects make the chemistry of FOX-7 unpredictable.^[4] Furthermore, the reactivity is low and the three possible active sites of this quite small molecule makes syntheses starting with FOX-7 extremely challenging.^[5] Consequently, the three types of reactions are: (1) nucleophilic substitution on the NH_2 groups, (2) reaction with the double bond and (3) electrophilic attacks on either the amino groups or the negatively charged carbon atom.^[6] In spite of that, rather a broad range of chemical reactions are reported, including alkylation, acylation, acetylation, coordination, halogenation, transamination, nitration and salification.^[6]

In an ongoing effort to seek less sensitive, powerful, green explosives the modification of the molecular structure of FOX-7 could be a promising route, to obtain new insensitive energetic materials. The enlargement of the planar π -system of FOX-7 with a carbamoyl group ($-\text{CONH}_2$) should be lead to a further improvement of the structure and enhance the stability. Additionally, the ability for the building up of hydrogen bonds is increased, due to added donor and acceptors groups. But what influence does this have on the physical properties and the explosive performance?

9.3 Results and Discussion

9.3.1 Synthesis

The lone pair electrons of the two amino groups make FOX-7 act as a nucleophilic molecule which undergo nucleophilic addition reactions. However, the nucleophilicity of FOX-7 is not very high therefore it reacts only with strong electrophilic reagents. An indication of the low reactivity of the amino nitrogen atoms is the low conversion rate with acetyl chloride or methyl isocyanate. Although in the presence of the catalyst hafnium triflate pure acetyl chloride reacts with FOX-7 only with 23% yield to the mono-*N*-acetyl product.^[7] For the conversion or implementation of an urea moiety to the FOX-7 structure only highly activated reagents would be considered. For this reason FOX-7 shows neither reactions with urea or ethyl carbamate in form of a nucleophilic substitution (transamination) nor nucleophilic addition to the isocyanic acid (HNCO) to form 1-(1-amino-2,2-dinitrovinyl)urea (**1**).



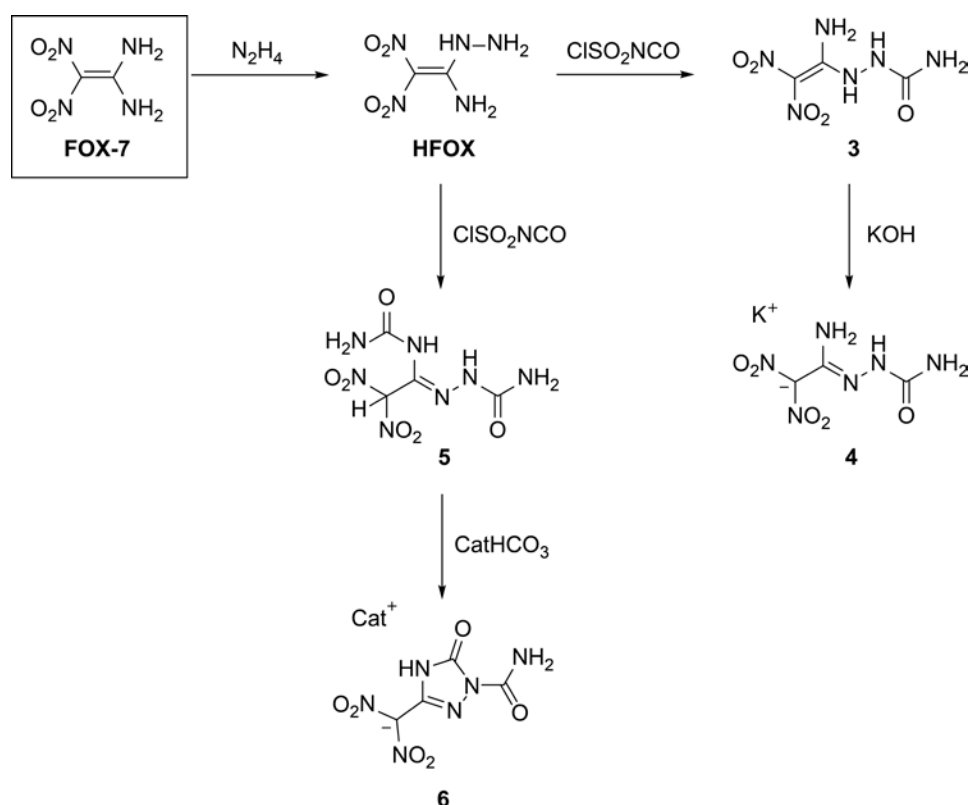
Scheme 9-2: Synthesis of 1-(1-amino-2,2-dinitrovinyl)urea (**1**) and its potassium salt (**2**).

First achievements were obtained with the two extremely activated isocyanates trichloroacetyl isocyanate (TAI) and chlorosulfonyl isocyanate (CSI). Both reagents are easy-to-handle liquids, which quickly react with nucleophiles mostly already at low temperatures.^[8] Advantageously is also the formation of a trichloroacetyl, respectively chlorosulfonyl intermediate, which prevent multiaddition during the reaction time. The new formed urea derivative is released by aqueous work-up of the reaction mixture.^[8d, 9] However, the expense of this TAI reagent prompted the use of the reagent chlorosulfonyl isocyanate (CSI) which is inexpensive and more activated, due to the strong electron withdrawing chlorosulfonyl group.^[8c, 8d]

During experiments with CSI and FOX-7, it became clear that the order of addition, the temperature, as well as the dilution are very critical parameters for a successful preparation of **1**. Furthermore, slow addition of CSI to FOX-7 resulted in the formation of different side products, by the reaction with the second active side the chlorosulfonyl group of CSI. This problem was overcome by rapid addition of the CSI reagent. A more practical solution was to adopt an inverse addition protocol with a quite large excess of the CSI reagent. This method reproducibly

afforded clean conversion of **1** (Scheme 9-2). The hydrolysis of the chlorosulfonyl intermediate was done upon addition of water to the reaction mixture. Subsequent concentration of the organic solvents and simple filtration allowed the isolation of pure **1** in a yield of 72%. No reaction of both amino groups of FOX-7 at any conditions could be observed.

The formation of the anion of **1** was carried out by the reaction of **1** with potassium hydroxide to form potassium 2-amino-2-(carbamoylimino)-1,1-dinitroethan-1-ide (**2**). The experimental procedure with cold aqueous KOH solution was one-to-one adopted from the synthesis of the potassium salt of FOX-7.^[10]



Scheme 9-3: Synthesis overview of reaction of 1-amino-1-hydrazino-2,2-dinitroethene (HFOX) and chlorosulfonyl isocyanate (CSI).

1-Amino-1-hydrazino-2,2-dinitroethene (HFOX) is the hydrazine derivative of FOX-7 and is synthesized by reacting this and hydrazine hydrate.^[11] In the literature it is reported that HFOX undergoes spontaneous energetic decomposition.^[11-12] The intention was to use the high energy of the hydrazine group in the HFOX molecule and add a carbamoyl moiety for the reduction of the sensitivity and safer handling. In contrast, the reaction of CSI and HFOX occurs more readily than with FOX-7, due to the higher electron density of the NH₂ group in the hydrazine moiety. The reaction to 2-(1-amino-2,2-dinitrovinyl)hydrazine-1-carboxamide (**3**) is very fast, proceeds

already at low temperature and without the need of an excess of CSI. Additionally, **3** was also reacted with potassium hydroxide to form potassium 2-amino-2-(2-carbamoylhydrazono)-1,1-dinitroethan-1-ide (**4**).

Furthermore, the amino group of the HFOX molecule is nucleophilic enough to attack a second CSI reagent to form the 2-(2,2-dinitro-1-ureidoethylidene)hydrazine-1-carboxamide (**5**). The structure of **5** contains no longer a C–C double bond. The dinitromethyl moiety is now protonated, which is also visible due to the colorless appearance of **5**. During recrystallization out of water the solution get immediately yellow, which is most likely from the proton transfer from the dinitromethyl unit to the hydrazine moiety by forming back the double bond. Such double bonds often absorb light in the visible blue region and thus appear as yellow material. The assumption to get the molecule with a C–C double bond by an induced proton transfer with slightly basic potassium bicarbonate failed. Instead a potassium salt of (1-carbamoyl-5-oxo-1,2,4-triazol-3-yl)dinitromethanide (**6_K**) emerged. This surprising intermolecular cyclization reaction of the heterocycle 1,2,4-triazol-5-on **6** is very fast with good yields. The reaction mechanism for this cyclization reaction is not further investigated but presumable the urea moiety is nucleophilic attacked by the neighboring hydrazino group whereupon ammonia is eliminated. This is even more remarkable since the hydrazino moiety is deactivated by the attached carbamoyl group. In the literature this type of reaction was observed only one time before by treating alkoxycarbonylthioamides with hydrazine under elimination of H₂S.^[13] This condensation-cyclization reaction with intramolecular elimination of ammonia could be a valuable synthetic tool for the preparation of 1,2,4-triazol-5-ones. The ammonia salt of (1-carbamoyl-5-oxo-1,2,4-triazol-3-yl)dinitromethanide (**6_NH₄**) was prepared similar by the reaction of **5** with ammonium bicarbonate. Both salts differ from each other, whereas the potassium salt **6_K** is poorly soluble the ammonium salt **6_NH₄** is very soluble in water.

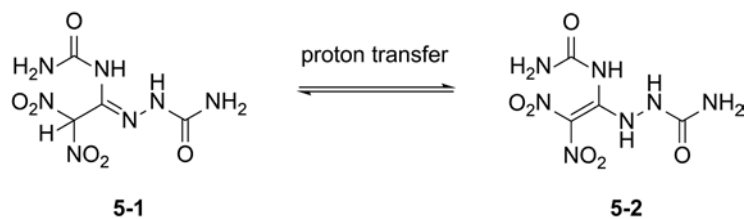
9.3.2 NMR Spectroscopy and Vibrational Spectroscopy

All compounds were thoroughly characterized by ^1H , ^{13}C and $^{14/15}\text{N}$ NMR spectroscopy (Table 9-1). In the ^1H NMR spectrum the attached carbamoyl group appears at 7.70/6.87 (**1**), 6.26 (**3**) and 7.70/7.67 ppm (**6_K**) and is often separated in two signals due to restricted rotation about the C–NH₂ bond.^[14] This phenomenon was also observed for the C–NH₂ group which has not reacted with CSI reagent. They appear at 10.71/10.58 (**1**) and 9.90/9.70 ppm (**3**), which is about 2 ppm shifted to lower field compared to the starting materials FOX-7 and HFOX. The C–NH groups are located at quite low field at 11.37 (**1**), 11.49 (**3**), 12.17 (**5**) and 12.15 ppm (**6_K**) and are the most acidic hydrogens.

Table 9-1: Multinuclear NMR data (^1H , ^{13}C , ^{15}N) of **1, **3**, **5** and **6_K** in ppm (number of hydrogens/multiplicity).**

		1	3	5	6_K	
	solvent	[D ₆]DMSO	[D ₆]DMSO	[D ₆]DMSO	CD ₃ CN	[D ₆]DMSO
^1H	CNH ₂	10.71/10.58 (2)	9.90/9.70 (2)			
	CONH ₂	7.70/6.87 (2)	6.26 (2)	6.93 (4)	3.64 (4)	7.70/7.67 (2)
	NH	11.37 (1)	11.49 (1)	12.17 (1)	6.44 (1)	12.15 (1)
	N(H)NHCO		8.83 (1)	7.69 (2)	7.68 (1)	
	CH				7.88 (1)	
$^{13}\text{C}\{^1\text{H}\}$	CNO ₂	128.5	125.6	123.5	104.8	123.9
	CNH ₂ /CN	156.8	158.9	140.5	135.3	140.7
	CO	155.1	157.6	154.0	153.4	154.0
	CO			149.5	149.0	149.6
^{15}N	CNH ₂	–253.0 (t)	–265.9 (t)			
	CONH ₂	–289.1 (t)	–305.5 (t)			–295.5 (t)
	NH	–250.1 (d)	–247.5 (d)			–235.3 (s)
	NH		–274.9 (d)		not measured	
	C=N					–115.5 (s)
	NNCO					–118.5(s)
	NO ₂	–25.8 (s)	–26.5 (s)		(^{14}N –24 (s))	–22.9 (s)

Compound **5** shows a special chemical behavior in different solvents. In the solid state as well as in acetonitrile a hydrogen is located at the dinitromethyl group, whereas in the slight basic DMSO a proton transfer to the hydrazine moiety takes place (Scheme 9-4).



Scheme 9-4: Tautomerization of 2-(2,2-dinitro-1-ureidoethylidene)hydrazine-1-carboxamide (5).

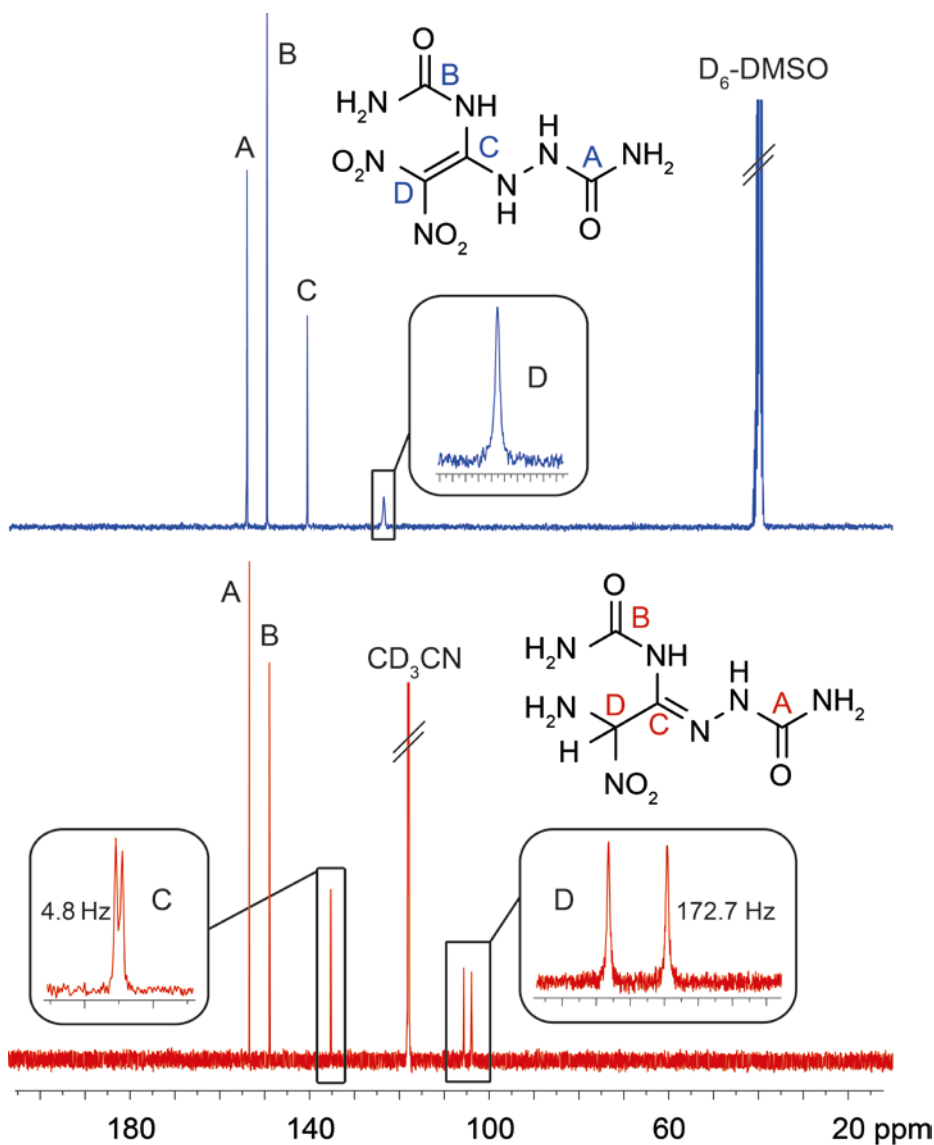


Figure 9-1: ¹³C NMR spectra of 2-(2,2-dinitro-1-ureidoethylidene)hydrazine-1-carboxamide (5) in CD₃CN (red) and [D₆]DMSO (blue).

This phenomenon is also observable in the ¹H and ¹³C NMR spectra. The assignments were based on the acquisition of different NMR experiments. The NH₂ moieties of the two chemical different -C(O)NH₂ groups are located in DMSO at 6.93 ppm and in CD₃CN at 3.64 ppm and in

both solvents with quite broad resonances. In DMSO three NH resonances at 12.17 (1H) and 7.69 ppm (2H) could be found, while in the CD₃CN solution two NH resonances at 7.68 and 6.44 ppm and one CH resonance at 7.88 ppm can be obtained. These chemical structures were also confirmed by the NMR measurement of ¹³C spectra coupled with ¹H which is shown in Figure 9-1. In acetonitrile the coupling of the hydrogen at the dinitromethyl is visible, causing a doublet at 104.8 ppm (**D**) with a coupling constant of ¹J_{CH} 171.9 Hz. The hydrogen couples also with the carbon of the CNHN group and creates a doublet at 135.3 ppm (**C**) with a smaller coupling constant of only ²J_{CH} 4.0 Hz. By contrast, in the spectrum with DMSO as solvent no ¹H–¹³C coupling of the dinitromethyl group (**D**) is visible.

In the ¹³C NMR spectra the most significant carbon resonances are of the carbonyl moieties. The signals of the carbonyl groups in the urea moieties are located in the small range of 154.0 to 157.6 ppm. When a second urea group is inserted the resonances are observed upfield at 149.5 (**5**) and 149.6 ppm (**6_K**). The carbon signal of the dinitromethyl moiety is observed in the range from 128.5 to 123.5 ppm. In the case of **5**, where the dinitromethyl group is protonated the resonance is shifted strong upfield to 104.8 ppm, due to the less located electron density on the carbon atom. The CNH₂N-group resonance is located at 155.1 (**1**) and 158.9 ppm (**3**), being less intense and broadened than the other groups. In the molecule **5** and in the ring system **6_K** the resonances are shifted to 140.5 (DMSO)/135.3 (CD₃CN) (**5**) and 140.7 ppm (**6_K**), due to the double bond imine character to one of the nitrogen atoms.

The ¹⁴N spectra of all compounds show only the resonances of the nitro groups in the range of –23 to –27 ppm as a singlet. The compounds **1**, **3** and **6_K** were further investigated by ¹⁵N NMR spectroscopy (Figure 9-2) and the assignments were based on comparison with theoretical calculations (MPW1PW91/aug-cc-pVDZ) and literature known analog derivatives.^[15] The compound **5** was not measured, due to its instability and slow conversion to **6**. The nitrogen resonance of the carbamoyl C(O)NH₂ group is located in the high-field area at –289.1 (**1**), –305.5 (**3**) and –295.5 ppm (**6_K**). The signals are splitted into a triplet, due to the ¹J coupling with the two bounded hydrogens. The triplets of the C–NH₂ moieties are shifted to lower fields at –253.0 (**1**) and –265.9 ppm (**3**) compared to the carbamoyl groups. The NH resonances which are split into duplets are located at –250.1 (**1**) and –247.5/274.9 ppm (**3**). The 1,2,4-triazol-5-on in compound **6_K** shows three resonances at –235.3, –188.5 and –115.5 ppm. The imine like nitrogen (**B**) is located at –115.5 ppm and the neighboring trivalent nitrogen (**C**) at –188.5 ppm. The resonance of the NH is located at –235.3 ppm (**D**), a N–H coupling is not observable probably due to the high acidity and therefore fast proton exchange in DMSO.

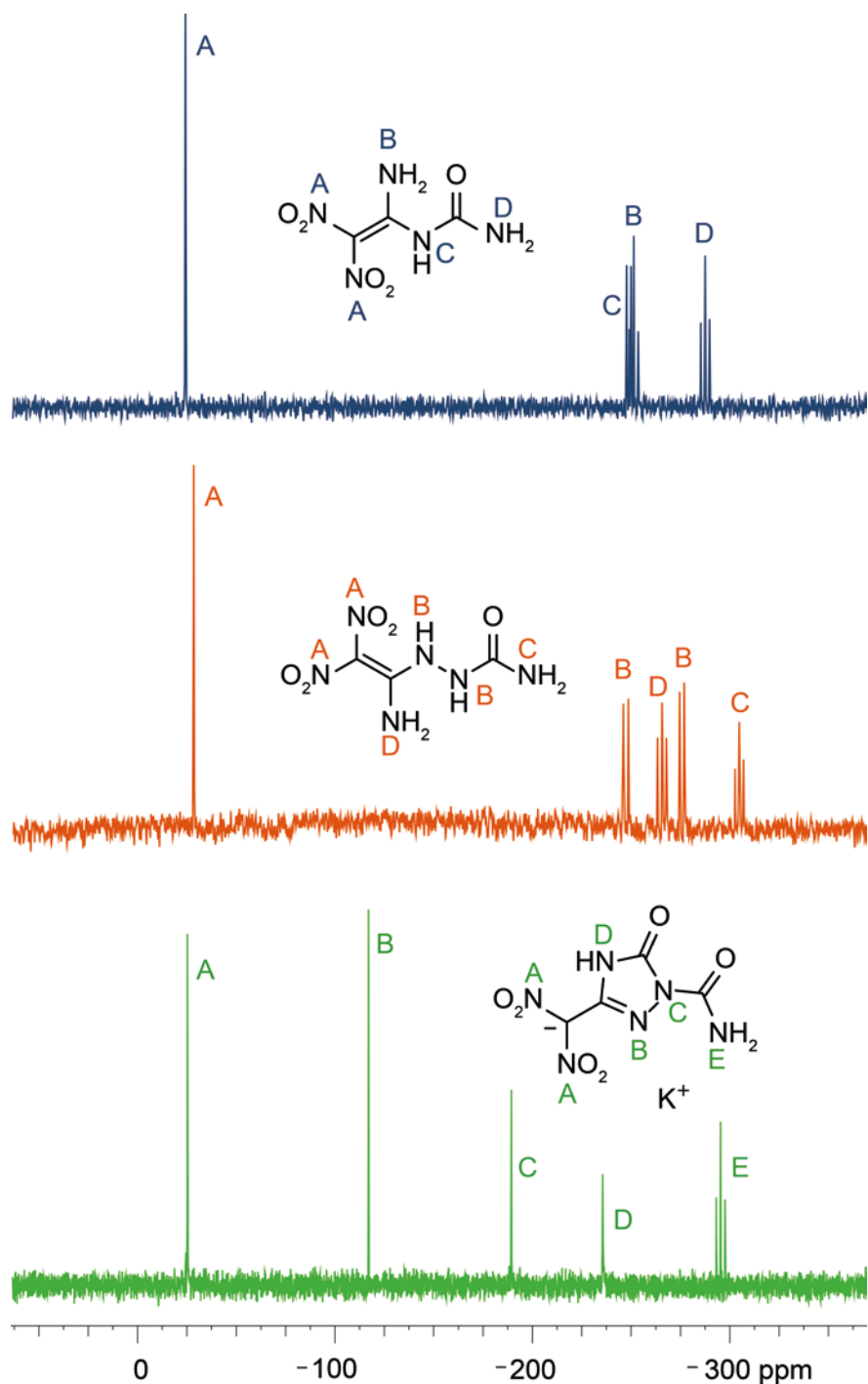


Figure 9-2: ^{15}N NMR spectrum of 1 (blue), 3 (orange) and 6_K (green) in $[\text{D}_6]\text{DMSO}$.

The vibrational analysis showed the characteristic asymmetric NO₂ stretching vibrations in the range of 1639 to 1604 cm^{-1} and the symmetric stretching vibrations at 1386 to 1337 cm^{-1} . The carbonyl group of the urea moieties absorbs around 1715 cm^{-1} . The N–H stretch absorption band for all compounds are quite dominant in the infrared spectrum and are in the range from 3450 to 3100 cm^{-1} which indicates strong hydrogen bonds.^[16]

9.3.3 Single Crystal Structure Analysis

Single crystals suitable for X-ray diffraction measurements were obtained by crystallization at room temperature from hot water. A full list of the crystallographic refinement parameters, structure data and additional information are displayed in the Appendix A.9. In Table 9-2 noteworthy atom distances and angles of all here presented structures, FOX-7 and HFOX are summarized.

Table 9-2: Measured bond lengths and torsion angles from FOX-7 derivatives all measured at 173 K.

	C-C	C-NH ₂	C-NH	C-N	C-NO ₂	N-N	∠, N-C-C-N	
FOX-7	1.456	1.322			1.413		177.8/172.9	
HFOX	1.476	1.293	1.297		1.373	1.404	90.6/89.4	
1	1.440	1.306	1.361		1.412		169.5/165.9	178.2/176.8 170.7/168.0
2	1.490	1.331		1.306	1.373		-83.4/-81.7	
3	1.448	1.316	1.342		1.410	1.382	175.8/173.6 175.2/172.6	
4	1.486	1.346		1.291	1.376	1.411	81.5/83.9	
5	1.500		1.381	1.274	1.510	1.370	102.8/-14.5	92.8/-24.6
6_K	1.461		1.375	1.295	1.380	1.394	88.9/90.5	
6_NH₄	1.448		1.378	1.313	1.391	1.393	170.8/167.3	

If more than one unique molecule is in the unit cell the average atom distance is given.

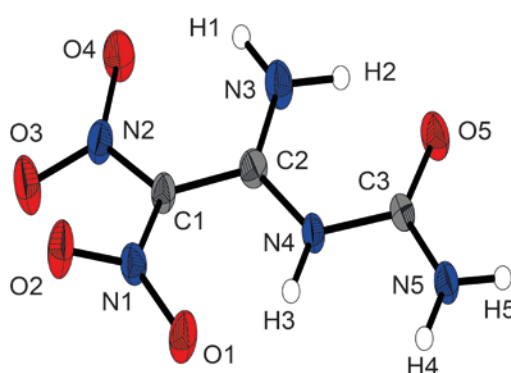


Figure 9-3: X-ray molecular structure of 1-(1-amino-2,2-dinitrovinyl)urea (1).

Selected atom distances (Å) and angles (deg.): O1-N1 1.234(3), O5-C3 1.227(3), N1-C1 1.418(3), N2-C1 1.404(3), N3-C2 1.309(3), N4-C2 1.362(3), N4-C3 1.408(3), N5-C3 1.327(3), C1-C2 1.443(3), N4-C2-N3 118.7(2), N4-C2-C1 119.9(2), N3-C2-C1 121.4(2), C2-C1-N1 122.1(2), N1-C1-N2 116.1(2), N2-C1-C2 121.7(2), N3-C2-C1-N1 -165.8(2), N2-C1-C2-N4 -169.8(2), N3-C2-N4-C3 5.5(4), N5-C3-N4-C2 175.1(2).

The compound **1** crystallizes in the triclinic space group $P\bar{1}$. The unit cell contains six molecules and the density is as high as FOX-7 with a value of 1.898 g cm^{-3} . The asymmetric unit consists of three nearly identical molecules; the molecular structure of one molecule is shown in Figure 9-3. The C–C atom distance is 1.440 \AA , which is very close to the starting material (1.456 \AA). The C2–N4 (1.361 \AA) bond is longer than the C2–N3 (1.306 \AA) bond where no carbamoyl group is attached. The C3–O5 (1.230 \AA) bond seems to be a normal carbonyl bond. The N4–C3 (1.408 \AA) is a bit and the C3–N5 (1.327 \AA) bond is significantly shorter than the atom distances of common amides/ureas.^[17] These shortened bonds indicates that the urea moiety participate in the π -system of the FOX-7 molecule.^[7] Another evidence is the essentially planarity of the molecule, only the nitro groups are little out of the plane with a twist from 3 to 14° . This behavior was also observed in the FOX-7 structure where the torsion angle N–C–C–N is around 5° .^[3c] An additional similarity is the molecular packing. In both cases infinite two dimensional layers are formed (Figure 9-4) with extensive intra- and intermolecular hydrogen bonds within the layers and weaker van der Waals interactions between the layers. The good physical-chemical properties of FOX-7, like the low sensitivity, are explained by the molecular packing structure with strong hydrogen bonds.^[18] In compound **1** the initial H-bond donors and acceptors are increased, due to the added carbamoyl group, which leads to higher cross-linking and thus a lower sensitivity. Intramolecular hydrogen bonds may also limited the free rotation of the two different amino groups, which in turn resulting in four different NH resonances in the ^1H NMR spectrum.

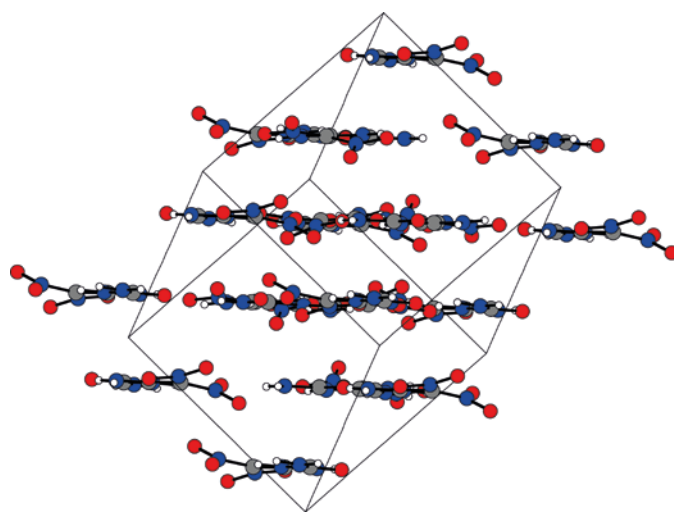


Figure 9-4: Representation of the layered structure of compound **1**.

The potassium salt **2** crystallizes in the orthorhombic space group $P2_12_12_1$ with four molecules in the unit cell and one molecule as asymmetric unit (Figure 9-5). The single crystal X-ray analysis

confirmed the assumption that the deprotonation takes place at the NH group with the highest acidity, which is induced by the neighboring electron withdrawing carbamoyl moiety. From Table 9-2, it can be seen that the C–C atom distance of 1.490 Å is elongated compared to **1** and thus closer to a single than a double bond distance. In contrast, the C–NO₂ bond lengths of C1–N1 (1.366 Å) and C1–N2 (1.382 Å) are shortened compared to FOX-7 and **1** for an enhanced delocalization and stabilization of the negative charge on the carbon C1. On the carbon C2 is as a result of the deprotonation of the neighboring nitrogen also a higher electron density which is reflected by a longer C2–N3 bond and a shorter C2–N4 bond. Furthermore, the higher negative charge on the nitrogen N4 leads to a poorer bonding ability of the carbonyl group and is displayed by the significant longer C3–O5 (1.253 Å) bond. The anion can be separated in two planar π -systems the dinitromethanide and the aminomethyl urea unit. Due to the almost orthogonal arrangement of the two π -systems no attractive interactions to each other are possible.

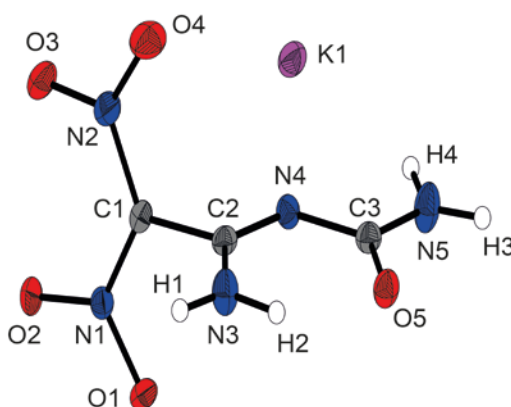


Figure 9-5: X-ray molecular structure of potassium 2-amino-2-(carbamoylimino)-1,1-dinitroethan-1-ide (2**).** Selected atom distances (Å) and angles (deg.): C1–C2 1.489(2), C1–N1 1.366(2), C1–N2 1.382(2), C2–N3 1.330(2), C2–N4 1.308(2), C3–N4 1.402(2), C3–N5 1.331(2), C3–O5 1.251(2), N1–O2 1.240(2), N1–C1–N2 122.7(1), N1–C1–C2 117.3(1), N2–C1–C2 120.0(1), N3–C2–N4 127.9(2), C2–N4–C3 119.5(1), N4–C3–N5 113.1(1), N2–C1–C2–N3 99.9(2), N1–C1–C2–N4 95.1(2), N3–C2–N4–C3 1.5(3), C2–N4–C3–N5 177.4(2), C2–N4–C3–O5 0.8(2).

The crystal structure HFOX was already investigated in the literature.^[19] For the better comparison the crystal structure measurement was repeated at 173 K, whereupon it was noticed that the literature measurement is not that good and the structure of the hydrazino moiety was misinterpreted. HFOX crystallizes in the orthorhombic space group *Pnma* and with a density of 1.855 g cm⁻³ (Figure 9-6). The molecule is divided by a mirror plane through the following atoms C1, C2, N2, N3, N4, H1 and H2 which leads to the asymmetric unit with just one nitro group and a disorder of H3. HFOX can be regarded as a zwitterion or dipolar ion, where the negative charge is located at C1 and the positive at C2.^[20] Albeit in the optimized computer calculated gas phase

structure the molecule is almost planar, in the solid state the dinitromethyl unit is twisted out of the 1-amino-1-hydrazinomethyl plane of 89.4° . The reason for this behavior may be the strong electrostatic interactions and the strong hydrogen bonds between the amino and nitro groups.^[11-12] This significant difference of the optimized gas phase structure and the solid structure could be a reason for the low stability and the quite high mechanical sensitivity of HFOX.

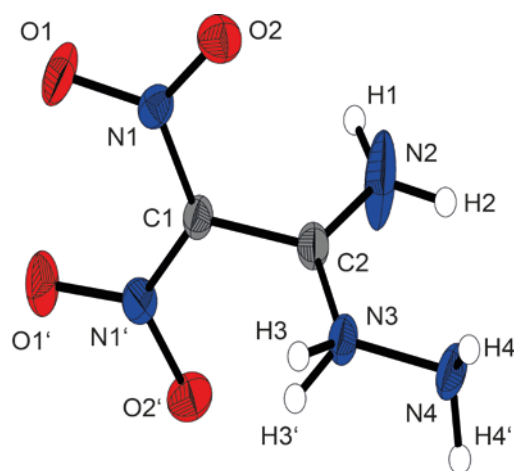


Figure 9-6: X-ray molecular structure of 1-amino-1-hydrazino-2,2-dinitroethene (HFOX).

Selected atom distances (Å) and angles (deg.): C1–C2 1.476, C1–N1 1.373, C1–N1' 1.373, C2–N2 1.294, C2–N3 1.297, N1–O1 1.245(2), N1–O2 1.252(2), N3–N4 1.404, N1–O1 1.245(2), N3–C2–N2 122, N3–C2–C1 117, N2–C2–C1 121, N1–C1–N1' 123.7, N4–N3–C2–C1 180, N2–C2–N3–N4 0, N3–C2–C1–N1 -90.6 , N2–C2–C1–N1 -89.4

Compound **3** crystallizes in the orthorhombic space group $Pca2_1$ with two molecules and one crystal water in the asymmetric unit (Figure 9-7). The molecular structure shows more matches with the FOX-7 structure than with HFOX. For instance the HFOX part of the molecule **3** is now planar, only the nitro groups are little rotated out of plane. Furthermore, the C–C, C–NH₂ and the C–NO₂ atom distances (Table 9-2) are in the same range than in FOX-7 and may explain the much higher stability of **3** compared to HFOX.

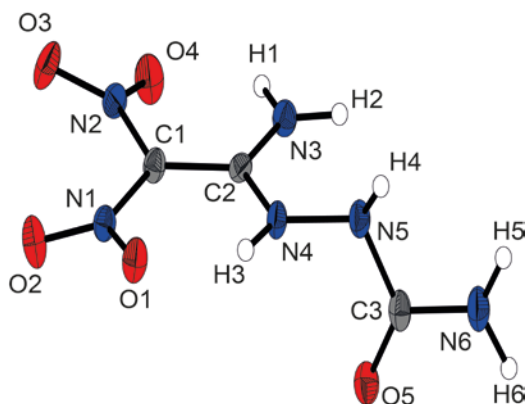


Figure 9-7: X-ray molecular structure of 2-(1-amino-2,2-dinitrovinyl)hydrazine-1-carboxamide (3).

Selected atom distances (Å) and angles (deg.): O5–C3 1.233(2), O2–N1 1.229(2), O1–N1 1.246(2), O4–N2 1.238(2), O3–N2 1.236(2), N2–C1 1.412(2), N1–C1 1.409(2), N4–N5 1.389(2), N4–C2 1.345(2), N3–C2 1.315(2), N5–C3 1.386(2), N5–H4 0.84(3), N6–C3 1.341(2), C1–C2 1.443(2), N1–C1–N2 115.5(1), N1–C1–C2 123.1(1), N2–C1–C2 121.4(1), C1–C2–N3 120.9(1), N3–C2–N4 118.7(1), C2–N4–N5 118.2(1), N4–N5–C3 118.0(1), N2–C1–C2–N4 172.6(1), N1–C1–C2–N3 175.2(1), C1–C2–N4–N5 –179.4(1), N6–C3–N5–N4 –170.6(1), O2–N1–C1–C2 –162.0(1), C2–N4–N5–C3 –99.7(1).

The attached urea unit inclusively the hydrazine group generate a second plane like structure which is shown by the torsion angle of N6–C3–N5–N4 –170.6(1) and is twisted to the HFOX unit by around 100° owing to the sp^3 hybridized nitrogen N5. The molecular packing with extensive hydrogen bonds leads to a layer structure of the HFOX units with interlocking urea groups between the layers.

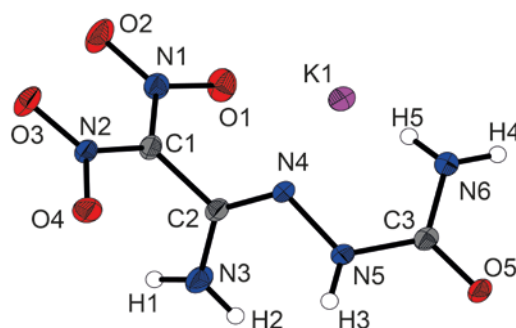


Figure 9-8: X-ray molecular structure of potassium 2-amino-2-(2-carbamoylhydrazono)-1,1-dinitroethan-1-ide (4).

Selected atom distances (Å) and angles (deg.): C1–C2 1.486(3), C1–N1 1.391(2), C2–N3 1.346(3), C2–N4 1.291(3), N1–O1 1.245(2), N4–N5 1.411(2), N2–C1–N1 122.1(2), N1–C1–C2 119.5(2), N3–C2–N4 127.8(2), C2–N4–N5 112.9(2), N4–N5–C3 119.7(2), C1–C2–N4 115.1(2), N1–C1–C2–N3 –99.3(2), N2–C1–C2–N4 –95.3(2), C2–N4–N5–C3 139.6(2).

The potassium salt of **3** the compound **4** crystallizes in the monoclinic space group $P2_1/n$ having four molecules in each unit cell (Figure 9-8). The structure is more similar to the HFOX structure and shows the same transformation than the potassium salt **2**. Here the structure is subdivided in three plane units, the dinitromethylene, the 1-amino-1-hydrazinomethyl and the urea part whereas the dinitromethylene unit is about 80° and the urea unit is about 40° twisted out of the 1-amino-1-hydrazinomethyl layer.

The C1–NO₂ (1.376 Å) and the C2–N4 (1.291 Å) bond lengths are shortened compared to the neutral compound **3** for a better stabilization of the negative partial charge on the carbon C1 and the nitrogen N4. Further effects of the deprotonation of the nitrogen N4 and the associated higher negative charge are the elongated C–NH₂ atom distances to the here observed maximum of 1.381 Å, as well as the very long N–N (1.411 Å) bond which is despite the attached carbamoyl group longer than in the starting material.

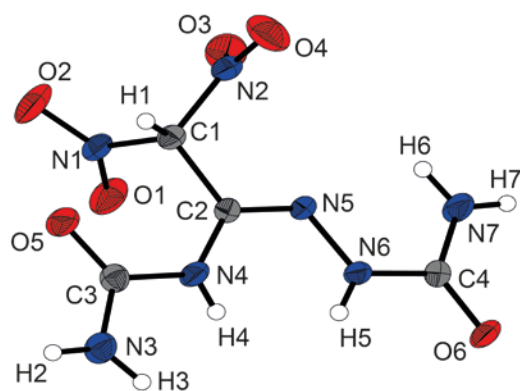


Figure 9-9: X-ray molecular structure of 2-(2,2-dinitro-1-ureidoethylidene)hydrazine-1-carboxamide (5).

Selected atom distances (Å) and angles (deg.): C1–C2 1.506(3), C1–N1 1.518(2), C1–N2 1.509(3), C1–H1 0.87(2), C2–N4 1.377(3), C2–N5 1.273(3), C3–N3 1.331(4), C3–N4 1.378(3), C3–O5 1.225(3), C4–N6 1.369(3), C4–N7 1.323(4), C4–O6 1.243(3), N1–O1 1.209(2), N5–N6 1.373(2), N1–C1–N2 105.5(2), N1–C1–C2 111.8(2), C2–N5–N6 118.3(2), N5–N6–C4 119.3(2), C2–N4–C3 127.2(2), N1–C1–C2–N4 $-77.0(2)$, N2–C1–C2–N4 165.9(2), N3–C3–N4–C2 $-179.9(2)$, N4–C2–N5–N6 $-1.2(3)$, C2–N5–N6–C4 176.5(2), N7–C4–N6–N5 3.6(3), O6–C4–N6–N5 $-177.7(2)$.

The disubstituted carbamoyl compound **5** crystallizes as colorless blocks in the triclinic space group $P\bar{1}$ with four molecules in the unit cell and a density of 1.732 g cm^{-3} . The asymmetric unit contains two nearly identical molecules one is displayed in Figure 9-9. The carbon atom C1 bearing the two nitro groups is rather protonated than the imine nitrogen N5. The C1–C2 (1.506 Å) bond distance as long as a single C–C bond (1.52 Å). The C–NO₂ bond lengths is compared to none protonated molecules significant elongated to about 1.51 Å which is longer than the average C–N bond distances (1.47 Å). Furthermore, the bond angle of N1–C1–N2

(105.5 °) in the $\text{CH}(\text{NO}_2)_2$ group is strongly compressed. This is caused by a $\text{N}\cdots\text{O}$ intramolecular attraction between the partial positive charged nitrogen N1 and O3 of the second nitro group and is confirmed by the very short distance of 2.575 Å. In contrast the chain with the two urea ends in contrast arranged in an almost perfect plane which builds up a π -system. This in turn leads to special interactions and a strong shortening of the imine C–N (1.274 Å) and the N–N (1.370 Å) bonds which are shorter than the regular C–N double (1.30 Å) and N–N single bonds (1.42 Å), respectively.

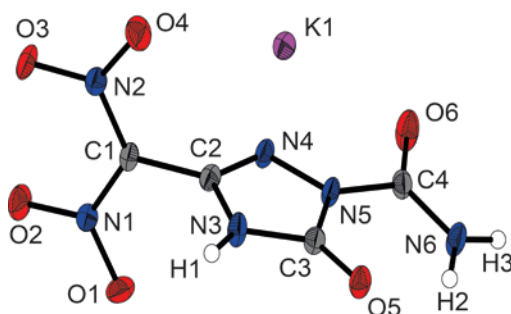


Figure 9-10: X-ray molecular structure of potassium (1-carbamoyl-5-oxo-1,2,4-triazol-3-yl)dinitromethanide (6_K).

Selected atom distances (Å) and angles (deg.): C1–C2 1.461(2), C1–N1 1.381(2), C1–N2 1.379(2), C2–N3 1.375(2), C2–N4 1.295(2), C3–N3 1.362(2), C3–N5 1.387(2), C3–O5 1.224(2), C4–N5 1.429(2), C4–N6 1.320(2), C4–O6 1.219(2), N1–O1 1.252(2), N4–N5 1.394(2), N1–C1–N2 122.0(1), N3–C2–N4 112.2(1), C2–N4–N5 104.0(1), N4–N5–C3 112.0(1), N5–C3–N3 103.1(1), C3–N3–C2 108.8(1), N1–C1–C2–N3 –86.3(2), N2–C1–C2–N4 –94.4(2), C1–C2–N3–C3 175.2(1), N3–C3–N5–C4 –175.0(1), C3–N5–C4–N6 8.7(2), C2–N4–N5–C4 175.3(1), O5–C3–N3–C2 179.9(1).

The potassium salt of the 1,2,4-triazol-5-on heterocycle **6_K** crystallizes in the orthorhombic space group *Pbca* containing eight molecules in the unit cell. The minimum asymmetric unit of the crystal structure made up of one cation and one anion and is displayed in Figure 9-10. The five-membered heterocyclic ring and the adjoining carbamoyl group are almost in a plane with small derivation of around 5 ° (N3–C3–N5–C4 –175.0 Å). On the other hand the heterocycle and the plane of the dinitromethyl unit are twisted of about 90 ° (N1–C1–C2–N3 –86.3 °, N2–C1–C2–N4 –94.4 °). A consequence of this arrangement, is a reduction of the C–NO₂ bond distance (1.380 Å) like in the structures of HFOX, **2** and **4** with the same orthogonal arrangement. Nevertheless the C1–C2 (1.461 Å) bond distances is shortened and is therefore in the range of FOX-7. The heterocyclic ring and the attached carbamoyl group form a big π -system supported by the conjugated C–N and C–O bonds and the sp^2 hybridized nitrogen N5.^[15b, 21] The ring forms not a regular pentagon (108 °), whereas the carbonyl group has the most acute angle (N5–C3–N3

103.1 °) and the N3–C2–N4 angle (112.2 °) shows the highest value. In the crystal structure, each potassium is connected to eight oxygen of the carbonyl and the nitro groups and to one nitrogen N4 of the imine moiety.

The ammonium salt **6**_{NH₄} crystallizes in the same orthorhombic space group *Pbca* with also eight molecules in the unit cell as the potassium salt **6**_K. The structure shows a high density of 1.848 g cm⁻³ and the asymmetric unit is illustrated in Figure 9-11. The atom distances and angles are almost equal between these two salts (Table 9-2). However, the ammonium salt has an important feature: The whole anion is in a planar. Only the nitro groups are rotated slightly out of the plane of about 9 and 12 °, due to disorder of one nitro group (N2).

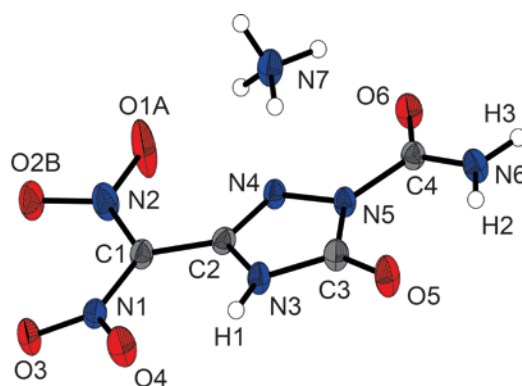


Figure 9-11: X-ray molecular structure of ammonium (1-carbamoyl-5-oxo-1,2,4-triazol-3-yl)dinitromethanide (6**_{NH₄}).**

Selected atom distances (Å) and angles (deg): C1–C2 1.448(2), C1–N2 1.380(2), C1–N1 1.403(2), C2–N3 1.378(2), C2–N4 1.313(2), C3–N3 1.355(2), C3–N5 1.379(2), C3–O5 1.229(2), C4–N5 1.426(2), C4–N6 1.317(2), C4–O6 1.221(2), N4–N5 1.393(2), N2–C1–N1 117.7(1), C2–N4–N5 104.2(1), N4–N5–C3 111.9(1), N5–C3–N3 103.5(1), C3–N3–C2 109.4(1), N3–C2–N4 111.0(1), O2B–N1–C1–C2 -164.0(2), N2–C1–C2–N4 170.8(1), N4–N5–C3–N3 -1.0(2), C2–N4–N5–C4 -177.3(1), C3–N3–C2–N4 -0.0(2), N4–N5–C4–N6 178.0(1).

The crystal packing consists of wave-like layers (Figure 9-12) with extensive strong intra- and intermolecular hydrogen bond forces within the layers and weak intermolecular forces between the molecular waved sheets (Figure 9-12), like it was also observed in the FOX-7 structure.^[22] The ammonium cation is here coordinated each time by four anion molecules, three within the layer and one between two layers.

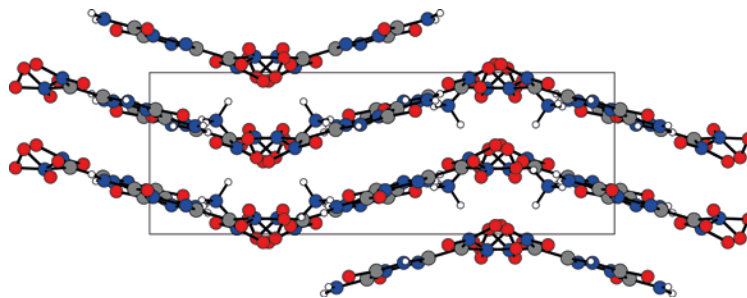


Figure 9-12: Representation of the wave-layered structure of 6_NH₄, view along the *a* axis.

9.3.4 Thermal Stabilities, Sensitivity and Energetic Properties

The investigated physical properties of all compounds are shown in Table 9-3. All compounds are stable toward moisture and air. Compound **1** shows a decomposition point of 209 °C which is thus less thermally stable than FOX-7 (218 °C) (Figure 9-13). However, the corresponding derivative of HFOX **3** shows a great improvement of the thermal stability from 110 °C (HFOX) to 170 °C (**3**). By an addition of two carbamoyl units, in compound **5** the decomposition point decrease to 129 °C. The here formed dinitromethyl unit with the strong acidic hydrogen next to the two nitro groups often show low thermal stabilities.^[23] The potassium and ammonium salt of (1-carbamoyl-5-oxo-1,2,4-triazol-3-yl)dinitromethanide show decomposition points of 198 °C (**6_K**) and 202 °C (**6_NH₄**).

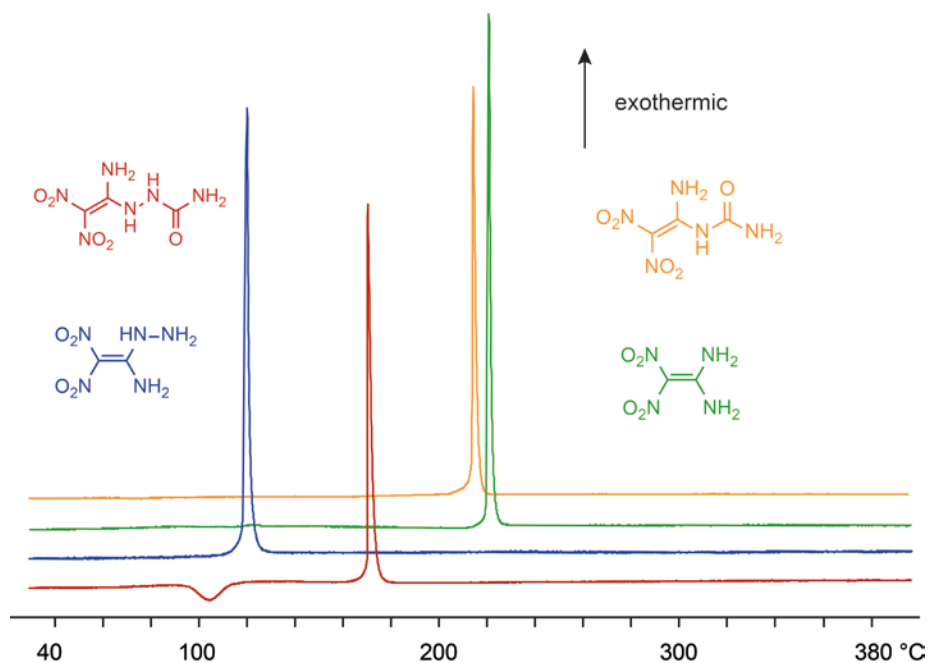


Figure 9-13: Comparison of DTA measurements (5 °C min⁻¹) of FOX-7 (green), HFOX (blue), **1** (yellow) and **3** (red).

Table 9-3: Physical properties of 1-5, 6_K and 6_NH₄ in comparison of the starting materials FOX-7 and HFOX.

	1	2	3	4	5
formula	C ₃ H ₅ N ₅ O ₅	C ₃ H ₄ N ₅ O ₅ K	C ₃ H ₆ N ₆ O ₅	C ₃ H ₅ N ₆ O ₅ K	C ₄ H ₇ N ₇ O ₆
T_m /°C (onset) ^[a]	-	155	-	-	-
T_{dec} /°C (onset) ^[b]	209	191	170	165	129
IS /J ^[c]	40	20	15	10	9
FS /N ^[d]	360	360	360	360	360
ESD /J ^[e]	1.0	0.5	0.3	0.3	0.2
N /% ^[f]	36.7	30.4	40.8	34.3	39.4
O /% ^[g]	41.9	34.8	38.8	32.6	38.5
$N+O$ /% ^[h]	78.6	65.2	79.6	66.9	77.9
Ω_{CO} /% ^[i]	-4.2	-4.2	-7.8	-7.8	-9.6
Ω_{CO_2} /% ^[j]	-29.3	-29.3	-31.0	-31.0	-35.3
	6_K	6_NH₄	FOX-7 ^[25]	HFOX	AP
formula	C ₄ H ₃ N ₆ O ₆ K	C ₄ H ₇ N ₇ O ₆	C ₂ H ₄ N ₄ O ₄	C ₂ H ₅ N ₅ O ₄	NH ₄ ClO ₄
T_m /°C (onset) ^[a]	-	-	-	-	-
T_{dec} /°C (onset) ^[b]	198	202	218	110	240
IS /J ^[c]	20	20	20	2	20
FS /N ^[d]	360	360	360	64	360
ESD /J ^[e]	0.5	0.5	0.5	0.1	0.50
N /% ^[f]	31.1	39.4	37.8	42.9	11.9
O /% ^[g]	35.5	38.5	43.2	39.2	54.5
$N+O$ /% ^[h]	66.6	77.9	81.0	82.1	66.4
Ω_{CO} /% ^[i]	0	-9.6	0	-4.9	+34.0
Ω_{CO_2} /% ^[j]	-27.6	-35.3	-21.6	-24.5	+34.0

[a] Onset melting T_m and [b] onset decomposition point T_{dec} from DSC measurement carried out at a heating rate of 5 °C min⁻¹. [c] Impact sensitivity. [d] Friction sensitivity. [e] Sensitivity toward electrostatic discharge. [f] Nitrogen content. [g] Oxygen content. [h] Sum of nitrogen and oxygen content. [i] Oxygen balance assuming the formation of CO and the formation of the formation of [j] CO₂ at the combustion.

For initial safety testing the impact and friction sensitivities as well as the electrostatic discharge sensitivity were determined and assigned according to the UN recommendations on the transport of dangerous goods.^[24] The friction sensitivity (FS) is determined by rubbing a small substance amount between a pin and a porcelain plate with different contact pressures.^[25] All compounds were classified as insensitive toward friction with exception of HFOX which must be classified as very sensitive to friction (≥ 360 N insensitive, 360–80 N sensitive, 80–10 N very sensitive, ≤ 10 N

extremely sensitive). The more important value for energetic compounds is the sensitiveness toward impact (IS) which is tested by the action of a dropping weight on a sample and at which benchmark a decomposition or explosion occurs.^[2] The HFOX exhibits an extraordinarily high sensitivity of 2 J and is therefore a most primary explosives classified in the most dangerous class (≥ 40 J insensitive, 40–35 J less sensitive, 35–4 J sensitive, ≤ 3 J very sensitive).^[2, 25] In comparison compound **3** shows only a impact sensitivity of 15 J and can hence be handled with much lower risk. FOX-7 is already very insensitive (20 J), but compound **3** (40 J) with the added carbamoyl unit is not sensitivity to impact any more. The corresponding salts **2** and **4** show slight higher impact sensitivities compared to their neutral compounds. Compound **5** has the lowest impact sensitivity (9 J) of all here presented compounds, due to the instable nature of such dinitromethyl groups. The ammonium and potassium salts of the 1,2,4-triazol-5-on are both quite insensitive toward impact (20 J) and are both in the range of FOX-7.

Table 9-4: Calculated heat of formation and predicted detonation parameters (using the EXPLO5 V6.02) for **1, **3**, **5** and **6_NH₄** in comparison of the starting material FOX-7 and HFOX.**

	1	3	5	6_NH₄	FOX-7	HFOX
density RT /g cm ⁻³ [a]	1.86	1.79	1.70	1.82	1.88	1.82
$\Delta_f H^\circ$ /kJ mol ⁻¹ [b]	-277	-153	-355	-337	-134	+46
$\Delta_f U^\circ$ /kJ kg ⁻¹ [c]	-1350	-641	-1325	-1254	-805	+373
Q_v /kJ kg ⁻¹ [d]	-4096	-4506	-3816	-3897	-4739	-5535
T_{ex} /K [e]	2913	3101	2823	2793	3218	3562
V_0 /L kg ⁻¹ [f]	768	808	802	790	780	827
P_{CJ} /kbar [g]	305	293	231	279	344	348
V_{det} /m s ⁻¹ [h]	8516	8507	7805	8359	8852	9036

[a] RT densities are recalculated from X-ray densities. [b] Enthalpy and [c] energy of formation calculated by the CBS-4 M method using Gaussian 09. [d] Heat of explosion. [e] Explosion temperature. [f] Volume of gaseous products. [g] Detonation pressure and [h] detonation velocity calculated by using the EXPLO5 (Version 6.02) program package.^[26]

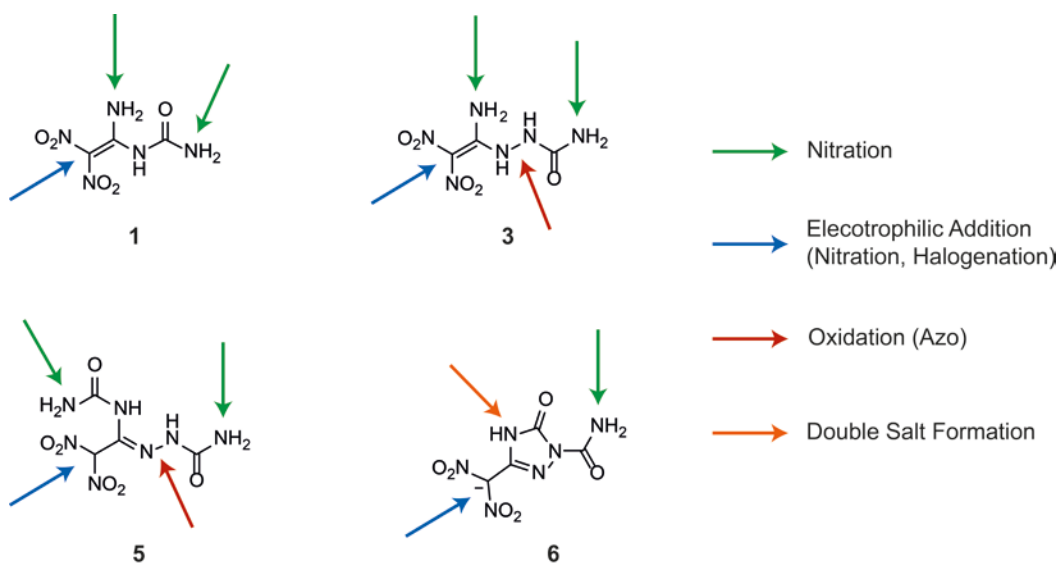
The main performance criterion of energetic materials is the detonation velocity V_{det} . The performance data were calculated by the computer code EXPLO5 V.6.02^[26] and based on the calculated energy of formation using CBS-4 M ab initio calculation. All detonation and combustion parameters for compounds **1**, **3**, **5** and **6_NH₄** are summarized in Table 9-4. The compounds **1** and **3** both demonstrate good detonation velocities V_{det} with values higher than 8500 m s⁻¹ which are only slightly lower than FOX-7 (8852 m s⁻¹). This high performance is even

more impressive considering the low sensitivity toward external mechanical stimuli. The ammonium salt **6**_{NH₄} show also quite good detonation velocities V_{det} of about 8359 m s⁻¹ and therefore achieve well known explosives like TNT (Trinitrotoluene, 7241 m s⁻¹) and PETN (Pentaerythritol tetranitrate 8403 m s⁻¹).

9.4 Conclusion

Several new energetic compounds based on the FOX-7 molecule were synthesized and thoroughly characterized. The molecular structures are discussed on the basis of single crystal X-ray diffraction studies and are compared with each other. Especially the neutral compounds **1** and **3** show good energetic properties with detonation velocities V_{det} of above 8500 m s⁻¹ and only low or no sensitivity against mechanic stimuli. Furthermore, the possibility of salt formation was demonstrated by the synthesis of the corresponding potassium salts **2** and **4**. Whereas the FOX-7 molecule reacts only once with the very reactive chlorosulfonyl isocyanate (CSI) the HFOX molecule reacted twice at the -NH₂ and -NHNH₂ groups to synthesize **5**, which is only possible due to the higher electron density of the hydrazinium moiety. The heterocycle (1-carbamoyl-5-oxo-1,2,3-triazol-3-yl)dinitromethanide **6** was formed by a cyclization reaction with elimination of ammonia by treating **5** with potassium bicarbonate. The ammonium salt of **6** has a high thermal stability, with low sensitivity against impact (20 J) and pleasing detonation properties. These new synthesis route for the formation of 1,2,4-triazol-5-on heterocycle may be transferred to other starting materials, like the semicarbazide group.

In the literature several further reactions for the FOX-7 unit are known.^[5b, 6, 10, 27] Most of these transformations were done for higher energetic performance and better physical properties. In this sense, these advancements can also be applied to the here newly synthesized compounds **1**, **3**, **5** and **6** (Scheme 9-5) being likely more stable due to higher hydrogen bond ability by the attached carbamoyl groups.



Scheme 9-5: Possible further reactions for better energetic properties.

9.5 Experimental Section

9.5.1 General Procedures

All chemicals were used as supplied. Raman spectra were recorded in a glass tube with a Bruker MultiRAM FT-Raman spectrometer with Nd:YAG laser excitation up to 1000 mW (at 1064 nm). Infrared spectra were measured with a Perkin–Elmer Spectrum BX-FTIR spectrometer equipped with a Smiths DuraSamplIR II ATR device. All spectra were recorded at ambient (25 °C) temperature. NMR spectra were recorded with a JEOL/Bruker instrument and chemical shifts were determined with respect to external Me_4Si (^1H , 399.8 MHz; ^{13}C , 100.5 MHz) and MeNO_2 (^{15}N , 40.6 MHz; ^{14}N , 28.9 MHz). Mass spectrometric data were obtained with a JEOL MStation JMS 700 spectrometer (DCI+, DEI+, FAB+, FAB–). Analysis of C/H/N were performed with an Elemental Vario EL Analyzer. Melting and decomposition points were measured with a Perkin-Elmer Pyris6 DSC and an OZM Research DTA 552-Ex with a heating rate of 5 °C min^{-1} in a temperature range of 15 to 400 °C and checked by a Büchi Melting Point B-540 apparatus (not corrected). The sensitivity data were performed using a BAM drophammer and a BAM friction tester.^[24]

9.5.2 Computational Details

All ab initio calculations were carried out using the program package Gaussian 09 (Rev. A.03)^[28] and visualized by GaussView 5.08^[29]. The initial geometries of the structures were taken from the corresponding, experimentally determined crystal structures. Structure optimizations and frequency analyses were performed with Becke's B3 three parameter hybrid functional using the LYP correlation functional (B3LYP). For C, H, N and O a correlation consistent polarized double- ξ basis set was used (cc-pVDZ). The structures were optimized with symmetry constraints and the energy is corrected with the zero point vibrational energy.^[30] The enthalpies (H) and free energies (G) were calculated using the complete basis set (CBS) method in order to obtain accurate values. The CBS models use the known asymptotic convergence of pair natural orbital expressions to extrapolate from calculations using a finite basis set to the estimated complete basis set limit. CBS-4 starts with a HF/3-21G(d) geometry optimization, which is the initial guess for the following SCF calculation as a base energy and a final MP2/6-31+G calculation with a CBS extrapolation to correct the energy in second order. The used CBS-4M method additionally implements a MP4(SDQ)/6-31+(d,p) calculation to approximate higher order contributions and

also includes some additional empirical corrections.^[31] The enthalpies of the gas-phase species were estimated according to the atomization energy method.^[32] The liquid (solid) state energies of formation (ΔH_f°) were estimated by subtracting the gas-phase enthalpies with the corresponding enthalpy of vaporization (sublimation) obtained by Trouton's rule.^[33] All calculations affecting the detonation parameters were carried out using the program package EXPLO5 V6.02 (EOS BKWG-S).^[26, 34] The detonation parameters were calculated at the Chapman–Jouguet (CJ) point with the aid of the steady-state detonation model using a modified Becker-Kistiakowski-Wilson equation of state for modeling the system. The CJ point is found from the Hugoniot curve of the system by its first derivative. The specific impulses were also calculated with the program package EXPLO5 V6.02 program, assuming an isobaric combustion of a composition of an oxidizer, aluminum as fuel, 6% polybutadiene acrylic acid, 6% polybutadiene acrylonitrile as binder and 2% bisphenol A as epoxy curing agent.^[26] A chamber pressure of 70.0 bar, an initial temperature of 3300 K and an ambient pressure of 1.0 bar with equilibrium expansion conditions were estimated for the calculations.

9.5.3 X-ray Crystallography

The low-temperature single-crystal X-ray diffraction of were performed on an Oxford XCalibur3 diffractometer equipped with a Spellman generator (voltage 50 kV, current 40 mA) and a KappaCCD detector operating with MoK α radiation ($\lambda = 0.7107 \text{ \AA}$). Data collection was performed using the CRYALIS CCD software.^[35] The data reduction was carried out using the CRYALIS RED software.^[36] The solution of the structure was performed by direct methods (SIR97)^[37] and refined by full-matrix least-squares on F2 (SHELXL)^[38] implemented in the WINGX software package^[39] and finally checked with the PLATON software^[40]. The absorptions were corrected by a SCALE3 ABSPACK multi-scan method.^[41] All non-hydrogen atoms were refined anisotropically. The hydrogen atom positions were located in a difference Fourier map. ORTEP plots are shown with thermal ellipsoids at the 50% probability level. Additional crystallographic data and structure refinement parameters are listed in the Appendix A.9.

9.5.4 Synthesis

1-(1-Amino-2,2-dinitrovinyl)urea (1): Dry acetonitrile (50 mL) was placed in an ice bath and chlorosulfonyl isocyanate (CSI) (2.12 g, 15 mmol) was added. The 1,1-diamino-2,2-dinitroethene (FOX-7) (1.48 g, 10 mmol) was added in portions and the mixture was further stirred 10 min. at

0 °C. The ice bath was removed, and stirring at room temperature was continued for 1.5 h whereby the solution became homogeneous. The clear reaction mixture was again cooled with an ice bath, and quenched carefully with water (20 mL). The stirring was continued at room temperature for 0.5 h. The organic solvent was removed on the rotary evaporator. The formed precipitate was filtered off, washed with water and dried under high vacuum to obtain yellow pure **1** (72%).

^1H NMR ($[\text{D}_6]\text{DMSO}$): $\delta = 11.37$ (s, 1H, NH), 10.71 (s, 1H, CNH_2), 10.58 (s, 1H, CNH_2), 7.70 (s, 1H, CONH_2), 6.87 (s, 1H, CONH_2) ppm. $^{13}\text{C}\{^1\text{H}\}$ NMR ($[\text{D}_6]\text{DMSO}$): $\delta = 156.8$ (CNH_2), 155.1 (CO), 128.5 (CNO_2) ppm. ^{15}N NMR ($[\text{D}_6]\text{DMSO}$): $\delta = -25.8$ (s, NO_2), -250.1 (d, NH, $^1J_{\text{NH}} = 90.8$ Hz), -253.0 (t, NH_2 , $^1J_{\text{NH}} = 91.8$ Hz), -289.1 (t, NH_2 , $^1J_{\text{NH}} = 90.0$ Hz) ppm. IR (ATR, cm^{-1}): $\nu = 3425$ (m), 3321 (m), 3304 (m), 3221 (m), 3188 (m), 1716 (s), 1639 (m), 1620 (w), 1536 (m), 1503 (s), 1374 (m), 1337 (m), 1269 (m), 1195 (s), 1153 (s), 1129 (m), 1103 (m), 1062 (m), 933 (w), 869 (w), 783 (w), 751 (m), 711 (m), 682 (w). Raman (1064 nm, 500 mW): $\nu = 3305$ (8), 1701 (9), 1629 (9), 1556 (5), 1493 (5), 1356 (29), 1334 (31), 1274 (44), 1204 (100), 1159 (27), 1131 (31), 1106 (8), 1065 (35), 941 (7), 871 (60), 788 (6), 685 (5), 602 (22). MS (DEI+) *m/e*: 191.2 [M^+], 148.2 [$(\text{M}-\text{HNCO})^+$]. Elemental analysis, calcd (%): $\text{C}_3\text{H}_5\text{N}_5\text{O}_5$ (191.10): C 18.86, H 2.64, N 36.36; found: C 19.01, H 2.59, N 36.38. DSC (5 °C min^{-1} , onset): 209 °C (dec.). BAM drophammer: 40 J. Friction tester: 360 N, ESD: 1.0 J (grain size <100 μm).

Potassium 2-amino-2-(carbamoylimino)-1,1-dinitroethan-1-ide (2): 1 (0.38 g, 2.0 mmol) was suspended in 4 mL water and was placed in an ice bath. To this suspension a cooled solution of potassium hydroxide (4 mL water, 0.12 g, 2.1 mmol) was added dropwise, whereas the reaction mixture became a clear solution. The solution formed was diluted with methanol (30 mL) and cooled in an ice bath. The resulting orange precipitate was filtered off, washed with methanol and dried to obtain the potassium salt **2** (82%).

^1H NMR ($[\text{D}_6]\text{DMSO}$): $\delta = 9.47$ (s, 1H, CNH_2), 8.52 (s, 1H, CNH_2), 6.11 (s, 1H, CONH_2), 5.90 (s, 1H, CONH_2) ppm. $^{13}\text{C}\{^1\text{H}\}$ NMR ($[\text{D}_6]\text{DMSO}$): $\delta = 167.0$ (CO), 157.1 (CNH_2), 133.6 (CNO_2) ppm. ^{14}N NMR ($[\text{D}_6]\text{DMSO}$): $\delta = -24$ (s, NO_2) ppm. IR (ATR, cm^{-1}): $\nu = 3443$ (w), 3276 (w), 3166 (w), 1674 (m), 1630 (w), 1595 (s), 1503 (s), 1367 (m), 1350 (m), 1302 (m), 1245 (vs), 1171 (m), 1155 (m), 1130 (vs), 1077 (m), 925 (w), 851 (w), 816 (w), 779 (w), 769 (w), 749 (w). Raman (1064 nm, 500 mW): $\nu = 3280$ (3), 1595 (5), 1503 (12), 1397 (32), 1352 (44), 1238 (31), 1172 (36), 1132 (39), 1123 (34), 1083 (4), 926 (10), 852 (100), 750 (9), 653 (9), 525 (12). Elemental analysis, calcd (%): $\text{C}_3\text{H}_4\text{N}_5\text{O}_5\text{K}$ (229.19): C 15.72, H 1.76, N 30.56; found: C 15.75, H 1.85, N 30.17. DSC

(5 °C min⁻¹, onset): 155 °C (melt.), 191 °C (dec.). BAM drophammer: 20 J. Friction tester: 360 N, ESD: 0.5 J (grain size <100 μm).

2-(1-Amino-2,2-dinitrovinyl)hydrazine-1-carboxamide (3): 1-Amino-1-hydrazino-2,2-dinitroethene (HFOX) (0.82 g, 5.0 mmol) was dissolved in dry acetonitrile (20 mL) and placed in an ice bath. Chlorosulfonyl isocyanate (CSI) (0.74 g, 5.2 mmol) was added slowly at 0 °C. The ice bath was removed, and stirring at room temperature was continued for 1 h. The reaction mixture was again cooled in an ice bath, water (10 mL) was added with caution, and the mixture was stirred for 10 min at room temperature. The organic solvent was removed on the rotary evaporator. The formed yellow precipitation was filtered off, washed with few cold water and dried to obtain pure **3** (77%). The water free product was obtained by dehydration at 70 °C for 24 h under high vacuum.

¹H NMR ([D₆]DMSO): δ = 11.49 (s, 1H, CNH), 9.90 (s, 1H, CNH₂), 9.70 (s, 1H, CNH₂), 8.83 (s, 1H, CONH), 6.26 (s, 2H, CONH₂) ppm. ¹³C{¹H} NMR ([D₆]DMSO): δ = 158.9 (CNH₂), 157.6 (CO), 125.6 (CNO₂) ppm. ¹⁵N NMR ([D₆]DMSO): δ = -26.5 (s, NO₂), -247.5 (d, NH, ¹J_{NH} = 102.7 Hz), -265.9 (t, NH₂, ¹J_{NH} = 90.5 Hz), -274.9 (d, NH, ¹J_{NH} = 95.8 Hz), -305.5 (t, NH₂, ¹J_{NH} = 85.3 Hz) ppm. IR (ATR, cm⁻¹): ν = 3588 (w), 3473 (w), 3369 (m), 3264 (w), 3197 (w), 1689 (s), 1610 (m) 1570 (m), 1522 (s), 1500 (s), 1363 (m), 1297 (w), 1227 (m), 1187 (vs), 1140 (s), 1093 (s), 1035 (m), 871 (w), 800 (m), 780 (w), 749 (w), 715 (w), 667 (w). Raman (1064 nm, 800 mW): ν = 3380 (5), 3290 (7), 1709 (7), 1589 (10), 1555 (25), 1535 (52), 1423 (21), 1379 (30), 1353 (76), 1300 (100), 1270 (46), 1206 (30), 1147 (27), 1103 (50), 1048 (26), 959 (7), 873 (91), 802 (9), 789 (8), 751 (13). MS (DEI+) *m/e*: 206.1 [M⁺]. Elemental analysis, calcd (%): C₃H₆N₆O₅×0.5H₂O (206.12): C 16.75, H 3.28, N 39.07; found: C 16.68, H 3.29, N 39.00. DSC (5 °C min⁻¹, onset): 97 °C (loss of water). 170 °C (dec.). BAM drophammer: 6 J. Friction tester: 360 N, ESD: 0.3 J (grain size <100 μm dehydrated).

Potassium 2-amino-2-(2-carbamoylhydrazono)-1,1-dinitroethan-1-ide (4): **3** (0.41 g, 2.0 mmol) was suspended in 4 mL water and was placed in an ice bath. To this suspension a cooled solution of potassium hydroxide (4 mL water, 0.12 g, 2.1 mmol) was added dropwise, whereas the reaction mixture became a clear solution. The solution formed was diluted with methanol (30 mL). The resulting yellow precipitate was filtered off, washed with methanol and dried to obtain the yellow potassium salt **4** (62%).

¹H NMR ([D₆]DMSO): δ = 8.17 (s, 1H, CNNH), 5.91 (s, 2H, CNH₂), 5.87 (s, 2H, CONH₂) ppm. ¹³C{¹H} NMR ([D₆]DMSO): δ = 158.2 (CO), 139.6 (CNN), 132.0 (CNO₂) ppm. ¹⁴N NMR

([D₆]DMSO): $\delta = -22$ (NO₂) ppm. IR (ATR, cm⁻¹): $\nu = 3595$ (w), 3495 (w), 3418 (m), 3329 (w), 3227 (w), 3038 (w), 2911 (w), 1726 (m), 1652 (m), 1621 (w), 1573 (w), 1495 (m), 1470 (m), 1383 (s), 1345 (m), 1203 (s), 1133 (m), 1095 (vs), 1065 (vs), 1001 (m), 850 (w), 753 (m), 738 (w). Raman (1064 nm, 500 mW): $\nu = 1668$ (14), 1622 (7), 1570 (4), 1510 (4), 1483 (5), 1442 (4), 1372 (29), 1347 (31), 1227 (9), 1205 (20), 1153 (14), 1105 (22), 1075 (11), 1010 (7), 853 (100), 774 (6), 762 (8). Elemental analysis, calcd (%): C₃H₅N₆O₅K (244.21): C 14.76, H 2.06, N 34.41; found: C 14.56, H 2.32, N 33.85. DSC (5 °C min⁻¹, onset): 165°C (dec.). BAM drophammer: 20 J. Friction tester: 360 N, ESD: 0.3 J (grain size <100 μm dehydrated).

2-(2,2-Dinitro-1-ureidoethylidene)hydrazine-1-carboxamide (5): 1-Amino-1-hydrazino-2,2-dinitroethene (HFOX) (1.64 g, 10.0 mmol) was dissolved in dry acetonitrile (20 mL) and placed in an ice bath. Chlorosulfonyl isocyanate (CSI) (3.54 g, 25.0 mmol) was added slowly at 0 °C. The ice bath was removed, and stirring at room temperature was continued for 2 h. The reaction mixture was again cooled in an ice bath, water (15 mL) was added with caution, and the mixture was stirred for 10 min at room temperature. The organic solvent was removed completely on the rotary evaporator. The formed colorless precipitate was filtered off and dried to obtain **5** (56%).

¹H NMR ([D₆]DMSO): $\delta = 12.17$ (s, 1H, CNH), 7.69 (s, 2H, CNH), 6.93 (s, 4H, CONH₂), ¹³C NMR ([D₆]DMSO): $\delta = 154.0$ (CO), 149.5 (CO), 140.5 (CNN), 123.5 (br, CNO₂) ppm. ¹⁵N NMR ([D₆]DMSO): $\delta = -26.5$ (s, NO₂), -247.5 (d, NH, ¹J_{NH} = 102.7 Hz), -265.9 (t, NH₂, ¹J_{NH} = 90.5 Hz), -274.9 (d, NH, ¹J_{NH} = 95.8 Hz), -305.5 (t, NH₂, ¹J_{NH} = 85.3 Hz) ppm. ¹H NMR (CD₃CN): $\delta = 7.88$ (s, 1H, CH), 7.68 (s, 1H, CNH), 6.44 (s, 1H, CNH), 3.6 (br s, 4H, CONH₂) ppm. ¹³C NMR (CD₃CN): $\delta = 153.4$ (CO), 149.0 (CO), 135.3 (d, CNN, ²J_{CH} = 4.0 Hz), 104.8 (d, CH(NO₂)₂, ¹J_{CH} = 171.9 Hz) ppm. ¹⁴N NMR ([CD₃CN): $\delta = -24$ (NO₂) ppm. IR (ATR, cm⁻¹): $\nu = 3636$ (m), 3363 (m), 3237 (w), 3005 (m), 2908 (w), 2761 (w), 2698 (w), 1760 (s), 1724 (s), 1629 (w), 1604 (s), 1584 (vs), 1498 (s), 1381 (m), 1357 (m), 1322 (s), 1299 (m), 1270 (m), 1241 (m), 1184 (m), 1150 (w), 1091 (m), 1013 (s), 936 (w), 867 (m), 826 (s), 791 (m), 759 (w), 746 (m), 715 (w), 683 (w). Raman (1064 nm, 800 mW): $\nu = 3125$ (12), 3007 (22), 1776 (14), 1603 (31), 1577 (81), 1398 (13), 1372 (25), 1323(24), 1243 (18), 1186 (22), 1153 ((26), 1104 (28), 939 (100), 914 (32), 870 (8), 795 (8), 619 (10), 573 (9), 538 (16). MS (DEI+) *m/e*: 249.2 [M⁺]. Elemental analysis, calcd (%): C₄H₇N₇O₆ (249.14): C 19.28, H 2.83, N 39.35; found: C 19.48, H 2.92, N 39.04. DSC (5 °C min⁻¹, onset): 129 °C (dec.). BAM drophammer: 9 J. Friction tester: 360 N, ESD: 0.2 J (grain size <100 μm).

Potassium (1-carbamoyl-5-oxo-1,2,4-triazol-3-yl)dinitromethanide (6_K): **5** (0.49 g, 2.0 mmol) was stirred in water (10 mL) and a saturated solution of potassium bicarbonate was

added to the reaction mixture until the pH value is stable around 7.5. The formed lemon yellow precipitate was filtered off and washed with water. The product was recrystallized from hot water to obtain pure **6_K** (81%).

^1H NMR ($[\text{D}_6]\text{DMSO}$): $\delta = 12.15$ (s, 1H, NH), 7.70 (s, 1H, NH_2), 7.67 (s, 1H, NH_2) ppm. $^{13}\text{C}\{^1\text{H}\}$ NMR ($[\text{D}_6]\text{DMSO}$): $\delta = 154.0$ (CO), 149.6 (CO), 140.7 (CNN), 123.9 (CNO_2) ppm. ^{15}N NMR ($[\text{D}_6]\text{DMSO}$): $\delta = -22.9$ (s, NO_2), -115.5 (s, CNNCONH₂), -188.5 (s, CNNCONH₂), -235.3 (s, NH), -295.5 (t, NH_2 , $^1J_{\text{NH}} = 90.3$ Hz) ppm. IR (ATR, cm^{-1}): $\nu = 3441$ (w), 3324 (m), 3285 (w), 1767 (m), 1736 (s), 1719 (m), 1583 (m), 1506 (m), 1485 (m), 1440 (w), 1386 (s), 1198 (vs), 1123 (vs), 1081 (s), 957 (s), 835 (w), 785 (w), 775 (w), 749 (s), 690 (m), 680 (m), 655 (w). Raman (1064 nm, 800 mW): $\nu = 3331$ (5), 1733 (7), 1590 (47), 1505 (9), 1442 (5), 1442 (5), 1379 (93), 1319 (10), 1288 (18), 1215 (30), 1155 (10), 1138 (38), 1087 (21), 959 (100), 836 (63), 794 (31), 758 (6), 681 (3). MS (FAB+) m/e : 233.3 $[(\text{M}+\text{H})^+]$, 188.3 $[(\text{M}-\text{HNCO})^+]$. Elemental analysis, calcd (%): $\text{C}_4\text{H}_3\text{N}_6\text{O}_6\text{K}$ (270.20): C 17.78, H 1.12, N 31.10; found: C 17.75, H 1.28, N 30.81. DSC ($5\text{ }^\circ\text{C min}^{-1}$, onset): $198\text{ }^\circ\text{C}$ (dec.). BAM drophammer: 20 J. Friction tester: 360 N, ESD: 0.3 J (grain size $<100\text{ }\mu\text{m}$ dehydrated).

9.6 References

- [1] N. V. Latypov, J. Bergman, A. Langlet, U. Wellmar, U. Bemm, *Tetrahedron* **1998**, *54*, 11525–11536.
- [2] T. M. Klapötke, *Chemistry of High-Energy Materials*, 2nd ed., deGruyter, Berlin, **2012**.
- [3] a) J. Evers, T. M. Klapötke, P. Mayer, G. Oehlinger, J. Welch, *Inorg. Chem.* **2006**, *45*, 4996–5007; b) M.-J. Crawford, J. Evers, M. Göbel, T. M. Klapötke, P. Mayer, G. Oehlinger, J. M. Welch, *Propellants, Explos., Pyrotech.* **2007**, *32*, 478–495; c) U. Bemm, H. Ostmark, *Acta Crystallogr., Sect. C: Struct. Chem.* **1998**, *54*, 1997–1999.
- [4] A. Bellamy, in *High Energy Density Materials, Vol. 125* (Ed.: T. M. Klapötke), Springer, Berlin, Heidelberg, **2007**, pp. 1–33.
- [5] a) J. Akhavan, *The Chemistry of Explosives*, 2nd ed., Royal Soc. of Chemistry, Cambridge, **2004**; b) T. T. Vo, J. Zhang, D. A. Parrish, B. Twamley, J. M. Shreeve, *J. Am. Chem. Soc.* **2013**, *135*, 11787–11790.
- [6] Y. Zhang, Q. Sun, K. Xu, J. Song, F. Zhao, *Propellants, Explos., Pyrotech.* **2015**, DOI:10.1002/prop.201500065.
- [7] G. Hervé, G. Jacob, *Tetrahedron* **2007**, *63*, 953–959.
- [8] a) M. Hirama, T. Oishi, *Trichloroacetyl Isocyanate*, John Wiley & Sons, Ltd, New York, **2001**; b) D. N. Dhar, P. Dhar, *The Chemistry of Chlorosulfonyl Isocyanate*, World Scientific, Singapore, **2002**; c) R. Graf, *Angew. Chem., Int. Ed.* **1968**, *7*, 172–182; d) R. Graf, *Chem. Ber.* **1956**, *89*, 1071–1079.
- [9] P. Kočovský, *Tetrahedron Lett.* **1986**, *27*, 5521–5524.
- [10] C. Sandberg, N. Latypov, P. Goede, R. Tryman, A. J. Bellamy, *New Trends Res. Energ. Mater., Proc. Semin., 5th* **2002**, pp. 292–299.
- [11] H. Gao, Y.-H. Joo, D. A. Parrish, T. Vo, J. M. Shreeve, *Chem. – Eur. J.* **2011**, *17*, 4613–4618.
- [12] A. J. Bellamy, A. E. Contini, N. V. Latypov, *Propellants, Explos., Pyrotech.* **2008**, *33*, 87–88.
- [13] B. George, E. P. Papadopoulos, *J. Org. Chem.* **1976**, *41*, 3233–3237.
- [14] M. Oki, *Applications of Dynamic NMR Spectroscopy to Organic Chemistry*, Wiley-VCH, Deerfield Beach, **1985**.
- [15] a) E. Bojarska-Olejnik, L. Stefaniak, M. Witanowski, G. A. Webb, *Magn. Reson. Chem.* **1986**, *24*, 911–914; b) J. C. Oxley, J. L. Smith, K. E. Yeager, *J. Energ. Mater.* **1995**, *13*, 93–105.
- [16] T. Steiner, *Angew. Chem., Int. Ed.* **2002**, *41*, 48–76.
- [17] F. Weinhold, *Discovering Chemistry With Natural Bond Orbitals*, John Wiley & Sons, New York, **2012**.
- [18] I. J. Lochert, *FOX-7 - A new insensitive explosive*, DSTO Aeronautical and Maritime Research Laboratory, Melbourne, **2001**.

- [19] C.-R. Chang, K.-Z. Xu, J.-R. Song, B. Yan, *Acta Chim. Sinica* **2008**, *66*, 1399–1404.
- [20] G. P. Moss, P. A. S. Smith, D. Tavernier, *Pure Appl. Chem.* **1995**, *67*, 1307–1375.
- [21] Q. Qiu, X. Yang, K. Xu, Z. Gao, J. Song, S. Yang, F. Zhao, *Inorg. Chim. Acta* **2013**, *405*, 356–361.
- [22] D. E. Taylor, F. Rob, B. M. Rice, R. Podeszwa, K. Szalewicz, *Phys. Chem. Chem. Phys.* **2011**, *13*, 16629–16636.
- [23] a) P. Duden, *Ber. Dtsch. Chem. Ges.* **1893**, *26*, 3003–3011; b) V. Grakauskas, A. M. Guest, *J. Org. Chem.* **1978**, *43*, 3485–3488; c) Z. Jalovy, J. Ottis, A. Ruzicka, A. Lycka, N. V. Latypov, *Tetrahedron* **2009**, *65*, 7163–7170.
- [24] M. Göbel, T. M. Klapötke, *Adv. Funct. Mater.* **2009**, *19*, 347–365.
- [25] R. Meyer, J. Köhler, A. Homburg, *Explosives*, Wiley-VCH, Weinheim, **2007**.
- [26] M. Sućeska, *EXPLO5 V.6.02*, Zagreb, **2013**.
- [27] a) T. T. Vo, D. A. Parrish, J. M. Shreeve, *Inorg. Chem.* **2012**, *51*, 1963–1968; b) H. Gao, J. M. Shreeve, *Angew. Chem., Int. Ed.* **2015**, *54*, 6335–6338; c) K.-Z. Xu, C.-R. Chang, J.-R. Song, F.-Q. Zhao, H.-X. Ma, X.-Q. LÜ, R.-Z. Hu, *Chin. J. Chem.* **2008**, *26*, 495–499; d) M. A. Ilyushin, I. V. Bachurina, A. V. Smirnov, I. V. Tselinskii, I. V. Shugalei, *Cent. Eur. J. Energ. Mater.* **2010**, *7*, 14–47.
- [28] M. J. Frisch, G. W. Trucks, H. B. Schlegel, G. E. Scuseria, M. A. Robb, J. R. Cheeseman, V. B. G. Scalmani, B. Mennucci, G. A. Petersson, H. Nakatsuji, M. Caricato, X. Li, H. P. Hratchian, A. F. Izmaylov, J. Bloino, G. Zheng, J. L. Sonnenberg, M. Hada, M. Ehara, K. Toyota, R. Fukuda, J. Hasegawa, M. Ishida, T. Nakajima, Y. Honda, O. Kitao, H. Nakai, T. Vreven, J. J. A. Montgomery, J. E. Peralta, F. Ogliaro, M. Bearpark, J. J. Heyd, E. Brothers, K. N. Kudin, V. N. Staroverov, R. Kobayashi, J. Normand, K. Raghavachari, A. Rendell, J. C. Burant, S. S. Iyengar, J. Tomasi, M. Cossi, N. Rega, J. M. Millam, M. Klene, J. E. Knox, J. B. Cross, V. Bakken, C. Adamo, J. Jaramillo, R. Gomperts, R. E. Stratmann, O. Yazyev, A. J. Austin, R. Cammi, C. Pomelli, J. W. Ochterski, R. L. Martin, K. Morokuma, V. G. Zakrzewski, G. A. Voth, P. Salvador, J. J. Dannenberg, S. Dapprich, A. D. Daniels, Ö. Farkas, J. B. Foresman, J. V. Ortiz, J. Cioslowski, D. J. Fox, *Gaussian 09*, Rev. A.02 ed., Gaussian, Inc., Wallingford CT, **2009**.
- [29] R. D. Dennington, T. A. Keith, J. M. Millam, *GaussView*, Ver. 5.08 ed., Semichem, Inc., Wallingford CT, **2009**.
- [30] J. A. Montgomery, M. J. Frisch, J. W. Ochterski, G. A. Petersson, *J. Chem. Phys.* **2000**, *112*, 6532–6542.
- [31] J. W. Ochterski, G. A. Petersson, J. A. Montgomery, *J. Chem. Phys.* **1996**, *104*, 2598–2619.
- [32] E. F. C. Byrd, B. M. Rice, *J. Phys. Chem.* **2005**, *110*, 1005–1013.
- [33] a) F. Trouton, *Philos. Mag.* **1884**, *18*, 54–57; b) M. S. Westwell, M. S. Searle, D. J. Wales, D. H. Williams, *J. Am. Chem. Soc.* **1995**, *117*, 5013–5015.
- [34] M. Sućeska, *Propellants, Explos., Pyrotech.* **1991**, *16*, 197–202.

- [35] Oxford Diffraction Ltd., *CrysAlis CCD*, Version 1.171.35. (release 16-05-2011 CrysAlis 171.Net), Abingdon, Oxford, **2011**.
- [36] Oxford Diffraction Ltd., *CrysAlis RED*, Version 1.171.35.11 (release 16-05-2011 CrysAlis 171.NET), Abingdon, Oxford, **2011**.
- [37] A. Altomare, M. C. Burla, M. Camalli, G. L. Cascarano, C. Giacovazzo, A. Guagliardi, A. G. G. Moliterni, G. Polidori, R. Spagna, *J. Appl. Crystallogr.* **1999**, *32*, 115–119.
- [38] a) G. M. Sheldrick, *SHELX-97, Programs for Crystal Structure Determination*, **1997**; b) G. M. Sheldrick, *Acta Crystallogr., Sect. A: Found. Crystallogr.* **2008**, *A64*, 112–122.
- [39] L. Farrugia, *J. Appl. Crystallogr.* **1999**, *32*, 837–838.
- [40] A. Spek, *Acta Crystallogr., Sect. D: Biol. Crystallogr.* **2009**, *65*, 148–155.
- [41] Oxford Diffraction Ltd., *SCALE3 ABSPACK - An Oxford Diffraction program 1.04*, Abingdon, Oxford, **2005**.

IV Appendix

1 Appendix A.1

Table A.1-1: Cell parameters of 2 and 3 at 25 °C.

	2	3
temperature /K	298(1)	298(1)
crystal system	monoclinic	monoclinic
space group	$P2_1/c$	$P2_1/c$
$a / \text{\AA}$	12.91(4)	10.79(4)
$b / \text{\AA}$	6.59(2)	11.540(3)
$c / \text{\AA}$	9.88(4)	8.76(4)
$\beta / ^\circ$	103.5(3)	108.2(4)
$V / \text{\AA}^3$	817(3)	1037(4)
Z	4	4
$\rho_{\text{calc.}} / \text{g cm}^{-3}$	1.821	1.722

Table A.1-2: Crystallographic data for 2 and 3.

	2d	3d
formula	C ₃ H ₄ N ₄ O ₈	C ₃ H ₃ N ₅ O ₁₀
formula weight /g mol ⁻¹	224.09	269.08
temperature /K	173(2)	243(2)
$\lambda_{\text{MoK}\alpha}$ /Å	0.71073	0.71073
crystal system	monoclinic	monoclinic
space group (No.)	<i>P</i> 2 ₁ / <i>c</i>	<i>P</i> 2 ₁ / <i>c</i>
<i>a</i> /Å	12.838(1)	10.784(2)
<i>b</i> /Å	6.572(1)	11.527(2)
<i>c</i> /Å	9.869(1)	8.752(2)
<i>a</i> /°	90	90
β /°	103.57(1)	108.20(2)
γ /°	90	90
<i>V</i> /Å ³	809.34(1)	1033.5(7)
<i>Z</i>	4	4
$\rho_{\text{calc.}}$ /g cm ⁻³	1.839(3)	1.730(2)
μ /mm ⁻¹	0.186	0.178
<i>F</i> (000)	456	544
crystal habit	colorless needle	colorless needle
crystal size /mm	0.28 x 0.10 x 0.05	0.25 x 0.02 x 0.02
<i>q</i> range /°	4.28 – 32.71	4.28 – 33.51
index ranges	$-7 \leq h \leq 15$ $-8 \leq k \leq 7$ $-12 \leq l \leq 12$	$-13 \leq h \leq 13$ $-13 \leq k \leq 14$ $-7 \leq l \leq 10$
reflections measured	3596	5001
reflections independent	1572	1945
reflections unique	1082	681
<i>R</i> _{int}	0.0234	0.0526
<i>R</i> ₁ , <i>wR</i> ₂ (2 σ data)	0.0292, 0.0574	0.062, 0.128
<i>R</i> ₁ , <i>wR</i> ₂ (all data)	0.0485, 0.0610	0.176, 0.153
data/restraints/parameters	1572/0/210	1945/1/245
GOOF on <i>F</i> ²	0.883	0.806
residual el. density /e Å ⁻³	-0.165/0.188	-0.198/0.362
CCDC	23988	23989

Table A.1-3: Hydrogen bonds of 2,2,2-trinitroethyl carbamate (2).

D-H...A			Sym. of A	H...A	D-H	D...A	∠, DHA
N1	H1	O1	$-x, 1-y, -z$	2.160	0.91	3.012	156.0
N1	H2	O5	$-x, -\frac{1}{2}+y; \frac{1}{2}-z$	2.709	0.87	3.189	116.3
N1	H2	O1	$x, \frac{1}{2}-y, \frac{1}{2}+z$	2.310	0.87	3.152	163.9
C2	H3A	O7	$x, \frac{1}{2}-y, -\frac{1}{2}+z$	2.634	0.99	3.379	132.1

Table A.1-4: Hydrogen bonds of 2,2,2-trinitroethyl nitrocarbamate (3).

D-H...A			Sym. of A	H...A	D-H	D...A	∠, DHA
N1	H1	O1	$x, \frac{1}{2}-y, -\frac{1}{2}+z$	2.015	0.82	2.797	159.8
N1	H1	O4	$x, \frac{1}{2}-y, -\frac{1}{2}+z$	2.634	0.82	3.117	119.3
C2	H2B	O3	$1-x, -\frac{1}{2}+y, \frac{1}{2}-z$	2.711	0.99	3.635	154.1
C2	H2B	O4	$1-x, -\frac{1}{2}+y, \frac{1}{2}-z$	2.516	0.99	3.424	157.2
C2	H2A	O10	$-x, -y, 1-z$	2.607	0.99	3.448	143.9

2 Appendix A.2

Table A.2-1: Crystallographic data for 3b, 2c and 3c.

	3b	2c	3c
formula	C ₃ H ₃ N ₄ O ₈ F	C ₅ H ₈ N ₄ O ₈	C ₅ H ₆ N ₆ O ₁₂
formula weight /g mol ⁻¹	242.08	252.14	342.13
temperature /K	173(2)	173(2)	100(2)
$\lambda_{\text{MoK}\alpha}$ /Å	0.71073	0.71073	0.71073
crystal system	monoclinic	orthorhombic	orthorhombic
space group (No.)	<i>P2</i> ₁ / <i>c</i> (14)	<i>Pna</i> 2 ₁ (33)	<i>Pbca</i> (61)
<i>a</i> /Å	14.716(3)	15.3762(12)	10.1269(5)
<i>b</i> /Å	5.9850(9)	9.3483(7)	9.6783(4)
<i>c</i> /Å	9.6928(12)	6.8213(6)	26.0397(12)
<i>a</i> /°	90	90	90
β /°	103.728(14)	90	90
γ /°	90	90	90
<i>V</i> /Å ³	829.3(2)	980.5(1)	2552.2(2)
<i>Z</i>	4	4	8
$\rho_{\text{calc.}}$ /g cm ⁻³	1.939	1.708	1.781
μ /mm ⁻¹	0.206	0.164	0.178
<i>F</i> (000)	488	520	1392
crystal habit	colorless plate	colorless needle	colorless needle
crystal size /mm	0.38 x 0.38 x 0.05	0.36 x 0.04 x 0.02	0.32 x 0.04 x 0.03
<i>q</i> range /°	4.34 – 31.37	4.36 – 32.33	4.21 – 26.37
index ranges	-13 ≤ <i>b</i> ≤ 18 -7 ≤ <i>k</i> ≤ 7 -12 ≤ <i>l</i> ≤ 11	-22 ≤ <i>b</i> ≤ 20 -5 ≤ <i>k</i> ≤ 13 -10 ≤ <i>l</i> ≤ 9	-12 ≤ <i>b</i> ≤ 10 -10 ≤ <i>k</i> ≤ 12 -32 ≤ <i>l</i> ≤ 32
reflections measured	6350	4820	8994
reflections independent	1690	2763	2603
reflections unique	1364	2185	2181
<i>R</i> _{int}	0.0284	0.0291	0.0243
<i>R</i> ₁ , wR ₂ (2 σ data)	0.0306, 0.0671	0.0420, 0.0718	0.0295, 0.703
<i>R</i> ₁ , wR ₂ (all data)	0.0419, 0.0735	0.0616, 0.0822	0.0388, 0.0762
data/restraints/parameters	1690/0/157	2763/1/186	2603/0/232
GOOF on <i>F</i> ²	1.043	1.047	1.051
residual el. density /e Å ⁻³	-0.198/0.228	-0.213/0.254	-0.215/0.302
CCDC	1053756	1053753	1053757

Table A.2-2: Crystallographic data for 2d, 3d and 2e.

	2d	3d	2e
formula	C ₄ H ₇ N ₃ O ₆	C ₄ H ₆ N ₄ O ₈	C ₅ H ₈ N ₄ O ₈
formula weight /g mol ⁻¹	193.11	238.11	252.15
temperature /K	100(2)	173(2)	173(2)
$\lambda_{\text{MoK}\alpha}$ /Å	0.71073	0.71073	0.71073
crystal system	monoclinic	monoclinic	monoclinic
space group (No.)	<i>P</i> 2 ₁ / <i>c</i> (14)	<i>P</i> 2 ₁ / <i>c</i> (14)	<i>P</i> 2 ₁ / <i>c</i> (14)
<i>a</i> /Å	13.471(3)	15.4551(6)	13.4225(8)
<i>b</i> /Å	6.3990(7)	6.2566(2)	10.2488(6)
<i>c</i> /Å	9.7370(13)	9.7445(4)	7.4690(5)
<i>a</i> /°	90	90	90
β /°	106.543(18)	105.824(4)	95.778(6)
γ /°	90	90	90
<i>V</i> /Å ³	804.6(2)	906.6(1)	1022.4(1)
<i>Z</i>	4	4	4
$\rho_{\text{calc.}}$ /g cm ⁻³	1.594	1.745	1.638
μ /mm ⁻¹	0.151	0.171	0.157
<i>F</i> (000)	400	488	520
crystal habit	colorless plate	colorless plate	colorless plate
crystal size /mm	0.12 x 0.12 x 0.02	0.38 x 0.18 x 0.04	0.38 x 0.32 x 0.06
<i>q</i> range /°	4.20 – 26.37	4.19 – 26.37	4.37 – 25.50
index ranges	-10 ≤ <i>b</i> ≤ 16 -7 ≤ <i>k</i> ≤ 6 -12 ≤ <i>l</i> ≤ 8	-19 ≤ <i>b</i> ≤ 19 -7 ≤ <i>k</i> ≤ 7 -12 ≤ <i>l</i> ≤ 11	-16 ≤ <i>b</i> ≤ 15 -12 ≤ <i>k</i> ≤ 12 -9 ≤ <i>l</i> ≤ 8
reflections measured	2921	6513	7159
reflections independent	1636	1849	1895
reflections unique	1241	1574	1487
<i>R</i> _{int}	0.0277	0.0238	0.0272
<i>R</i> ₁ , wR ₂ (2 σ data)	0.0507, 0.1211	0.0312, 0.0742	0.0573, 0.1542
<i>R</i> ₁ , wR ₂ (all data)	0.0712, 0.1350	0.0387, 0.0791	0.0737, 0.1684
data/restraints/parameters	1636/0/136	1849/0/169	1895/0/186
GOOF on <i>F</i> ²	1.066	1.051	1.057
residual el. density /e Å ⁻³	-0.219/0.272	-0.214/0.230	-0.353/0.535
CCDC	1053754	1053758	1053755

Table A.2-3: Crystallographic data for 3e.

3e	
formula	C ₅ H ₇ N ₅ O ₁₀
formula weight /g mol ⁻¹	297.16
temperature /K	173(2)
$\lambda_{\text{MoK}\alpha}$ /Å	0.71073
crystal system	orthorhombic
space group (No.)	<i>P</i> 2 ₁ 2 ₁ 2 ₁ (19)
<i>a</i> /Å	8.5690(10)
<i>b</i> /Å	10.8030(8)
<i>c</i> /Å	25.5310(5)
α /°	90
β /°	90
γ /°	90
<i>V</i> /Å ³	2363.4(3)
<i>Z</i>	8
$\rho_{\text{calc.}}$ /g cm ⁻³	1.672
μ /mm ⁻¹	0.164
<i>F</i> (000)	1216
crystal habit	colorless needle
crystal size /mm	0.25 x 0.04 x 0.04
<i>q</i> range /°	4.38 – 25.86
index ranges	-6 ≤ <i>b</i> ≤ 10 -13 ≤ <i>k</i> ≤ 13 -30 ≤ <i>l</i> ≤ 31
reflections measured	13957
reflections independent	4786
reflections unique	3367
<i>R</i> _{int}	0.0559
<i>R</i> ₁ , <i>wR</i> ₂ (2σ data)	0.0760, 0.2012
<i>R</i> ₁ , <i>wR</i> ₂ (all data)	0.1046, 0.2352
data/restraints/parameters	4786/1/369
GOOF on <i>F</i> ²	1.033
residual el. density /e Å ⁻³	-0.318/0.613
CCDC	1053759

Table A.2-4: Halogen and hydrogen bonds of 2-fluoro-2,2-dinitroethyl nitrocarbamate (3b).

D-H...A			Sym. of A	H...A	D-H	D...A	∠, DHA
C2	H1	F1	$x, \frac{1}{2}-y, \frac{1}{2}+z$	2.762	0.96	3.485	131.7
C2	H1	F1	$x, \frac{1}{2}-y, -\frac{1}{2}+z$	2.776	0.96	3.485	131.7
C2	H1	O4	$x, \frac{1}{2}-y, \frac{1}{2}+z$	2.526	0.96	3.439	158.5
C2	H2	O4	$x, 1.5-y, \frac{1}{2}+z$	2.702	0.93	3.554	152.8
N3	H3	O6	$x, \frac{1}{2}-y, -\frac{1}{2}+z$	2.103	0.80	2.893	169.8
C2	H1	O4	$x, \frac{1}{2}-y, \frac{1}{2}+z$	2.528	0.96	3.439	158.5

Table A.2-5: Hydrogen bonds of 2,2-dinitropropane-1,3-diyl dicarbamate (2c).

D-H...A			Sym. of A	H...A	D-H	D...A	∠, DHA
N1	H1	O8	$-\frac{1}{2}+x, \frac{1}{2}-y, 1+z$	2.02	0.92	2.913	164.5
N1	H2	O8	$\frac{1}{2}-x, \frac{1}{2}+y, \frac{1}{2}+z$	2.060	0.88	2.913	161.5
C2	H3	O5	$\frac{1}{2}-x, -\frac{1}{2}+y, \frac{1}{2}+z$	2.715	0.97	3.536	144.0
C2	H4	O6	$\frac{1}{2}-x, -\frac{1}{2}+y, -\frac{1}{2}+z$	2.842	0.97	3.691	146.7
C4	H5	O5	$\frac{1}{2}-x, -\frac{1}{2}+y, \frac{1}{2}+z$	2.712	0.95	3.502	141.9
C4	H6	O6	$\frac{1}{2}-x, -\frac{1}{2}+y, -\frac{1}{2}+z$	2.562	0.94	3.494	170.1
N4	H7	O1	$\frac{1}{2}-x, \frac{1}{2}+y, -\frac{1}{2}+z$	2.152	0.83	2.941	159.5
N4	H8	O1	$\frac{1}{2}+x, \frac{1}{2}-y, -1+z$	2.162	0.87	2.963	152.1
N4	H8	O6	$1-x, 1-y, -\frac{1}{2}+z$	2.834	0.87	3.476	131.7

Table A.2-6: Hydrogen bonds of 2,2-dinitropropane-1,3-diyl bis(nitrocarbamate) (3c).

D-H...A			Sym. of A	H...A	D-H	D...A	∠, DHA
N2	H1	O3	$-\frac{1}{2}-x, \frac{1}{2}+y, z$	2.08	0.81	2.873	166.1
C2	H2	O5	$-x, -\frac{1}{2}+y, \frac{1}{2}-z$	2.572	0.97	3.484	158.0
C2	H2	O6	$-x, -\frac{1}{2}+y, \frac{1}{2}-z$	2.961	0.97	3.679	132.2
C2	H2	O7	$-\frac{1}{2}+x, y, \frac{1}{2}-z$	2.992	0.97	3.614	123.0
C2	H3	O1	$-\frac{1}{2}-x, -\frac{1}{2}+y, z$	2.586	0.93	3.429	153.0
C4	H4	O2	$-\frac{1}{2}-x, \frac{1}{2}+y, z$	2.605	0.93	3.296	131.3
C4	H5	O1	$1+x, y, z$	2.952	0.93	3.521	120.7
C4	H5	O8	$\frac{1}{2}-x, \frac{1}{2}+y, z$	2.460	0.93	3.305	151.4
N5	H6	O10	$\frac{1}{2}-x, -\frac{1}{2}+y, z$	1.980	0.83	2.813	177.2

Table A.2-7: Hydrogen bonds of 2,2-dinitropropyl carbamate (2d).

D-H...A			Sym. of A	H...A	D-H	D...A	∠, DHA
C1	H1	O3	x, -1+y, z	2.632	0.99	3.372	132.0
C1	H2	O2	-x, -y, 1-z	2.660	0.99	3.650	175.3
C1	H3	O2	-x, -1/2+y, 1.5-z	2.730	0.99	3.507	135.6
C1	H3	O4	x, -1/2-y, 1/2+z	2.821	0.99	3.621	138.5
C3	H4	O4	x, 1/2-y, 1/2+z	2.879	0.95	3.630	138.8
C3	H5	O4	x, -1/2-y, 1/2+z	2.965	0.93	3.774	147.9
N3	H6	O6	x, -1/2-y, -1/2+z	2.224	0.79	2.999	168.8
N3	H7	O6	1-x, -1-y, 2-z	2.071	0.90	2.923	158.7

Table A.2-8: Hydrogen bonds of 2,2-dinitropropyl nitrocarbamate (3d).

D-H...A			Sym. of A	H...A	D-H	D...A	∠, DHA
C1	H1	O2	1-x, 1/2+y, 1/2-z	2.772	0.95	3.535	138.3
C1	H1	O4	x, 1.5-y, -1/2+z	2.892	0.95	3.610	133.8
C1	H2	O2	1-x, 1-y, 1-z	2.645	0.97	3.606	176.0
C1	H3	O3	x, 1+y, z	2.503	0.97	3.277	137.3
C3	H4	O4	x, 1.5-y, -1/2+z	2.609	0.93	3.435	149.7
C3	H5	O3	x, 1/2-y, -1/2+z	2.918	0.95	3.492	120.7
C3	H5	O4	x, 1/2-y, -1/2+z	2.977	0.95	3.763	141.9
C3	H5	O7	-x, 1-y, -z	2.854	0.95	3.558	132.2
N3	H6	O6	x, 1.5-y, 1/2+z	2.112	0.84	2.931	168.4

Table A.2-9: Hydrogen bonds of 4,4,4-trinitrobutyl carbamate (2e).

D-H...A			Sym. of A	H...A	D-H	D...A	∠, DHA
C4	H5	O1	x, y, -1+z	2.882	0.98	3.542	125.2
N4	H8	O8	-x, -1/2+y, 1.5-z	2.818	0.83	3.391	130.6
C3	H3	O8	-x, 1-y, 1-z	2.875	0.99	3.771	153.5
N4	H7	O8	-x, 1-y, 2-z	2.102	0.82	2.917	173.8
C2	H2	O3	1-x, 1-y, 1-z	2.779	0.89	3.541	146.4
C2	H1	O5	x, 1/2-y, -1/2+z	2.692	0.92	3.509	148.5
N4	H8	O6	x, 1/2-y, -1/2+z	2.592	0.83	3.299	145.5
C2	H2	O2	x, 1.5-y, -1/2+z	2.790	0.89	3.555	146.5
C4	H5	O2	x, 1.5-y, -1/2+z	2.723	0.98	3.571	145.7
C4	H6	O8	x, 1.5-y, -1/2+z	2.776	0.98	3.495	131.0

Table A.2-10: Hydrogen bonds of compound 4,4,4-trinitrobutyl nitrocarbamate (3e).

D-H...A			Sym. of A	H...A	D-H	D...A	∠, DHA
C2	H1	O13	x, y, z	2.802	0.990	3.686	149.0
C4	H6	O3	-1+x, y, z	2.545	0.990	3.308	134.2
C4	H6	O6	-1/2+x, 1.5-y, -z	2.542	0.990	3.330	135.6
N4	H7	O18	-1+x, 1+y, z	2.012	1.00	2.862	142
N4	H7	O20	-1+x, 1+y, z	2.134	1.00	2.896	132
N9	H14	O8	x, 1+y, z	2.117	0.73	2.787	154
C9	H12	O11	-1+x, y, z	2.792	0.990	3.601	139.2
C9	H13	O13	-1+x, y, z	2.732	0.990	3.505	135.3
C8	H11	O11	-1/2+x, 1/2-y, -z	2.907	0.990	3.794	150.8
C9	H12	O16	-1/2+x, 1/2-y, -z	2.782	0.990	3.498	130.2
C7	H8	O20	2-x, -1/2+y, 1/2-z	2.701	0.990	3.494	137.8

Table A.2-11: Further calculated detonation and combustion parameters using EXPLO5 V6.02.

	2a	3a	2b	3b	2c	3c	2d	3d	2e	3e	AP
density RT	1.82	1.72	1.58	1.92	1.69	1.76	1.57	1.73	1.63	1.66	1.95
formula	$C_3H_4N_4O_8$	$C_3H_3N_5O_{10}$	$C_3H_4N_3O_6F$	$C_3H_3N_4O_8F$	$C_5H_8N_4O_8$	$C_5H_6N_6O_{12}$	$C_4H_7N_3O_6$	$C_4H_6N_4O_8$	$C_3H_8N_4O_8$	$C_3H_7N_5O_{10}$	NH_4ClO_4
$\Delta H_f^\circ / \text{kJ mol}^{-1}$	-459	-366	-659	-573	-902	-709	-553	-455	-523	-428	-296
$Q_v / \text{kJ kg}^{-1}$	-5286	-4456	-3922	-4342	-3260	-5088	-3779	-4839	-4547	-5184	-1422
T_{ex} / K	3780	3618	3178	3444	2487	3712	2740	3434	3160	3689	1735
$V_0 / \text{L kg}^{-1}$	761	750	749	707	768	743	803	743	770	752	885
P_{CJ} / kbar	302	232	211	338	196	275	186	271	221	262	158
$V_{Det} / \text{m s}^{-1}$	8530	7704	7273	8526	7256	8157	7130	7945	7524	7858	6368
I_s / s	246	232	227	237	182	245	196	242	220	251	157
I_s / s (5% Al)	250	244	239	248	202	249	205	246	233	258	198
I_s / s (10% Al)	253	248	244	250	213	256	223	255	245	262	224
I_s / s (15% Al)	254	251	248	252	228	254	238	259	253	265	235
I_s / s (20% Al)	255	252	252	254	236	255	244	261	254	265	244
I_s / s (25% Al)	255	252	246	254	236	255	242	256	248	260	247
I_s / s (30% Al)	251	251	234	248	230	247	237	244	241	247	247
I_s / s (5% Al, 14% binder)	228	252	203	234	184	222	201	216	217	225	250
I_s / s (10% Al, 14% binder)	239	256	219	244	196	234	212	233	222	239	257
I_s / s (15% Al, 14% binder)	247	261	233	248	214	244	225	243	237	249	261
I_s / s (20% Al, 14% binder)	246	255	233	245	228	243	235	243	240	246	263

3 Appendix A.3

Table A.3-1: Crystallographic data for 2 and 3.

	2	3
formula	C ₉ H ₁₂ N ₈ O ₁₆	C ₉ H ₂₄ N ₁₂ O ₁₆
formula weight /g mol ⁻¹	488.24	556.36
temperature /K	100(2)	173(2)
$\lambda_{\text{MoK}\alpha}$ /Å	0.71073	0.71073
crystal system	tetragonal	orthorhombic
space group (No.)	<i>P</i> -42 ₁ <i>c</i> (114)	<i>Pbca</i> (61)
<i>a</i> /Å	9.7350(5)	12.9274(5)
<i>b</i> /Å	9.7350(5)	12.7948(4)
<i>c</i> /Å	9.6921(5)	27.2880(8)
<i>a</i> /°	90	90
β /°	90	90
γ /°	90	90
<i>V</i> /Å ³	918.5(1)	4513.5(3)
<i>Z</i>	2	8
$\rho_{\text{calc.}}$ /g cm ⁻³	1.765	1.638
μ /mm ⁻¹	0.172	0.155
<i>F</i> (000)	500	2320
crystal habit	colorless block	colorless block
crystal size /mm	0.32 x 0.20 x 0.18	0.29 x 0.22 x 0.20
<i>q</i> range /°	4.19 – 27.2	4.60 – 31.5
index ranges	-10 ≤ <i>b</i> ≤ 12 -5 ≤ <i>k</i> ≤ 12 -12 ≤ <i>l</i> ≤ 8	-15 ≤ <i>b</i> ≤ 15 -15 ≤ <i>k</i> ≤ 14 -30 ≤ <i>l</i> ≤ 33
reflections measured	3874	33060
reflections independent	1069	4171
reflections unique	933	3486
<i>R</i> _{int}	0.0362	0.0261
<i>R</i> ₁ , <i>wR</i> ₂ (2 σ data)	0.0355, 0.0751	0.0498
<i>R</i> ₁ , <i>wR</i> ₂ (all data)	0.0378, 0.0789	0.0561, 0.1406
data/restraints/parameters	1069/0/87	4171/1/406
GOOF on <i>F</i> ²	1.072	1.075
res. electron density /e Å ⁻³	-0.192, 0.163	-0.323, 0.713
CCDC number	1003442	1003443

Table A.3-2: Hydrogen bonds of pentaerythritol tetranitrocarbamate (2).

D-H...A			Symm. of A	H...A	D-H	D...A	∠, DHA
N1	H3	O2	$y^{-1/2}, x+1/2, z^{-1/2}$	1.92	0.86	2.777	167.0
C2	H1	O4	$y^{-1/2}, x+1/2, z+1/2$	2.64	0.95	3.412	160.1
C2	H2	O3	$X+1/2, -y+1/2, -z+1/2$	2.73	0.91	3.607	138.8

Table A.3-3: Hydrogen bonds of tetraammonium salt of pentaerythritol tetranitrocarbamate (3).

D-H...A			Symm. of A	H...A	D-H	D...A	∠, DHA
C2	H1	O2	$x+1/2, y, z+1/2$	2.45	0.96	3.275	143.2
C4	H3	O10	$x, 1+y, z$	2.68	0.99	3.475	137.5
C7	H5	O8	x, y, z	2.68	0.93	3.452	140.2
C8	H7	O16	$1/2+x, y, 1/2z$	2.45	0.99	3.452	134.4
N9	H9	O3	x, y, z	1.99	0.86	2.837	166.1
N9	H9	O1	x, y, z	2.48	0.86	3.005	120.1
N9	H10	O7	$x, -y+1/2, z+1/2$	2.18	0.83	2.991	162.2
N9	H11	N2	$x+1/2, y, -z+1/2$	2.18	0.87	3.037	167.2
N9	H12	O16	$-x+1/2, y+1/2, z$	2.15	0.84	2.936	156.1
N9	H12	O8	$x, -y+1/2, z+1/2$	2.63	0.84	3.096	116.9
N10	H13	O10	$x+1/2, -y+1/2, -z$	2.35	0.85	3.069	142.6
N10	H13	N5	$x+1/2, -y+1/2, -z$	2.69	0.85	3.527	165.9
N10	H14	O14	$x+1/2, y, -z+1/2$	2.01	0.86	2.839	162.2
N10	H14	O15	$x+1/2, y, -z+1/2$	2.62	0.86	3.188	125.1
N10	H15	N7	x, y, z	2.11	0.87	2.974	175.5
N10	H16	O3	$-x+1/2, y-1/2, z$	2.28	0.85	3.058	152.6
N11	H17	O12	$x+1/2, -y+1/2, -z$	1.93	0.88	2.774	159.5
N11	H17	O9	$x+1/2, -y+1/2, -z$	2.43	0.88	3.039	126.8
N11	H18	O1	$x+1/2, y, -z+1/2$	2.10	0.87	2.966	168.7
N11	H19	N3	$-x+1/2, y+1/2, z$	2.33	0.85	3.124	154.6
N11	H19	O5	$-x+1/2, y+1/2, z$	2.59	0.85	3.150	124.7
N11	H20	O10	$-x, -y+1, -z$	2.05	0.90	2.921	163.9
N12	H21	N6	$-x+1/2, y-1/2, z$	2.32	0.87	3.133	155.4
N12	H21	O11	$-x+1/2, y-1/2, z$	2.61	0.87	3.257	132.7
N12	H22	O6	$x+1/2, -y+1/2, -z$	1.86	0.87	2.725	169.5
N12	H22	O7	$x+1/2, -y+1/2, -z$	2.57	0.87	3.100	120.1
N12	H23	O15	$x+1/2, y, -z+1/2$	2.17	0.88	3.004	158.6
N12	H24	O8	$-x+1, -y, -z$	2.25	0.85	3.039	153.2

4 Appendix A.4

Table A.4-1: Crystallographic data for 2a, 3a and 3b.

	2a	3a	3b
formula	C ₄ H ₈ N ₂ O ₄	C ₄ H ₆ N ₄ O ₈	C ₆ H ₈ N ₆ O ₁₂ (C ₂ H ₃ N) ₂ ·H ₂ O
formula weight /g mol ⁻¹	148.12	238.11	456.28
temperature /K	173(2)	173(2)	173(2)
λ _{MoKα} /Å	0.71073	0.71073	0.71073
crystal system	monoclinic	orthorhombic	triclinic
space group (No.)	<i>P2₁/c</i> (14)	<i>Fdd2</i> (43)	<i>P</i> -1 (2)
<i>a</i> /Å	8.8363(5)	16.3442 (5)	8.2936 (4)
<i>b</i> /Å	5.1148(4)	44.4286 (14)	10.2439 (4)
<i>c</i> /Å	7.0213(7)	4.7335 (2)	13.9157 (5)
<i>a</i> /°	90	90	97.091 (5)
<i>β</i> /°	95.482(7)	90	106.829 (5)
<i>γ</i> /°	90	90	113.799 (7)
<i>V</i> /Å ³	315.88(4)	3437.20 (20)	995.67 (10)
<i>Z</i>	2	16	2
ρ _{calc.} /g cm ⁻³	1.557	1.841	1.522
μ /mm ⁻¹	0.139	0.181	0.141
<i>F</i> (000)	156	1952	472
crystal habit	colorless block	colorless block	colorless plate
crystal size /mm	0.18 x 0.06 x 0.06	0.12 x 0.06 x 0.06	0.23 x 0.15 x 0.04
<i>q</i> range /°	4.61 – 29.36	4.44 – 28.98	4.33 – 25.34
index ranges	-11 ≤ <i>b</i> ≤ 11 -7 ≤ <i>k</i> ≤ 6 -9 ≤ <i>l</i> ≤ 3	-21 ≤ <i>b</i> ≤ 20 -60 ≤ <i>k</i> ≤ 59 -6 ≤ <i>l</i> ≤ 6	-9 ≤ <i>b</i> ≤ 9 -12 ≤ <i>k</i> ≤ 12 -16 ≤ <i>l</i> ≤ 16
reflections measured	1276	11070	16346
reflections independent	758	2097	3613
reflections unique	594	2016	2960
<i>R</i> _{int}	0.025	0.022	0.028
<i>R</i> ₁ , <i>wR</i> ₂ (2σ data)	0.0437, 0.1021	0.0214, 0.0535	0.0426, 0.1071
<i>R</i> ₁ , <i>wR</i> ₂ (all data)	0.0583, 0.1157	0.0231, 0.0517	0.0527 0.1172
data/restraints/parameters	758/0/62	2097/1/163	3613/3/322
GOOF on <i>F</i> ²	1.069	1.069	1.046
residual el. density /e Å ⁻³	-0.233/0.283	-0.167/0.122	-0.382/0.496
CCDC	1429437	1429438	1429439

Table A.4-2: Crystallographic data for 3c and 3d.

	3c	3d
formula	C ₇ H ₉ N ₇ O ₁₄ (C ₂ H ₃ N) ₂	C ₆ H ₆ N ₄ O ₈
formula weight /g mol ⁻¹	497.29	262.13
temperature /K	100(2)	294
λ _{MoKα} /Å	0.71073	0.71073
crystal system	monoclinic	monoclinic
space group (No.)	<i>P</i> 2 ₁ / <i>c</i> (14)	<i>P</i> 2 ₁ / <i>n</i> (14)
<i>a</i> /Å	9.8297 (4)	4.3479 (5)
<i>b</i> /Å	16.5363 (7)	14.8725 (13)
<i>c</i> /Å	26.6880 (11)	7.9973 (7)
<i>a</i> /°	90	90
<i>β</i> /°	94.572 (4)	93.696 (10)
<i>γ</i> /°	90	90
<i>V</i> /Å ³	4324.2 (3)	516.1(1)
<i>Z</i>	8	2
ρ _{calc.} /g cm ⁻³	1.528	1.687
μ /mm ⁻¹	0.142	0.159
<i>F</i> (000)	2048	268
crystal habit	colorless plate	colorless plate
crystal size /mm	0.22 x 0.19 x 0.03	0.28 x 0.22 x 0.05
<i>q</i> range /°	4.24 – 25.50	4.84 – 26.37
index ranges	-8 ≤ <i>b</i> ≤ 11 -20 ≤ <i>k</i> ≤ 18 -32 ≤ <i>l</i> ≤ 26	-5 ≤ <i>b</i> ≤ 5 -18 ≤ <i>k</i> ≤ 11 -9 ≤ <i>l</i> ≤ 7
reflections measured	17232	2469
reflections independent	7997	1054
reflections unique	6280	810
R _{int}	0.023	0.020
R ₁ , wR ₂ (2σ data)	0.0437, 0.1051	0.0388, 0.0949
R ₁ , wR ₂ (all data)	0.0604, 0.1170	0.0537, 0.1054
data/restraints/parameters	7997/0/671	1054/0/94
GOOF on <i>F</i> ²	1.027	1.051
residual el. density /e Å ⁻³	-0.461/0.542	-0.214/0.230
CCDC	1429441	1429440

Table A.4-3: Calculated heat of formation, predicted detonation and combustion parameters (using the EXPLO5 V6.02 code) for 3a–3d and ethylene glycol dinitrate EGDN and nitroglycerin NG.

	3a	3b	3c	3d	EGDN	NG
$\Delta H_f^\circ / \text{kJ mol}^{-1}$	-685	-985	-1023	-339	-371	-241
$\Delta U_f^\circ / \text{kJ kg}^{-1}$	-2784	-2676	-2373	-1208	-1540	-1487
$Q_v / \text{kJ kg}^{-1}$	-4013	-4064	-4294	-4816	-6065	-6409
T_{ex} / K	2944	3038	3216	3406	4321	4469
$V_0 / \text{L kg}^{-1}$	731	727	734	745	727	810
$P_{\text{CJ}} / \text{kbar}$	278	261	248	236	232	209
$V_{\text{det}} / \text{m s}^{-1}$	8014	7842	7703	7594	7748	7502

5 Appendix A.5

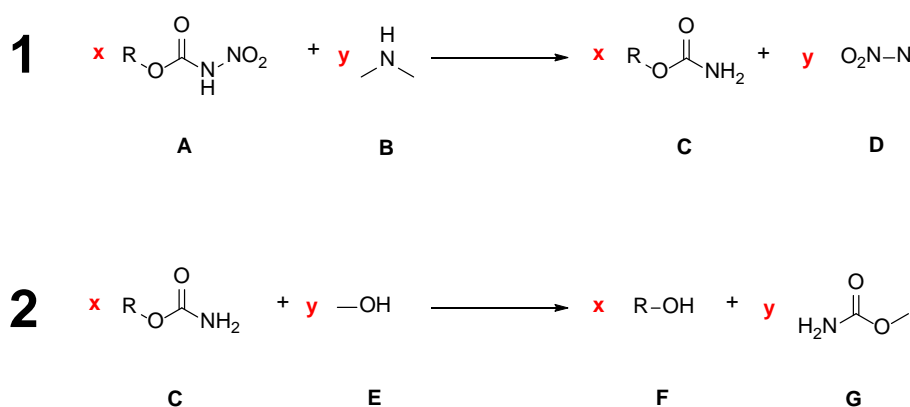
Table A.5-1: Crystallographic data for 2b and 3a.

	2b	3a
formula	C ₁₂ H ₁₈ N ₆ O ₁₂ H ₂ O	C ₈ H ₁₀ N ₈ O ₁₆ 2(H ₂ O)
formula weight /g mol ⁻¹	456.32	510.24
temperature /K	173	173
$\lambda_{\text{MoK}\alpha}$ /Å	0.71073	0.71073
crystal system	orthorhombic	monoclinic
space group (No.)	<i>Pbca</i> (61)	<i>P2₁/n</i> (14)
<i>a</i> /Å	15.4602 (5)	8.8865 (7)
<i>b</i> /Å	8.0901 (2)	10.1358 (9)
<i>c</i> /Å	30.0960 (11)	11.2758 (6)
<i>a</i> /°	90	90
β /°	90	98.951 (6)
γ /°	90	90
<i>V</i> /Å ³	3764.2 (2)	1003.26 (13)
<i>Z</i>	8	2
$\rho_{\text{calc.}}$ /g cm ⁻³	1.610	1.689
μ /mm ⁻¹	0.147	0.168
<i>F</i> (000)	1904	524
crystal habit	colorless plate	colorless plate
crystal size /mm	0.28x0.22x0.02	0.21x0.12x0.02
<i>q</i> range /°	4.53 – 27.59	4.39 – 31.23
index ranges	-18 ≤ <i>b</i> ≤ 18 -9 ≤ <i>k</i> ≤ 9 -36 ≤ <i>l</i> ≤ 36	-10 ≤ <i>b</i> ≤ 10 -11 ≤ <i>k</i> ≤ 12 -13 ≤ <i>l</i> ≤ 13
reflections measured	23700	6479
reflections independent	3456	1892
reflections unique	2719	1581
<i>R</i> _{int}	0.0600	0.0231
<i>R</i> ₁ , μ <i>R</i> ₂ (2 σ data)	0.0600, 0.1000	0.0474, 0.1231
<i>R</i> ₁ , μ <i>R</i> ₂ (all data)	0.0442, 0.1089	0.0568, 0.1317
data/restraints/parameters	3456/0/4352	1892/0/175
GOOF on <i>F</i> ²	1.027	1.038
residual el. density /e Å ⁻³	-0.460/0.792	-0.172/0.683
CCDC	1423039	1423040

Quantum Chemical Calculations and Isodesmic Reactions

All *ab initio* calculations were carried out using the program package Gaussian 09 (Rev. A.03)^[1] and visualized by GaussView 5.08^[2]. Structure optimizations and frequency analyses were performed with Becke's B3 three-parameter hybrid functional using the LYP correlation functional (B3LYP). For C, H, N, and O, a correlation consistent polarized double- ζ basis set was used (cc-pVDZ).^[3]

The heats of formations were calculated by the use of isodesmic reactions. This was necessary due to the high molecular weight and associated difficulties with complete basis set (CBS) calculation method. Isodesmic reactions can be hypothetical in which reactants and products have the same number of electron pairs. Due to the constant number of bonds of a given bond-type, the reaction energies of isodesmic reactions can be predicted quite accurately by cheap theoretical method.^[4] The subsequent two isodesmic reactions (Scheme A.5-1) were selected because the equal number of bonds, hybridisation and the number of attached hydrogen's generates a very good estimation.^[4]



Scheme A.5-1: General isodesmic reaction for the calculation of the heats of formation of polyvalent nitrocarbamates.

$$\Delta n(1) = x + y - x - y = 0 \quad \text{Eq. 1}$$

$$\Delta n(2) = x + y - x - y = 0 \quad \text{Eq. 2}$$

$$\Delta n(1 + 2) = 0 \quad \text{Eq. 3}$$

Reaction Energy in the gas phase at 0 K:

$$\Delta_R G(1) = -xG(A) - yG(B) + xG(C) + yG(D) \quad \text{Eq. 4}$$

$$\Delta_R G(2) = -xG(C) - yG(E) + xG(F) + yG(G) \quad \text{Eq. 5}$$

$$\Delta_R G(1+2) = \Delta_R G(1) + \Delta_R G(2) \quad \text{Eq. 6}$$

$$\Delta_R G(1+2) = -xG(A) - yG(B) + yG(D) - yG(E) + xG(F) - yG(G) \quad \text{Eq. 7}$$

Reaction Energy in the Gas Phase at 298 K:

$$\Delta_R G^\circ(1+2)(298K) = \Delta_R G^\circ(1+2) + \Delta_R G^\circ_{trans}(298K) + \Delta_R G^\circ_{rot}(298K) + \Delta_R G^\circ_{vib}(298K) \quad \text{Eq. 8}$$

$$\Delta_R G^\circ_{trans}(298K) = \sum_{i=1}^N \nu_i \frac{3}{2} RT = \Delta n * \frac{3}{2} RT = 0 * \frac{3}{2} RT = 0 \quad \text{Eq. 9}$$

$$\Delta_R G^\circ_{rot}(298K) = \sum_{i=1}^N \nu_i \frac{F_{rot}^i}{2} RT = \Delta n * F_{rot}^i * \frac{1}{2} RT = 0 * F_{rot}^i * \frac{1}{2} RT = 0 \quad \text{Eq. 10}$$

$$\Delta_R G^\circ_{vib}(298K) = \Delta \Delta_R G_{vib}(298K) + \Delta_R G_{ZPVE} \quad \text{Eq. 11}$$

The values of $\Delta \Delta_R G_{vib}$ and $\Delta_R G_{ZPVE}$ are given from Gaussian calculation (B3LYP/cc-pVDZ).

Reaction Enthalpy in the Gas Phase at 298 K:

$$\Delta H = \Delta G + p\Delta V \quad \text{Eq. 12}$$

$$\Delta_R H^\circ(1+2)(298K) = \Delta_R G(1+2)(298K) + p\Delta_R V \quad \text{Eq. 13}$$

Work by Gas:

$$p\Delta_R V = \Delta n RT = 0 * RT = 0 \quad \text{Eq. 14}$$

$$\Delta_R H^\circ(1+2)(298K) = \Delta_R G(1+2)(298K) \quad \text{Eq. 15}$$

Standard Enthalpy of Formation in the Gas Phase at 298 K of Compound A:

$$\Delta_R H^\circ(1+2) = -x\Delta_f H^\circ(A) - y\Delta_f H^\circ(B) + y\Delta_f H^\circ(D) - y\Delta_f H^\circ(E) + x\Delta_f H^\circ(F) - y\Delta_f H^\circ(G) \quad \text{Eq. 16}$$

$$\Delta_f H^\circ(A) = [\Delta_R H^\circ(1+2) - y\Delta_f H^\circ(B) + y\Delta_f H^\circ(D) - y\Delta_f H^\circ(E) + x\Delta_f H^\circ(F) - y\Delta_f H^\circ(G)]/x \quad \text{Eq. 17}$$

The values of the heat of formation $\Delta_f H^\circ$ were taken from the NIST database^[5] or calculated by CBS-4 M (MP4(SDQ)/6-31+(d,p)) method and by estimating according to the atomization energy method.^[6]

$\Delta_f H^\circ_{solid}(A)$ using the Trouton's Rule^[7]:

$$\Delta_{sub}H = C_{sub} * T_{melt} \sim 188 \frac{J}{mol \cdot K} * T_{melt} \quad \text{Eq. 18}$$

$$\Delta_f H_{solid}^\circ(A) = \Delta_f H_{(g)}^\circ - \Delta_{sub}H \quad \text{Eq.19}$$

Erythritol tetranitrocarbamate (3a):

R-OH: E_OH, erythritol

Basis Set: B3LYP/cc-pVDZ

Valency: 4

Isodesmic reaction mechanism:



Table A.5-2: Results from GAUSSIAN 09 calculation.

coefficient	compound	Sum of electronic and thermal free energies ($\mathcal{E}_0 + G_{\text{corr}}$) hartree
1	ROCONHNO ₂	-1951.982198
4	Me ₂ NH	-135.100304
4	Me ₂ NNO ₂	-339.614923
1	ROCONH ₂	-1134.047874
4	MeOH	-115.694776
4	MeOCONH ₂	-284.407134
1	ROH	-459.215600

$$\Delta_r G^\circ(\text{Reaction I}) = -0.124152 \text{ Ha}$$

$$\Delta_r G^\circ(\text{Reaction II}) = -0.017158 \text{ Ha}$$

$$\Delta_r G^\circ(\text{Reaction I+II}) = -0.017158 \text{ Ha}$$

Table A.5-3: Heat of formation in the gas phase $\Delta_f H^\circ_{\text{gas}}$ of the isodesmic reactions.

compound	kJ/mol	coefficient	\sum kJ/mol	Literature / Source
Me ₂ NH	-19	4	-76	Issoire, J.; Long, C. <i>Bull. Soc. Chim. France</i> 1960 , 2004–2012.
MeOH	-201	4	-804	Hine, J.; Arata, K. <i>Bull. Chem. Soc. Jpn.</i> 1976 , <i>49</i> , 3089–3092.
Me ₂ NNO ₂	-5	4	-20	Matyushin, Yu. N.; V'yunova, I. B.; Pepekin, V. I.; Apin, A. Ya. <i>Bull. Acad. Sci. USSR, Div. Chem. Sci.</i> 1971 , 2320–2323.
E_OH	-768	1	-768	From CBS-4 Calculation, GAUSSIAN09
MeOCONH ₂	-425	4	-1700	Bernard, M.A.; Boukari, Y.; Busnot, F. <i>Thermochim. Acta</i> 1976 , <i>16</i> , 267–275.

$$\Delta_f H^\circ_{\text{sub}}(\mathbf{3a}) = 0.032520 \text{ Ha}$$

$$\Delta_f H^\circ_{\text{gas}}(\mathbf{3a}) = -0.471145 \text{ Ha}$$

$$\Delta_f H^\circ_{\text{solid}}(\mathbf{3a}) = -0.503664 \text{ Ha} = -1322 \text{ kJ mol}^{-1}$$

myo-Inositol hexanitrocarbamate (3b):

R-OH: I_OH, *myo-inositol*

Basis Set: B3LYP/cc-pVDZ

Valency: 6

Isodesmic reaction mechanism:



Table A.5-4: Results from GAUSSIAN 09 calculation.

coefficient	compound	Sum of electronic and thermal free energies ($\mathcal{E}_0 + G_{\text{corr}}$) hartree
1	ROCONHNO ₂	-2926.193054
6	Me ₂ NH	-135.100304
6	Me ₂ NNO ₂	-339.614923
1	ROCONH ₂	-1699.29411
6	MeOH	-115.694776
6	MeOCONH ₂	-284.407134
1	ROH	-685.063427

$$\Delta_i G^\circ(\text{Reaction I}) = -0.188770 \text{ Ha}$$

$$\Delta_i G^\circ(\text{Reaction II}) = -0.043565 \text{ Ha}$$

$$\Delta_i G^\circ(\text{Reaction I+II}) = -0.232335 \text{ Ha}$$

Table A.5-5: Heat of formation in the gas phase $\Delta_f H^\circ_{\text{gas}}$ of the isodesmic reactions.

compound	kJ/mol	coefficient	\sum kJ/mol	Literature / Source
Me ₂ NH	-19	6	-114	Issoire, J.; Long, C. <i>Bull. Soc. Chim. France</i> 1960 , 2004–2012.
MeOH	-201	6	-1206	Hine, J.; Arata, K. <i>Bull. Chem. Soc. Jpn.</i> 1976 , <i>49</i> , 3089–3092.
Me ₂ NNO ₂	-5	6	-30	Matyushin, Yu. N.; V'yunova, I. B.; Pepekin, V. I.; Apin, A. Ya. <i>Bull. Acad. Sci. USSR, Div. Chem. Sci.</i> 1971 , 2320–2323.
I ₂ OH	-1072	1	-1072	From CBS-4 Calculation, GAUSSIAN09
MeOCONH ₂	-425	6	-2550	Bernard, M.A.; Boukari, Y.; Busnot, F. <i>Thermochim. Acta</i> 1976 , <i>16</i> , 267–275.

$$\Delta_f H^\circ_{\text{sub}}(\mathbf{3c}) = 0.032591 \text{ Ha}$$

$$\Delta_f H^\circ_{\text{gas}}(\mathbf{3c}) = -0.697774 \text{ Ha}$$

$$\Delta_f H^\circ_{\text{solid}}(\mathbf{3c}) = -0.730365 \text{ Ha} = -1918 \text{ kJ mol}^{-1}$$

D-Mannitol hexanitrocarbamate (3c):

R–OH: M_OH, mannitol

Basis Set: B3LYP/cc-pVDZ

Valency: 6

Isodesmic reaction mechanism:

**Table A.5-6: Results from GAUSSIAN 09 calculation.**

coefficient	compound	Sum of electronic and thermal free energies ($\mathcal{E}_0 + G_{\text{corr}}$) hartree
1	ROCONHNO ₂	-2927.344781
6	Me ₂ NH	-135.100304
6	Me ₂ NNO ₂	-339.614923
1	ROCONH ₂	-1700.455444
6	MeOH	-115.694776
6	MeOCONH ₂	-284.407134
1	ROH	-687.063527

$$\Delta_r G^\circ(\text{Reaction I}) = -0.198377 \text{ Ha}$$

$$\Delta_r G^\circ(\text{Reaction II}) = -0.045931 \text{ Ha}$$

$$\Delta_r G^\circ(\text{Reaction I+II}) = -0.244308 \text{ Ha}$$

Table A.5-7: Heat of formation in the gas phase $\Delta_f H^\circ_{\text{gas}}$ of the isodesmic reactions.

compound	kJ/mol	coefficient	\sum kJ/mol	Literature / Source
Me ₂ NH	-19	6	-114	Issoire, J.; Long, C. <i>Bull. Soc. Chim. France</i> 1960 , 2004–2012.
MeOH	-201	6	-1206	Hine, J.; Arata, K. <i>Bull. Chem. Soc. Jpn.</i> 1976 , <i>49</i> , 3089–3092.
Me ₂ NNO ₂	-5	6	-30	Matyushin, Yu. N.; V'yunova, I. B.; Pepekin, V. I.; Apin, A. Ya. <i>Bull. Acad. Sci. USSR, Div. Chem. Sci.</i> 1971 , 2320–2323.
M_OH	-1182	1	-1182	From CBS-4 Calculation, GAUSSIAN09
MeOCONH ₂	-425	6	-2550	Bernard, M.A.; Boukari, Y.; Busnot, F. <i>Thermochim. Acta</i> 1976 , <i>16</i> , 267–275.

$$\Delta_f H^\circ_{\text{sub}}(\mathbf{3c}) = 0.029727 \text{ Ha}$$

$$\Delta_f H^\circ_{\text{gas}}(\mathbf{3c}) = -0.673232 \text{ Ha}$$

$$\Delta_f H^\circ_{\text{solid}}(\mathbf{3c}) = -0.702959 \text{ Ha} = -1846 \text{ kJ mol}^{-1}$$

References:

- [1] M. J. Frisch, G. W. Trucks, H. B. Schlegel, G. E. Scuseria, M. A. Robb, J. R. Cheeseman, V. B. G. Scalmani, B. Mennucci, G. A. Petersson, H. Nakatsuji, M. Caricato, X. Li, H. P. Hratchian, A. F. Izmaylov, J. Bloino, G. Zheng, J. L. Sonnenberg, M. Hada, M. Ehara, K. Toyota, R. Fukuda, J. Hasegawa, M. Ishida, T. Nakajima, Y. Honda, O. Kitao, H. Nakai, T. Vreven, J. J. A. Montgomery, J. E. Peralta, F. Ogliaro, M. Bearpark, J. J. Heyd, E. Brothers, K. N. Kudin, V. N. Staroverov, R. Kobayashi, J. Normand, K. Raghavachari, A. Rendell, J. C. Burant, S. S. Iyengar, J. Tomasi, M. Cossi, N. Rega, J. M. Millam, M. Klene, J. E. Knox, J. B. Cross, V. Bakken, C. Adamo, J. Jaramillo, R. Gomperts, R. E. Stratmann, O. Yazyev, A. J. Austin, R. Cammi, C. Pomelli, J. W. Ochterski, R. L. Martin, K. Morokuma, V. G. Zakrzewski, G. A. Voth, P. Salvador, J. J. Dannenberg, S. Dapprich, A. D. Daniels, Ö. Farkas, J. B. Foresman, J. V. Ortiz, J. Cioslowski, D. J. Fox, *Gaussian 09*, Rev. A.02 ed., Gaussian, Inc., Wallingford CT, **2009**.
- [2] R. D. Dennington, T. A. Keith, J. M. Millam, *GaussView*, Ver. 5.08 ed., Semichem, Inc., Wallingford CT, **2009**.
- [3] J. A. Montgomery, M. J. Frisch, J. W. Ochterski, G. A. Petersson, *J. Chem. Phys.* **2000**, *112*, 6532–6542.
- [4] S. E. Wheeler, K. N. Houk, P. v. R. Schleyer, W. D. Allen, *J. Am. Chem. Soc.* **2009**, *131*, 2547–2560.
- [5] H. Y. Afeefy, J. F. Liebman, S. E. Stein, in *NIST Chemistry WebBook, NIST Standard Reference Database Number 69* Eds. P.J. Linstrom and W.G. Mallard, National Institute of Standards and Technology, Gaithersburg MD, 20899, <http://webbook.nist.gov>.
- [6] a) E. F. C. Byrd, B. M. Rice, *J. Phys. Chem.* **2005**, *110*, 1005–1013; b) J. W. Ochterski, G. A. Petersson, J. A. Montgomery, *J. Chem. Phys.* **1996**, *104*, 2598–2619.
- [7] M. S. Westwell, M. S. Searle, D. J. Wales, D. H. Williams, *J. Am. Chem. Soc.* **1995**, *117*, 5013–5015.

6 Appendix A.6

Table A.6-1: Crystallographic data for 2 and 4.

	2	4
formula	C ₄ H ₆ N ₄ O ₈	C ₇ H ₁₀ N ₈ O ₁₃ C ₂ H ₅ OH
formula weight /g mol ⁻¹	238.11	460.27
temperature /K	173(2)	173(2)
$\lambda_{\text{MoK}\alpha}$ /Å	0.71073	0.71073
crystal system	monoclinic	orthorhombic
space group (No.)	<i>P2₁/c</i> (14)	<i>Pnma</i> (62)
<i>a</i> /Å	12.846 (2)	11.7691 (4)
<i>b</i> /Å	7.5006 (10)	21.9210 (6)
<i>c</i> /Å	9.5234 (13)	7.6200 (5)
α /°	90	90
β /°	99.254 (15)	90
γ /°	90	90
<i>V</i> /Å ³	905.71 (20)	1965.89 (15)
<i>Z</i>	4	4
$\rho_{\text{calc.}}$ /g cm ⁻³	1.746	1.555
μ /mm ⁻¹	0.171	0.148
<i>F</i> (000)	488	952
crystal habit	colorless plate	colorless block
crystal size /mm	0.12 x 0.08 x 0.02	0.18 x 0.16 x 0.15
<i>q</i> range /°	4.21 – 25.99	4.23 – 28.88
index ranges	-15 ≤ <i>b</i> ≤ 12 -5 ≤ <i>k</i> ≤ 9 -9 ≤ <i>l</i> ≤ 11	-15 ≤ <i>b</i> ≤ 1 -29 ≤ <i>k</i> ≤ 28 -10 ≤ <i>l</i> ≤ 10
reflections measured	4035	13975
reflections independent	1737	2440
reflections unique	1434	13364
<i>R</i> _{int}	0.020	0.084
<i>R</i> ₁ , <i>wR</i> ₂ (2 σ data)	0.0565, 0.1537	0.0570, 0.1151
<i>R</i> ₁ , <i>wR</i> ₂ (all data)	0.0668, 0.1638	0.1250, 0.1397
data/restraints/parameters	1737/2/170	2440/0/250
GOOF on <i>F</i> ²	1.060	1.017
residual el. density /e Å ⁻³	-0.26/0.60	-0.23/0.33
CCDC	-	-

7 Appendix A.7

Table A.7-1: Crystallographic data for 1, 2 and 4.

	1	2	4
formula	C ₄ H ₆ N ₄ O ₇	C ₄ H ₅ N ₃ O ₈	C ₄ H ₄ N ₆ O ₇
formula weight /g mol ⁻¹	222.11	223.11	248.13
temperature /K	100(2)	100(2)	100(2)
$\lambda_{\text{MoK}\alpha}$ /Å	0.71073	0.71073	0.71073
crystal system	triclinic	monoclinic	triclinic
space group (No.)	<i>P</i> -1(2)	<i>P</i> 2 ₁ / <i>n</i> (14)	<i>P</i> -1(2)
<i>a</i> /Å	6.1081(5)	6.1307(7)	7.4160(5)
<i>b</i> /Å	7.5366(6)	16.7082(6)	7.5385(6)
<i>c</i> /Å	8.8543(7)	8.5025(4)	9.0347(8)
<i>a</i> /°	80.728(7)	90	70.713(8)
β /°	87.505(7)	98.296(4)	80.100(7)
γ /°	88.355(6)	90	81.601(7)
<i>V</i> /Å ³	401.80(6)	861.82(7)	467.47(6)
<i>Z</i>	2	4	2
$\rho_{\text{calc.}}$ /g cm ⁻³	1.836	1.720	1.763
μ /mm ⁻¹	0.177	0.171	0.168
<i>F</i> (000)	228	456	252
crystal habit	colorless plate	colorless block	colorless block
crystal size /mm	0.35 x 0.21 x 0.05	0.25 x 0.22 x 0.18	0.35 x 0.27 x 0.25
<i>q</i> range /°	4.27 – 28.27	4.15 – 26.37	4.20 – 26.36
index ranges	-8 ≤ <i>b</i> ≤ 8 -10 ≤ <i>k</i> ≤ 10 -11 ≤ <i>l</i> ≤ 11	-7 ≤ <i>b</i> ≤ 5 -18 ≤ <i>k</i> ≤ 20 -8 ≤ <i>l</i> ≤ 10	-9 ≤ <i>b</i> ≤ 9 -9 ≤ <i>k</i> ≤ 9 -11 ≤ <i>l</i> ≤ 11
reflections measured	3448	3513	4352
reflections independent	1971	1750	1909
reflections unique	1685	1484	1653
<i>R</i> _{int}	0.019	0.019	0.021
<i>R</i> ₁ , <i>wR</i> ₂ (2 σ data)	0.0308, 0.0735	0.0306, 0.0708	0.0309, 0.0726
<i>R</i> ₁ , <i>wR</i> ₂ (all data)	0.0380, 0.0794	0.0384, 0.0764	0.0384, 0.0782
data/restraints/parameters	1971/0/154	1750/0/156	1909/0/170
GOOF on <i>F</i> ²	1.060	1.040	1.040
res. electron density /e Å ⁻³	-0.228/0.388	-0.198/0.228	-0.215/0.302
CCDC number	-	-	-

Table A.7-2: Crystallographic data for 6, 7 and 9.

	6	7	9
formula	C ₃ H ₇ N ₄ O ₆ Cl H ₂ O	C ₃ H ₇ N ₄ O ₆ ·NO ₃	C ₆ H ₆ N ₆ O ₁₄
formula weight /g mol ⁻¹	248.58	257.14	386.14
temperature /K	100(2)	173(2)	173(2)
λ _{MoKα} /Å	0.71073	0.71073	0.71073
crystal system	triclinic	orthorhombic	monoclinic
space group (No.)	<i>P</i> -1(2)	<i>P</i> 2 ₁ 2 ₁ 2 ₁ (14)	<i>P</i> 2 ₁ / <i>n</i> (14)
<i>a</i> /Å	6.7434(6)	5.6622(4)	5.7264(3)
<i>b</i> /Å	7.8045(8)	10.2826(7)	21.6530(11)
<i>c</i> /Å	10.0663(10)	16.2582(18)	11.0910(6)
<i>a</i> /°	90.393(8)	90	90
β /°	98.800(8)	90	93.555(4)
γ /°	114.135(9)	90	90
<i>V</i> /Å ³	476.36(8)	946.59(14)	1372.57(12)
<i>Z</i>	2	4	4
ρ _{calc.} /g cm ⁻³	1.733	1.804	1.869
μ /mm ⁻¹	0.430	0.181	0.188
<i>F</i> (000)	256	528	784
crystal habit	colorless plate	colorless plate	colorless plate
crystal size /mm	0.32 x 0.27 x 0.08	0.32 x 0.28 x 0.08	0.12 x 0.11 x 0.04
<i>q</i> range /°	4.23 – 28.28	4.11 – 31.44	4.14 – 27.09
index ranges	-7 ≤ <i>b</i> ≤ 8 -10 ≤ <i>k</i> ≤ 8 -13 ≤ <i>l</i> ≤ 13	-8 ≤ <i>b</i> ≤ 7 -15 ≤ <i>k</i> ≤ 7 -11 ≤ <i>l</i> ≤ 23	-3 ≤ <i>b</i> ≤ 7 -21 ≤ <i>k</i> ≤ 27 -14 ≤ <i>l</i> ≤ 14
reflections measured	4182	5194	6223
reflections independent	2345	3069	3023
reflections unique	2050	2567	2572
<i>R</i> _{int}	0.021	0.029	0.021
<i>R</i> ₁ , w <i>R</i> ₂ (2σ data)	0.0287, 0.0641	0.0424, 0.0793	0.0301, 0.0652
<i>R</i> ₁ , w <i>R</i> ₂ (all data)	0.0355, 0.0680	0.0584, 0.0883	0.0390, 0.0700
data/restraints/parameters	2345/0/172	3069/0/175	3023/0/259
GOOF on <i>F</i> ²	1.083	1.058	1.025
residue electron density /e Å ⁻³	-0.292/0.336	-0.229/0.418	-0.240/0.379
CCDC number	-	-	-

Table A.7-3: Hydrogen bonds of 4,4,4-trinitrobutanamide (1).

D-H...A			sym. of A	H...A	D-H	D...A	∠, DHA
C3	H3	O5	1-x, 1-y, -z	2.702	0.96	3.600	155.6
C2	H2	O4	1-x, 1-y, 1-z	2.434	0.95	3.276	145.7
N4	H6	O7	2-x, -y, 1-z	2.073	0.89	2.933	170.9
N4	H5	O6	2-x, 1-y, -z	2.440	0.86	3.314	168.3
C2	H1	O7	2-x, 1-y, 1-z	2.640	0.95	3.531	156.2

Table A.7-4: Hydrogen bonds of 4,4,4-trinitrobutanoic acid (2).

D-H...A			sym. of A	H...A	D-H	D...A	∠, DHA
C2	H1	O1	-1+x, y, z	2.628	0.96	3.565	166.3
O8	H5	O7	1-x, -y, -z	1.769	0.86	2.632	176.5
C2	H2	O4	-1/2+x, 1/2-y, -1/2+z	2.547	0.94	3.253	136.1
C2	H2	O2	-1/2+x, 1/2-y, 1/2+z	2.653	0.94	3.389	132.5

Table A.7-5: Hydrogen bonds of 4,4,4-trinitrobutanoyl azide (4).

D-H...A			sym. of A	H...A	D-H	D...A	∠, DHA
C2	H2	O1	-x, 1-y, -z	2.535	0.96	3.373	144.7
C2	H1	O7	1-x, 1-y, -z	2.386	1.00	3.221	141.3

Table A.7-6: Hydrogen bonds of 3,3,3-trinitropropan-1-amine hydrochloride (6).

D-H...A			sym. of A	H...A	D-H	D...A	∠, DHA
N4	H6	O7		1.909	0.88	2.779	168.7
N4	H7	Cl1	-x+1, -y+2, -z+1	2.549	0.88	3.254	137.6
N4	H7	O5	x+1, y+1, z	2.574	0.88	3.206	129.3
N4	H8	Cl1		2.273	0.88	3.146	169.6
O7	H9	Cl1	x+1, y, z	2.469	0.82	3.235	155.2
O7	H10	Cl1	-x+1, -y+1, -z+1	2.380	0.82	3.184	169.0

Table A.7-7: Hydrogen bonds of 3,3,3-trinitropropan-1-amine nitrate (7).

D-H...A			sym. of A	H...A	D-H	D...A	\angle , DHA
N4	H5	O9	$-x+1, y-1/2, -z+1/2$	1.948	0.91	2.859	173.6
N4	H6	O7		1.957	0.90	2.818	160.0
N4	H6	N5		2.667	0.90	3.391	138.3
N4	H7	O7	$-x+2, y-1/2, -z+1/2$	2.080	0.92	2.954	158.0
N4	H7	O9	$-x+2, y-1/2, -z+1/2$	2.361	0.92	3.094	136.5
N4	H7	N5	$-x+2, y-1/2, -z+1/2$	2.570	0.92	3.465	164.4
C2	H2	O7	$-x+2, y-1/2, -z+1/2$	2.546	0.91	3.286	138.4

Table A.7-8: Hydrogen bonds of compound 2,2,2-trinitroethyl-4,4,4-trinitrobutanoate (9).

D-H...A			sym. of A	H...A	D-H	D...A	\angle , DHA
C2	H3	O6	$-1+x, y, z$	2.673	0.95	3.556	155.5
C5	H6	O10	$-1+x, y, z$	2.612	0.94	3.388	140.4
C2	H4	O7	$-x, 1-y, 1-z$	2.509	0.96	3.391	152.1
C3	H1	O12	$-1/2+x, 1/2-y, 1/2+z$	2.618	0.95	3.419	142.1

8 Appendix A.8

Table A.8-1: Crystallographic data for 4, 5 and 6.

	4	5	6
formula	C ₇ H ₁₀ N ₈ O ₁₃	C ₈ H ₁₀ N ₈ O ₁₄	C ₈ H ₈ N ₆ O ₁₆
formula weight /g mol ⁻¹	414.20	442.21	444.18
temperature /K	173	173	173
$\lambda_{\text{MoK}\alpha}$ /Å	0.71073	0.71073	0.71073
crystal system	orthorhombic	monoclinic	monoclinic
space group (No.)	<i>Pccn</i> (56)	<i>P2₁/c</i> (14)	<i>P2₁/c</i> (14)
<i>a</i> /Å	12.2453(6)	9.8760(6)	10.9196(7)
<i>b</i> /Å	40.795(3)	15.2750(10)	6.7591(4)
<i>c</i> /Å	9.3517(4)	11.2720(9)	11.8923(8)
<i>a</i> /°	90	90	90
β /°	90	93.027(7)	98.330(5)
γ /°	90	90	90
<i>V</i> /Å ³	4671.6(5)	1698.1(2)	868.5(1)
<i>Z</i>	12	4	2
$\rho_{\text{calc.}}$ /g cm ⁻³	1.767	1.730	1.699
μ /mm ⁻¹	0.171	0.167	0.169
<i>F</i> (000)	2544	904	452
crystal habit	colorless plate	colorless block	colorless plate
crystal size /mm	0.18x0.16x0.02	0.32x0.25x0.22	0.24x0.15x0.09
<i>q</i> range /°	4.43 – 30.23	4.24 – 28.22	4.57 – 32.02
index ranges	-7 ≤ <i>b</i> ≤ 15 -50 ≤ <i>k</i> ≤ 40 -6 ≤ <i>l</i> ≤ 11	-12 ≤ <i>b</i> ≤ 12 -17 ≤ <i>k</i> ≤ 18 -13 ≤ <i>l</i> ≤ 13	-11 ≤ <i>b</i> ≤ 13 -7 ≤ <i>k</i> ≤ 8 -10 ≤ <i>l</i> ≤ 14
reflections measured	13453	6716	3723
reflections independent	4756	3321	1582
reflections unique	3554	2541	1361
<i>R</i> _{int}	0.0632	0.0231	0.0195
<i>R</i> ₁ , <i>wR</i> ₂ (2 σ data)	0.0938, 0.1201	0.0385, 0.0568	0.0370, 0.0443
<i>R</i> ₁ , <i>wR</i> ₂ (all data)	0.1745, 0.1856	0.0777, 0.0869	0.0854, 0.0902
data/restraints/parameters	4756/5/494	3321/0/311	1582/0/152
GOOF on <i>F</i> ²	1.175	1.019	1.060
residual el. density /e Å ⁻³	-0.330/0.356	-0.358/0.323	-0.255/0.333
CCDC	1062382	1062383	1062384

Table A.8-2: Crystallographic data for 7, 8 and 9.

	7	8	9
formula	C ₄ H ₆ N ₄ O ₈	C ₄ H ₅ N ₅ O ₁₀	C ₅ H ₇ N ₇ O ₁₂
formula weight /g mol ⁻¹	238.11	283.11	357.02
temperature /K	173	295	173
$\lambda_{\text{MoK}\alpha}$ /Å	0.71073	0.71073	0.71073
crystal system	orthorhombic	orthorhombic	monoclinic
space group (No.)	<i>Pbca</i> (61)	<i>Pcn</i> (56)	<i>P2₁/c</i> (14)
<i>a</i> /Å	7.3738(3)	10.5771(6)	18.5978(12)
<i>b</i> /Å	9.7135(4)	23.7040(12)	9.6138(3)
<i>c</i> /Å	25.2033(10)	8.8283(4)	11.5247(5)
<i>a</i> /°	90	90	90
β /°	90	90	106.059(6)
γ /°	90	90	90
<i>V</i> /Å ³	1805.2(1)	2213.3(2)	1980.2(2)
<i>Z</i>	8	8	2
$\rho_{\text{calc.}}$ /g cm ⁻³	1.752	1.699	1.797
μ /mm ⁻¹	0.172	0.171	0.178
<i>F</i> (000)	976	1152	1092
crystal habit	colorless plate	colorless block	colorless plate
crystal size /mm	0.38x0.24x0.01	0.10x0.10x0.09	0.10x0.08x0.02
<i>q</i> range /°	4.83 – 32.17	3.12 – 23.83	4.42 – 27.61
index ranges	$-7 \leq h \leq 9$ $-10 \leq k \leq 12$ $-31 \leq l \leq 31$	$-12 \leq h \leq 11$ $-26 \leq k \leq 26$ $-10 \leq l \leq 9$	$-22 \leq h \leq 22$ $-11 \leq k \leq 5$ $-13 \leq l \leq 8$
reflections measured	13212	29604	6861
reflections independent	1835	1698	3669
reflections unique	1707	1297	2864
<i>R</i> _{int}	0.0183	0.0282	0.0211
<i>R</i> ₁ , wR_2 (2 σ data)	0.0284, 0.0308	0.0840, 0.1020	0.0424, 0.0611
<i>R</i> ₁ , wR_2 (all data)	0.0681, 0.0695	0.2392, 0.2577	0.0886, 0.0981
data/restraints/parameters	1835/0/169	1698/0/176	3669/0/353
GOOF on <i>F</i> ²	1.062	1.083	1.034
residual el. density /e Å ⁻³	-0.161/0.270	-0.342/0.409	-0.231/0.348
CCDC	1062385	1062386	1062387

Table A.8-3: Crystallographic data for 10.

10	
formula	C ₅ H ₆ N ₈ O ₁₄
formula weight /g mol ⁻¹	402.15
temperature /K	173
$\lambda_{\text{MoK}\alpha}$ /Å	0.71073
crystal system	monoclinic
space group (No.)	<i>Pc</i> (7)
<i>a</i> /Å	5.9260(3)
<i>b</i> /Å	11.3220(4)
<i>c</i> /Å	11.9577(6)
α /°	90
β /°	118.944(4)
γ /°	90
<i>V</i> /Å ³	702.1(1)
<i>Z</i>	2
$\rho_{\text{calc.}}$ /g cm ⁻³	1.902
μ /mm ⁻¹	0.192
<i>F</i> (000)	408
crystal habit	colorless needle
crystal size /mm	0.18x0.05x0.02
<i>q</i> range /°	5.27 – 30.01
index ranges	$-8 \leq h \leq 7$ $-15 \leq k \leq 15$ $-16 \leq l \leq 15$
reflections measured	6578
reflections independent	3144
reflections unique	2770
<i>R</i> _{int}	0.0414
<i>R</i> ₁ , <i>wR</i> ₂ (2 σ data)	0.0367, 0.0448
<i>R</i> ₁ , <i>wR</i> ₂ (all data)	0.0759, 0.0817
data/restraints/parameters	3144/2/323
GOOF on <i>F</i> ²	1.032
residual el. density /e Å ⁻³	-0.221/0.270
CCDC	10623828

Table A.8-4: Hydrogen bonds of bis(3,3,3-trinitropropyl) urea (4).

D-H...A			sym. of A	H...A	D-H	D...A	\angle , DHA
C2	H2	O8	$\frac{1}{2}-x, y, -\frac{1}{2}+z$	2.791	0.89	3.682	174.9
C3	H3	O18	x, y, z	2.643	0.95	3.583	166.9
C3	H3	O19	$\frac{1}{2}-x, y, -\frac{1}{2}+z$	2.728	0.95	3.450	133.7
C3	H3	O20	x, y, z	2.907	0.95	3.823	160.0
C3	H4	O16	$x, y, -1+z$	2.611	1.03	3.624	169.2
C3	H4	O19	$x, y, -1+z$	2.556	1.03	3.384	136.6
N4	H5	O19	$x, y, -1+z$	2.829	0.69	3.323	130.8
N4	H5	O21	$x, y, -1+z$	2.976	0.69	3.533	139.2
N4	H5	O7	$\frac{1}{2}-x, y, -\frac{1}{2}+z$	2.349	0.69	2.985	154.0
N5	H6	O7	$\frac{1}{2}-x, y, -\frac{1}{2}+z$	2.151	0.85	2.946	154.7
C5	H7	O12	$-\frac{1}{2}+x, -y, -\frac{1}{2}-z$	2.487	1.11	3.463	145.4
C5	H8	O9	$-x, -y, -z$	2.756	1.05	3.535	131.2
C9	H11	O5	x, y, z	2.555	0.95	3.503	174.6
C9	H12	O1	$x, y, -1+z$	2.895	0.89	3.697	151.0
C9	H12	O2	$x, y, -1+z$	2.896	0.89	3.647	143.2
C10	H13	O2	$x, \frac{1}{2}-y, -\frac{1}{2}+z$	2.772	1.01	3.586	138.3
C10	H14	O14	$x, \frac{1}{2}-y, -\frac{1}{2}+z$	2.743	0.98	3.702	165.8
N15	H15	O23	$1.5-x, y, -\frac{1}{2}+z$	2.104	0.88	2.947	159.7

Table A.8-5: Hydrogen bonds of bis(3,3,3-trinitropropyl) oxalamide (5).

D-H...A			sym. of A	H...A	D-H	D...A	\angle , DHA
C2	H1	O9	x, y, z	2.836	0.96	3.279	131.0
C2	H1	O5	$x, \frac{1}{2}-y, -\frac{1}{2}+z$	2.572	0.96	3.625	140.5
C2	H2	O13	$1+x, y, z$	2.895	0.93	3.694	135.6
C2	H2	O1	$x, \frac{1}{2}-y, -\frac{1}{2}+z$	2.968	0.93	3.715	147.4
C3	H3	O10	$2-x, \frac{1}{2}+y, 1.5-z$	2.641	0.97	3.604	172.7
N4	H5	O14	x, y, z	2.061	0.84	2.845	155.5
C6	H6	O1	$1+x, \frac{1}{2}-y, \frac{1}{2}+z$	2.977	0.96	3.859	154.1
C6	H7	O5	$x, \frac{1}{2}-y, \frac{1}{2}+z$	2.945	0.93	3.785	150.2
C7	H8	O3	$1+x, y, z$	2.860	0.96	3.789	163.4
N8	H10	O7	$1+x, y, z$	2.054	0.84	2.845	157.8

Table A.8-6: Hydrogen bonds of bis(3,3,3-trinitropropyl) oxalate (6).

D-H...A			sym. of A	H...A	D-H	D...A	∠, DHA
C2	H2	O7	$x, \frac{1}{2}-y, \frac{1}{2}+z$	2.687	0.96	3.446	136.6
C3	H3	O1	$-x, \frac{1}{2}+y, \frac{1}{2}-z$	2.611	0.95	3.204	121.1
C3	H3	O8	$x, \frac{1}{2}-y, \frac{1}{2}+z$	2.664	0.95	3.458	142.0
C3	H4	O4	$x, -1+y, z$	2.809	0.94	3.460	127.3
C3	H4	O5	$1-x, -\frac{1}{2}+y, \frac{1}{2}-z$	2.847	0.94	3.727	129.5
C3	H4	O6	$1-x, -\frac{1}{2}+y, \frac{1}{2}-z$	2.882	0.94	3.554	156.4

Table A.8-7: Hydrogen bonds of 3,3,3-trinitropropyl carbamate (7).

D-H...A			sym. of A	H...A	D-H	D...A	∠, DHA
N1	H1	O1	$1-x, -y, -z$	2.074	0.86	2.925	170.4
N1	H2	O1	$\frac{1}{2}-x, \frac{1}{2}+y, z$	2.090	0.85	2.938	174.0
C2	H3	O8	$\frac{1}{2}-x, -\frac{1}{2}+y, z$	2.633	0.95	3.378	135.1
C2	H4	O7	$-\frac{1}{2}-x, -\frac{1}{2}+y, z$	2.784	0.98	3.457	126.3
C3	H5	O3	$-\frac{1}{2}-x, -\frac{1}{2}+y, z$	2.614	0.98	3.380	135.4
C3	H6	O5	$\frac{1}{2}+x, y, \frac{1}{2}-z$	2.692	0.96	3.555	149.3

Table A.8-8: Hydrogen bonds of 3,3,3-trinitropropyl nitrocarbamate (8).

D-H...A			sym. of A	H...A	D-H	D...A	∠, DHA
N2	H1	O3	$\frac{1}{2}-x, y, -\frac{1}{2}+z$	1.922	0.94	2.784	150.7
N2	H1	O2	$\frac{1}{2}-x, y, -\frac{1}{2}+z$	2.318	0.94	3.034	132.2
C2	H2A	O1	$-\frac{1}{2}+x, 1-y, \frac{1}{2}-z$	2.796	0.97*	3.718	159.1
C3	H3A	O2	$-\frac{1}{2}+x, 1-y, \frac{1}{2}-z$	2.574	0.97*	3.285	130.3
C3	H3B	O7	$-\frac{1}{2}-x, y, -\frac{1}{2}+z$	2.875	0.97*	3.622	134.5
C3	H3B	O8	$-\frac{1}{2}-x, y, -\frac{1}{2}+z$	2.976	0.97*	3.763	139.0

Table A.8-9: Hydrogen bonds of 3,3,3-trinitro-*N*-(2,2,2-trinitroethyl)propan-1-amine (9).

D-H...A			sym. of A	H...A	D-H	D...A	∠, DHA
C2	H1	O3	$x, 1.5-y, -\frac{1}{2}+z$	2.533	0.96	3.389	148.2
N4	H3	O5	$1-x, -\frac{1}{2}+y, 1.5-z$	2.966	0.92	3.566	166.2
C3	H4	O18	$-1+x, y, z$	2.768	0.89	3.523	150.3
C3	H5	O7	$x, \frac{1}{2}-y, -\frac{1}{2}+z$	2.867	0.88	3.258	133.1
C3	H5	O15	$-1+x, 1.5-y, \frac{1}{2}+z$	2.575	0.88	3.370	136.5
C4	H6	O4	$1-x, 1-y, 1-z$	2.589	0.88	3.574	148.7
C4	H7	O9	$x, \frac{1}{2}-y, -\frac{1}{2}+z$	2.817	0.94	3.622	138.0
C8A	H8A	O10	$1-x, -\frac{1}{2}+y, \frac{1}{2}-z$	2.496	0.99*	3.622	138.8
C8A	H8A	O14	$2-x, -\frac{1}{2}+y, \frac{1}{2}-z$	2.666	0.99*	3.306	135.9
C8A	H9A	O12	$-1+x, y, z$	2.640	0.99*	3.447	171.3
C7A	H10A	O11	$1-x, 1-y, -z$	2.850	0.99*	3.810	163.6
C7A	H11A	O14	$x, 1.5-y, -\frac{1}{2}+z$	2.693	0.99*	3.615	155.1

Table A.8-10: Hydrogen bonds of *N*-(2,2,2-trinitroethyl)-*N*-(3,3,3-trinitropropyl) nitramide (10).

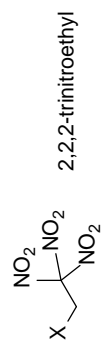
D-H...A			sym. of A	H...A	D-H	D...A	∠, DHA
C3	H4	O8	$-1+x, y, z$	2.634	0.89	3.595	171.3
C2	H2	O7	$-1+x, y, z$	2.569	0.95	3.342	138.7
C4	H6	O9	$-1+x, y, z$	2.474	0.95	3.401	154.1
C4	H5	O14	$x, -y, -\frac{1}{2}+z$	2.920	0.95	3.724	143.0
C2	H2	O2	$-1+x, 1-y, -\frac{1}{2}+z$	2.710	0.95	3.434	133.5
C3	H3	O10	$x, -y, -\frac{1}{2}+z$	2.692	0.91	3.595	169.8
C2	H1	O5	$x, 1-y, -\frac{1}{2}+z$	2.700	0.93	3.607	166.5
C3	H4	O8	$-1+x, y, z$	2.634	0.89	3.595	171.3
C2	H2	O7	$-1+x, y, z$	2.569	0.95	3.342	138.7
C4	H6	O9	$-1+x, y, z$	2.474	0.95	3.401	154.1

Table A.8-11: Further calculated detonation and combustion parameters using EXPLO5 V6.02.

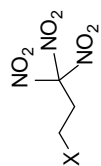
	4	5	6	7	8	9	10	AP
density RT	1.75	1.71	1.67	1.73	1.70	1.78	1.89	1.95
formula	$C_7H_{10}N_8O_{13}$	$C_8H_{10}N_8O_{14}$	$C_8H_8N_6O_{16}$	$C_4H_6N_4O_8$	$C_4H_5N_3O_{10}$	$C_5H_7N_7O_{12}$	$C_5H_6N_8O_{14}$	NH_4ClO_4
$\Delta H_f^\circ / \text{kJ mol}^{-1}$	-359.1	-522.3	-789.4	-503.5	-401.7	-86.4	-66.8	-295.8
$\Delta U_f^\circ / \text{kJ kg}^{-1}$	-774.1	-1091.5	-1693.5	-2021.0	-1331.3	-151.7	-79.7	-2623.2
$Q_v / \text{kJ kg}^{-1}$	-5385	-5095	-5126	-4662	-5809	-6565	-6377	-1422
T_{ex} / K	3692	3605	3808	3328	4175	4445	4420	1735
$V_0 / \text{L kg}^{-1}$	739	732	724	724	755	738	756	885
$P_{\text{CJ}} / \text{kbar}$	294	268	256	265	269	330	367	158
$V_{\text{Det}} / \text{m s}^{-1}$	8227	7937	7732	7896	8134	8713	9119	6368
I_s / s	254	245	250	237	256	272	264	157
$I_s / \text{s (5\% Al)}$	259	253	255	246	257	273	266	198
$I_s / \text{s (10\% Al)}$	265	259	257	252	260	274	268	224
$I_s / \text{s (15\% Al)}$	267	263	259	256	261	274	269	235
$I_s / \text{s (20\% Al)}$	268	267	260	262	262	274	269	244
$I_s / \text{s (25\% Al)}$	257	247	258	252	261	271	267	247
$I_s / \text{s (30\% Al)}$	245	240	246	242	254	262	262	247
$I_s / \text{s (5\% Al, 14\% binder)}$	227	220	223	213	238	254	261	250
$I_s / \text{s (10\% Al, 14\% binder)}$	242	235	237	227	247	261	266	257
$I_s / \text{s (15\% Al, 14\% binder)}$	251	245	246	240	253	261	267	261

Table A.8-12: Comparison of physical and chemical properties of the 3,3,3-trinitropropyl and 2,2,2-trinitroethyl group with different moieties.

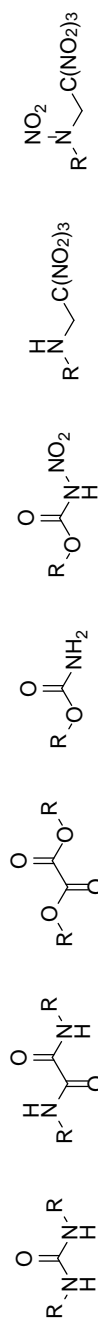
moiety	4		5		6		7		8		9		10						
	urea	ethyl	oxamide	ethyl	oxalate	propyl	ethyl	carbamate	propyl	ethyl	nitrocarbamate	propyl	ethyl	amine	propyl	ethyl	nitramine		
propyl <i>vs</i> ethyl	propyl	ethyl	propyl	ethyl	propyl	ethyl	propyl	ethyl	propyl	ethyl	propyl	ethyl	propyl	ethyl	propyl	ethyl	propyl	ethyl	
$T_m / ^\circ\text{C}$ (onset)	-	185	-	n.a.	121	115	78	91	68	109	65	114	141	94	153	96	2	64	28.9
$T_{dec} / ^\circ\text{C}$ (onset)	160	187	181	n.a.	170	201	152	169	134	153	96	114	153	96	114	153	7	64	28.9
IS / J	20	3	10	n.a.	> 40	10	> 40	40	> 30	10	7	5	7	2	7	2	2	2	2
FS / N	120	160	160	n.a.	> 360	> 360	> 360	64	> 288	96	120	120	160	64	120	160	64	64	28.9
N / %	27.1	29.0	25.3	27.1	18.9	20.2	23.5	25.0	24.7	26.0	27.5	28.6	27.9	28.6	27.9	28.9	28.9	28.9	28.9
O / %	50.2	53.9	50.7	54.1	57.6	61.5	53.8	57.1	56.5	59.5	53.8	56.0	55.7	56.0	55.7	57.7	57.7	57.7	57.7
N+O / %	77.3	82.9	76.0	81.2	76.5	81.7	77.3	82.1	81.2	85.5	81.3	84.6	83.6	84.6	83.6	86.6	86.6	86.6	86.6
$\Omega_{CO} / \%$	+3.9	+20.7	+3.6	+19.3	+14.4	+30.8	+6.7	+21.4	+19.8	+32.7	+15.7	+25.7	+23.9	+25.7	+23.9	+33.0	+33.0	+33.0	+33.0
$\Omega_{CO_2} / \%$	-20.2	+0.0	-20.3	-3.9	-14.4	+7.7	-20.2	0.0	-2.8	+14.9	-6.7	+7.0	+4.0	+7.0	+4.0	+16.5	+16.5	+16.5	+16.5
$r_{calc.} / \text{g cm}^{-3} \text{RT}$	1.75	1.86	1.71	1.80	1.67	1.86	1.73	1.82	1.70	1.72	1.78	1.84	1.89	1.84	1.89	1.92	1.92	1.92	1.92
$\Delta_f H_m^\circ / \text{kJ mol}^{-1}$	-359.1	-306.8	-522.3	-446.5	-789.4	-689.1	-503.5	-459.1	-401.7	-366.1	-86.4	-74.8	-66.8	-74.8	-66.8	-5.7	-5.7	-5.7	-5.7
$\Delta_f U^\circ / \text{kJ kg}^{-1}$	-774.1	-707.7	-1091.5	-994.2	-1693.5	-1578.6	-2021.0	-1960.8	-1331.3	-1278.2	-151.7	-131.4	-79.7	-131.4	-79.7	+68.3	+68.3	+68.3	+68.3



or



R =



9 Appendix A.9

Table A.9-1: Crystallographic data for HFOX, 1 and 2.

	HFOX	1	2
formula	C ₂ H ₅ N ₅ O ₄	C ₃ H ₅ N ₅ O ₅	C ₃ H ₄ N ₅ O ₅ K
formula weight /g mol ⁻¹	163.09	191.10	229.21
temperature /K	173(2)	173(2)	173(2)
$\lambda_{\text{MoK}\alpha}$ /Å	0.71073	0.71073	0.71073
crystal system	orthorhombic	triclinic	orthorhombic
space group (No.)	<i>Pnma</i> (62)	<i>P</i> -1 (2)	<i>P2₁2₁2₁</i> (14)
<i>a</i> /Å	6.2255(10)	9.5204(8)	7.2940(3)
<i>b</i> /Å	7.6807(9)	9.7709(7)	8.9920(3)
<i>c</i> /Å	12.2111(17)	10.9656(8)	12.0159(5)
<i>a</i> /°	90	97.989(6)	90
β /°	90	96.485(7)	90
γ /°	90	90.246(6)	90
<i>V</i> /Å ³	583.89(14)	1003.48(13)	788.09(5)
<i>Z</i>	4	6	4
$\rho_{\text{calc.}}$ /g cm ⁻³	1.855	1.898	1.932
μ /mm ⁻¹	0.174	0.178	0.684
<i>F</i> (000)	336	588	464
crystal habit	orange needle	yellow block	yellow plate
crystal size /mm	0.32x0.04x0.04	0.30x0.22x0.19	0.21x0.12x0.06
<i>q</i> range /°	4.53 – 27.47	4.13 – 26.73	4.39 – 32.39
index ranges	-5 ≤ <i>b</i> ≤ 8	-12 ≤ <i>b</i> ≤ 11	-10 ≤ <i>b</i> ≤ 10
	-9 ≤ <i>k</i> ≤ 9	-12 ≤ <i>k</i> ≤ 12	-12 ≤ <i>k</i> ≤ 13
	-14 ≤ <i>l</i> ≤ 15	-12 ≤ <i>l</i> ≤ 13	-17 ≤ <i>l</i> ≤ 17
reflections measured	4223	7187	9745
reflections independent	713	4191	2631
reflections unique	593	2853	2335
<i>R</i> _{int}	0.034	0.032	0.038
<i>R</i> ₁ , <i>wR</i> ₂ (2 σ data)	0.0386, 0.0953	0.0517, 0.1110	0.0332, 0.0655
<i>R</i> ₁ , <i>wR</i> ₂ (all data)	0.0492, 0.1048	0.0816, 0.1348	0.0424, 0.0722
data/restraints/parameters	713/1/68	4191/0/412	2631/0/143
GOOF on <i>F</i> ²	1.102	1.055	1.071
residual el. density /e Å ⁻³	-0.451/0.367	-0.350/0.593	-0.346/0.303

Table A.9-2: Crystallographic data for 3, 4 and 5.

	3	4	5
formula	2(C ₃ H ₆ N ₆ O ₅) H ₂ O	C ₃ H ₅ N ₆ O ₅ K	C ₄ H ₇ N ₇ O ₆
formula weight /g mol ⁻¹	430.29	244.21	249.14
temperature /K	173(2)	173(2)	173(2)
$\lambda_{\text{MoK}\alpha}$ /Å	0.71073	0.71073	0.71073
crystal system	orthorhombic	monoclinic	triclinic
space group (No.)	<i>Pca</i> 2 ₁ (29)	<i>P</i> 2 ₁ / <i>n</i> (14)	<i>P</i> -1 (2)
<i>a</i> /Å	6.7941(2)	9.4515(4)	8.4279(7)
<i>b</i> /Å	12.5486(5)	8.2373(4)	9.5361(6)
<i>c</i> /Å	18.4107(7)	11.1018(5)	13.4489(11)
<i>a</i> /°	90	90	102.602(6)
β /°	90	92.513(4)	102.644(7)
γ /°	90	90	107.809(6)
<i>V</i> /Å ³	1569.63(10)	863.50(7)	955.66(13)
<i>Z</i>	4	4	4
$\rho_{\text{calc.}}$ /g cm ⁻³	1.821	1.879	1.732
μ /mm ⁻¹	0.170	0.634	0.160
<i>F</i> (000)	888	496	512
crystal habit	yellow block	yellow block	colorless plate
crystal size /mm	0.38 x 0.11 x 0.11	0.18 x 0.14 x 0.10	0.12 x 0.11 x 0.02
<i>q</i> range /°	4.42 – 32.39	4.32 – 26.36	4.17 – 26.37
index ranges	-10 ≤ <i>b</i> ≤ 10	-11 ≤ <i>b</i> ≤ 11	-9 ≤ <i>b</i> ≤ 10
	-10 ≤ <i>k</i> ≤ 18	-10 ≤ <i>k</i> ≤ 10	-11 ≤ <i>k</i> ≤ 11
	-27 ≤ <i>l</i> ≤ 26	-13 ≤ <i>l</i> ≤ 13	-14 ≤ <i>l</i> ≤ 16
reflections measured	16685	6374	6961
reflections independent	5107	1762	3884
reflections unique	4241	1432	2807
<i>R</i> _{int}	0.031	0.037	0.028
<i>R</i> ₁ , <i>wR</i> ₂ (2σ data)	0.0404, 0.0901	0.0329, 0.0770	0.0436, 0.0903
<i>R</i> ₁ , <i>wR</i> ₂ (all data)	0.0545, 0.0990	0.0463, 0.0865	0.0701, 0.1022
data/restraints/parameters	5107/1/305	1762/0/156	3884/0/363
GOOF on <i>F</i> ²	1.028	1.068	1.037
residual el. density /e Å ⁻³	-0.309/0.531	-0.360/0.335	-0.235/0.230

Table A.9-3: Crystallographic data for 6_K and 6_NH₄.

	6_K	6_NH ₄
formula	C ₄ H ₃ N ₆ O ₆ K	C ₄ H ₃ N ₆ O ₆ NH ₄
formula weight /g mol ⁻¹	270.22	249.14
temperature /K	173(2)	173(2)
$\lambda_{\text{MoK}\alpha}$ /Å	0.71073	0.71073
crystal system	orthorhombic	orthorhombic
space group (No.)	<i>Pbca</i> (61)	<i>Pbca</i> (61)
<i>a</i> /Å	13.7655(5)	14.2816(6)
<i>b</i> /Å	7.2622(2)	6.5952(3)
<i>c</i> /Å	18.3782(6)	19.0169(7)
<i>a</i> /°	90	90
β /°	90	90
γ /°	90	90
<i>V</i> /Å ³	1837.23(10)	1791.20(13)
<i>Z</i>	8	8
$\rho_{\text{calc.}}$ /g cm ⁻³	1.954	1.848
μ /mm ⁻¹	0.614	0.171
<i>F</i> (000)	1088	1024
crystal habit	yellow block	yellow plate
crystal size /mm	0.35 x 0.27 x 0.19	0.24 x 0.18 x 0.03
<i>q</i> range /°	4.23 – 26.37	4.21 – 27.09
index ranges	-17 ≤ <i>h</i> ≤ 16 -9 ≤ <i>k</i> ≤ 9 -22 ≤ <i>l</i> ≤ 22	-18 ≤ <i>h</i> ≤ 16 -8 ≤ <i>k</i> ≤ 8 -21 ≤ <i>l</i> ≤ 24
reflections measured	13724	12202
reflections independent	1867	1959
reflections unique	1708	1555
<i>R</i> _{int}	0.026	0.042
<i>R</i> ₁ , <i>wR</i> ₂ (2 σ data)	0.0252, 0.0666	0.0362, 0.0829
<i>R</i> ₁ , <i>wR</i> ₂ (all data)	0.0278, 0.0686	0.0514, 0.0916
data/restraints/parameters	1867/0/166	1959/0/189
GOOF on <i>F</i> ²	1.068	1.038
residual el. density /e Å ⁻³	-0.300/0.289	-0.255/0.231

Table A.9-4: Hydrogen bonds of 1-(1-amino-2,2-dinitrovinyl)urea (1).

D-H...A			sym. of A	D-H	H...A	D...A	\angle , DHA
N4	H3	O1		0.90	1.859	2.592	137.01
N4	N3	O7	$-x, -y+1, -z+1$	0.90	2.600	3.343	140.23
N14	H13	O11		0.84	1.896	2.572	137.15
N10	H10	O5	$-x+1, -y, -z+1$	0.91	2.116	2.959	153.95
N5	H5	O15	$x, y, z+1$	0.88	2.067	2.915	161.79
N9	H8	O6		0.92	1.849	2.587	135.50
N9	H8	O12	$-x+1, -y+1, -z+1$	0.92	2.620	3.388	141.37
N5	H4	O7 [$x, -y+1, -z+1$	0.89	2.129	2.958	155.75
N5	H4	O8	$-x, -y+1, -z+1$	0.89	2.345	3.034	134.70
N8	H7	O10		0.84	1.919	2.603	137.54
N8	H7	O3	$-x, -y, -z$	0.84	2.442	2.907	115.63
N3	H1	O4		0.89	1.931	2.573	127.80
N3	H1	O14	$x, y-1, z$	0.89	2.273	2.967	134.79
N8	H6	O9		0.88	1.908	2.577	131.66
N8	H6	O4	$-x, -y, -z$	0.88	2.304	2.979	133.79
N15	H15	O10	$-x+1, -y, -z$	0.86	2.124	2.930	156.74
N13	H12	O15		0.88	1.929	2.638	136.94
N13	H12	O8	$-x, -y+1, -z$	0.88	2.446	2.925	114.91
N10	H9	O12	$-x+1, -y+1, -z+1$	0.91	2.134	3.002	160.43
N10	H9	O13	$-x+1, -y+1, -z+1$	0.91	2.283	2.965	131.87
N13	H11	O14		0.87	1.857	2.558	136.33
N13	H11	O9	$-x, -y+1, -z$	0.87	2.352	2.993	130.73
N3	H2	O5		0.97	1.834	2.612	134.66
N3	H2	O13	$x, y-1, z$	0.97	2.343	2.870	113.17
N15	H14	O2	$x+1, y, z$	0.89	2.222	3.076	160.40
N15	H14	O3	$x+1, y, z$	0.89	2.388	3.039	130.02

Table A.9-5: Hydrogen bonds of potassium 2-amino-2-(carbamoylimino)-1,1-dinitroethan-1-ide (2).

D-H...A			sym. of A	D-H	H...A	D...A	\angle , DHA
N3	H1	N4	$-x+2, y-1/2, z+3/2$	0.86	2.551	3.292	144.63
N3	H2	O5		0.96	1.972	2.633	124.41
N3	H2	O3	$x+1, y, z$	0.96	2.330	2.962	123.10
N5	H3	N4	$x+1/2, -y+1/2, -z+2$	0.93	2.124	3.025	164.18
N5	H4	O5	$x-1/2, -y+1/2, -z+2$	0.86	2.068	2.911	165.40

Table A.9-6: Hydrogen bonds of compound 1-amino-1-hydrazino-2,2-dinitroethene (HFOX).

D-H...A			sym. of A	D-H	H...A	D...A	\angle , DHA
N2	H1	O1	$x-1/2, -y+3/2, -z+1/2$	0.85	2.640	3.331	139.7
N2	H1	O1	$x-1/2, y, -z+1/2$	0.85	2.640	3.331	139.7
N2	H2	O2	$-x+1, -y+1, -z$	0.85	2.507	3.195	139.0
N2	H2	O2	$-x+1, y+1/2, -z$	0.85	2.507	3.195	139.0
N3	H3	O2	$-x+2, -y+1, -z$	0.86	2.202	3.007	156.9
N3	H3	O2	$-x+2, y+1/2, -z$	0.86	2.557	3.007	113.9
N3	H3	O1	$-x+2, -y+1, -z$	0.86	2.632	3.125	117.9
N3	H3	N1	$-x+2, -y+1, -z$	0.86	2.693	3.361	136.0
N4	H4	O1	$-x+3/2, -y+1, z-1/2$	0.82	2.450	3.166	146.3
N4	H4	O2	$-x+3/2, -y+1, z-1/2$	0.82	2.658	3.359	144.4
N2	H1	O1	$x-1/2, -y+3/2, -z+1/2$	0.85	2.640	3.331	139.7
N2	H1	O1	$x-1/2, y, -z+1/2$	0.85	2.640	3.331	139.7
N2	H2	O2	$-x+1, -y+1, -z$	0.85	2.507	3.195	139.0

Table A.9-7: Hydrogen bonds of 2-(1-amino-2,2-dinitrovinyl)hydrazine-1-carboxamide (3).

D-H...A			sym. of A	D-H	H...A	D...A	\angle , DHA
N4	H3	O1		0.90	1.873	2.567	132.01
N4	H3	O5	$x+1/2, -y+1, z$	0.90	2.251	2.991	138.90
N3	H1	O4		0.95	1.929	2.614	127.15
N3	H1	O1	$x-1, y, z$	0.95	2.174	2.828	125.07
N3	H3	O5	$x-1/2, -y+1, z$	0.92	2.043	2.906	155.73
N5	H4	O11		0.84	1.948	2.783	170.22
N6	H6	O2	$-x+1, -y+1, z-1/2$	0.93	2.323	3.009	130.23
N6	H6	O3	$-x+1, -y+1, z-1/2$	0.93	2.379	3.204	147.52
N6	H5	O4	$-x+1/2, y, z-1/2$	0.89	2.402	3.188	147.06
N9	H8	O10	$x-1/2, -y+2, z$	0.95	2.437	3.164	133.47
N9	H8	O11		0.95	2.564	3.395	146.62
N9	H7	O9		0.98	1.852	2.558	126.72
N9	H7	O6	$x-1, y, z$	0.98	2.167	2.894	130.11
N10	H9	O6		0.90	1.832	2.538	133.78
N10	H9	O10	$x+1/2, -y+2, z$	0.90	2.351	3.023	131.54
N11	H10	O3	$-x+3/2, y, z-1/2$	0.88	2.062	2.901	159.42
N12	H12	O8	$-x+2, -y+2, z-1/2$	0.84	2.397	3.093	140.98
N12	H12	O7	$-x+2, -y+2, z-1/2$	0.84	2.493	3.173	139.03
N12	H11	O9	$-x+3/2, y, z-1/2$	0.87	2.399	3.071	134.40
N12	H11	O3	$-x+3/2, y, z-1/2$	0.87	2.620	3.291	134.73
O11	H14	O2	$-x+3/2, y, z-1/2$	0.88	2.188	2.990	150.96
O11	H14	O8	$-x+3/2, y, z-1/2$	0.88	2.422	2.979	121.51
O11	H13	O10	$x-1/2, -y+2, z$	0.89	1.850	2.688	155.27

Table A.9-8: Hydrogen bonds of potassium 2-amino-2-(2-carbamoylhydrazono)-1,1-dinitroethan-1-ide (4).

D-H...A			sym. of A	D-H	H...A	D...A	\angle , DHA
N3	H1	O5	$x-1/2, -y+3/2, z+1/2$	0.88	1.999	2.879	175.82
N3	H2	O4	$1, -y+1, -z$	0.84	2.656 1	3.411	50.54
N5	H3	O4	$-x+1, -y+1, -z$	0.85	2.215	2.946	144.30
N6	H4	O5	$-x+3/2, y+1/2, -z-1/2$	0.87	2.170	2.960	151.16
N6	H5	O3	$-x+3/2, y+1/2, -z+1/2$	0.82	2.341	2.954	132.47

Table A.9-9: Hydrogen bonds of 2-(2,2-dinitro-1-ureidoethylidene)hydrazine-1-carboxamide (5).

D-H...A			sym. of A	D-H	H...A	D...A	\angle , DHA
N10	H10	O8	$x-1, y, z$	0.86	2.445	3.063	129.65
N10	H10	N3		0.86	2.604	3.157	123.35
N14	H14	O1	$x+1, y-1, z$	0.79	2.650	3.431	168.39
N11	H11	O6	$x, y-1, z$	0.76	2.223	2.979	170.69
N10	H9	O11	$-x+1, -y+1, -z$	0.96	1.934	2.892	173.45
N3	H2	O6	$x, y-1, z$	0.84	2.322	3.099	154.14
N3	H3	O12	$x, y+1, z$	0.84	2.426	3.142	143.28
N3	H3	O3	$x+1, y, z$	0.84	2.473	3.078	129.45
N4	H4	O12	$x, y+1, z$	0.72	2.035	2.752	173.22
N13	H12	O6	$x, y-1, z$	0.80	2.348	3.138	168.10
N13	H12	O9	$-x+1, -y, -z$	0.80	2.635	3.024	111.54
N14	H13	O7	$-x+2, -y, -z$	0.89	2.571	3.208	129.42
N6	H5	O12	$x, y+1, z$	0.77	2.292	3.054	173.81
N7	H7	O5	$x, y+1, z$	0.81	2.145	2.911	159.19
N7	H6	N5		0.84	2.242	2.624	107.95

Table A.9-10: Hydrogen bonds of potassium (1-carbamoyl-5-oxo-1,2,4-triazol-3-yl)dinitromethanide (6_K).

D-H...A			sym. of A	D-H	H...A	D...A	∠, DHA
N3	H1	O1	$-x+1/2, y+1/2, z$	0.83	2.253	2.900	134.94
N3	H1	O6	$x-1/2, y, -z+3/2$	0.83	2.344	2.988	134.82
N6	H2	O5		0.85	2.173	2.776	127.55
N6	H2	O3	$x, -y+1/2, z+1/2$	0.85	2.362	2.979	129.61
N6	H2	O2	$x, -y+1/2, z+1/2$	0.85	2.484	3.177	139.04
N6	H3	O4	$-x+1, y-1/2, -z+3/2$	0.83	2.313	3.058	149.30
N6	H3	O1	$-x+1, y+1/2, -z+3/2$	0.83	2.366	2.917	124.32

Table A.9-11: Hydrogen bonds of ammonium (1-carbamoyl-5-oxo-1,2,4-triazol-3-yl)dinitromethanide (6_NH4).

D-H...A			sym. of A	D-H	H...A	D...A	∠, DHA
N3	H1	O4		0.85	2.038	2.556	118.66
N3	H1	O6	$x-1/2, -y+1/2, -z$	0.85	2.262	3.025	149.35
N6	H2	O5		0.85	2.106	2.752	132.66
N6	H2	O2B	$x, -y+1/2, z-1/2$	0.85	2.160	2.855	139.03
N6	H2	O2A	$x, -y+1/2, z-1/2$	0.85	2.572	3.071	118.75
N6	H3	O4	$x+1/2, -y+1/2, -z$	0.86	2.045	2.833	151.37
N7	H4	O5	$x+1/2, -y+1/2, -z$	0.92	1.905	2.805	164.48
N7	H5	N4		0.89	2.148	3.031	173.37
N7	H5	O6		0.89	2.455	2.916	112.80
N7	H6	O2A	$-x+1, y-1/2, -z+1/2$	0.93	1.968	2.767	143.20
N7	H6	O2B	$-x+1, y-1/2, -z+1/2$	0.93	2.063	2.964	163.34
N7	H6	O3	$-x+1, y-1/2, -z+1/2$	0.93	2.352	3.020	128.68
N7	H7	O3	$x+1/2, y, -z+1/2$	0.90	2.135	2.980	155.50

10 Curriculum Vitae

Quirin Josef Axthammer

15.01.1985 in Munich, Germany

EDUCATION

- 12/2011 – 02/2016 **Dissertation,**
Ludwig-Maximilian University Munich
Research Group Prof. T. M. Klapötke
Chair of Inorganic Chemistry – Energetic Materials
- 12/2008 – 08/2011 **Master of Science (Chemistry),**
Ludwig-Maximilian University Munich
Master thesis in the Research Group Prof. T. M. Klapötke
Chair of Inorganic Chemistry – Energetic Materials
- 10/2005 – 11/2008 **Bachelor of Science (Chemistry and Biochemistry),**
Ludwig-Maximilian University Munich
Master thesis in the Research Group Prof. H. Langhals
Chair of Organic and Macromolecular Chemistry

11. Bibliography

Publications:

Q. J. Axthammer, T. M. Klapötke, B. Krumm, R. Moll, S. F. Rest

"The Energetic Nitrocarbamate $O_2NN(H)CO[OCH_2C(NO_2)_3]$ Derived from Phosgene"

Z. Anorg. Allg. Chem. **2014**, *640*, 76–83.

Q. J. Axthammer, T. M. Klapötke, B. Krumm

"Pentaerythritol-Based Energetic Materials Related to PETN"

Eur. J. Org. Chem. **2015**, *2015*, 723–729.

Q. J. Axthammer, T. M. Klapötke, B. Krumm

"Synthesis of Energetic Nitrocarbamates from Polynitro Alcohols and Their Potential as High Energetic Oxidizers"

J. Org. Chem. **2015**, *80*, 6329–6335.

Q. J. Axthammer, T. M. Klapötke, B. Krumm, R. Scharf

"A Study of the 3,3,3-Trinitropropyl Unit as a Potential Energetic Building Block"

Chem. Eur. J. **2015**, *21*, 16229–16239.

Q. J. Axthammer, T. M. Klapötke, B. Krumm

"Primary Nitrocarbamates of Sugar Alcohols: From Food to Explosives"

Chem. Asian. J. **2015**, *11*, 568–575.

Q. J. Axthammer, T. M. Klapötke, B. Krumm

"Selected Nitrocarbamates of Glycerine and Co."

Z. Anorg. Allg. Chem. **2016**, *642*, 211–218.

Q. J. Axthammer, T. M. Klapötke, B. Krumm

"Studies on the Synthesis and Properties of 1,1,1-Trinitroprop-2-yl"

Z. Naturforsch., B: J. Chem. Sci. **2016**, *in press*.

Conference Posters:

Q. J. Axthammer, C. Evangelisti, T. M. Klapötke

"Synthesis and Characterization of 2,2,2-Trinitroethyl carbamate and 2,2,2-Trinitroethyl Nitrocarbamate"

16th New Trends in Research of Energetic Materials, Proceedings of the Seminar, Pardubice, Czech Republic, **2013**, 2, 511–521.

Q. J. Axthammer, C. Evangelisti, T. M. Klapötke

"Characterization, Bomb Calorimetric Measurements and Quantum Chemical Calculations of High Energetic Dense Oxidizers (HEDO)"

44th International Annual Conference of the Fraunhofer Institute ICT, Karlsruhe, Germany, **2013**, 44, 88/1–88/15.

Q. J. Axthammer, C. Evangelisti, T. M. Klapötke, R. Meyer

"Michael Addition of Nitroform as a Source of Energetic Materials, Synthesis and Characterization"

17th New Trends in Research of Energetic Materials, Proceedings of the Seminar, Pardubice, Czech Republic, **2014**, 2, 549–562.

Q. J. Axthammer, V. K. Golubev, T. M. Klapötke, T. Witkowski,

"New Pentaerythritol based Energetic Materials Related to PETN"

18th New Trends in Research of Energetic Materials, Proceedings of the Seminar, Pardubice, Czech Republic, **2015**, 2, 448–458.

Conference Talks:

Q. J. Axthammer, M. A. Kettner, T. M. Klapötke, R. Moll, S. F. Rest

"Progress in the Development of High Energy Dense Oxidizers based on CHNO(F) Materials"

16th New Trends in Research of Energetic Materials, Proceedings of the Seminar, Pardubice, Czech Republic, 2013.

Q. J. Axthammer, M. A. Kettner, T. M. Klapötke, R. Moll, S. F. Rest

"Development of High Energy Dense Oxidizers based on CHNO(F) Materials"

5th European Conference for Aeronautics and Space Sciences (EUCASS), Munich, Germany, 2013.

Q. J. Axthammer, C. Evangelisti, T. M. Klapötke

"Characterization, Bomb Calorimetric Measurements and Quantum Chemical Calculations of High Energetic Dense Oxidizers (HEDO)"

44th International Annual Conference of the Fraunhofer Institute ICT, Karlsruhe, Germany, 2013.

Q. J. Axthammer, T. M. Klapötke

"The Combination of Alcohols with the Energetic Functionality of Nitrocarbamate Arises a Innovative Subgroup of Energetic Materials "

45th International Annual Conference of the Fraunhofer Institute ICT, Karlsruhe, Germany, 2014.

Q. J. Axthammer, T. M. Klapötke

"The Nitrocarbamate Moiety for Safer Energetic Materials"

Greener and Safer Energetic and Ballistic Systems, Bucharest, Romania, 2015.